Aus dem Institut für Prophylaxe und Epidemiologie der Kreislaufkrankheiten (IPEK)
des Klinikums der Ludwig-Maximilians-Universität München

Direktor: Univ.-Prof. Dr. med. Christian Weber

Cell type-specific CD40-CD40L interaction in atherosclerosis

Dissertation
zum Erwerb des Doktorgrades der Naturwissenschaften
an der Medizinischen Fakultät
der Ludwig-Maximilians-Universität München
vorgelegt von

Christina Bürger
aus Kamen

2017

Gedruckt mit Genehmigung der Medizinischen Fakultät
der Ludwig-Maximilians-Universität München

Betreuer:	Prof. Dr. rer. nat. Sabine Steffens
Zweitgutachter:	Prof. Dr. rer. nat. Jürgen Bernhagen
Dekan:	Prof. Dr. med. dent. Reinhard Hickel
Abgabe der Dissertation:	01.02.2017
Tag der mündlichen Prüfung:	04.09.2017

Eidesstattliche Versicherung

Bürger, Christina

Name, Vorname

Ich erkläre hiermit an Eides statt, dass ich die vorliegende Dissertation mit dem Thema:

Cell type-specific role of CD40 and CD40L in atherosclerosis

selbständig verfasst, mich außer der angegebenen keiner weiteren Hilfsmittel bedient und alle Erkenntnisse, die aus dem Schrifttum ganz oder annähernd übernommen sind, als solche kenntlich gemacht und nach iher Herkunft unter Bezeichnung der Fundstelle einzen nachgewiesen habe.

Ich erkläre des Weiteren, dass die hier vorgelegte Dissertation nicht in gleicher oder in ähnlicher Form bei einer anderen Stelle zur Erlangung eines akademischen Grades eingereicht wurde.

_____ _____

Ort, Datum Unterschrift Doktorandin

The results of this work were presented at the following conferences as poster and oral presentations:

Oral presentation

84th EAS European Atherosclerosis Society Congress, Innsbruck, Austria, 29 May-1 June 2016
Title: ‘T-cell-specific CD40L promotes to Atherosclerosis´.

Poster presentation

ATVB/PVD Arteriosclerosis, Thrombosis and Vascular Biology | Peripheral Vascular Disease 2016 Scientific Sessions**,** Nashville, Tennessee, USA**,** 4–6 May 2016 |
Title: ‘T-cell-specific CD40L promotes to Atherosclerosis´.

Für Nina & Sven

TABLE OF CONTENTS

ABBREVIATIONS

^{3}H	Tritium
APC	Antigen Presenting Cell
ApoA1	Apolipoprotein A1
ApoB	Apolipoprotein B
ApoE	Apolipoprotein E
ATP	Adenosine Triphosphate
Bcl-xL	B-Cell Lymphoma-Extra Large
Blimp-1	PR Domain Zinc Finger Protein 1
BMDM	Bone Marrow-Derived Macrophages
bp	Base Pair
BSA	Bovine Serum Albumin
CCL5	Chemokine (C-C motif) Ligand 5
CCR5	Chemokine (C-C motif) Receptor 5
CD206	Mannose Receptor 1
CD25	IL-2 receptor α chain
CD40L	CD40 Ligand, CD154,
cDNA	Complimentary DNA
CEA	Carotid Endarterectomy
CFSE	Carboxyfluorescein Succinimidyl Ester
CHS	Contact Hypersensitivity
CO_2	Carbon Dioxide
CTLA-4	Cytotoxic T-lymphocyte-associated protein 4
CVD	Cardiovascular Disease
CX3CL1	Chemokine (C-X3-C motif) Ligand 1, also known as Fractalkine
CXCL1	Chemokine (C-X-C motif) Ligand 1
CXCL10	Chemokine (C-X-C motif) 10
CXCR5	Chemokine (C-X-C motif) Receptor type 5
Cy	Cyanine
DAMP	Danger-associated Molecular Pattern
DAPI	4',6-diamidino-2-phenylindole
DC	Dendritic Cell
DMEM	Dulbecco's Modified Eagle Medium
DMSO	Dimethylsulfoxid

DNA	Deoxyribonucleic acid
DNase	Deoxyribonuclease
DNFB	1-Fluoro-2,4-dinitrobenzene
dNTP	Deoxynucleotide Triphosphate
Dnmt	DNA Methyltransferase
EAE	Experimental Autoimmune Encephalitis
EBV	Epstein-Barr Virus
EC	Endothelial Cell
EDTA	Ethylenediaminetetraacetic Acid
ELISA	Enzyme-linked Immunosorbent Assay
ER	Endoplasmatic Reticulum
EVG	Elastic Von Gieson Stain
FACS	Fluorescence-Activated Cell Sorting
FCA	Fibrous Cap Atheroma
FCCP	Carbonyl Cyanide-p-Trifluoromethoxyphenylhydrazone
FBS	Fetal Bovine Serum
FcγR	Fragment Crystallizable Gamma Receptor
FITC	Fluorescein Isothiocyanate
Foxp3	Forkhead Box P3
GAPDH	Glyceraldehyde 3-Phosphate Dehydrogenase
Gata3	GATA Binding Protein-3 (gata s consensus sequence)
GM-CSF	Granulocyte-macrophage Colony-stimulating Factor
H&E	Hematoxylin and Eosin
HCL	Hydrochloric Acid
HDAC1	Histone Deacetylase 1
HDL	High-density Lipoprotein
HEPES	4-(2-hydroxyethyl)-1-piperazineethanesulfonic Acid
WD	High Fat, Cholesterol-enriched, Western Type Diet
HRP	Horseradish Peroxidase
HSP	Heat Shock Protein
ICAM-1	Intercellular Adhesion Molecule 1
IFNγ	Interferon Gamma
IgG	Immunoglobulin G
IL-6	Interleukin 6
IRF4	Interferon Regulatory Factor 4

IX	Intimal Xanthoma
JNK	C-Jun-N-terminal Kinase
KC	Keratinocyte
$KHCO_3$	Potassium Bicarbonate
LC	Langerhans Cell
LCMV	Lymphocytic Choriomeningitis Virus
LDL(R)	Low-density Lipoprotein (Receptor)
LFA-1	Lymphocyte Function-associated Antigen 1
LOX1	Lectin-Type oxLDLR1
LPS	Lipopolysaccharide
LXR	Liver X Receptor
MCP1	Monocyte Chemotactic Protein 1
M-CSF	Macrophage Colony-stimulating Factor
MDA-LDL	Malondialdehyde-LDL
MEK	Mitogen-activated Protein Kinase
MFI	Mean Fluorescence Intensity
$MgCl_2$	Magnesium Chloride
MHC	Major Histocompatibility Complex
MMP	Matrix Metalloproteinase
MOG	Myelin Oligodendrocyte Glycoprotein
mTEC	Medullary Thymic Epithelial Cells
NaN_3	Sodium Azide
NaOH	Sodium Hydroxide
NFκB	Nuclear Factor Kappa-light-chain-enhancer Of Activated B cells
NH_4Cl	Ammonium Chloride
NK cells	Natural Killer Cells
NLRP3	NACHT, LRR And PYD Domains-containing Protein 3
NO	Nitric Oxide
OCR	Oxygen Consumption Rate
OM	Oligomycin
oxLDL	Oxidized LDL
OXPHOS	Oxidative Phosphorylation
PAMP	Pathogen-associated Molecular Pattern
PBS	Phosphate-buffered Saline
PBS-T	PBS-Tween

PCR	Polymerase Chain Reaction
PD-1	Programmed Cell Death Protein 1
PE	Phycoerythrin
PerCP	Peridinin Chlorophyll
PFA	Paraformaldehyde
PI	Propidium Iodide
PI3K	Phosphatidylinositol-4,5-bisphosphate 3-kinase
PIT	Pathological Intimal Thickening
PRR	Pattern Recognition Receptor
RA	Rheumatoid Arthritis
RAG2	Recombinase Activating Gene 2
RANK	Tumor Necrose Factor Family Member 11a
RNA	Ribonucleic Acid
RNase	Ribonuclease
Rorγt	RAR-related Orphan Receptor Gamma t
ROS	Reactive Oxygen Species
RPMI 1640	Roswell Park Memorial Institute 1640
SD	Standard Deviation
SDS	Sodium Dodecyl Sulfate
SEM	Standard Error Of The Mean
SLE	Systemic Lupus Erythematosus
SMC	Smooth Muscle Cell
STAT6	Signal Transducer And Activator Of Transcription 6
TBS	Tris-buffered Saline
TCR	T Cell Receptor
Th	T Helper
TFH	T Follicular Helper
TGFβ	Transforming Growth Factor Beta
TLR2	Toll-like Receptor 2
TMB	3,3',5,5'-Tetramethylbenzidine
TNF(R)	Tumor Necrosis Factor (Receptor)
Tr1	IL-10-producing Tregs
TRAF2	TNFR-associated Factor 2
Treg	Regulatory T cell
TRIS	Tris (hydroymethyl) aminoethamine

VCAM-1	Vascular Cell Adhesion Molecule-1
VLDL	Very Low-Density Lipoprotein
ASMA/α-SMA	Alpha Smooth Muscle Actin

1 INTRODUCTION

1.1 Cellular players of adaptive and innate immunity - An Overview

When we talk about the immune system, (Latin, immunis, English, unaffected, free, pure), we refer to the biological defense system of higher organisms, which prevents tissue damage by pathogens. It protects the body from invading microorganisms and foreign substances and is also able to destroy defective endogenous cells.

The immune system is a complex network of various organs, cell types and molecules and is the central subject of research in immunology. The immune system is of paramount importance for the physical health of living beings, since all organisms are constantly exposed to the influences and potential threats by the environment. If for example harmful microorganisms enter the body, they can lead to malfunctions and diseases. Characteristic pathogens are bacteria, viruses, fungi, and unicellular (e.g. protozoa such as Plasmodium) or multicellular parasites (e. g. Tapeworms). Even changes inside the own body can pose potential threats for the existence of a living being. The cells of the body that lose their proper function usually die via two distinct pathways. They have to be dismantled (necrosis) or undergo controlled death, apoptosis. In rare cases, they can also pathologically degenerate and lead to the development of cancer. Fortunately, all living beings harbor protective functions. Even simple organisms have such a defense mechanism, which is called the non-specific (innate) immune response.

Innate immunity has emerged very early in the evolutionary history of organisms and since its basic mechanisms remained largely unchanged. In addition to these defense mechanisms, vertebrates developed a complex, adaptable, so-called adaptive immune system, which protects more effectively against pathogens. Both innate and the adaptive immune response depend upon the activities of white blood cells or leukocytes. These cells originate from the bone marrow and many of them also mature there. The innate immune system is based on the detection of certain types of molecules that are common to many pathogens, but are absent in the host. Those so called pathogen associated molecular patterns (PAMPs) are molecular signatures of pathogens that are recognized by the host germ-line encoded pattern recognition receptors (PRRs). These comprise soluble receptors in the blood (components of the complement system) and membrane-bound receptors on the surface of host cells like macrophages and neutrophils. They display a variety of cell-surface receptors that enable them to recognize and engulf pathogens. These include PRRs such as the toll like receptors (TLRs). Additionally, they have cell-surface receptors for the fragment crystallizable region (FcγR) of antibodies produced by the adaptive immune system, as well as for the C3b component of complement system[1,2]. The

activation of cell-surface receptors is usually quickly followed by its engulfment by phagocytic macrophages and neutrophils. The activation of an array of biochemical reactions, leads to the activation of transcription factors such as nuclear factor kappa B (NFκB) and interferon (IFN) regulatory factors (IRFs) for induction of inflammatory cytokine and type-I IFNs, respectively[3]. The released signaling molecules trigger an inflammatory response and begin to marshal the forces of the adaptive immune system via dendritic cells (DCs), B (B cells) and T lymphocytes (T cells). Both of these reactions can occur quickly, even if the host has never been exposed to a particular pathogen[4,5]. Unlike the innate immune system, the first formation of the specific (adaptive) part of the immune system only occurs after birth: The adaptive immune system of an organism evolves in the course of its life time by direct examination of various pathogens. Since the responses to recognized pathogens or associated molecules are destructive, it is crucial that they gain activity only in response to molecules that are foreign to the host while sparing host-derived molecules. The ability to distinguish foreign molecules from the hosts' endogenous molecules is a fundamental feature of the adaptive immune system. Whenever the system fails to make this distinction it will react destructively against the molecules of the host. Such dysregulations known as autoimmune disorders can be disastrous.

However, when the adaptive immune responses are carried out correctly they can be divided in two different groups, the antibody responses and the cell-mediated immune responses. Adaptive immunity elicits very specific and strong immune responses, but is slower as it requires antigen presentation by antigen presenting cells (APCs), as well as selection and clonal expansion of its highly-specialized effector cells, namely the B cells and T cells. In antibody responses, B cells are activated to secrete specific antibodies, proteins which are called immunoglobulins. The antibodies circulate in the bloodstream and other body fluids, where they bind specifically to the foreign antigen that initially induced their production. The binding of an antibody can then lead to inactivation of viruses and microbial toxins by blocking their ability to bind to receptors on host cells and also marks invading pathogens for destruction, mainly by ingestion of phagocytic cells of the innate immune system[5].

1.2 Atherosclerosis – a chronic inflammatory disease

The term atherosclerosis was first introduced by Johan Lobestein in 1829 and the first theories regarding the pathogenesis of atherosclerosis followed in the middle of the 19th century[6]. Since then a broad range of theories has been employed to describe the development of atherosclerosis. Atherosclerosis was previously considered merely a lipid deposit-driven narrowing of the vessel lumen. Nowadays, it is recognized that both the innate and adaptive immune system engage in disease onset and progression[7]. Despite the long history of atherosclerosis research, the main clinical manifestations of the disease including coronary artery disease, stroke, and peripheral arterial disease, still represent the leading causes of death in Europe and North America[8,9]. Atherosclerosis, as a chronic inflammation elicited by hyperlipidemia and perpetuated by a dysbalanced immune response, is characterized by the development of lipid-rich lesions, or plaques, which preferentially arise at the sites of disturbed blood flow in medium- to large-sized arteries[10]. The origin of those plaques lies in an initial local dysfunction and activation of the endothelium, as lipoproteins and lipids in the vessel wall accumulate to a degree exceeding the capacity of clearance and are retained in the extracellular matrix of the vessel wall[11]. Specifically, a shear stress-responsive element, identified in the regulatory region of several genes, has been show to promote a local platelet-induced activation of the endothelium, which triggers an initial leukocyte-endothelial cell (EC) interaction and the activation of ECs[12]. Activated ECs entail the expression of adhesion molecules such as intercellular adhesion molecule-1 (ICAM-1) and vascular cell adhesion molecule-1 (VCAM-1), leading to the adherence of circulating leukocytes and their subsequent migration into the sub-endothelial space along a chemokine gradient produced by the inflamed intima, establishing the nascent atherosclerotic lesion (Figure 1)[13,14]. The local inflammation and concomitant persistent hyperlipidemia, together contribute further to an enhanced endothelial dysfunction resulting in the infiltration and retention of lipoprotein particles in the sub-endothelial space[15]. The retained lipoprotein particles such as low-density lipoprotein (LDL) then may undergo chemical modifications. Assumingly, oxidation of LDL-cholesterol is induced by free radicals produced by macrophages, ECs, or smooth-muscle cells (SMCs). Whereas native LDL is not ingested by phagocytic cells, oxidized LDL (oxLDL) can be taken up by macrophages through scavenger receptors[16]. This increased uptake of lipid particles by macrophages leads to a cytosolic accumulation of those particles and these macrophages gain a “foamy” appearance, thus their designation as foam cells, and become one of the primary components of the fatty streak, the earliest visible manifestation of atherosclerosis. Due to the massive cholesterol scavenging, foam cells will undergo different ways of cell death (i.e. apoptosis, necroptosis, and necrosis)

forming the necrotic core of the plaque[17]. The necrotic core and the increased apoptosis of invaded macrophages are elaborate sources of inflammatory cytokines, which fuel the immune reaction by recruiting more leukocytes including lymphocytes to the lesion site.[18] The recruited immune cells within the atherosclerotic lesion will release further proteases and cytokines which reduce the survival and proliferation of SMCs and the degradation or impaired synthesis, respectively, of matrix proteins (e.g. collagen) which could compromise the stability of the fibrous cap.

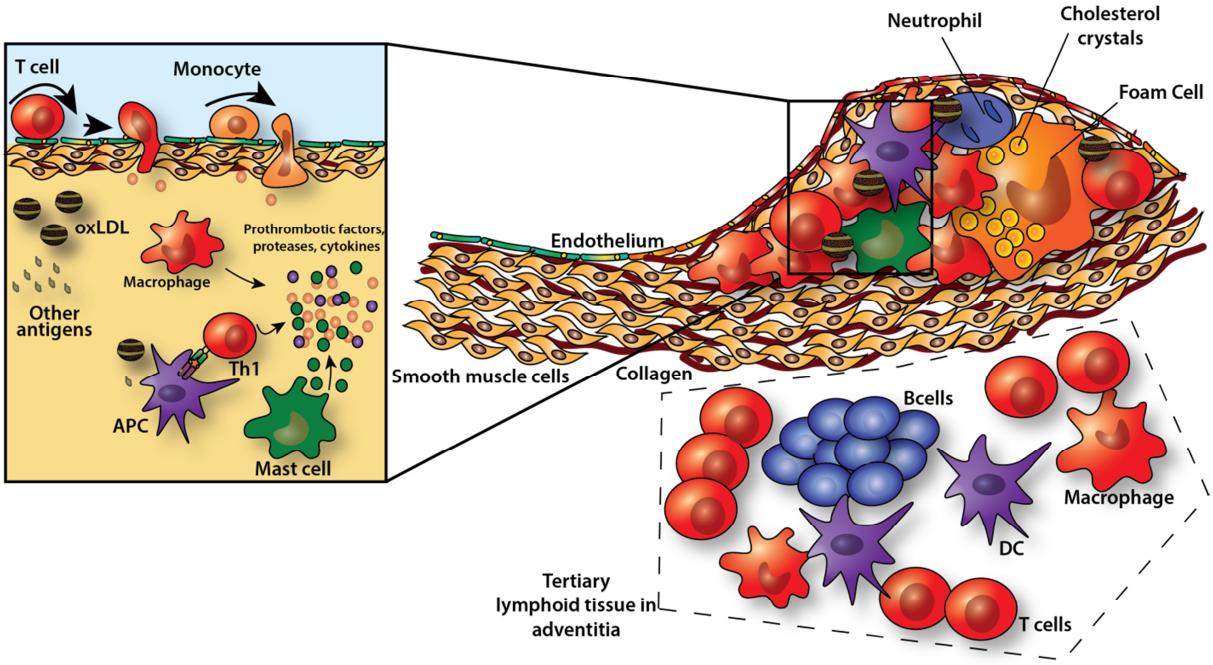

Figure 1. Immune components of the atherosclerotic plaque. The atheroma builds up in the intima, the innermost layer of the artery. The atheroma has a core of lipids, including cholesterol crystals, living and apoptotic cells and a fibrous cap with smooth muscle cells and collagen. Plasma lipoproteins accumulate in the sub-endothelial region. Several types of cells of the immune response are present throughout the atheroma including macrophages, T cells, mast cells and DCs. Outside the intima, the media contains smooth muscle cells that regulate blood pressure and regional perfusion, and further abluminal, the adventitia continues into the surrounding connective tissue. Here, cells of the immune response accumulate outside advanced atheroma and may develop into tertiary lymphoid structures with germinal centers, APC, antigen-presenting cell; DC, dendritic cell; oxLDL, oxidized LDL. Modified from Hansson *et al* and Spitz *et al*[10,19].

Ultimately, the rupture of the destabilized plaque leads to a release of highly-coagulant substances into the blood stream causing rapid thrombus formation, an acute occlusion of the vessel ceasing blood supply to vital organs and thereby to its life-threatening clinical manifestations, namely myocardial infarction and stroke[7] .

1.3 Use of mouse models in atherosclerosis research

Atherosclerosis and its pathogenesis may be studied in a variety of mammalian species, as the basic mechanisms for this pathology are similar in most of organisms. Animal models used for the investigation of atherosclerosis have included rabbits, pigs, and nonhuman primates. Yet, the greatest part of the mechanistic insight into the evolution of the plaque derives from the study of mouse models[20].

One of the most common models used for investigation of atherosclerosis is the LDL receptor-deficient (*Ldlr*$^{-/-}$) mouse, which is a murine model for familial hypercholesterolemia. The LDL receptor is a widely expressed plasma membrane protein that is responsible for the clearance of plasma lipoproteins containing either apoliprotein (Apo) B100 or E. These mice have elevated plasma cholesterol levels when compared to wild type mice but do not exhibit profound atherosclerosis while maintained on a regular chow diet. However, when feeding a cholesterol-enriched, atherogenic diet atherosclerotic plaques occur throughout the arterial vasculature[21].

The apolipoprotein E-deficient (*Apoe*$^{-/-}$) mouse is the other highly popular hypercholesterolemic mouse model that, in contrast to wild type and *Ldlr*$^{-/-}$ mice, develops atherosclerosis on a regular chow diet while aging[22,23]. ApoE is carried on plasma lipoproteins, mostly chylomicron remnants, very low-density lipoprotein (VLDL) and large high-density lipoprotein (HDL). It serves as a ligand for the hepatic uptake of non-HDL lipoproteins by members of the LDL receptor superfamily of receptors[24]. Accordingly, mice that are deficient for ApoE develop severe hypercholesterolemia and their total cholesterol can reach levels ~10 times higher than those in wildtype C57BL/6 mice[23]. Among available models, the *Apoe*$^{-/-}$ mouse is particular popular because of its propensity to spontaneously develop atherosclerotic lesions. In addition, the disease pattern can be aggravated by feeding the fat- and cholesterol-enriched Western-type diet (WD)[25]. Since hypercholesterolemia is exaggerated by administration of a WD, the innate immune system overrides effects caused by adaptive immune cells[26]. Several studies also demonstrated the importance of cholesterol levels, when studying the adaptive immune responses in experimental atherosclerosis[27–30]. In fact it is essential to avoid exaggerated hypercholesterolemic conditions (e.g., WD in *Apoe*$^{-/-}$ mice) as innate immune cells dominate the inflammatory response under such conditions and adaptive immunity becomes increasingly irrelevant for the disease progression[26,28]. Therefore the use of either the *Ldlr*$^{-/-}$ -or the *Apoe*$^{-/-}$ model in atherosclerosis research depends on whether the involvement of specific cells, products of the immune system or hypercholesterolemia in general, should be addressed.

1.4 Dendritic cells in atherosclerosis

DCs are characterized by their capability to engulf and process antigens for presentation to naïve T cells and are therefore members of the group of the so called APCs[31].

They originate from precursors, that reside in the bone marrow, or from monocytes and can be found in both lymphoid and non-lymphoid tissues throughout the body[32]. DCs to some point share similar features with macrophages. Parallel to macrophages, DCs can engulf lipids to adopt a foam cell-like appearance thereby constitute the earliest stages of plaque initiation and formation but nevertheless they represent a unique and potent subset of professional APCs capable of activating naive lymphocytes[33,34]. Mature DCs are typically characterized by the surface expression of CD11c, their ability to strongly upregulate and express high levels of the major histocompatibility complex (MHC) II, the costimulatory molecules CD80 and CD86 and various members of tumor necrosis factor receptor (TNFR) superfamily, such as CD40. Additionally they hold a distinct morphologically feature, the dendrites, which give them their name (δένδρον or déndron being Greek for "tree"). The murine DC population can be divided into four main categories, conventional DCs (cDCs), plasmacytoid (pDCs), monocyte-derived DCs and Langerhans cells a special population of yolk sac-derived DCs[3536]. Here, I will mainly but not exclusively, focus on murine cDCs and pDCs.

Although splenic DCs were first discovered in 1973 by Steinman and colleagues, it took nearly 25 years before DCs were discovered in the arteries of mice and man[37,38]. Only few DCs are found in arterial vessels of healthy mice and humans but an accumulation of DCs was observed in atherosclerosis. Moreover, an increased abundance of DCs seems to correlate with signs of increased plaque vulnerability in humans[39]. Two of the four subtypes of DC were identified in atherosclerotic lesions, cDCs which mainly recognize bacterial signatures and pDCs which specialize in sensing viral fragments and have the unique potential of producing large amounts of type-I IFN. DCs play a central role in atherogenesis as they are directly implicated in cholesterol homeostasis and the immune response[40]. Lipid-loaded $CD11c^+$ DCs can already be detected in the aorta of *Ldlr*$^{-/-}$ mice which consumed a high fat diet for a few days [40] .

In atherosclerotic plaques T cells and DCs are found in close proximity and several studies imply that antigen-presentation by DCs fosters atherosclerosis progression[41–44]. The uptake of lipids by DCs leads to the induction of maturation markers and enhances antigen presentation to T cells and facilitates CD40- and TLR-induced DC maturation. Their enhanced maturation and activation status consecutively leads to an increased ability to stimulate T cells via costimulatory molecules[45,46]. These findings were underpinned by Buono *et al*, who demonstrated that the lack of the costimulatory molecules CD80 and CD86, which are known to be involved in

immunological synapse formation and activation of T cells, reduces atherosclerotic plaque size in *Ldlr*$^{-/-}$ mice[47]. Interestingly, mice lacking CD74 (MHCII-associated protein invariant chain, which regulates antigen processing and inhibits DC motility *in vivo*) also demonstrate marked reduction of atherosclerosis[48,49]. Further studies using the transfer, depletion or modulation of DCs indicated that DCs are capable of skewing immune responses in atherosclerosis towards either an athero-protective or promoting profile[40,50–52]. Under atherosclerotic conditions, some subtypes of DCs may take up atherosclerosis-specific antigens, become locally activated, and migrate to draining lymph nodes, where they then present the antigen to naïve T cells and leading to T cell activation and proliferation[51]. During progression of atherosclerosis, the emigration rate of DCs from aorta to secondary lymphoid organs decreases, which could lead to accumulation of antigen-loaded DCs in the plaque area[53]. These DCs in turn may then stimulate T cells and propagate a local, antigen-specific immune response. Finally these processes perpetuate local inflammation and increased plaque progression. Besides their ability to take up lipids and antigens, DCs can also produce various amounts of anti- and pro-inflammatory cytokines. The engagement of TLR for example, can result in the production of pro-inflammatory and pro-atherogenic cytokines including TNFα, interleukin (IL)-6 and IL-12, but also to the production of the anti-atherogenic cytokine IL-10[54–57]. IL-12 affects atherosclerosis by driving the presumably pro-inflammatory helper cell 1 (Th1) polarization and T cell recruitment (Figure 2). IL-12p40 deficient *Apoe*$^{-/-}$ mice have smaller lesions, whereas the injection of IL-12 increases the atherosclerotic lesion size[58].

As a prototypic anti-inflammatory cytokine, IL-10 down-regulates Th1 cytokines such as IL-12 and IL-18 leading to inhibition of Th1-biased immune response and polarization of the Th1/Th2 balances toward Th2[59,60]. Induction of a regulatory T cell type 1 response attenuates the development of atherosclerosis in *Apoe*$^{-/-}$ mice by decreasing the Th1 response, decreasing the production of IFNγ and increasing IL-10 production[61].

In conclusion, DCs can influence atherosclerosis through different mechanisms such as production of cytokines, antigen presentation and lipid uptake, which either promote inflammation or induce tolerance. However, the exact role of DCs in directing different T and B cell subsets during atherosclerosis is not fully understood.

1.5 T cells in atherosclerosis

Although cells of the innate immune system dominate the inflammatory response and are the most abundant immune cells in the atherosclerotic plaque, several studies have proven a pivotal role for T cells in the pathogenesis of atherosclerosis[62]. Elhage and colleagues demonstrated the importance of various T lymphocyte subsets in atherosclerosis by investigating *Apoe*$^{-/-}$ mice which were genetically deficient in specific lymphocyte subpopulation[63]. Whereas TCR$\alpha\beta^+$ T lymphocytes appeared to play a modest role, absence of TCR$\alpha\beta^+$ T lymphocytes significantly prevented early and late atherosclerosis at all arterial sites. Interestingly, the lack of CD4$^+$ T cells led to a dramatic increase in early lesion abundance[63]. This emphasizes the pro-inflammatory role of CD4$^+$ T cells, which are the most abundant T cell subset within human atherosclerotic lesions[63,64]. Moreover, the adoptive transfer of CD4$^+$ T cells into *scid/scid Apoe*$^{-/-}$ mice, lacking a functional adaptive immune system, clearly demonstrates the pro-atherogenic role of CD4$^+$ T cells in immune-deficient conditions[27]. Further studies with mice deficient for the recombinase activating gene 2 (RAG-2), which do not harbor any T- or B cells, because the gene re-arrangement of immunoglobulins (Ig)- and T cell receptor (TCR) depends on RAG-2, were performed. The atherosclerosis-prone *Rag2*$^{-/-}$ mice developed reduced atherosclerosis under mildly-elevated hypercholesterolemia underlining the importance of those cells for plaque progression[28]. Despite of the increasing understanding of the role of different subsets of CD4$^+$ cells in disease pathology it still remains a topic of controversial and sometimes contradictory results.

Although T cell activation accelerates early progression of atherosclerosis, it is not required for its initiation, as shown using conditional ablation of dividing T cells in *Apoe*$^{-/-}$ mice[65]. Several subsets of CD4$^+$Tcells (Th1, Th2, Th17, T follicular helper (TFH) and regulatory T cells (Tregs)) are found in the arterial wall and play a major role in atherosclerosis (Figure 2)[18]. The commitment of naïve T cells to a certain subpopulation is regulated for the most part by the cytokine milieu and the network of transcription factors that are induced downstream of cytokine signaling. The presence of IL-12 and IL-18 initiate Th1 skewing, IL-4 leads to a Th2 commitment of naïve CD4$^+$ T cells, the differentiation towards the Th17 lineage requires several cytokines including IL-6, TGFβ, IL-23 and IL-1β and the presence of IL-10 and TGFβ are required for Treg commitment[66,67]. APCs including B cells, DCs and macrophages express MHC II on their surface displaying antigen to CD4$^+$ T cells, a process usually occurring in secondary lymphoid organs. The antigen leading to T cell activation in atherosclerosis are not known with certainty, but appear to involve epitopes of oxLDL and possibly heat shock protein 60/65 (HSP60/65)[68–70]. Upon recognition of cognate antigen presented by APCs, naïve CD4$^+$ T

cells undergo differentiation during their activation in response to TCR ligation and costimulatory signals via CD28 which binds to costimulatory molecules CD80/CD86 provided by the APCs[71].

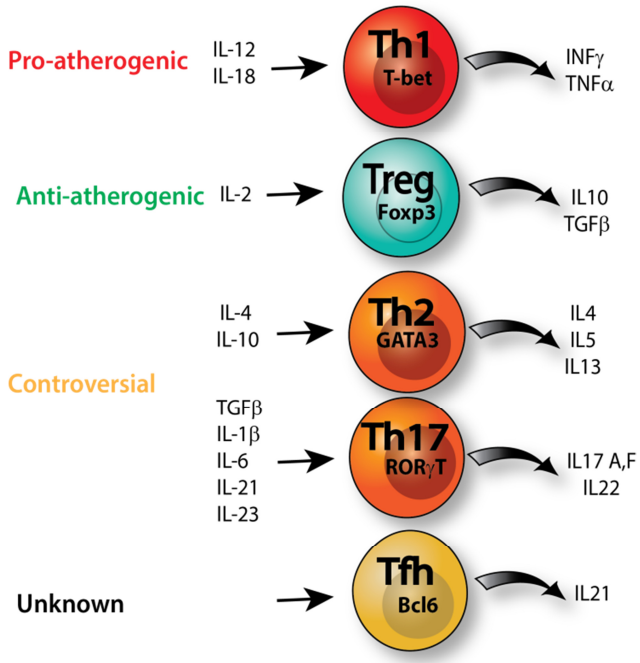

Figure 2. The effects of T-cell subsets on atherosclerosis.
Pro-atherogenic: Th1 (red). The presence of IL-12 and IL-18 causes Th1 skewing. IL-12 results in activation of the downstream transcription factor, T-bet. T-bet activation results in pro-inflammatory cytokine production, including IFN-γ and TNF-α. Athero-protective: Treg (blue). IL-10 and TGFβ are required for Treg commitment. Tregs express the transcription factor Foxp3 and can produce IL-10 and/or TGFβ. Controversial: Th2 (orange, top) and Th17 (orange, bottom). Naive $CD4^+$ T cells commit to a Th2 lineage under the influence of IL-4. In a positive feedback loop, IL-4 increases expression of the transcription factor GATA3, which produces additional IL-4 and inhibits IFNγ production. Th17 differentiation requires a combination of several cytokines, including IL-6, TGFβ, IL-21, IL-23 and IL-1β. These cells express the transcription factor RORγT, and produce IL-17A/F and IL-22. Unknown: Follicular helper T cells (yellow). These are $CD4^+$ T cells found in the B cell follicles of secondary lymphoid organs. They secrete IL-21 and express the transcription factor Bcl6. Modified from Tse *et al*[62].

The activation induces the production of IL-2 which leads to an IL-2- dependent activation of signal transducer and activator of transduction 5 (STAT5) and the entry into the cell cycle[72]. Thereafter their development is initiated by STAT1, which is activated in response to IFNγ and IL-27 that are produced by natural killer (NK) cells and APCs, respectively. STAT1 activation induces the transcription of the T-box transcription factor (T-bet), which in turn fosters the production of IFNγ and suppression of IL-4 thus promoting Th1 differentiation whilst inhibiting Th2 differentiation[73,74]. Th1 cells exceed the number of Th2 cells in atherosclerotic lesions and are considered the prototypical pro-inflammatory and pro-atherogenic T cells[75]. Additionally atherosclerotic lesions contain a substantial amount of IFNγ , supporting the idea that the predominant T cells in the lesion are IFNγ-releasing Th1 cells[76]. IFNγ enhances recruitment of T cells and macrophages to the plaque, inhibits SMC function and proliferation, reduces collagen

production and increases the synthesis of extracellular matrix-degrading proteins leading to compromised plaque stability[77]. Deficiency of T-bet decreases atherosclerotic burden in mice accompanied by reduced IFNγ levels and an enhanced, athero-protective Th2-mediated antibody response[78]. Additional cytokine associated with Th1 cells are IL-12 and IL-18[66,67]. IL-12 is typically produced by DC, macrophages, neutrophils and a subset of T cells. IL-12 stabilizes the Th1 subset by promoting the production of the IFNγ. *Il12*$^{-/-}$ mice exhibit impaired IFNγ production and increased levels of IL-4 indicating an dysfunctional Th1 response leading to reduced plaque development[56]. Furthermore, IL-12 increases expression of MHCII, CD80, and CD86 on APCs thereby enabling an efficient immune response. IL-18 synergizes with IL-12 to favor the differentiation of naïve T cells towards the Th1 lineage and to induce the production of IFNγ in T cells, natural killer cells, in certain macrophages, and even in SMC[67,79–81]. Mallat and colleagues suggested a role for the Th1 response in plaque destabilization by IL-18-mediated mechanisms[82]. Overall the IFNγ, IL-12, IL-18 axis of cytokines is strongly inflammatory and promotes and accelerates lesion development. IL-4, IL-5, and IL-13 are Th2-associated hallmark cytokines. Th2 commitment occurs in presence of IL-4 which increases expression of the transcription factor GATA-binding protein 3 (GATA3), which through a positive feedback loop potentiates IL-4 expression and inhibits IFNγ expression[83]. IL-4 counteracts the production of IFNγ and lack of IL-4 leads to increased athero-progression. Since IL-4 inhibits Th1 differentiation, yet its deficiency leads to mildly enhanced atherosclerotic lesion formation in *Apoe*$^{-/-}$ mice the role of the Th2 pathway in the development of atherosclerosis remains controversial[56]. Contrasting effects were also observed in *Ldlr*$^{-/-}$ mice where the lack of IL-4 led to decreased lesion formation [84]. Furthermore, IL-4 can mediate numerous effects on non-T cell populations in the lesion leading to increased lipid oxidation in the arterial wall, enhanced leukocyte adhesion and attraction, increased uptake of modified lipoproteins and foam-cell formation, and promotes an M2-like macrophage phenotype[85,86]. Moreover, IL-4 activates mast cells which secrete mediators (e.g. serine proteases) promoting apoptosis of SMCs, reducing collagen production, and increasing production of proteases thereby potentially destabilizing the plaque[87]. Bone marrow transplant studies using IL-13-deficient donors demonstrated reduced macrophage content in lesions of *Apoe*$^{-/-}$ mice and limited recruitment of monocytes into the plaque by decreasing VCAM-1 expression. Furthermore, *in vitro* experiments revealed an IL-13-mediated switch towards M2 macrophages which show a higher capacity in clearing oxLDL[88]. In sum, different studies show reduced and unaltered atherogenesis in hypercholesterolemic mice deficient for Th2 hallmark cytokines, the role of Th2 cells remains unclear and requires further evaluation. Overall, the Th2 response appears not to play a pivotal role in atherosclerosis, in

particular in murine models of atherosclerosis which are mainly performed in mice of the C57Bl/6 strain which inherently displays a weak Th2 response[56,89,90].

The role of the rather recently discovered Th17 cells in atherosclerosis is also still controversial[91,92]. Naïve $CD4^+$ T cells differentiate into Th17 cells by signaling cues requiring TGFβ and either IL-6 or IL-21, IL-1β, and IL-23 which influences the expression of the transcription factor STAT3, RORγT and RORα[93]. Th17 cells secrete IL-17A, IL-17F, and IL-23[94,95]. A recent study illustrated the presence of T cells producing IL-17 and IFNγ in atherosclerosis, but opposing effects of IL-17 in atherogenesis are reported [96,97]. Th17 cells infiltrate coronary plaques, subsequently inducing vascular SMCs to produce pro-inflammatory cytokines and chemokines. Several studies demonstrated a pro-atherogenic role for Th17 cells in hyperlipidemic mice, whereas others suggested a protective role of IL-17 in atherosclerosis[96,98–102]. Madhut and colleagues, however, employing a genetically deficient mouse model showed that IL-17A is involved in systemic and vascular inflammation, but did not alter plaque burden in experimental atherosclerosis [103]. Th17 and Treg development both depend on TGFβ. In addition, the cytokine milieu and fatty acid metabolism are critical in shifting the balance towards the of one of these cell type polarizations[93,104,105].

Since the first descriptions in the year 2000, TFH cells only recently became established as a distinct CD4 T cell type, and one of great importance for protective immunity. TFH cells depend on the expression of the master regulator transcription factor B cell lymphoma 6 (Bcl6). Distinguishing features of TFH cells are the expression of CXC- chemokine receptor type 5 (CXCR5), Programmed cell death protein 1 (PD-1), IL-21, and Inducible T cell costimulator (ICOS), and the absence of PR domain zinc finger protein 1 (Blimp-1)[106–108]. TFH cells are important for the formation of germinal centers and antibody production[109]. Due to its rather recent research history the role of TFH cells in atherosclerosis has not been investigated yet[110].

Tregs are generally characterized as $CD4^+CD25$ $(IL2R)^+$ cells co-expressing the Forkhead box P3 (Foxp3) transcription factor[111,112]. Treg commitment is mainly driven by the presence of TGFβ and IL-10. Recently it has been shown commitment to this lineage is influenced by activated DCs that appear to have a supportive role in Treg differentiation[113–115]. Tregs are characterized as negative key regulators of immune effector cells. $Foxp3^+$ Tregs suppress the proliferation of tissue-specific T cells and their differentiation into the Th1, Th2, and Th17 lineage. Moreover, they inhibit polyclonal T cell activation and the function of other immune cells including B cells, macrophages, and DCs[116]. They are further separated according to their functional phenotype in natural Tregs (nTregs) and inducible Tregs (iTregs). Both groups harbor a powerful anti-inflammatory arsenal and are versatile in the modes of action by which they prevent autoimmunity or tissue damage by host-derived immune cells. Tregs constantly express

Cytotoxic T-lymphocyte-associated protein 4 (CTLA-4), a co-inhibitory molecule which binds to CD80/CD86. Thus, Tregs prevent the activation of naïve T cells[117]. Furthermore, engagement of CTLA-4 with CD80/CD86 leads to their internalization further reducing their surface abundance and rendering the APC tolerogenic[118]. In parallel the high expression of CD25 enables Tregs to deprive the micro milieu from the T cell autocrine growth and activation factor IL-2, thus limiting survival and proliferation of effector T cells. Furthermore, Tregs are potent sources of the anti-inflammatory cytokines IL-10, IL-35, and TGFβ which modulate and reduce the activation of APCs and other cells. Additionally, similar to $CD8^+$ T cells, Tregs are equipped with the molecular machinery to produce and release granzyme B and perforin, which can negatively modulate function and survival of conventional T cells, B cells, and NK cells[119].

With the help of mouse models, the importance of Tregs in atherosclerosis became apparent within the past decade. Mouse models which employed genetic deficiencies or cell depletion clearly demonstrated a protective role for Tregs in atherosclerosis with studies demonstrating decreased Treg numbers in conditions of hypercholesterolemia and atherosclerosis[120–122]. In 2006 Ait-Oufella and colleagues demonstrated that Tregs conferred atheroprotection in hyperlipidemic mice. The authors observed decreased Treg development and abundance in *Ldlr*$^{-/-}$ mice after reconstitution with CD80/CD86- or CD28-deficient bone marrow accompanied by an increased atherosclerotic burden. Furthermore they showed that the injection of an anti-CD25 antibody in hyperlipidemic mice reduced abundance of Tregs and concomitantly increased lesion size and infiltration of macrophages and conventional T cells[123]. Vice versa, the adoptive transfer of Tregs in *Apoe*$^{-/-}$ mice protected them from the development of atherosclerosis [124]. In addition, Lievens and colleagues provided evidence that the interaction of the costimulatory molecule CD40 with CD40 Ligand (L) on platelets mediates the numbers of Tregs leading to accelerated atherosclerosis by rendering the Treg/T effector cell homeostasis[125]. Conversely, a treatment with anti-CD25 antibody in *Apoe*$^{-/-}$ mice completely prevented the observed protective effects of platelet CD40L deficiency on atherosclerosis. However, the presence of CD25 is not sufficient to characterize Tregs reliably as it is also present on activated T cells, NK cells, and myeloid DCs, leaving $CD25^+$ cell populations contaminated and only enriched for natural Tregs. Accordingly, experiments employing CD25-depleting antibodies should be interpreted with caution and do not provide final evidence for a Treg-mediated phenotype. Klingenberg *et al.* confirmed the anti-atherogenic propensities of Treg directly. Hyperlipidemic *Ldlr*$^{-/-}$ mice were transplanted with bone marrow from transgenic mice expressing the diphtheria toxin receptor (DTR) under control of the Foxp3 promotor. Treatment of the resulting chimeric bone marrow mice with diphtheria toxin (DT) induced cell death of all $Foxp3^+$ Tregs resulting in their systemic ablation. Depletion of $Foxp3^+$ Tregs in these chimeric mice led to increased atherosclerosis but

also aggravated hypercholesterolemia ascribing Tregs an additional regulatory function in lipoprotein metabolism[126]. Although these findings provide yet further steps in understanding the athero-protective functions of Tregs in cardiovascular diseases it remains challenging to distinguish effects of a lesion-specific or systemic function/depletion of Tregs as the latter may indirectly affect local inflammatory response in the atherosclerotic vasculature.

The role of $CD8^+$ T cells in atherosclerosis is a topic of controversial debate. Although infiltration of $CD8^+$ T cells in human atherosclerotic lesions were described 30 years ago, the role of these cells in lesion development has long remained inscrutable[127]. In murine models of atherosclerosis, $CD8^+$ T cells are found in atherosclerotic lesions by immunohistochemistry in *Apoe*$^{-/-}$ mice or by flow cytometric analyses of vascular tissue in *Ldlr*$^{-/-}$ animals[128,129] . In the past years, however, more refined research models have proposed both athero-protective and pro-atherogenic functions for $CD8^+$ T cells. A number of studies have focused on $CD8^+$ T cells in atherosclerosis, and suggested that, similar to $CD4^+$ T cells, the role of $CD8^+$ T cells in atherogenesis is complex and subset-dependent. To explore the role of $CD8^+$ T cells in atherosclerosis, Elhage and colleagues analyzed atherosclerotic lesion development in $CD8^+$ T cell-deficient *Apoe*$^{-/-}$*Cd8*$^{-/-}$ mice. In these mice, cytotoxic T cell responses were dramatically decreased, whereas B- as well as $CD4^+$ T lymphocyte populations and function were described to be unaltered[63]. The *Apoe*$^{-/-}$ mice lacking $CD8^+$ T cells did not show any significant changes in atherosclerotic lesion size in the aortic root and descending aorta, suggesting that $CD8^+$ T cells do not play a major role in atherosclerosis. In contrast to that, the adoptive transfer of $CD8^+CD25^+$ T cells, a $CD8^+$ subset that is considered anti-inflammatory and exerting suppressive effects, decreased atherosclerotic burden in *Apoe*$^{-/-}$ mice[130]. A recent report showed that depletion of $CD8^+$ T cells in *Apoe*$^{-/-}$ mice reduced atherosclerotic lesion development, lesional inflammation, and cell death and that perforin/granzyme B-mediated cytotoxicity was key to the pro-atherogenic effect of transferred $CD8^+$ T cells[131]. Overall, the data on $CD8^+$ T cells in atherosclerosis indicate that $CD8^+$ T cells are pro-atherogenic, but their contribution to atherogenesis seems to depend on timing and the subset.

1.6 B cells and Immunoglobulins in atherosclerosis

B cells originate from the bone marrow and play an important role in humoral immune response. They are characterized by the presence of a B cell receptor (BCR) and are classically known for their ability to produce antibodies important for the clearance of antigens. Like DCs, B cells possess antigen presenting capacities, activating $CD4^+$ and $CD8^+$ T cells. In addition, they can produce a broad number of cytokines (e.g. IFNγ, IL-2, IL-12, IL-4, IL-6 and IL-10). B cells can be categorized into two developmentally-distinct lineages, B-1 and conventional B-2 cells. B-1 B cells include the B-1a and B-1b B cell subsets and conventional B-2 B cells include follicular B cells and marginal zone B cells[132–134]. Upon antigen recognition all mature B cell subtypes are capable of differentiating into plasma cells and produce natural antibodies like Immunoglobulin (Ig) M and IgA. Conventional follicular B-2 B cells undergo isotype switching in the spleen and lymph nodes in response to T cell-dependent antigens to either become plasma cells that secrete large amounts of antibody (adaptive IgM, followed by IgG (IgG_1, $IgG_{2a/c}$, IgG_3), IgA, or IgE antibodies), or become memory B cells with the ability to produce specific antibodies upon re-exposure to the same antigen[135–138]. Unlike the follicular B-2 B cells of the adaptive immune system, marginal zone B cells are considered to be part of the innate immune system[139,140]. They reside in the spleen and are positioned to immediately respond to antigens in the blood that are filtering through the spleen. In contrast to follicular B cells they do not have the ability to become memory B cells[139,140].

In contrast to the role of T cells, which has been extensively studied for decades, the role of B cells only recently has gained attention. New studies have identified differential effects of different B cell-subsets and helped to clarify the still poorly understood mechanisms by which B cells act. Only low B cells numbers can be detected in atherosclerotic lesions[141]. Galkina *et al* were able to show that B cells participate in lymphocyte infiltrates of the adventitia surrounding arteries and in tertiary lymphoid organs.[142]. Although only a few were detected occasionally in the intima of atherosclerotic lesions, early lesions contain considerable amounts of IgG, IgM, and IgG antibodies[143].

Various studies reviewed by Perry *et al* and Kyaw *et al* have recently pointed out an important role for B cells in atherogenesis[144,145]. B cells may affect atherosclerosis potentially through mechanisms like the production of immunoglobulins and the subsequent formation of immune complexes with their cognate antigens. The first evidence for a functional role of B cells in experimental atherosclerosis came from studies, which demonstrated that the removal of the spleen, as a large B cell reservoir, resulted in aggravated atherosclerosis in *Apoe*$^{-/-}$ mice and that this effect could be reversed through the adoptive transfer of unfractionated splenic B

cells[146]. In agreement, Major *et al* demonstrated that the transfer of with B cell–deficient bone marrow from µ*MT* mice into cholesterol-fed *Ldlr*$^{-/-}$ mice resulted in an increased plaque formation compared with mice reconstituted with wild-type bone marrow[147]. Although the results from the different studies indicated an overall protective role of B cells, some studies also reported pro-atherogenic effects for B cells. Anti-CD20–mediated B-cell depletion in atherosclerotic *Apoe*$^{-/-}$ and *Ldlr*$^{-/-}$ mice results in a significant reduction of lesion size[148,149]. Furthermore, the deficiency or adoptive transfer of B2 B cells revealed a pro-atherogenic role of this B cell subtype[149]. These contradictory findings do not only exclusively imply that B cells have both pro and anti-atherogenic roles in atherosclerosis, but also indicate that B cell subtypes are differently involved in atherosclerosis progression.

A spate of studies has pointed toward a differential role of B1 and B2 cells in atherogenesis and there is conflicting evidence concerning the role of B2 cells in atherogenesis. Although the role of B2 cells in atherosclerosis is controversial, the role for B1 cells, which represent a much smaller subset of B cells, particularly B1a cells, seems clearer. B1a cells clearly prevent atherosclerosis in mice[150]. An intact spleen is required for B1a cell maintenance, because splenectomized or genetically modified asplenic mice have significantly lower B1 cell numbers in the circulation and peritoneal cavity[151]. Moreover, it has been shown that the splenic microenvironment enhances the antibody production capacity of B1 cells and a splenectomy therefore may result in the loss of this potentially athero-protective B-cell subset[152]. Indeed, Kyaw *et al* demonstrated that the number of peritoneal B1a cells of splenectomized *Apoe*$^{-/-}$ mice was reduced by 50% and that the transfer of peritoneal B1a cells but not splenic B2 cells into splenectomized *Apoe*$^{-/-}$ mice resulted in higher concentrations of IgM and an amelioration of the splenectomy-induced accelerated atherosclerosis[153]. It is currently not known whether B1b cells have the same athero-protective potential as B1a cells.

Secretion of natural IgM antibodies is one of the major functions of B1 cells. Accordingly, it has been hypothesized that the athero-protective effect of B1 cells depends on the secretion of IgM antibodies[153150]. Splenectomy of *Apoe*$^{-/-}$ mice is associated with decreased IgM levels, and patients subjected to splenectomy after trauma have been reported to have significantly lower serum IgM titers[154]. Of note, unlike transfer of wild-type B1a cells, those isolated from *sIgM*$^{-/-}$ donor mice, which express but do not secrete IgM, failed to attenuate the accelerated atherosclerosis in splenectomized mice, demonstrating that the IgM conferred the atheroprotection[153].The class of IgM antibodies comprises both, natural IgM antibodies and adaptive IgM antibodies.

Natural antibodies are primarily derived from B1 cells that spontaneously secrete antibodies independently from T cells, whereas adaptive IgMs are secreted by B2 cells in a T cell–

dependent manner. In naïve mice, up to 90% of the total IgM pool is derived from B1 cells[155]. Natural IgM antibodies are pre-existing germline-encoded products that do not require exogenous antigen stimulation for their generation[30,144,156,157]. Due to their specificity for microbial antigens, they play an important role in the first-line defense against infections with bacteria, viruses, and fungi. Natural antibodies also exhibit specificity for certain self-antigens, and in addition to their antimicrobial properties, possess so called “housekeeping functions” by regulating the safe disposal of apoptotic cells and self-antigens[158]. Natural antibodies facilitate the removal of cellular debris, because their repertoire includes specificities for highly conserved structures on apoptotic cells and other self-antigens, such as oxidation specific epitopes (OSE) that are found on apoptotic cells and on the highly immunogenic oxLDL[159]. Several studies could demonstrate that OSEs are a major target of natural IgM antibodies and that IgG and IgM autoantibodies to oxLDL can be easily detected in both humans and animal models of atherosclerosis[160–163]. OxLDL-specific antibody IgM titers associate with athero-protection, while oxLDL- specific IgGs correlate with atherosclerosis progression[164,165]. OxLDL generates various oxidation-specific neoepitopes, such as malondialdehyde-modified (MDA-modified) LDL (MDA-LDL) or the phosphatidylcholine (PC) headgroup of oxidized phospholipids (oxPLs)[164]. Shaw *et al* isolated a panel of oxLDL-specific B cell lines that secrete IgM antibodies which specifically bind to the PC headgroup of oxPLs[164]. Of considerable interest is the fact that all of these PC-specific autoantibodies recognized the lipid moiety of oxLDL, as well as the delipidated modified apoB (the protein moiety of oxLDL), but not native LDL[164]. The antibodies were found structurally and functionally identical to classic "natural" T15 anti-PC antibodies that are of B-1 cell origin and are reported to provide optimal protection from virulent pneumococcal infection[164]. Accordingly, Binder *et al* showed that pneumococcal vaccination of *Ldlr*$^{-/-}$ mice reduced atherosclerosis by expanding T15 natural antibodies[166]. The group also performed vaccination studies by immunization with MDA-LDL. They indicated that the athero-protective effect seen after the immunization was due to an increase in T15 antibody titers that resulted from IL-5 production of Th2 T cells[166]. In addition they confirmed their theory by using a bone marrow transplantation model and showed that the deficiency in bone marrow IL-5, a cytokine which is important for maturation and Ig secretion of B1 cells, reduces the levels of oxLDL-reactive IgM and lead to an acceleration of atherosclerosis[167]. Taken together these data and supporting results from animal and clinical studies underline the athero-protective properties of IgM[168,169].

In contrast to IgM, antigen-driven IgG response are considered pro- atherogenic. IgG is the main immunoglobulin subtype in the circulation of humans. The IgG consists of 4 different subclasses in both humans (IgG1, IgG2, IgG3, and IgG4) and in mice (IgG1, IgG2$_{a/c}$, IgG2$_b$, and IgG3) and each of the IgG subtypes exhibits different fragment crystallizable gamma receptor (FcγR)

affinity and harbors different capacities to activate the complement system[170,171]. As already mentioned above oxLDL-specific IgG antibodies are detected in atherosclerotic lesions and the depletion of B cells lowered atherosclerotic burden and concomitantly titers of oxLDL-specific IgG antibodies and to a lesser extent those of IgM antibodies[149]. There are several studies which document positive or negative correlation of anti-oxLDL IgG with manifestations of cardiovascular disease (CVD)[172]. The inconsistent results may lose their significance when analyzed in combination with other CVD risk factors or could be explained by the fact that a reproducible antigen to perform reliable measurements (e.g. MDA-LDL) was missing. Despite the discrepancy between the different studies IgG antibodies have often been suggested to be pro-atherogenic. However, there is little experimental evidence for the functional role of IgG antibodies in atherosclerosis. Most information about IgG antibodies in atherosclerosis were derived from immunization approaches with HSP65 or oxLDL. The immunization of normocholesterolemic rabbits with HSP65 for example, induced accelerated atherosclerosis on a cholesterol-enriched diet[173].These effects were reproduced in studies using *Ldlr*$^{-/-}$ mice fed a regular chow diet, which developed high anti-HSP65 IgG antibodies and increased atherosclerotic lesions[69]. The pro-atherogenic effect of anti-HSP65 IgG was also demonstrated by George *et al*, who showed that injecting chow-fed *Ldlr*$^{-/-}$ mice with IgG preparations from Hsp65-immunized mice promoted fatty streak formation[174]. Taken together these data suggest a pro-atherogenic role of HSP65-specific IgGs. The immunization of hyperlipidemic mice with MDA-LDL resulted in increased amounts of specific antibodies and was atheroprotective[175,176]. Contradictory results were obtained *in vitro*, where plasma of mice with high MDA-LDL-IgG titers inhibited oxLDL uptake by macrophages whereas recombinant human athero-protective MDA-LDL–specific IgG1 promoted uptake of oxLDL by macrophages[177,178]. In summary, there is still information missing to understand the biological roles and functions of oxLDL-specific IgGs in atherosclerosis.

IgE antibodies have been extensively studied in allergy and asthma and their role was only indirectly tested in atherosclerosis. Although a few epidemiological studies exist that suggest a contribution for IgE immunoglobulins to atherosclerosis. Kovanen *et al* could show, that high IgE levels are a prognostic factor for myocardial infarction and cardiac death in dyslipidemic men[179]. The results were later confirmed by Wang *et al* and several others[180]. Thus, epidemiological data suggest a pro-atherogenic role for IgE antibodies. Even though the role of IgE antibodies in experimental atherosclerosis has not been directly investigated, additional indirect evidence came from studies in atherosclerosis-prone mice deficient in Fcε receptors and just recently from studies in mice with a deficiency of secreted IgM (sIGM)[180,181]. *Apoe*$^{-/-}$ mice deficient for the high-affinity FcεRI receptors contained smaller atherosclerotic lesions accompanied by reduced

macrophage and apoptotic cell. However, these effects were achieved with IgE concentrations that were 200-fold higher than the concentrations measured *in vivo* in atherosclerotic mice. Therefore, these effects may not entirely reflect an *in vivo* situation[180]. In the beginning of 2017 Tsiantoulas et al identified a previously unsuspected mechanism by which sIgM deficiency aggravates atherosclerosis through strongly increased plasma IgE level[181]. Insights into a direct role of IgE in atherosclerosis are still missing. Moreover, it will be important to demonstrate whether such effects are dependent on certain antibody specificities for relevant antigens, or whether they are antigen independent.

Another Ig subclass is represented by IgA which confers mucosal protection against pathogens. Substantial IgA amounts are found in the circulation of humans. Epidemiologic studies correlate circulating IgA titers with myocardial infarction, CVD, and cardiac death in hyperlipidemic humans[182]. However the mechanistic contribution of IgA to atherosclerosis is not resolved yet.

Comparable to T cells, the B cell population also harbors B cell subsets which are capable of dampening immune responses. These regulatory B cells modulate the immune response through mechanisms similar to Tregs. They either produce cytokines like IL-10 and TGFβ or interact with other immune cells via antigen presentation and secretion of antibodies. With the help of those mechanisms regulatory B cells might be capable to interact with pathogenic T cells to dampen harmful immune responses[183]. But their functions and impact on atherosclerosis still remains elusive.

1.7 Platelets in atherosclerosis

Platelets are anucleated cell fragments of cytoplasm that are derived from the megakaryocytes in the bone marrow, and enter the circulation. Megakaryocytes first undergo nuclear endomitosis, organelle synthesis, and dramatic cytoplasmic maturation and expansion. The entire megakaryocyte cytoplasm afterwards is converted into a mass of proplatelets, which are released from the cell[184]. The nucleus is eventually extruded from the mass of proplatelets, and individual platelets are released from proplatelet ends[184]. Therefore the most of functional proteins may derive from different origins and are delivered to the major storage compartment in platelets, the α-granules. Von Willebrand factor (vWF) is synthesized in the megakaryocyte, while fibrinogen (340 kDa), also a major component of α-granules, is not synthesized by the megakaryocytes, but is exclusively recruited from plasma[185–188]. The platelet α-granule therefore represents a unique storage compartment that stores both endogenously synthesized proteins, as well as proteins derived from endocytic origin.[189] Endocytosis and incorporation of glycoproteins into the α-granules require surface binding, internalization, and proper intracellular targeting. Little is known about the intracellular trafficking of proteins in megakaryocytes and platelets, especially with regard to the intracellular routing of glycoproteins following internalization and delivery to α–granules.

Although central role of platelets lies in the prevention of bleeding, platelets probably contribute to diverse processes that extend beyond hemostasis and thrombosis. The process of thrombus formation is site dependent. Thrombosis inside veins is associated with high coagulation activity and the production of large amounts of fibrin. Arterial thrombosis however, is connected to high platelet activation. Therefore the thrombi contain high amounts of platelets [190]. In arteries the activation of platelets occurs at the sites of injury such as ruptured atherosclerotic lesions where platelets are exposed to plaque components like vWF and Tissue Factor (TF)[191]. There is a constantly growing recognition that platelets modulate immune responses since platelets are well-equipped to facilitate leukocyte recruitment to sites of vascular injury and inflammation[192]. While their hemostatic and thrombotic roles are already well-established, their function as potent immune cells emerged rather recently. These studies implicated platelets as essential effectors in inflammatory conditions like sepsis, experimental autoimmune encephalomyelitis (a model for multiple sclerosis), allergy, rheumatoid arthritis, host defense during bacterial infection and cancer[193–197].

Besides the cell types that are present in the atherosclerotic lesion, circulating platelets today are also known to be important contributors to atherosclerosis[198]. Activated platelets promote leukocyte arrest on the vascular endothelium, which is believed to be a key process in the

development of atherosclerosis[199] and they seem to play a role in all relevant stages of atherosclerosis by initiating or sustaining the chronic inflammatory process. Platelets facilitate the recruitment of inflammatory cells to inflamed lesion sites and dysfunctional endothelium by interacting with endothelial cells (ECs) and a plethora of circulating leukocytes like monocytes, neutrophils, DCs, T cells and progenitor cells[200–208]. A range of molecules present on the platelet surface or stored in platelet granules such as glycoproteins, costimulatory molecules (CD40, CD40L), cell adhesion molecules (e.g. P-selectin), junctional adhesion molecules (e.g. JAM-A), TLRs, chemokine receptors, scavenger receptors and protease-activated receptors contributes to the cross-talk of platelets with other inflammatory cells during the vascular inflammation involved in the development and progression of atherosclerosis[209–214].

Over 30 years ago Fitzgerald *et al* were the first to detect activated platelets, as defined by P-selectin surface expression, in peripheral blood of patients with unstable atherosclerotic disease[215]. Later circulating activated platelets were also detected in the blood of atherosclerotic patients with stable coronary disease [216,217]. Activated platelets can contribute to atherosclerosis via different ways, through the interaction with the endothelium and through the interaction with leukocytes. Both interactions can occur via direct or indirect mechanisms. The ability of activated platelets to interact with the endothelium was shown in the postcapillary venules in mice with hypercholesterolemia and after stimulation with the calcium ionophore A23187[218,219]. Hoe *et al*. could show that this interaction was an exclusive property of activated but not resting platelets[220]. The observed platelet endothelium interactions were mainly characterized by transient tethering, rolling, and firm adhesion and an essential role was ascribed to P-selectin during the interaction of activated platelets with atherosclerotic arteries[220]. Employing a similar *in vivo* model Massberg *et al* showed that platelet GPIb and GPIIb/IIIa are crucial for platelet translocation and firm adhesion, respectively[221]. Later the VWF was identified as another important molecule for both resting and activated platelet recruitment to atherosclerosis-prone sites of arteries of rabbits with hypercholesterolemia[222]. In addition to these findings Huo and colleagues showed that circulating activated platelets promote monocyte recruitment to atherosclerotic arteries and accelerate atherosclerosis in *Apoe*$^{-/-}$ mice[220,221]. The increase in lesion size was halted when the activated platelets were P-selectin negative[220,221]. During the adhesion process to the endothelium, platelets become activated and release an arsenal of potent inflammatory and mitogenic substances into the local microenvironment, thereby altering chemotactic, adhesive, and proteolytic properties of ECs. The engagement of GP IIb/IIIa receptor during platelet adhesion induces upregulation of P-Selectin and CD40L on platelets, resulting in CD40L-dependent endothelial activation[210,223]

Besides their direct interaction with the endothelium platelets also induce inflammation through their indirect interaction with other cell types of the immune system. The recruitment from, and the interaction with leukocytes requires multistep adhesive and signaling events, including selectin-mediated attachment and rolling, leukocyte activation, integrin-mediated firm adhesion, and diapedesis, which result in the infiltration of inflammatory cells into the blood vessel wall[224]. When adhered to the endothelium, platelets can attract leukocytes by secretion and deposit of chemokines and then provide a surface for their adhesion to the vessel wall[213]. During these interactions platelets, leukocytes, and the endothelium, become activated in a cascade-like manner. Upon activation, platelets release different adhesive and pro-inflammatory substances. The main organelles which are involved in this release are the α-granules, the most important storage compartments within the platelets. The released molecules contain chemokines like Platelet factor 4 (PF4, CXCL4), Regulated on activation, normal T cell expressed and secreted (RANTES, CCL5) or the Macrophage inflammatory protein 1α (MIP1α)[225]. PF4 a member of the C-X-C subfamily of chemokines, is derived by limited proteolysis from platelet basic protein. PF4 causes chemotaxis of monocytes and other leukocytes and enhances the binding of oxLDL to vascular wall cells, including endothelial cells and smooth muscle cells[225]. PF4 when co-localized with oxLDL in atherosclerotic lesions, especially in macrophage-derived foam cells, is able to dramatically increase the oxLDL esterification by macrophages[225]. RANTES and MIP1α are members of the C-C chemokine subfamily. RANTES, first purified as a product of activated T cells, is a powerful chemoattractant for memory T lymphocytes and also monocytes[226]. MIP1α additionally causes chemotaxis of $CD8^+$ T lymphocytes[220]. PF4, RANTES, and MIP1α deposition by platelets mainly promotes atherosclerosis by triggering monocyte arrest on the endothelium of atherosclerotic lesions[202,220,225].

Besides their direct effects, platelets induce inflammation also by indirect interactions with other cell types, especially EC and monocytes. They induce the expression of intercellular adhesion receptors (e.g. E-selectin or VCAM-1), the production of cytokines (IL-6, IL-8) and the production of matrix metalloproteinase (MMP) 9[210,227,228]. Although it is clear that platelets affect all phases of immune responses, further research is required to fully understand how platelets directly and indirectly affect atherosclerosis.

1.8 An introduction to the CD40/CD40L dyad

To generate and mount a successful adaptive immune response, a variety of molecular signals is required. The initial signal is the binding of a cognate antigen to an antigen receptor (TCR or BCR) expressed by T or B cells. However, synergistic signaling by costimulatory molecules is also necessary to sustain and integrate TCR/BCR signaling and to stimulate optimal T or B cell proliferation and differentiation. Multiple secondary signals involve the engagement of costimulatory molecules expressed by T and B cells with their respective ligands. Due to its essential role in immunity, CD40 and its ligand CD40 ligand (CD40L) is one of the best characterized costimulatory molecule pair.

Costimulatory molecules can be broadly divided into two groups based on their respective homologies. On one hand the CD28/B7 family includes CD28 and cytotoxic T lymphocyte antigen 4 (CTLA4) that binds to the ligands CD80 and CD86. On the other, the tumor necrosis factor receptor (TNFR) family, which includes CD40 in addition to the name-giving TNF isoforms and others[229–232]. Costimulatory molecules can be further subdivided based on their functions. For example, molecules containing positive costimulatory function, such as CD40L binding to CD40 can be grouped together while coinhibitory molecules such as CTLA-4 build another group[233].

CD40 was originally detected in immunohistochemical studies using an antibody recognizing a 50 kD protein on bladder cancer cells over three decades ago[234,235]. Those initial studies showed that with the status of B cell activation and proliferation, the expression level of a specific molecule originally named Bp50, varies[234,235]. Later studies showed that this activation of B cells required direct contact with T helper cells rather than soluble lymphokines[236].This led to the hypothesis of the presence of an unknown ligand on T cells[236]. In further studies the identity of this antigen was elucidated by cloning of the murine and human ligand for CD40, termed CD40L or CD154 and cell surface tumor necrosis factor-related activation protein (TRAP), a 39 kD cell surface glycoprotein and member of the tumor necrosis factor (TNF) family, which originally thought to be restricted to activated $CD4^+$ helper T cells[237,238]. The CD40L gene is located at X chromosome and is preferentially expressed by activated $CD4^+$ T cells. Nowadays it is known that CD40L is also expressed by activated B cells and platelets, although it is variably induced on monocytic cells, natural killer cells, mast cells, and basophils under inflammatory conditions[210,239]. CD40 expression can be detected in DCs, B cells, monocytes, epithelial cells, fibroblasts and ECs, as well as in SMC under pro-inflammatory conditions[240–243]. This broad distribution of CD40 and CD40L points to the likely involvement of this receptor/ligand dyad in chronic inflammatory disease.

Initially, the importance of CD40 and CD40L and the crucial role of both, receptor and ligand, in T cell-dependent B cell differentiation and activation could be established. The performed studies provided evidence for the important impact of CD40 and CD40L, by using blocking antibodies which prevented an immune response to T cell-dependent antigens and affected the development of memory B lymphocytes and germinal centers[244–246]. The role of CD40/CD40L interaction in T cell-dependent B cell activation and differentiation nowadays can be best illustrated and understood by analyzing the consequences of certain genetic polymorphisms in the human CD40L gene. Several point mutations in the human CD40 ligand gene, interfering with receptor interactions, were identified as the cause of the X-linked immunodeficiency hyper IgM-syndrome (XHIGM), a disease associated with drastic or complete inhibition in the T cell-dependent humoral immune response[247]. This disease is not exclusively characterized by elevated concentrations of serum IgM and decreased amounts of other immunoglobulin isotypes, but also by a reduced activation and proliferation of B cells[248]. Because CD40L is not only required in the functional maturation of T cells and B cells but also in the activity of DC and macrophages, patients with XHIGM also have a variable defect in T cell, DC, and macrophage effector function[247]. Patients with XHIGM have increased susceptibility to infections with a wide variety of bacteria, viruses, fungi, and parasites[247]. In addition, they have increased risk for developing autoimmune disorders and malignancies[249]. In consequence patients with this syndrome suffer from chronic infections of the upper respiratory tract as well as a number of opportunistic or viral infections[250]. Moreover, Th1-dependent inflammatory reactions are weakened indicating even more important functions of CD40/CD40L interactions in the regulation of the cellular immune response[251]. Apart from the importance of CD40/CD40L interaction for the mounting of an appropriate immune response, more recent studies associated this costimulatory pathway with the exaggerated reaction in various chronic inflammatory and autoimmune diseases, such as asthma, rheumatoid arthritis, psoriasis, type I diabetes and multiple sclerosis, to name a few, but also in atherosclerosis[252].

CD40 does not feature any intrinsic signaling activity and requires the help of adaptor molecules to relay its activation into subsequent signaling pathways. In accordance, the binding of CD40L to CD40 promotes the clustering of CD40 and induces the recruitment of adapter proteins (TNFR-associated factors (TRAFs)) to the cytoplasmic domain of CD40[253]. The TRAF family contains seven members (TRAF1-7) and five of them (TRAF1,2,3,5, and 6) are able to bind to CD40 via three different TRAF bindings domains[254]. The binding site for TRAF1, TRAF2, and TRAF3 are situated at the membrane distal domain of the intracellular tail of CD40 and is most often occupied by TRAF2 and TRAF3[255]. Recently a second alterative binding site for TRAF2 was identified[256]. TRAF6 is recruited to the membrane proximal domain of CD40 which

exclusively binds to TRAF6[257]. Until now there is no consensus whether TRAF5 binds directly or indirectly to CD40[257,258]. After the binding to its domains the TRAF proteins activate different signaling pathways including the canonical and non-canonical nuclear factor κB (NFκB)-signaling pathways, the mitogen-activated protein kinases (MAPKs), phosphoinositide 3-kinase (PI3K), as well as the phospholipase Cγ (PLCγ) pathway[259]. Accordingly, the activated signaling cascade depends on the TRAF family member expressed on the activated cell type and the surrounding conditions. In conclusion, CD40 primarily mediates signaling through TRAF proteins, which can activate or inhibit different signaling pathways dependent upon the cell type. TRAF proteins drive a wide range of cellular and immune processes and the complex pathways elicit the essential signals mediated by CD40 to support its diverse cellular processes.

1.9 CD40/CD40L signaling in cell-mediated immunity

Over time it has become evident that CD40 and CD40L are expressed on the majority of cell types involved in perpetuating and regulating proper immune responses in the body. To gain a better understanding of the importance of the CD40/CD40L dyad and to unravel its role in the different aspects of the immune system, it is necessary to understand CD40/CD40L signaling on the distinct cell types which play a role especially in the adaptive part of the immune response. APCs and particularly DCs, represent the central cell type of the immune system since they immediately sense pathogens and provide the first link to the adaptive immune response by activating T cells[5,260]. Their proper function relies crucially on the costimulatory signaling of CD40 and CD40L. As already mentioned, the successful T cell priming depends on three individual signals, cognate TCR interaction, costimulation and instructing cytokines. Immature DCs have a low expression of costimulatory molecules on their surface and consequently have poor T cell priming capacity. However, upon specific antigen activation, DCs switch from an antigen capturing cell phenotype to that of a professional APC. The switch is accompanied by the upregulation of MHCII and costimulatory molecules expression. CD40 signaling has been shown to be an important step in this transition[261]. Notably, functional interactions between CD40 and CD40L are bidirectional. The interaction of CD40 on DCs with CD40L expressed on T cells leads to an activation of the DC enabling them to prime T cells and produce cytokines[261]. The interaction of CD40 with CD40L or, experimentally, an anti-CD40 antibody induces the upregulation of costimulatory molecules, adhesion molecules, and the Th1-polarizing cytokine IL-12 in both mouse and human DCs[262–264]. However, CD40-dependent maturation of DCs is far more complex than the simple upregulation of costimulatory molecules and cytokine production. The first *Cd40*$^{-/-}$ mice were generated by two different groups, one with the CD40 defect of all

hematopoietic cells and the other, with the defect restricted to lymphocytes and both groups showed that both types of CD40 deficient mice were impaired in the generation of a T cell dependent antibody responses[265,266]. With the help of these newly generated CD40 deficient mice, Mackey and others could show that CD40 signaling on DCs is important for the expression and increased stability of the MHC/alloantigen complex in the context of cardiac allograft rejection[31,267]. Indeed, the alloantigen-presenting, non-matured DCs induce abortive activation and anergy of the host alloreactive T cell pool[31,267]. Their increased life span after CD40L ligation is considered to be another major factor in the success of CD40-triggered DCs in driving cell-mediated immunity. CD40-mediated survival is based on the upregulation of the anti-apoptotic factor B cell lymphoma extra-large (Bcl-XL) and is NFκB dependent[268,269].

Later, Wykes and MacPherson showed that the expression of CD40 on DCs and B cells is required for optimal proliferation of B cells in absence of any exogenous stimuli. CD40 deficient mice displayed a decreased number of proliferating B cells and a reduced survival of B cells[26]. While the mechanism of this interaction has not been established, they suggested that CD40 expressed on DCs plays a direct role in regulating B cell proliferation and potentially more important in regulation of B cell homeostasis[270]. In addition, Litinskiy *et al.* could prove that DCs activated by CD40L induces the expression of the TNF family member cytokines B lymphocyte stimulator protein (BLyS, also known as B cell activating factor (BAFF)) and proliferation-inducing ligand (APRIL)[271]. BAFF and APRIL promoted B cell survival, class switch recombination and secretion of IgG and IgA antibodies[272]. The addition of antibodies to neutralize DC-derived BAFF or APRIL abrogated antibody production and class switching, but was not observed after the addition of a CD40 neutralizing antibody. Accordingly, the authors concluded that B cell antibody responses are regulated by cytokines produced during CD40 signaling on DCs, and not by DC-induced CD40 signaling on B cells[272]. Through its expression on B cells (CD40) as well as on T cells (CD40L) CD40-CD40L interactions play a crucial role in humoral adaptive immune responses[273,274]. Activated T helper cells express CD40L which binds to the constitutively expressed CD40 on the B cell surface. Together with cytokines produced by the T helper cell, this leads to the proliferation of B cells and finally to their differentiation into plasma cells[273,274].The signal provided by the CD40-CD40L interactions also induces the Ig Isotype switch (IgM to IgG, IgE and IgA)[236,274]. In the absence of signals from T helper cells B cells will only produce IgM. An example for the consequence of the missing T helper cell signal constitutes the XHIGM syndrome which is characterized by low or absent levels of IgG, IgE and IgA in serum, but normal or elevated serum levels of IgM[247,248]. The constitutive expression of CD40 was first ascribed to B cells, and then extended to most APC (DC and macrophages); this property helped to decipher the APC function of activated/memory B cells and their use

alongside MHC molecules[275]. In their role as APC, B cells and DCs are tightly connected to T cells because they provide the antigen-specific (via TCR) and the antigen-unspecific signals (costimulatory molecules) which are essential for proper T cell activation. The ligation of T cell CD40L to CD40 on APCs leads to the upregulation of costimulatory activity (e.g. E-selectin, MHCII, CD40) and the production of pro-inflammatory cytokines like IL-1, IL-6, IL-12, and TNFα[251]. In lymphoid tissues, naïve T cells will be activated by APCs that present antigens leading to the differentiation and proliferation of the naïve T cell into an inflammatory T helper cell phenotype. Smook *et al* showed that CD40 signaling is crucial for the induction of Tregs by interacting with APCs[276,277]. They reported that the amount of Tregs was markedly reduced in *Cd40*$^{-/-}$ mice since APCs lacking CD40 failed to induced Tregs and resulted in T cell autoreactivity[277]. An additional impact on T cell immunity can be achieved by the inhibition of CD40L. The blockade of CD40L leads to passive apoptosis of T cells induced by the absence of growth and survival factors, such as IL-2, IL-7, and IL-15[278–280].

In addition to the CD40L expression on T cells, CD40L can also be released from the cell surface as a soluble form (sCD40L)[180]. Today, the biological effect of T cell-derived sCD40L is still not known and only limited information regarding the mechanisms that controls the production of sCD40L is available. Currently, platelets are thought to be the main source of sCD40L producing nearly 95% of the plasma sCD40L pool and the role of circulating sCD40L in atherothrombosis is widely accepted[281]. Without any direct cell-cell interaction, sCD40L, retains its biological activity and acts as a cytokine. Of note, sCD40L concentrations are used as a reliable biomarker to detect inflammation and to predict the risk for several cardiovascular diseases[281–283]. Interestingly, T cells can also express CD40. The mechanisms behind T cell CD40 function, however, have not been clearly defined yet[282]. Burgeois *et al* demonstrated that in addition to bearing CD40L, both activated $CD4^+$ and $CD8^+$ cells express CD40. CD40-deficient $CD8^+$ T cells are unable to differentiate into memory cells and do not react to signals from $CD4^+$ T helper cells[284]. The authors suggested that $CD8^+$ T cells receive $CD4^+$ T cell help directly through CD40 and that this interaction is fundamental for the generation of CD8+ memory T cells[284].

In addition to the cells which are considered to be an important part of the adaptive immunity, activated cellular participants of the innate immune system are also known to express CD40. Monocytes and macrophages are central cells of the innate part of the immune system, responsible for defending against diverse pathogens. Although monocytes represent an important part of the host defense, accumulation of monocytes can be harmful and aggravate diseases such as atherosclerosis, arthritis, and multiple sclerosis[285]. Monocytes stimulated by ECs up-regulate CD40 expression in the presence of T cells. When T cells were separated from

monocyte-EC interaction, these monocytes did not show CD40 up-regulation[286]. The interaction between T cells and monocytes is bidirectional and activated monocytes are capable of activating other T cells. The binding of CD40L on monocytes induces IL-12 secretion, which elicits CD40L expression on T cells and the production of the pro-inflammatory cytokine IL-1β[287]. Signaling via CD40 in monocytes/macrophages results in nitric oxide generation, rescue from apoptosis and induction of MMP production[262,288,289]. The importance of CD40-dependent macrophage activation in host defense is supported by the finding that *Cd40l*$^{-/-}$ mice have defective macrophage effector function[290].

Besides the main players of cellular immunity, platelets are also well-equipped to facilitate leukocyte recruitment to sites of vascular injury and inflammation [192]. Henn *et al* were first to prove that platelets interaction with leukocytes is also regulated strongly via the CD40-CD40L axis[210]. CD40L is rapidly presented to the platelet surface after platelet stimulation. The surface-expressed CD40 ligand is then cleaved from the platelet over a period of minutes to hours subsequently generating sCD40L[226]. When expressed on the surface of platelets and exposed to CD40-bearing vascular cells, platelet-associated CD40L is capable of initiating various inflammatory responses, including expression of inflammatory adhesion receptors (e.g. E-selectin, VCAM-1), expression of tissue factor, and release of chemokines (e.g. MCP1 and IL-8) and the production of matrix metalloproteinase (MMP) 9 [227,228,291]. As mentioned before, platelets contribute to more than 95% of the circulating sCD40L. Aside from CD40L and sCD40L, platelets can also express the receptor CD40. The role of this receptor on platelets is still under debate but it was shown that sCD40L is able to activate platelets in an autocrine manner and cause them to upregulate P-selectin expression and induce release of the chemoattractant β-thromboglobulin and serotonin. Whereas the membrane-bound form from T cells triggers the release of biologically active RANTES stored in the platelets granules. The released RANTES activates ECs and mediates further T cell recruitement[292]. Platelets are known to interact with neutrophils and ECs[293]. CD40 was reported to be expressed on neutrophils and Vanichakaran *et al* demonstrated that the release of sCD40L from activated platelets stimulates neutrophils to release reactive oxygen species (ROS) which can subsequently stimulate more platelets[293]. In another study by Li *et al*, incubation with activated platelets led to enhanced MAC-1 expression on neutrophils, an effect diminished by addition of anti CD40L or anti P selectin antibodies[294]. In the same study they were able to show, that sCD40L promoted platelet-leukocyte activation and recruitment[294]. These findings suggest a mechanism in the recruitment of leukocytes and the formation of platelet-leukocyte aggregates through CD40-CD40L signaling.

ECs also actively participate in both innate and adaptive immune responses. ECs are one of the first cell types to detect foreign pathogens and endogenous metabolite-related danger signals in

the bloodstream, in which ECs function as sensors for danger signals. Treatment with lipopolysaccharide (LPS) activates ECs, causing the production of pro-inflammatory cytokines and chemokines, which amplify the immune response by recruiting immune cells. Thus, ECs function as immune effectors and immune cell mobilizers. They induce cytokine production by immune cells that consecutively lead to an activation or suppression of the immune cell functions. Under certain conditions, ECs express CD40 as well as CD40L and serve as APCs by expressing MHC I and II molecules and presenting antigens to T cells. The function of the endothelium is influenced by multiple factors as a consequence of cell-cell interactions. The expression of adhesion molecules on vascular ECs determines the pattern of migration and extravasation of leucocytes in inflammation and immunity. The cell-cell communication between ECs and platelets has only recently received attention in systematic studies. In 2000 Kotowicz *et al* showed that costimulation with CD40L and IL-4 or IL-13 gives rise to a unique pattern of adhesion molecule expression by human umbilical vein ECs (HUVEC). CD40 ligation alone enhanced expression of VCAM-1, ICAM-1 and E-selectin whereas IL-4 and IL-13 increased expression of VCAM-1 and P-selectin. Just recently Gerdes *et al* extended the knowledge about platelet CD40-dependent EC interaction. The group demonstrated that *Cd40*$^{-/-}$ platelets showed less abundant adhesion to the endothelium *in vivo*[295]. Moreover, *ex vivo* stimulation of EC with either activated *Apoe*$^{-/-}$ or *Cd40*$^{-/-}$*Apoe*$^{-/-}$ platelets revealed that also other adhesion molecules, such as VCAM-1, platelet EC adhesion molecule (PECAM), VE-cadherin, and P-selectin, were significantly decreased in the absence of platelet CD40[295]. These results implicate CD40/CD40L interactions between platelets and give rise to specific patterns of adhesion molecule expression and cytokine production that may have important implications for lymphocyte migration and function at sites of inflammation[296].

In summary studies in both mouse and man showed, that by virtue of the interaction of CD40 and CD40L positive immune cells, the CD40L/CD40 pathway is critical to a variety of cell-mediated immune responses and in the induction of inflammation.

1.10 The role of CD40/CD40L costimulation in atherosclerosis

The CD40/CD40L dyad is one of the best- described costimulatory pair in the pathogenesis of atherosclerosis. The expression of both CD40 and CD40L was found on the vast majority of immune cells and non-immune cells present in the atherosclerotic lesion as well as on monocytes and circulating platelets[252,297,298]. In other words, nearly all atherosclerosis-related cell types are known to express at least one part of the receptor ligand dyad[252,297,298]. CD40 and CD40L are already expressed in early stages of atherosclerosis and are highest in late stage atherosclerotic lesions which are prone to rupture[299]. In general, stimulation of all CD40-expressing cell types induces cell functions that contribute to inflammation, such as activation of chemokine and cytokine synthesis, enhancement of costimulatory and adhesion molecules, as well as up-regulation of proteolytic enzymes[300].

In 1997 Mach *et al* were the first to describe CD40L expression by human vascular ECs, SMC, and macrophages *in vitro*, and the co-expression with its receptor CD40 on all three cells types in human atherosclerotic lesions[301]. Shortly after the first description of CD40 and CD40L expression in atherosclerotic plaques Mach *et al* were also able to prove the functional relevance of CD40L in atherosclerosis[302]. They showed that the treatment of hyperlipidemic *Ldlr*$^{-/-}$ mice with an anti-CD40L antibody significantly reduces the size and lipid content of aortic atherosclerotic lesions[302]. The atheroma of mice treated with the anti-CD40L antibody contained fewer macrophages and T lymphocytes and exhibited decreased expression of vascular cell adhesion[302]. One year later Lutgens and colleagues revealed that CD40–CD40L signaling is important in late atherosclerotic changes, such as lipid core formation and plaque destabilization[303]. *Apoe*$^{-/-}$*Cd40l*$^{-/-}$ mice exhibited a nearly 6-fold decrease in plaque area and displayed a remarkable change in plaque phenotype[303]. Advanced atherosclerotic lesions of *Apoe*$^{-/-}$ *Cd40l*$^{-/-}$ contained increased amounts of collagen and SMC, while plaque lipid levels and the number of inflammatory cells were strongly reduced[303]. In a follow up study Lutgens *et al* used an anti-CD40L antibody (MR-1) to block CD40 signaling in *Apoe*$^{-/-}$ mice either during the onset of disease or when advanced atherosclerotic lesions had formed[304]. In addition to limiting lesion progression, the anti-CD40L treatment changed the composition of atheroma in manners thought to favor plaque stability by reducing relative content of macrophages and lipid, as well as increasing relative content of SMC and collagen[304]. Both early and delayed treatment with an anti-CD40L antibody did not affect atherosclerotic lesion initiation but did result in the development of a lipid-poor collagen-rich stable plaque phenotype[304].Corroborating these results, Schönbeck *et al* showed similar effects while using a different anti-CD40L antibody (M158) in *Ldlr*$^{-/-}$ mice which consumed a hypercholesterolemic diet[305].

In contrast to the findings regarding CD40L, the results for CD40 were contradictory. Zirlik *et al* reported that *Ldlr*$^{-/-}$ *Cd40*$^{-/-}$ mice do not exhibit any changes in atherosclerosis and reported the discovery of Mac-1 as a novel alternative receptor for CD40L[306]. However, *Cd40*$^{-/-}$ Apoe$^{-/-}$ mice displayed decreased atherosclerosis with lesions only containing a few inflammatory cells[306]. This also holds true when transferring bone marrow of *Apoe*$^{-/-}$*Cd40*$^{-/-}$ into irradiated *Ldlr*$^{-/-}$ mice[298].

The previous investigations towards the role of CD40 and CD40L in atherosclerosis all agree in the fact that they focus on the consequences of a complete inhibition of CD40- CD40L signaling on all cell types in the different mouse models. Lievens *et al* were the first to study the CD40-CD40L signaling in a more cell type-specific way, by injecting CD40L-deficient activated platelets into *Apoe*$^{-/-}$ mice[125]. The repeated injections of activated *Cd40l*$^{-/-}$ platelets into *Apoe*$^{-/-}$ mice strongly decreased both platelet and leukocyte adhesion to the endothelium and decreased plasma levels of the important pro-inflammatory chemokine CCL2 compared with platelets from wild type mice. Moreover, *Cd40l*$^{-/-}$ platelets failed to form pro-inflammatory platelet-leukocyte aggregates[125]. In addition they revealed the importance of CD40L expression on platelets for platelet-induced atherosclerosis as injection of *Cd40l*$^{-/-}$ platelets in contrast to *Cd40l*$^{+/+}$ platelets did not promote lesion formation[125]. This was the first study to show that CD40L plays a pivotal role in atherosclerosis, not only by affecting platelet-platelet interactions but especially by activating leukocytes, thereby increasing platelet-leukocyte and leukocyte-endothelium interactions. In 2016 Gerdes *et al* confirmed the supposed role of CD40 and CD40L in the interaction of platelets, leukocytes and the endothelium[295]. The group showed that activated platelets isolated from *Apoe*$^{-/-}$*Cd40*$^{-/-}$ mice adhered less to the endothelium upon injection into *Apoe*$^{-/-}$ mice when compared with CD40-sufficient platelets[295]. Furthermore, the lack of CD40 on injected platelets led to reduced leukocyte recruitment to the carotid artery[295]. When compared to mice that received *Apoe*$^{-/-}$ platelets, those injected with *Apoe*$^{-/-}$*Cd40*$^{-/-}$ platelets exhibited a more than 2-fold reduction in atherosclerosis. The plaques of mice receiving CD40-deficient platelets were less advanced, contained less macrophages, neutrophils, and collagen, and displayed smaller lipid cores[295].

In addition to the investigations towards the role of CD40 and CD40L in atherosclerosis Lutgens *et al* did the first steps in unravelling the signaling mechanisms of CD40 and CD40L in atherosclerosis. To obtain insights about CD40-TRAF interactions and which of them are required in atherosclerosis, they used mice with targeted mutations at the CD40-TRAF2/3/5, CD40-TRAF6 and CD40-TRAF2/3/5/6 recognition sites. The mice with defective CD40-TRAF6 signaling displayed a strong decrease in atherosclerotic plaque size. The data unveil a role for CD40–TRAF6, but not CD40–TRAF2/3/5, interactions in atherosclerosis[298].

1.11 Hypothesis and outline of the thesis

Many genes and processes are implicated in the pathogenesis of atherosclerosis. In addition, interaction between cells and their gene products is manifold and varies greatly during lesion maturation. Considering this and the limited knowledge regarding the cell type-specific CD40 and CD40L interactions in athero-progression, the present studies aim to specify the cell type-specific influence of costimulation via CD40/CD40L on atherosclerosis at early and late time points of atherogenesis. The research presented here will provide novel insights in the complex field of adaptive immunity and in the particular effects exerted by CD40 and CD40L in atherogenesis. As the CD40/CD40L dyad plays an imminent role in the interaction of T cells, B cells and DCs, it is important to understand the different pathways elicited by CD40 and CD40L to modulate and improve potential therapies. Cell type-specific gene modification is a useful technique for determining the role of a gene product in certain cell types, or when global modification is lethal. The cre/loxP system can be used to delete or activate a gene of choice in a cell type-specific manner. Accordingly, we use the system to create different, athero-prone *Apoe*$^{-/-}$ *Cd40*$^{fl/fl}$cre^{+} and *Apoe*$^{-/-}$ *Cd40l*$^{fl/fl}$cre^{+} mice with conditional CD40 or CD40L deficiencies on T cells, dendritic cells and platelets, to investigate the cell type-specific impact of these costimulatory molecules on the generation of atherosclerosis. In addition to atherosclerosis-specific parameters such as plaque size and plaque phenotype, other organs and tissues will be analyzed to examine whether and how the different cell subsets of the adaptive and innate immune system are influenced by a deficiency of either CD40 or CD40L. Furthermore, *in vitro*-based assays will be performed to elucidate the function of immune cells isolated and generated from different *Apoe*$^{-/-}$*Cd40*$^{fl/fl}$Cre^{+} and *Apoe*$^{-/-}$*Cd40l*$^{fl/fl}$Cre^{+} mice lines and their potential contribution to atherosclerosis.

2 MATERIALS AND METHODS

2.1 General equipment

Table 1: General equipment used for this thesis

Equipment	Modell	Source
Autoclave	VX150	Systex, Linden, Germany
Balance	BP2100S R160P	Sartorius, Goettingen, Germany
Centrifuges	5415R 5810	Eppendorf, Hamburg, Germany
	Multifuge 3S-R Heraeus Multifuge 40R Heraeus	Thermo Scientific, Waltham, MA, USA
Cryotome	CM3050S	Leica, Wetzlar, Germany
Flow cytometer	FACS Canto II FACS Aria III	BD Biosciences, San Jose, CA, USA
Heating block	SBH130DC	Stuart, Staffordshire, UK
Incubator	Binder CB150	Binder, Tuttlingen, Germany
Laminar Flow Hood	Herasafe (Heraeus)	Thermo Scientific
Luminex xMAP instrument	MAGPIX	Luminex, Austin, TX, USA
Microplate reader	Tecan GENios	Tecan Group, Maennedorf, Switzerland
Microscopes	DMLB DM6000 SP8 3X	Leica
Microtome	RM2155	Leica
pH-meter	HI2211 pH/ORP meter	Hanna Instruments, Voehringen, Germany
Plate shaker	Titramax 101	Heidolph, Schwabach, Germany
qPCR system	7900 HT Fast Real-Time PCR System ViiA 7 Real-Time PCR System	Thermo Scientific
Spectrometer	ND1000 Nanodrop Peqlab	VWR, Radnor, PA, USA
Thermal cyclers	MyCyclerT100	Bio-Rad, Hercules, CA, USA
Tube Rotator	MACS Mix Tube Rotator	Miltenyi, Bergisch-Gladbach, Germany
Water purification system	Milli Q Direct Q 16	Merck Millipore, Billerica, MA, USA

2.2 Mice

2.2.1 Generation of *Apoe*$^{-/-}$ *Cd40*$^{flox/flox}$ and *Apoe*$^{-/-}$ *Cd40l*$^{flox/flox}$ mouse lines

Cd40$^{flox/flox}$ mice and *Cd40l*$^{flox/flox}$ mice were crossed with *Apoe*$^{-/-}$ mice (stock No. 002052, The Jackson Laboratory, Bar Harbor, Maine, USA) mice to generate *Cd40*$^{flox/flox}$ *Apoe*$^{-/-}$ mice or *Cd40l*$^{flox/flox}$ *Apoe*$^{-/-}$ mice, respectively. *Cd40*$^{flox/flox}$ mice were custom-designed and generated by Ozgene Pty Ltd (Bentley, Australia). A conditional allele was created by inserting loxP sites upstream of exon 2 and downstream of exon 3. Cre-mediated deletion of the two "floxed" exons induces a frameshift mutation (from translational reading frame 0 to 1). The resulting knockout (KO) is similar, in principle, to two previously published non-conditional alleles in which neomycin (neo) selection cassettes were used to disrupt exon 3[265,307]. *Cd40l*$^{flox/flox}$ mice were generated similarly by custom-design at Ozgene. For this purpose two loxP sites upstream and downstream of exon 3 were introduced. Cre-mediated deletion of exon 3 cause a translational frameshift (from phase 0 to 1), rendering the downstream exons non-function.

2.2.2 Generation of *Apoe*$^{-/-}$ *Cd40*$^{fl/fl}$ *Cre* and *Apoe*$^{-/-}$ *Cd40l*$^{fl/fl}$ *Cre* mouse lines

We then introduced several cell-specific CD40 and CD40L deficient mouse lines by crossbreeding *Cd40*$^{flox/flox}$ *Apoe*$^{-/-}$ *Cre* and *Cd40l*$^{flox/flox}$ *Apoe*$^{-/-}$ *Cre* mice with different transgenic mice in which Cre- recombinase was expressed under the control of cell type-specific enhancers, promoters or silencer.

Table 2: Description of cre-recombinase positive mice used in this thesis

Cell type	Promotor	Method
T cells	CD4	The cre-recombinase is expressed under the control of the CD4 enhancer/promoter/silencer, which becomes active at sequential stages of T cell development[308].
Dendritic Cells	CD11c	The recombination cassette containing the cre-recombinase open reading frame, followed by the bovine growth hormone (BGH) polyA signal and the FRT site-flanked prokaryotic Zeocin resistance cassette (ZeoR), replace the coding part of the first CD11c exon, and the ZeoR cassette was subsequently removed by FLP-mediated recombination[309].
Platelets	Pf4	A codon-improved cDNA for re-recombinase, inserted by homologous recombination into bacterial artificial chromosome (BAC) DNA containing the mouse Pf4 promotor[310].

Heterozygous mice then were intercrossed and *Apoe*$^{-/-}$ *Cd40*$^{flox/flox}$ and *Apoe*$^{-/-}$*Cd40l*$^{flox/flox}$ littermates, respectively, were used to cross with different cre^{+}-Mice. Housing and breeding of mice followed institutional guidelines. All animal experiments were approved by the local ethical committee for animal experimentation.

2.3.1 Genotyping

Newly weaned mice were marked by individual ear notches and holes produced by an ear punch device. A tail biopsy of 1-2 mm length was taken for genotypic analysis of mice. The tail biopsy was incubated overnight at 56°C in 250 µl tissue lysis buffer (see 2.8) supplemented 1:100 with proteinase k solution (Qiagen, Hilden, Germany). Subsequently, automatic DNA isolation was performed with the QIAxtractor (Qiagen) according the manufacturer's instructions. The isolated DNA was kept at 4°C and applied for polymerase chain reaction (PCR).

The following PCR mastermixes were prepared for CD40, CD40L and ApoE genotyping reactions:

	Stock concentration	Volume in µl
Dnase-/Rnase-free H_2O	-	12.75
GoTaq Flexi buffer	5x	5
$MgCl_2$	25 mM	2
dNTP mix	10 mM each	0.5
forward Primer	10 µM	1.25
reverse Primer	10 µM	1.25
GoTaq DNA Polymerase	5 U/µl	0.25
Genomic DNA	100 ng/µl	2

GoTaq Flexi DNA polymerase and GoTaq Flexi buffer were obtained from Promega (Promega, Fitchburg, WI, USA). Dnase-/Rnase-free H_2O, primer, magnesium chloride ($MgCl_2$), and the deoxynucleotide triphosphate (dNTP, containing deoxyadenosine/-guanosine/-cytidine/-thymidine triphosphate) mix were obtained from Sigma (Sigma Aldrich, St. Louis, USA). Two mastermixes each were prepared for CD40 and CD40L genotyping containing either wildtype or mutant allele detecting primer and an additional primer to detect the transposon of the delivering vector. The reaction has to be run in to separate mixes as the mutant fragment does not amplify in heterozygous samples. The PCR program for CD40 DNA detection was composed of an initial step at 94°C for 2 min followed by 35 cycles of each 30 sec at 94°C, 30 sec at 60°C, and 1 min at 72°C. Subsequently, the samples were incubated at 72°C for 5 min and 21°C for 5 min.

Primer sequences for CD40 genotyping:

CD40 12398 5' GTG AGA TGC TAG CCC TCC TG 3'
CD40 12399 5'CAC GTC ATC TGC TGG TTT TC 3'
CD40 12400 5' CGT GCA ATC CAT CTT GTT CA3'

The amplified PCR products were each electrophoretically separated applying the QIAexcel Advanced System (Qiagen) according to the manufacturer's instructions. Expected results are a wildtype product at 594 base pair (bp) length and a mutant product at 685 bp length. DNA samples from heterozygous mice would yield a product at 594 bp and 685 bp length. Also for CD40L and Apoe genotyping two mastermixes were prepared with the common CD40L or Apoe forward primer and either the wildtype reverse primer or the mutant reverse primer. The PCR program was composed of an initial step at 94°C for 5 min followed by 35 cycles of each 30 sec at 94°C, 30 sec at 60°C, and 1 min at 72°C. Subsequently, the samples were incubated at 72°C for 5 min and 21°C for 5 min.

Primer sequences for CD40L genotyping:

CD40L mutant forward	5' GCC CTG AAT GAA CTG CAG GAC G3'
CD40L mutant reverse	5' GGG TAG CCA ACG CTA TGT C3'
CD40L wildtype forward	5' GTT CCT CCA CCT AGT CAT TCA TC3'
CD40L wildtype reverse	5'CCC AAG TGT ATG AGC ATG TGT GT

Expected results for CD40L are a wildtype product at 250 bp length and a mutant product at 500 bp length. DNA samples from heterozygous mice would yield a product at 250 bp and 500 bp length.

Primer sequences Apoe genotyping:

Apoe common forward	5' GCC TAG CCG AGG GAG AGC CG 3'
Apoe wildtype reverse	5' TGT GAC TTG GGA GCT CTG CAG C 3'
Apoe mutant reverse	5' GCC GCC CCG ACT GCA TCT 3'

Expected results for Apoe are a wildtype product at 150 bp length and a mutant product at 245 bp length. DNA samples from heterozygous mice would yield a product at 150 bp and 245 bp length.

Primer sequences for Cre genotyping

Pf4 cre forward	5' CCC ATA CAG CAC ACC TTT TG 3'
Pf4 cre reverse	5' TGC ACA GTC AGC AGG TT 3'

Expected results for Pf4 cre are no product for wildtype mice and a product at 450 bp length for Pf4 cre-positive animals.

CD4 cre forward	5' CGA TGC AAC GAG TGA TGA GG 3'
CD4 cre reverse	5' GCA TTG CTG TCA CTT GGT CGT 3'

Expected results for CD4 cre are no product for wildtype mice and a product at 250 bp length for CD4 cre-positive animals.

CD11c internal control forward	5' GAT GTG CTC CAG GCT AAA GTT 3'
CD11c internal control reverse	5' AGA AAC GGA ATG TTG TGG AGT 3'
CD11c cre forward	5' TAT CTT CTA TAT CTT CAG GCG C 3'
Cd11c cre reverse	5' GTG AAC GAA CCT GGT CGA AAT CAG 3'

Expected results for CD4 cre are no product for wildtype mice and a product at 200 bp length for CD4 cre-positive animals. DNA samples from mice would yield a 500 bp length product for a successful PCR and no product for a failure of the PCR protocol.

2.3.2 Surgical procedure

Mice were administered a normal chow diet for 28 weeks or a high fat diet for 6 weeks, mice were euthanized i.p. with Ketamine/Xylazine and blood was obtained via cardiac puncture. Spleen, abdominal aorta, liver, aortic root, and lymph nodes were harvested after perfusion of the arterial tree with sodium nitroferricyanide(III) dehydrate (Sigma Aldrich) followed by 1% paraformaldehyde (PFA) in phosphate-buffered saline (PBS) perfusion (Sigma Aldrich). Parts of the tissue were stored in RNAlater (Life Technologies, Carlsbad, USA) for 24 h at room temperature and afterwards at -80°C. Hearts were isolated and frozen in Tissue-tek (Sakura Finetek, Torrance, USA). The aortic arch and its main branch points were excised, fixed overnight in 1% PFA in PBS, and embedded in paraffin.

2.3.2.1 Contact Hypersensitivity

Mice were shaved and the skin of their abdomens using a small animal clipper. Then the mice were sensitized by the epicutaneous application of 20 µl 0.5% 2,4-dinitro-1-fluorobenzene (DNFB, Sigma-Aldrich) in 4:1 aceton-olive oil (AO, Sigma-Aldrich), onto the shaved abdomen. After 5 days the baseline ear thickness is measured prior to initiation of the efferent phase with a Dial Thickness Gage (Mitutoyo). Finally, the ear is treated epicutaneously with 10 µl of 0,2% DNFB (in 4:1 AO on each side of the right ear). Ear thickness of the treated (right) and the untreated (left) ear is measured 24 hours after treatment. The change in ear thickness was measured by calculating the difference between treated ear and untreated ear. Mice were anaesthetized and blood was obtained via cardiac puncture. Spleen and lymph nodes were

harvested. Parts of the tissue were stored in RNAlater (Life Technologies) for 24 h at room temperature and afterwards at -80°C. Ears were excised, fixed overnight in 1%PFA in PBS, and embedded in paraffin.

2.4 Protein assays

2.4.1 Flow cytometry

Aortae were digested with an enzymatic cocktail (Collagenase I, 450 U/ml; collagenase XI, 250 U/ml; hyaluronidase, 120 U/ml; deoxyribonuclease (DNase) I, 120 U/ml; all Sigma Aldrich) in PBS containing 20 mM 4-(2-hydroxyethyl)-1-piperazineethanesulfonic acid (HEPES) (Thermo Scientific) for 30 min at 37°C as previously described.[209] Single cell suspensions of the aortic lysates were prepared by filtering the aortic tissue through a 50 µm cell strainer (BD Biosciences). Aortic lysates were washed with 1x PBS and resuspended in 100 µl 1x PBS/staining mix (maximum 2 staining panels were applied due to low abundance of leukocytes). Cell suspensions were prepared from harvested spleens and lymph nodes by tearing the tissues apart. Single cell suspensions were prepared by meshing the tissue through a 70 µm cell strainer (BD Biosciences). Splenic cells were erylysed (6 ml for a whole spleen) for 3 min on ice, washed and filtered through a 70 µm cell strainer. Freshly-drawn blood was incubated with red blood cell lysis buffer (5 ml for 1 ml blood) for 10 min at room temperature and subsequently washed. If the pellet was still containing too many red blood cells, another lysis step was performed (3 ml, 3 min, wash). Wash steps were performed with 1x PBS. Pellets from lymph nodes were resuspended in 1 ml PBS and pellets from whole spleens in 6 ml PBS. Blood leukocytes were resuspended in 100 µl/staining mix. Subsequently, 100 µl of cell suspension were stained with a viability dye (Live/Dead fixable Aqua/Violet/Near-Infrared; Life Technologies) to discriminate between living and dead cells according the manufacturer's instruction concomitantly with Fc-Block (anti-CD16/32-antibody, functional grade, clone:93, 1:100, eBioscience, San Diego, CA, USA). 1x PBS was used for Live/Dead staining as protein components of buffers, such as bovine serum albumin (BSA), could reduce staining efficacy thus producing false negative results. Single cell suspensions were incubated (20 min, dark, room temperature) and washed with FACS buffer to remove remnant Live/Dead dye. Subsequently, cells were incubated for 20 min on ice with 50 µl of antibody mixes with antibodies from BD Biosciences, eBioscience, Biolegend (San Diego, CA, USA), or Novus Biologicals (Littleton, CO, USA) (Table 3). An additional washing step was performed after antibody-staining with FACS buffer to remove unbound antibodies. In case intracellular stainings were performed the Foxp3/Transcription Factor Staining Buffer Set was used according the manufacturer's

instructions (eBioscience). To determine the level of apoptosis, stainings were performed for fluorochrome-conjugated Annexin V (Biolegend) and simultaneous exclusion of dead cells determined by Live/Dead staining (Life Technologies) according the manufacturer's protocol. Apoptosis stainings were analyzed immediately. Other stainings were fixed with 1% PFA in FACS buffer and analyzed within the following days. Single cell suspensions were analyzed using a FACS Canto II (BD Biosciences) and data were analyzed using Flowjo v.10 (Flowjo, LLC, Ashland, USA).

Table 3: Antibodies used for flow cytometry

Antigen	Source and reactivity	Clone	Dilution	Source
CD45 APCe780	Rat-anti-mouse (IgG2b, κ)	30-F11	1:400	eBioscience
CD4 V500	Rat-anti-mouse (IgG2a, κ)	RM4-5	1:200	BD Biosciences
CD8a e450	Rat-anti-mouse (IgG2a, κ)	53-6.7	1:200	eBioscience
Foxp3 PE	Rat-anti-mouse/rat/pig/canine/bovine (IgG2b, κ)	FJK-16s	1:40	eBioscience
CD3 FITC	Armenian Hamster-anti-mouse (IgG)	45-2C11	1:200	eBioscience
CD25 APC	Rat-anti-mouse (IgG1, λ)	PC61.5	1:300	eBioscience
CD44 APC	Rat-anti-mouse/human (IgG2b, κ)	IM7	1:1000	eBioscience
CD25 APC	Rat-anti-mouse (IgG2b, κ)	RM134L	1:100	Biolegend
CD40 PE	Rat-anti-mouse (IgG2a, κ)	1C10	1:100	eBioscience
CD70 PE	Rat-anti-mouse (IgG2b, κ)	FR70	1:100	eBioscience
CD154 PE-Cy7	Armenian Hamster-anti-mouse (IgG)	MR1	1:100	Biolegend
CD62L PE-Cy7	Rat-anti-mouse (IgG2a, κ)	MEL-14	1:800	eBioscience
CD11b PerCp-Cy5.5	Rat-anti-mouse (IgG2b, κ)	M1/70	1:300	eBioscience
MHC II	Rat-anti-mouse (IgG2b, κ)	M5/114.15.2	1:500	Biolegend
CD11c PE-Cy7	Armenian Hamster-anti-mouse (IgG)	N418	1:1000	eBioscience
CD21/CD35	Rat-anti-mouse (IgG2a, λ)	eBio8D9	1:100	eBioscience
IgD FITC	Rat-anti-mouse (IgG2a, κ)	1-26c(11-26)	1:100	eBioscience

APC =Allophycocyanin, PE=Phycoerythrin, FITC = Fluorescein Isothiocyanate, PerCp = Peridinin chlorophyll, Cy = Cyanine

2.4.3 Plasma preparation and lipid analysis

Plasma was isolated by centrifugation (500 x g, 15 min, 4°C) of EDTA-anticoagulated blood. Plasma cholesterol concentration was determined using a colorimetric assay (Roche, Basel, Switzerland) modified to microtiter format. In brief, the plasma samples were diluted 1:5 with 0.9% saline on ice. A standard (Roche/Hitachi; 152 mg/dl accordingly 3.95 mmol/l) was serially diluted 1:2, 1:4, 1:8, 1:16 and 1:32 with 0.9% saline on ice. Subsequently, 2 µl of each standard, sample and blank (0.9% saline) were transferred to a flat bottom microtiterplate (BD Biosciences) on ice. To increase the range of the standard 2 µl and 4 µl undiluted standard was added to the respective wells. After adding 200 µl reagent CHOD-PAP (Roche) to each well the microtiter-plate was gently mixed. Following incubation at room temperature for 30 min absorbance at 505 nm wavelength was measured using a 96-well plate reader (Tecan GENios). For calculating the cholesterol content of the sample the following equation was used:

$$\text{Concentration (mmol/l)} = \frac{\text{Sample (mean) x standard-concentration (mmol/l)}}{\text{Standard (mean)}}$$

Hematologic analysis was performed with a ScilVet abc Plus+ (ScilVet, Viernheim, Germany).

2.4.4 Plasma analysis

Murine plasma was analyzed for cytokine levels, general Ig levels and oxLDL-reactive Ig using multiplex bead-based assays (eBioscience) and enzyme-linked immunosorbent assays (ELISA).

2.4.4.1 Anti-oxLDL-Ig ELISA

The abundance of antibodies detecting oxLDL in plasma of mice was detected via ELISA. In brief, a 96-well polystyrene microplate (Costar 3690, Corning, Corning NY, USA) was incubated with 50 µl per well of 10 µg/ml oxLDL in PBS pH 7.4 at 4°C overnight. Wells were washed twice with PBS, blocked 1h at room temperature with 1% gelatin (Sigma Aldrich) in PBS and washed twice with PBS. Subsequently, 50 µl of pre-diluted mouse plasma (1:20, 1:200, 1:1000) in 0.1% gelatin/Tris-buffered saline (TBS) were added per well and incubated for 2 h at room temperature. After incubation, wells were washed thrice with 0.05% PBS-Tween (PBS-T) and 50 µl of the biotinylated anti-mouse IgG-antibodies listed below were added (each antibody was diluted 1:25000 in 0.1% gelatin/TBS):

- Biotin-SP-conjugated Goat anti-mouse IgG_1,
- Biotin-SP-conjugated Goat anti-mouse IgM, µ chain,
- Biotin-SP-conjugated Goat anti-mouse total IgG,

- Biotin-SP-conjugated Goat anti-mouse total IgG_{2b},
- Biotin-SP-conjugated Goat anti-mouse total IgG_3,
- Biotin-SP-conjugated Goat anti-mouse total IgG_{2a},

All antibodies were obtained from Jackson ImmunoResearch Labs and handled according the manufacturer's data sheets. Subsequent to incubation for 1 h at room temperature with biotinylated antibodies, wells were washed thrice in 0.05% PBS-T and 50 µl of streptavidin conjugated to horse radish peroxidase (HRP, 1:1000 in 0.1% gelatin/TBS) were added (1 h, room temperature, dark). After washing with 0.05% PBS-T (4x), 50 µl 3,3',5,5'-Tetramethylbenzidin (TMB) substrate (1-Step Ultra TMB ELISA substrate, Thermo Scientific) were added for 2-10 min depending of titers. The substrate is converted into blue product in presence of HRP activity. The addition of 1 M hydrochloric acid (HCL) stopped the reaction and changes the substrate to a yellow color. Absorbance was analyzed with an 96-well plate reader (Tecan GENios) at 450 nm wavelength with reference wave length set at 570 nm.

2.4.4.3 Cytometric bead Arrays

Murine plasma from 28-week-old mice was analyzed for T helper cytokine abundance with the mouse Th1/2/17/22 13-plex kit FlowCytomix Multiplex Kit (eBioscience) which allows for the simultaneous detection of, IL-1α, IL-2, IL-4, IL-5, IL-6, IL-10, IL-13, IL-17, IL-21, IL-22, IL-27, IFNγ and TNFα. Levels of circulating Ig subclasses (IgA, IgG1, IgG2a, IgG2b, IgG3, IgM) from the same mice were assessed with the mouse Ig isotyping 6-plex kit (eBioscience). Both assays are bead-based and follow a similar principal as a sandwich ELISA. Analysis was performed with a flow cytometer (BD FACS Canto II, BD Biosciences). In brief, fluorescently-marked polystyrol beads are pre-coupled with antibodies specifically detecting the respective analyte(s) of interest. A single bead population was only coupled with one specific capturing antibody. A mixture of different bead populations was incubated with plasma samples for 2 h. The bead-bound-analyte from the plasma sample was detected by a biotinylated detection antibody. Subsequent 1 h incubation with PE-conjugated streptavidin- binding to the biotinylated analyte-bead-complex allowed for quantification of the respective analyte. The bead samples were acquired with a BD FACS Canto II (BD Biosciences). Up to 20 bead sets could be analyzed in one fluorescent channel as the beads are distinguishable by size (4 µm and 5 µm) and different intensities of the fluorochrome labeling the bead populations. Here, beads were labeled with a fluorochrome emitting in the far-red channel at 690 nm wavelength. First beads were separated by size by displaying size (front scatter) and granularity (side scatter). Gating on the size-separated bead populations allowed for further discrimination in fluorescence intensity by displaying fluorescence

emitted in the APC channel. Mean fluorescence intensities (MFI) of each bead population for fluorescence emitted in the PE channel were acquired and standard curves based on the MFI obtained from standard cytokine beads were used for quantification of sample analyte concentration. Flow cytometer data was analyzed with the FlowCytomix Pro 3.0 analysis software to obtain plasma cytokine or Ig concentrations. During the course of this thesis the manufacturer replaced the bead array technology analyzed by flow cytometry with the ProcartaPlex immunoassays using Luminex xMAP technology for the multi-analyte detection. Here, we applied the ProcartaPlex mouse Th1/Th2/Th9/Th17/Th22/Treg cytokine panel (17 plex) to simultaneously analyze plasma concentration of IL-1α, IL-2, IL-4, IL-5, IL-6, IL-9, IL-10,IL-12, IL-13, IL-17, IL17A, IL18, IL-21, IL-22, IL-27, IFNγ , TNFα and GM-CSF. Plasma was obtained from *Cd40*$^{flox/flox}$ *Apoe*$^{-/-}$ *Cd11cCre*$^{+}$, *Cd40*$^{flox/flox}$ *Apoe*$^{-/-}$ *CD11Cre*$^{-}$, *Cd40l*$^{flox/flox}$ *Apoe*$^{-/-}$ *Cd4Cre*$^{+}$ and *Cd40l*$^{flox/flox}$ *Apoe*$^{-/-}$ *Cd4Cre*$^{-}$. The xMAP technology is also a bead-based technique which applies beads which are internally labeled with fluorescent dyes to produce a specific spectral address. The beads are magnetized thus allowing for convenient washing steps in a 96-well plate. The beads are coupled with antibodies which will capture the specific analyte which in turn will be bound by a biotinylated detection antibody. Quantification will follow the binding of streptavidin-PE-conjugates to the detection antibody. Again, MFI of each bead population for fluorescence emitted in the PE channel were acquired and standard curves based on the MFI obtained from standard cytokine incubated with beads were used for quantification of sample analyte concentration. The samples were analyzed with the Luminex platform MAGPIX (Luminex). Data was analyzed with the xPONENT software controlling the MAGPIX platform (Luminex).

2.4.5 Histochemistry (morphometry and histology)

Hearts were cut in 8 µm-thick serial sections beginning from the onset of the aortic valves until the valves disappeared. Serial sections were stained with Oil Red O (Sigma) to determine lipid depositions and analyzed with a Leica DM6000 microscope (Leica Microsystems) equipped with a computerized morphometry system (LAS 4.6 analysis, Leica Microsystems). In brief, air-dried cryostat sections were pre-incubated with 60% 2-propanol (10x dipping) and subsequently kept 15 min in the Oil Red O-working solution (180 ml Oil red O-stock solution and 120 ml deionized water filtered 1 h after mixing to remove precipitated salts). Excess Oil Red O solution was washed away by dipping 10 x in 60% 2-propanol. The sections were rinsed 5 min in tap water and counterstained with hemalaun (Sigma) in deionized water for 30 s followed by rinsing 5 min in tap water. Oil red O-stained sections were embedded in Immu-Mount (Thermo Scientific).

Serial paraffin sections of the aortic arch, the abdominal aorta and ears were stained with Hematoxylin & Eosine (H&E) and analyzed with a Leica DM6000 microscope (Leica Microsystems). Paraffin section were first deparaffinized with xylene and then rehydrated with the help of an descending ethanol (ETOH) series (100% ETOH, 96% ETOH, 70%ETOH, 50%ETOH) and deionized water. The sections were then stained with hematoxylin in deionized water for 2 min followed by rinsing 10 min in tap water. Afterwards the sections were counterstained with Eosine for 5 min. Excess Eosine was washed away by dipping 1x in deionized water. Finally the sections were dehydrated with the help of an ascending ethanol series (50%ETOH, 70%ETOH, 96%ETOH, 100%ETOH) and fixated in xylene for 2 min. H&E-stained sections were embedded in Immu-Mount (Thermo Scientific).The tissue sections with insufficient quality were excluded from further analysis, which may influence the individual parameter group size.

2.4.6 Immunohistochemistry

Selected murine tissue cryosections were fixed in ice-cold acetone prior to incubation with antibodies against alpha smooth muscle actin (α-SMA), CD3, CD4, Foxp3 and MAC3. The primary antibody binding of non-fluorescent conjugated antibodies was detected either by incubation with fluorochrome- (Alexa Fluor 488, Alexa Fluor 594, Cy3 or horse-radish peroxidase-conjugated secondary antibodies and diaminobenzidine (ABC kit, Vector Labs, Burlingame, USA). To amplify signal strength for α-SMA staining, a primary antibody against α-SMA conjugated with FITC and secondary antibody directed against FITC and conjugated with Alexa Fluor 488 were used. Tissue sections were counterstained with hematoxylin or 4',6-Diamidino-2-phenylindol (DAPI, Life Technologies), respectively, mounted with DAKO fluorescent mounting medium (Dako, Agilent Technologies, Santa Clara, CA, USA), and images were recorded with a Leica DM6000 microscope equipped with a DFC295 and DFC365FX camera (Leica).CD4- and Foxp3-stained cells were counted. α-SMA-, MAC3-positive areas were analyzed by applying color threshold measurements. Tissue sections with insufficient quality were excluded from further analysis, which influences the individual parameter group size.

Table 4: Primary antibodies used in immunohistochemistry

Antigen	Source and reactivity	Clone	Dilution	Source
CD3	Armenian Hamster-anti-mouse (IgG1, κ)	145-2C11	1:100	BD Biosciences
CD4	Rat-anti-mouse (IgG2a, κ)	RM4-5	1:100	BD Biosciences
Foxp3	Rat-anti-mouse/rat/pig/canine/bovine (IgG2b, κ)	FJK-16s	1:50	eBioscience
α–SMA-	Mouse-anti-mouse/rabbit/human/pig (IgG2a) FITC conjugated	1A4	1:1000	Sigma Aldrich
CD8	Rat-anti-mouse (IgG2a)	YTS105.18	1:100	AbD Serotec, Puchheim, Germany
MAC3	Rat-anti-mouse (IgG1, κ)	M3/84	1:200	BD Biosciences

Table 5: Secondary antibodies used in immunohistochemistry

Source and Reactivity	Conjugate	Dilution	Source
Donkey-anti-rat	Alexa Fluor488	1:300	Thermo Scientific
Mouse-anti-FITC	Alexa Fluor488	1:400	Jackson ImmunoResearch, West Grove, PA, USA
Goat-anti-armenian hamster	Cy3	1:300	Thermo Scientific
Goat-anti-mouse	Alexa Fluor594	1:300	Thermo Scientific
Goat-anti-rabbit	Star 635P	1:300	Abberior, Goettingen, Germany

2.5 Cell culture and functional assays

Cell culture was performed under sterile conditions in a laminar flow hood. Cells were maintained in a carbon dioxide incubator at 37°C and a humidified 5% CO_2 atmosphere. FBS was incubated at 56°C for 30 min to inactivate the complement proteins and stored at -20°C until use. According to cell types specific media were used.

2.5.1 CD4$^+$ T cell isolation

T cells were sorted isolated from spleen and lymph nodes. CD4$^+$ T cells were negatively sorted using antibody-conjugated magnetic beads (Dynabeads Untouched Mouse CD4, Life Technologies) and dynal isolation buffer. In brief, an antibody-mix was used to label non-CD4$^+$ T cells. The addition of Fc-binding magnetic beads bound the labeled cells in the tube while separating untouched CD4$^+$ T cells. Tregs were sorted by either flow cytometry sorting for CD3$^+$CD4$^+$CD25^{high} cells (BD FACS Aria III, BD Biosciences) or using an untouched CD4 negative magnetic bead-sort followed by a CD25 positive magnetic bead sort according to the instructions of the manufacturer (Dynabeads Flowcomp Mouse CD4$^+$CD25$^+$ Treg cells kit, Life Technologies). T Cells were cultured in T cell medium (see 2.9).

2.5.2 T cell proliferation assay

Sorted CD4$^+$ T cells from *Apoe*$^{-/-}$ mice were stained with carboxyfluorescein succinimidyl ester (CFSE, Life Technologies). In brief, T cells were adjusted to 1x10^6/100 µl in 37°C pre-warmed PBS and stained with 3 µM CFSE for 15 min at 37°C in a water bath while shaking the tube every 2 min. Subsequently, the T cells were washed twice with T cell medium and adjusted to 1x10^6/ml. 5x10^4 CFSE-labeled T cells were co-cultured in a 1:1 ratio with anti-CD3/CD28 antibody-conjugated beads (Life Technologies) for 72 hours. T cell proliferation was determined by CFSE dilution measured by flow cytometry.

The proliferation index was calculated by multiplying the percentages of cells in a specific CFSE-dilution-population with the number of their respective generation starting from the first proliferated generation defined as “1” (undevided is”0”).

$$PI = ((n1\% \times 1) + (n2\% \times 2) + (n3\% \times 3) + (n4\% \times 4) + (n5\% \times 5) + (n6\% \times 6))$$

PI= Proliferationindex, n= CFSE Dilution, % percentage of total cells

2.5.3 Treg suppression assay

CFSE-labeled T cells ($5x10^4$), as described above, were co-cultured in a 1:1 ratio with anti-CD3/CD28 antibody-conjugated beads (Life Technologies) and varying concentrations of Tregs from *Apoe*$^{-/-}$ *Cd4Cre*$^{+}$ and *Cd40l*$^{flox/flox}$ *Apoe*$^{-/-}$ *Cd4Cre*$^{-}$ mice for 72 h. T cell proliferation was determined by CFSE dilution measured by flow cytometry.

2.6 Biomolecular methods

2.6.1 RNA isolation

All reagents were obtained from Qiagen if not stated otherwise. Total ribonucleic acid (RNA) was isolated from tissue stored in RNAlater (Ambion, Thermo Scientific) at -80°C according to the protocol of Qiagen RNeasy Mini Kit II. The entire procedure was performed under RNase-free conditions and partly on ice. The tissue samples were thawed and the amount of tissue was determined to use a maximum of 100 mg per sample. A stainless steel bead (7 mm diameter) was added along with the tissue sample removed from RNAlater to a 2 ml tube and kept on ice. Before placing the tube in the TissueLyser with a 12-Tube LT Adapter 1 ml Qiazol Lyses Reagent was added. Lysis was performed for 5 min at 50 Hz. The lysate was transferred to a new microcentrifuge tube and incubated at room temperature for 5 min so nucleoprotein complexes were able to dissociate. After incubation 200 µl Roti® - Phenol/C I (Roth, Karlsruhe, Germany) was added and the tube was shaken vigorously for 15 s. Another incubation step for 3 min. at room temperature was performed and thereafter all samples were centrifuged at 12,000 x g for 15 min at 4°C. After centrifugation 3 (or 4) Phases appeared in the tube: a) an upper, colorless, aqueous phase containing RNA b) a white interphase c) a lower, red, organic phase and d) a clear phase below the red phase (only in tissues with high fat content). The upper, aqueous phase was transferred gently to a new tube without interfering with DNA- and protein-containing phases. One volume of 70% ethanol was added to the transferred RNA-containing phase and the tube was vortexed. Up to 700 µl of sample was transferred to an RNeasy Mini spin column placed in a supplied 2 ml tube. After closing the lid, the sample was centrifuged for 15 sec at 8,000 x g at room temperature. The flow-through was discarded. This procedure was repeated until the entire remainder of the sample was used. For digestion of potentially contaminating genomic DNA the ribonuclease (RNase)-Free DNase set supplied with DNase I, buffer RDD and RNase-free water was used. Lyophilized DNase I was dissolved in 550 µl of RNase-free water to prepare a DNase I stock solution. After adding 350 µl of buffer RW1 to the RNeasy spin column the column was centrifuged at 5000 x g for 15 sec at room temperature.

For each sample 10 µl DNase I stock solution were added to 70 µl buffer RDD. Subsequently, 80 µl of DNase I incubation mix was directly added to the middle of the RNeasy spin column membrane and incubated for 15 min at room temperature. Following incubation 350 µl RW1 buffer was applied to the RNeasy spin column and the column centrifuged for 15 sec at 8000 x g. The obtained flow-through was discarded. The membrane of the RNeasy spin column was washed twice with 500 µl buffer RPE supplied with 96% Ethanol. Following centrifuging the column for 15 sec at 8000 x g, a second drying step at 8000 x g for 2 min was performed. All flow-through was discarded. For elution of the RNA the RNeasy spin column was placed in a new 1.5 ml collection tube and 50 µl of RNase-free water was added to the membrane. The column was centrifuged for 1 min at 8000 x g. Purity and yield of total RNA of each preparation were assessed spectrophotometrically at OD_{260}/OD_{280} employing a nanodrop (Peqlab). A value of OD_{260}/OD_{280} lower than 1.7 led to the disqualification of these samples. Samples were stored at -80°C until further use.

2.6.2 cDNA synthesis

RNA isolated from aortas was reverse transcribed with the SuperScript® VILO™ complimentary DNA (cDNA) Synthesis Kit (Invitrogen) according to the manufacturer's instructions. In brief, 4 µl 5X VILO™ Reaction Mix and 2 µl 10X SuperScript® Enzyme Mix were added on ice. The concentration of RNA adjusted to the sample with the lowest concentration with DNAse-/RNAse-free water (Sigma Aldrich) for equal amounts of starting material, and 14 µl of RNA were added. The total reaction volume was 20 µl. The content of the tubes was mixed gently and incubated at 25°C for 10 min. Subsequently, the mixture was incubated at 42°C for 1 h and the reaction stopped by heating to 85°C for 5 min.

2.6.3 Real-time polymerase chain reaction

Quantitative PCR (qPCR) was performed with TagMan® gene expression assays (Thermo Fisher Scientific) on a 7900HT Fast Real Time PCR system (Thermo Fisher Scientific). TagMan® pobes were obtained from Thermo Fisher Scientific. TagMan® probes are listed below (see 2.6.4).

For a single real-time PCR reaction

5 µl	2 ng/µl cDNA,
5µl	2x FAST® Mastermix
0.5µl	TagMan® assay

were mixed on ice. If higher sample numbers were processed a master mix was prepared in a tube on ice and kept in the dark. Each PCR reaction was pipetted in duplicate. The PCR program was composed of an initial step at 95°C for 20 sec followed by 40 cycles of each 1 sec at 95°C and 20 sec at 60°C. Subsequently, a dissociation cycle was performed with 15 sec at 95°C, 1 min at 60°C, and followed by 15 sec at 95°C with a 2% ramp rate. The obtained data from real-time PCR for the respective genes and tissues was analyzed by applying the $2^{-\Delta\Delta C_T}$ method.[210] β-actin expression was considered to be equal in a respective tissue upon administration of atherogenic diet and therefore was used as reference.

2.6.4 Table 6: List of genes and TagMan® probes for gene expression analysis

Gene	TagMan probe
IL-1β	Mm00434228_m1 (Thermo Fisher Scientific)
IL-2	Mm01340213_m1 Thermo Fisher Scientific
IL-6	Mm00446190_m1 Thermo Fisher Scientific
Il-10	Mm00439614_m1 Thermo Fisher Scientific
IL-12 p35	Mm00434165_m1 Thermo Fisher Scientific
Foxp3	Mm00475162_m1 Thermo Fisher Scientific
IFNγ	Mm01168134_m1 Thermo Fisher Scientific
CD69	Mm01183378_m1 Thermo Fisher Scientific
TGFβ	Mm01178820_m1 Thermo Fisher Scientific
TNFα	Mm00443258_m1 Thermo Fisher Scientific

2.7 Statistical analysis

Data is presented as average ± standard deviation (SD). Student's t test was used to analyze data for statistical significance with GraphPad Prism v.5 software (GraphPad Software Inc., La Jolla, USA). A *p* value of <0.01 was considered statistical significant.

2.8 Buffers

Tissue lysis buffer

10 mM Tris

10 mM EDTA

10 mM Sodium chloride (NaCl)

0.5% Sarcosyl (N-Lauroylsarcosine sodium salt)

adjusted to 0.5 Liter with distilled H_2O.

Erythrocyte lysis buffer

10 mM Potassium hydrogen carbonate ($KHCO_3$)

150 mM Ammonium chloride (NH_4Cl)

0.1 mM EDTA

adjusted to 1 Liter with distilled H_2O and pH 7.2-7.4.

FACS buffer

1x PBS

0.5% BSA

0.01% Sodium azide (NaN_3)

Fixation/Permeabilization working solution (from Foxp3 staining set, eBioscience)

Dilute 3x Fixation/Permeabilization 3 times in Fixation/Permeabilization diluent.

Permeabilization buffer (from Foxp3 staining set, eBioscience)

Dilute the 10x Permeabilization Buffer (00-8333-56) 10 times in distilled water.

Dynal isolation buffer

1x PBS

0.1% BSA

2 mM EDTA

CFSE label buffer

1x PBS

0.1% BSA

Citrate saline buffer

135 mM Potassium chloride

15 mM Sodium citrate

In distilled H_2O.

Oil Red O-stock solution

1 g Oil Red O (Sigma Aldrich)

200 ml 99% 2-propanol

2.9 Media

T cell medium

All reagents were obtained from (A) Thermo Scientific and (B) Sigma Aldrich.

RPMI1640 with Glutamax (A)

10% FBS (A)

100 U/ml Penicillin (A)

100 µg/ml Streptomycin (A)

10 mM Hepes (B)

1x MEM non-essential amino acids (B)

1 mM Sodium pyruvate (B)

50 µM 2-Mercaptoethanol (B)

D10 medium

DMEM (Dulbecco's Modified Eagle Medium) with 4,5 g/L glucose and pyruvate (Life Technologies)

10% FBS

100 U/ml Penicillin

100 µg/ml Streptomycin

3 RESULTS

3.1 Experimental setup of the cell type-specific CD40-CD40L study and generation of cell type-specific deletion of CD40 and CD40L.

Apoe$^{-/-}$ mice were crossed with *Cd40*$^{fl/fl}$ or *Cd40l*$^{fl/fl}$ mice and bred with mice expressing the recombinase cre under control of a cell type-specific promotor. The resulting cre^{+} animals and their cre^{-} littermates were sacrificed at the age of 28 weeks on regular chow diet or after consuming a hypercholesterolemic diet (0.15% cholesterol, 21% fat) for 6 weeks. Cryo sections (8µm) of the aortic sinus and paraffin sections of the aortic arch (4µm) including its main branch points (brachiocephalic trunk, left common carotid artery, left subclavian artery) were prepared and analyzed for atherosclerotic lesion size, histology, and cellular composition of the atherosclerotic plaques. Flow cytometry was performed to monitor potential changes in the abundance, activation status and survival of immune cells in lymph nodes, blood, and spleen (Figure 4 A).To confirm the cell type-specific deletion of either CD40 or CD40L different assays were used, depending on the cell type that was supposed to be depleted of CD40 or CD40L.Flow cytometric measurements of splenocytes from *Apoe*$^{-/-}$*Cd40*$^{fl/fl}$*Cd11cCre*$^{+}$ and *Apoe*$^{-/-}$ *Cd40*$^{fl/fl}$*Cd11cCre*$^{-}$ animals demonstrated specific deletion of CD40 on B220^{-}/CD11c^{+} splenocytes (Figure 4 B). To prove the specific deletion of CD40L on CD4^{+} T cells via cre-recombinase, CD4^{+} and CD4^{-} cells were isolated and analyzed for CD40L mRNA expression. Indeed, mRNA isolated from isolated CD4^{+} cells, or isolated CD4^{-} cells of the *Apoe*$^{-/-}$ *Cd40l*$^{fl/fl}$*Cd4Cre*$^{+}$ mice did not show detectable CD40L expression, even after 40 cycles of the qPCR program. In contrast mRNA from CD4^{+} cells isolated from *Apoe*$^{-/-}$*Cd40l*$^{fl/fl}$*Cd4Cre*$^{-}$ mice showed a CD40L expression after 11 to 18 cycles of the qPCR program (Figure 4 C).

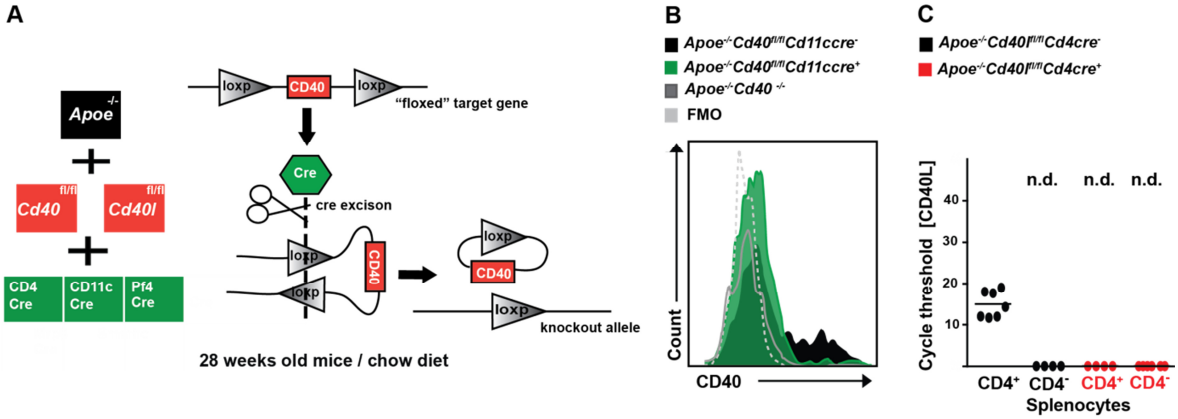

Figure 4. Experimental setup of the cell type-specific CD40-CD40L study.
(**A**) *Apoe*$^{-/-}$mice were crossed with *Cd40*$^{fl/fl}$ or *Cd40l*$^{fl/fl}$ mice and a cell type-specific cre-recombinase was introduced through breeding with cre^{+} or *cre*$^{-}$ mice. (**B**) The cell type-specific deletion of CD40 in CD11c^{+} cells is shown via a representative flow cytometric histogram (right), CD40 expression on splenic CD11c^{+} cells from wild type *(Apoe*$^{-/-}$ *Cd40*$^{fl/fl}$*CD11cCre*$^{-}$*)*, *Apoe*$^{-/-}$*Cd40*$^{fl/fl}$*CD11cCre*$^{+}$, mice with a global CD40 deletion (*Apoe*$^{-/-}$*Cd40*$^{-/-}$) and a fluorescence minus one (FMO) are represented. (**C**) Cycle threshold of CD40L mRNA (left), analyzed via qPCR, from isolated CD4^{+} or CD4^{-}splenocytes of *Apoe*$^{-/-}$*Cd40l*$^{fl/fl}$*Cd4Cre*$^{+}$ and *Apoe*$^{-/-}$*Cd40l*$^{fl/fl}$*Cd4Cre*$^{-}$ mice (n.d.= not detectable).

3.2 T cell-specific deletion of CD40L decreases atherogenesis in early and late stage of atherosclerosis and promotes a stable plaque phenotype.

CD40L is predominately found on activated cells, the most characteristic of which are activated and/or differentiated T cells[251]. Therefore we started our studies by investigating the role of role of T cell-specific CD40L in atherosclerosis. To identify and characterize the possible effect of T cell-specific CD40L we decided to use a mild form of hyperlipidemia for our initial experiments, where we fed mice for 28 weeks on a normal chow diet. Prior to our studies, we wanted to exclude any secondary effects of T cell CD40L deficiency on the cholesterol mechanism or blood parameters. Accordingly, we measured body weight, plasma cholesterol concentration and basic hematological parameters of 28 week old male *Apoe*$^{-/-}$*Cd40l*$^{fl/fll}$*Cd4Cre*$^{+}$ and *Apoe*$^{-/-}$*Cd40l*$^{fl/fl}$*Cd4Cre*$^{-}$ mice. These analyses did not reveal any significant differences between *Apoe*$^{-/-}$*Cd40l*$^{fl/fll}$*Cd4Cre*$^{+}$ and *Apoe*$^{-/-}$*Cd40l*$^{fl/fl}$*Cd4Cre*$^{-}$ mice (Table7).

■ *Apoe*$^{-/-}$*Cd40l*$^{fl/fl}$*Cd4cre*$^{-}$ ■ *Apoe*$^{-/-}$*Cd40l*$^{fl/fl}$*Cd4cre*$^{+}$

Body weight [g]	33.00	±1.89	32.20	±2.32
Lymphocytes [%]	72.35	±4.51	71.54	±8.93
Monocytes [%]	3.95	±0.87	4.06	±1.52
Granulocytes [%]	23.70	±4.40	24.45	±5.05
Platelets [10^3/µl]	1233	±248	1202	±205
Erythrocytes [10^6/µl]	8.57	±0.58	8.38	±2.78
Leukocytes [10^3/µl]	2.75	±1.63	3.76	±2.02
Lymphocytes [10^3/µl]	1.88	±4.51	2.74	±1.08
Monocytes [10^3/µl]	0.05	±0.05	0.08	±0.05
Granulocytes [10^3/µl]	0.73	±0.34	1.09	±0.58
Plasma Cholesterol [mM]	2.60	±0.20	2.56	±0.40

Table 7. Body weight, hematological parameters, and plasma cholesterol content in *Apoe*$^{-/-}$*Cd40l*$^{fl/fll}$*Cd4Cre*$^{-}$ mice (n=17) and *Apoe*$^{-/-}$*Cd40l*$^{fl/fl}$*Cd4Cre*$^{+}$mice (n=19. Data is presented as mean±SD.

Since the deletion of CD40L on T cells did not interfere with blood parameters or cholesterol metabolism we analyzed the atherosclerotic lesion area in the aortic arch and in the aortic sinus. Quantification of atherosclerotic lesion development in mouse models is of primary interest, since it enables the evaluating of risk factors and disease development. The histological examination of H&E-stained paraffin sections of the aortic arch revealed significantly reduced lesion areas in *Apoe*$^{-/-}$*Cd40l*$^{fl/fll}$*Cd4Cre*$^{+}$ mice. The absolute atherosclerotic lesion area in the aortic arch, whit its three main branch points (brachiocephalic trunk, left common carotid artery and left subclavian artery) of 28 week old male *Apoe*$^{-/-}$*Cd40l*$^{fl/fll}$*Cd4Cre*$^{+}$ mice displayed a nearly 30% reduction in lesion area compared to *Apoe*$^{-/-}$*Cd40l*$^{fl/fl}$*Cd4Cre*$^{-}$ littermate controls (Figure 5 A, B).

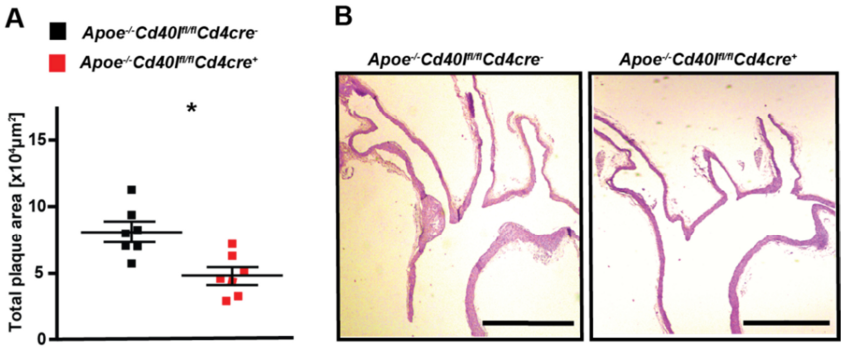

Figure 5. T cell-specific deletion of CD40L does reduce early plaque formation in the aortic arch.
Total atherosclerotic plaque area sections hematoxylin-and-eosin-stained longitudinal section of the aortic arch, including the brachiocephalic trunk, left carotid, and left subclavian artery from 28 week-old male *Apoe*$^{-/-}$*Cd40l*$^{fl/fl}$*Cd4Cre*$^{-}$ *or Apoe*$^{-/-}$*Cd40l*$^{fl/fl}$*Cd4Cre*$^{+}$ mice. (**A**) Quantification of total plaque size and (**B**) representative photomicrographs of hematoxylin-and-eosin-stained longitudinal section. n=7 (*Apoe*$^{-/-}$*Cd40l*$^{fl/fl}$*Cd4Cre*$^{-}$), n=8 (*Apoe*$^{-/-}$*Cd40l*$^{fl/fl}$*Cd4Cre*$^{+}$) Scale bar = 200 µm. Data is presented as mean±SD. *=p<0.01

To further analyze the effect of the T cell-specific CD40L deficiency on lesion initiation and to validate our finding of a significantly decreased absolute plaque area in the aortic arches of *Apoe*$^{-/-}$*Cd40l*$^{fl/fl}$*Cd4cre*$^{+}$ mice, we analyzed lesion size in cryosections of the aortic sinus, as a second main region of lesion progression. This analysis revealed a 30% reduction in absolute and relative lesion area in *Apoe*$^{-/-}$*Cd40l*$^{fl/fl}$*Cd4Cre*$^{+}$ compared to *Apoe*$^{-/-}$*Cd40l*$^{fl/fl}$*Cd4Cre*$^{-}$ mice confirming the findings in the aortic arch (Figure 6 A-C).

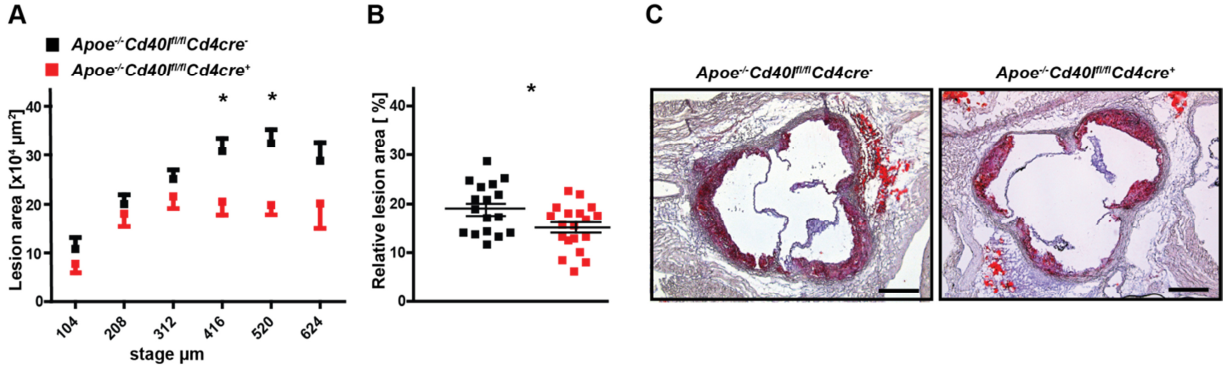

Figure 6. T cell-specific deficiency of CD40L alleviates atherosclerosis
Quantification of lesion area and atherosclerotic plaque area in cross-sections at indicated positions of the aortic sinus at different stages from 28-week-old, male *Apoe*$^{-/-}$*Cd40l*$^{fl/fl}$*Cd4Cre*$^{-}$ *or Apoe*$^{-/-}$*Cd40l*$^{fl/fl}$*Cd4Cre*+ mice. (**A**) Lesion areas in stages 104-624. (**B**) Average of lesions area stages 312-520 as percentage of total vessel area. (**C**) Representative photomicrographs showing Oil-Red-O-stained sections. n= 13-17 (*Apoe*$^{-/-}$*Cd40l*$^{fl/fl}$*Cd4Cre*$^{-}$); n=16-19 (*Apoe*$^{-/-}$*Cd40l*$^{fl/fl}$*Cd4Cre*$^{+}$) Scale bar = 200 µm. data is presented as mean±SD:*=p<0.0

Measuring lesion size is required to determine if a particular pharmacological treatment or genetic loss/enhancement of function has a direct effect on atherosclerosis. However, evaluation of atherosclerosis should not solely be determined by measuring the size of an atherosclerotic lesion. In fact, even more information about the process of atherogenesis can be gathered from a detailed histological and morphological examination as it pertains to the cellular and extracellular composition of the lesion which may offer significant mechanistic insight into the

atherogenic process itself. Thus, we determined the cellular composition of the lesions of the aortic sinus from 28 week- old male *Apoe*$^{-/-}$*Cd40l*$^{fl/fl}$*Cd4Cre*$^{+}$ *Apoe*$^{-/-}$*Cd40l*$^{fl/fl}$*Cd4Cre*$^{-}$ mice. Our detailed immunohistomorphological quantification of lesional macrophages and SMCs, the most abundant cell types in atherosclerosis, revealed a significantly decrease in infiltrated macrophages and a significant increase in the SMC content in the late stage lesions of the aortic sinus of 28 week- old male *Apoe*$^{-/-}$*Cd40l*$^{fl/fl}$*Cd4Cre*$^{+}$ mice, characteristics which are associated with a stable plaque phenotype (Figure 7 A, B).

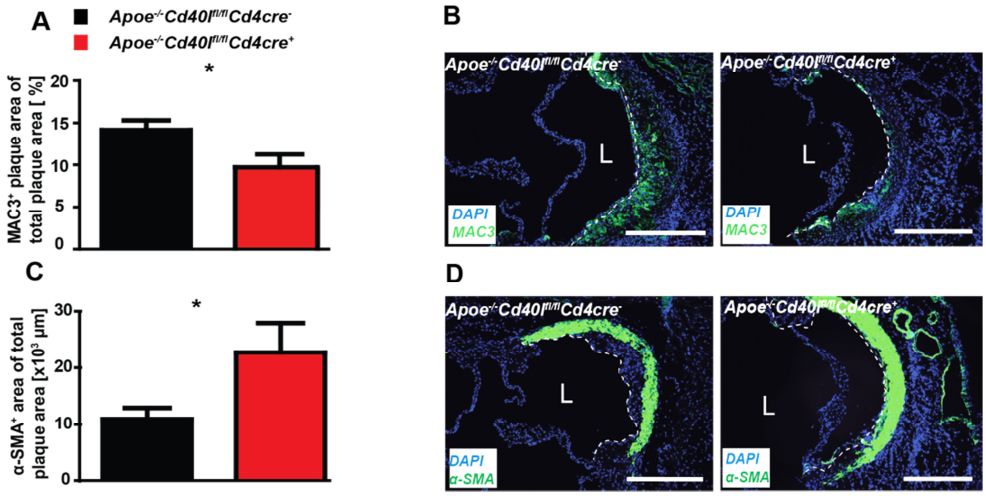

Figure 7. Lack of T cell-specific CD40L alters cellular plaque composition.
Immunofluorescent stainings in cross-sections of the aortic sinus from 28-week-old, male *Apoe*$^{-/-}$*Cd40l*$^{fl/fl}$*Cd4Cre*$^{-}$ *or* *Apoe*$^{-/-}$*Cd40l*$^{fl/fl}$*Cd4Cre*+ mice. Quantifications and representative photomicrographs are displayed for each staining. The dashed lines separate the atherosclerotic lesion from the lumen (L). Analyzed for (**A**) MAC3^{+} area and (**B**) α-SMA^{+} area. n=8-10 (*Apoe*$^{-/-}$*Cd40l*$^{fl/fl}$*Cd4Cre*) n=7-10 (*Apoe*$^{-/-}$*Cd40l*$^{fl/fl}$*Cd4Cre*$^{+}$). Scale bar = 200 µm. Data is presented as mean±SD.*=p<0.01

Immunohistological stainings for CD4^{+} cells demonstrated a lower amount of CD4^{+} cells in the plaque of 28 week- old *Apoe*$^{-/-}$*Cd40l*$^{fl/fl}$*Cd4Cre*$^{+}$ mice compared to the littermate controls (Figure 8 A, B).

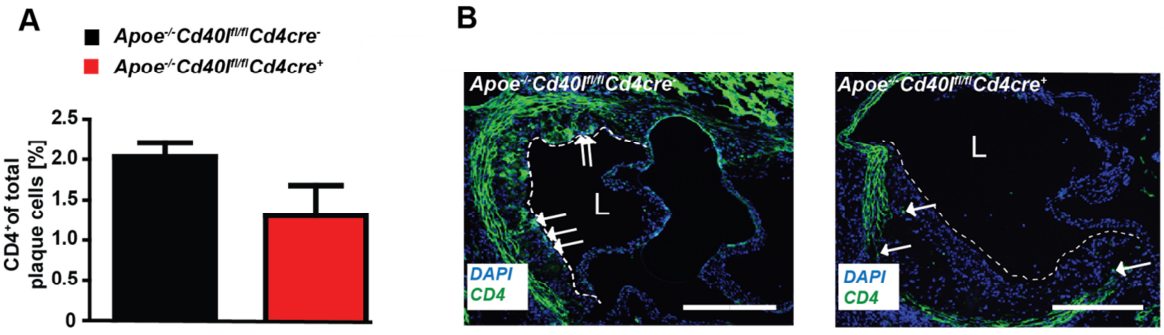

Figure 8. Lack of CD4 specific CD40L alters cellular plaque composition and reduces invasion of CD4^{+} cells.
Immunofluorescent stainings in cross-sections of the aortic sinus from 28-week-old, male *Apoe*$^{-/-}$*Cd40l*$^{fl/fl}$*Cd4Cre*$^{-}$ *or* *Apoe*$^{-/-}$*Cd40l*$^{fl/fl}$*Cd4Cre*+ mice analyzed for CD4^{+} cells. The dashed lines separate the atherosclerotic lesion from the lumen (L). Quantification (**A**) and representative photomicrographs (**B**) are displayed for each staining. n=9-10 (*Apoe*$^{-/-}$*Cd40l*$^{fl/fl}$*Cd4Cre*) n=8-10 (*Apoe*$^{-/-}$*Cd40l*$^{fl/fl}$*Cd4Cre*$^{+}$) Scale bar = 200 µm. Data is presented as mean±SD.

The first aim of the study was to provide a broad overview about the role of T cell-specific CD40L in the different stages of atherosclerosis as well as under the influence of different hyperlipidemic conditions. To this end we employed a second mouse model to identify an association between T cell CD40L deficiency and appearance of atherosclerotic lesions in more severe hypercholesterolemia. This status is achieved by feeding a fat- and cholesterol-enriched Western type diet for 6 weeks. *Apoe*$^{-/-}$*Cd40l*$^{fl/fl}$*Cd4Cre*$^{+}$ mice showed a 50% reduced lesion area compared to littermate controls consuming a WD for 6 weeks (Figure 9 A-C).

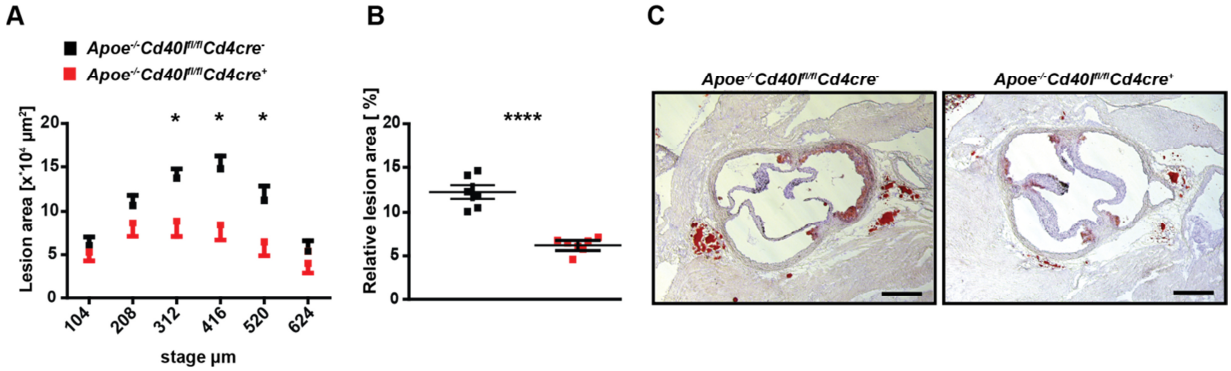

Figure 9 T cell-specific CD40L deficiency influence diet induced atherosclerosis.
Quantification of lesion area and atherosclerotic plaque area in cross-sections at indicated positions of the aortic root at different stages after administering a hypercholesterolemic diet for 6 weeks to male *Apoe*$^{-/-}$*Cd40l*$^{fl/fl}$*Cd4Cre*$^{-}$ *or* *Apoe*$^{-/-}$*Cd40l*$^{fl/fl}$*Cd4Cre*$^{+}$ mice. (**A**) Lesion areas in stages 104-624. (**B**) Average lesion area in stages 312-520 as percentage of total vessel area. (**C**) Representative photomicrographs of Oil Red O-stained sections. n=11-14 (*Apoe*$^{-/-}$*Cd40l*$^{fl/fl}$*Cd4Cre*$^{-}$), n=10-13 (*Apoe*$^{-/-}$*Cd40l*$^{fl/fl}$*Cd4Cre*$^{+}$) Scale bar = 200 µm. Data is presented as mean±SD.*=p<0.01; ****=p<0.0001

Resembling the immunohistological data from the 28 weeks study, the reduction in plaque size in diet-induced atherosclerosis was also accompanied by changes in the cellular composition in the plaques of *Apoe*$^{-/-}$*Cd40l*$^{fl/fl}$*Cd4Cre*$^{+}$ mice. Analysis of the distribution of single plaques scaled by size showed that *Apoe*$^{-/-}$*Cd40l*$^{fl/fl}$*Cd4Cre*$^{+}$ tend to acquire more “small-” and “medium-” sized plaques, whereas *Apoe*$^{-/-}$*Cd40l*$^{fl/fl}$*Cd4Cre*$^{-}$ mice displayed more than 60% of their plaques in the “large” plaque tertile (Figure 10 A). In addition, the plaques of the *Apoe*$^{-/-}$*Cd40l*$^{fl/fl}$*Cd4cre*$^{+}$ mice presented more nuclei per area resembling a higher cellularity of the atherosclerotic plaque (Figure 10 B). This increased cellularity was mostly derived from an increase in SMCs, suggesting a less inflammatory and rather pro-fibrotic plaque phenotype. This hypothesized less inflammatory plaque phenotype was further substantiated by the decreased number of infiltrated macrophages in the lesions of *Apoe*$^{-/-}$*Cd40l*$^{fl/fl}$*Cd4cre*$^{+}$ mice (Figure 7 C, D).

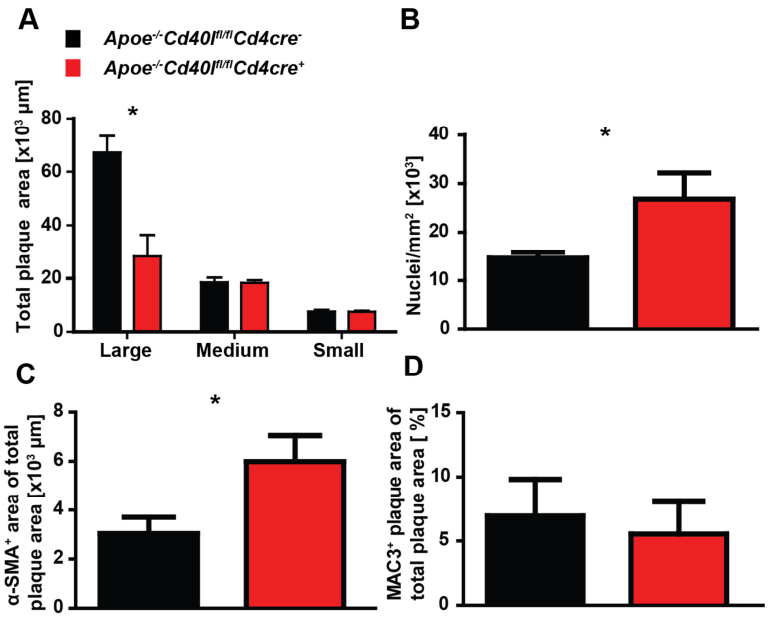

Figure 10. Lack of T cell-specific CD40L alters cellular plaque composition in diet induced atherosclerosis.
Quantifications of immunofluorescent staining in cross-sections of the aortic sinus from *Cd40l$^{fl/fl}$Cd4cre^{-}* and *Cd40l$^{fl/fl}$Cd4cre^{+}* mice after administering a hypercholesterolemic diet for 6 weeks. Quantifications are displayed for each staining.
(**A**) Analyzed for distribution of "large" (>20*10^{3}µm),"medium" (10-20*10^{3}µm) and "small" (<10*10^{3}µm) plaque sizes, (**B**) plaque cellularity represented as DAPI+ nuclei per mm^2 plaque area, (**C**) α-SMA$^+$ area and MAC3$^+$ area (**D**). n=8-10 (*Apoe$^{-/-}$Cd40l$^{fl/fl}$Cd4Cre*) n=7-10 (*Apoe$^{-/-}$Cd40l$^{fl/fl}$Cd4Cre^{+}*). Data is presented as mean±SD.*=p<0.01

By immunohistochemistry we were able to demonstrate, that the variance of plaque sizes in this model was also attended by a smaller amount of infiltrated CD4$^+$ cells in the plaque of ascending aortas of *Apoe$^{-/-}$Cd40l$^{fl/fll}$Cd4Cre^{+}* mice compared to those of littermate controls (Figure 11 A, B).

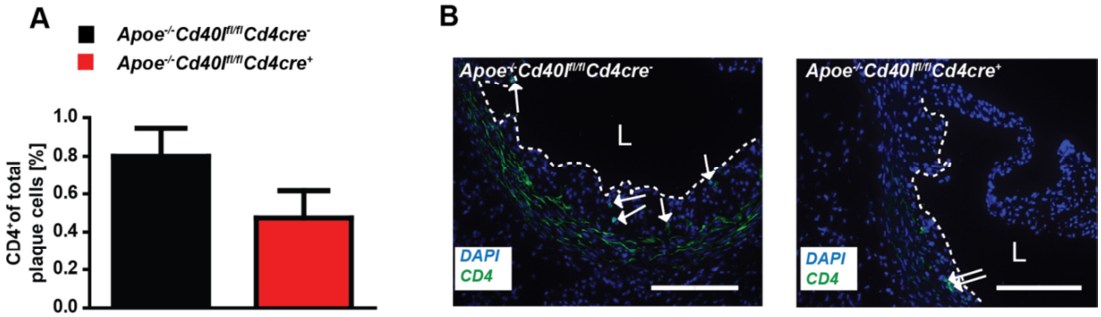

Figure 11. Lack of T cell specific CD40L alters cellular plaque composition and reduces invasion of CD4$^+$ cells in diet accelerated form of atherosclerosis.
Immunofluorescent stainings in cross-sections of the ascending aorta after administering a hypercholesterolemic diet for 6 weeks to male *Apoe$^{-/-}$Cd40l$^{fl/fl}$Cd4Cre^{-} or Apoe$^{-/-}$Cd40l$^{fl/fl}$Cd4Cre+* mice analyzed for CD4$^+$ cells The dashed lines separate the atherosclerotic lesion from the lumen (L). (**A**) Quantifications of analyzed CD4$^+$ cells and representative photomicrographs (**B**) are displayed for each staining. n=8-10 (*Apoe$^{-/-}$Cd40l$^{fl/fl}$Cd4Cre*) n=7-10 (*Apoe$^{-/-}$Cd40l$^{fl/fl}$Cd4Cre^{+}*) Scale bar = 200 µm. Data is presented as mean±SD.

In sum, mice lacking CD40L on T cells showed smaller lesions and more stable plaque phenotypes characterized by a decreased infiltration of CD4$^+$ cells in both models of early and late stage atherosclerosis and under the influence of different hypercholesterolemic burden.

3.3 T cell-specific CD40L deficiency decreases systemic and thymic Treg abundance without altering their regulatory capacity

Interestingly, our data of both models, advanced atherosclerosis after 28 week chow diet and accelerated atherosclerosis after 6 week WD, indicated that the abundance of lesional $CD4^+$ T cells is decreased in *Apoe*$^{-/-}$*Cd40l*$^{fl/fl}$*Cd4Cre*$^+$ mice. To evaluate this phenomenon, to test its local or systemic appearance and to examine the reason for the reduced $CD4^+$ T cell population in *Apoe*$^{-/-}$*Cd40l*$^{fl/fl}$*Cd4Cre*$^+$ mice, we analyzed the abundance of $CD4^+$ Tregs in *Apoe*$^{-/-}$*Cd40l*$^{fl/fl}$*Cd4Cre*$^+$ mice.

Flow cytometric measurements of lymphoid organs and blood of *Apoe*$^{-/-}$*Cd40l*$^{fl/fl}$*Cd4cre*$^-$ and Cre^+ animals were used to investigate possible changes in the Treg abundance. These analyses showed that the lack of T cell-specific CD40L led to significant decreased Treg numbers. As shown by flow cytometry of $Foxp3^+$ T cells in spleen, lymph node and blood, the results suggested a systemic rather than local phenomenon causing the reduced $CD4^+$ population (Figure 12 A, B, C).

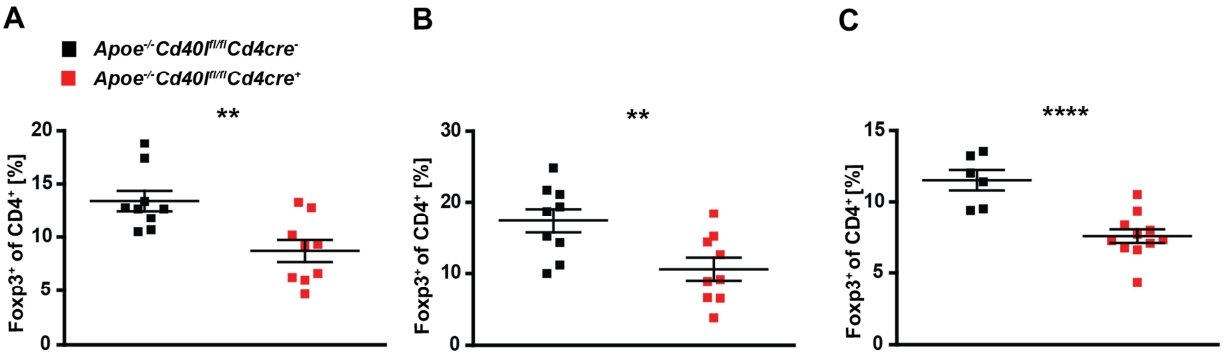

Figure 12. Loss of $CD4^+$ specific CD40L decreases systemic and aortic Treg abundance.
Flow cytometric analysis of splenic, lymphoid and blood cells for Foxp3+ cells from 28 weeks old, male *Apoe*$^{-/-}$*Cd40l*$^{fl/fl}$*Cd4Cre*$^+$ or *Apoe*$^{-/-}$*Cd40l*$^{fl/fl}$*Cd4Cre*$^-$ mice. (**A)** Flow cytometry analysis of splenic cells, (**B**) lymphoid cells and (**C**) blood cells, from *Apoe*$^{-/-}$*Cd40l*$^{fl/fl}$*Cd4Cre*$^+$ or *Apoe*$^{-/-}$*Cd40l*$^{fl/fl}$*Cd4Cre*$^-$ mice analyzed for $Foxp3^+$ cells. n= 8-10 (both groups). Data is presented as mean±SD. *=p<0.01;**=p<0.001; ****=p<0.0001

In addition to the systemic reduction of Tregs, the immunohistological stainings for $Foxp3^+$ cells in the plaque of ascending aorta of *Apoe*$^{-/-}$*Cd40l*$^{fl/fl}$*Cd4Cre*$^+$ mice at 28 weeks of age also revealed decreased lesional Treg numbers (Figure 13 A, B).

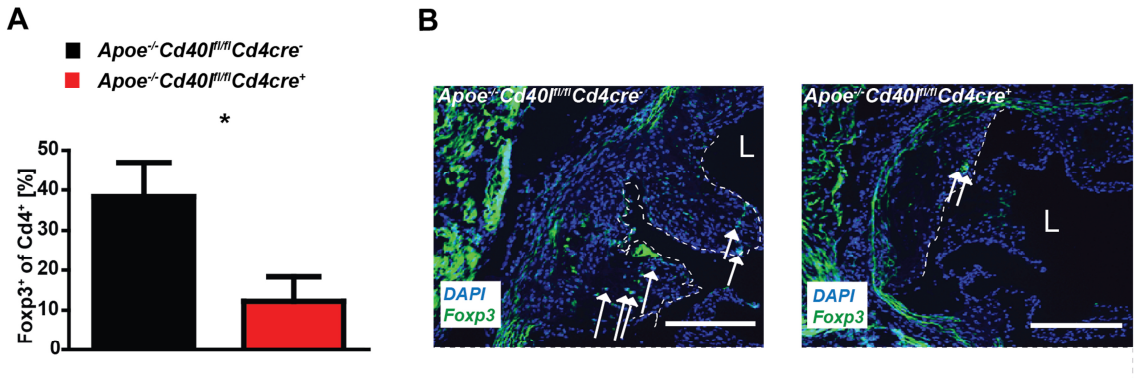

Figure 13. Loss of CD4$^+$ specific CD40L decreases systemic and aortic Treg abundance.
Immunofluorescent staining in cross-sections of the ascending aorta analyzed for Foxp3+ cells from 28 weeks old, male *Apoe$^{-/-}$Cd40l$^{fl/fl}$ Cd4Cre$^+$* or *Apoe$^{-/-}$Cd40l$^{fl/fl}$Cd4Cre$^-$* mice. The dashed lines separate the atherosclerotic lesion from the lumen (L). (**A**) Quantification of immunofluorescent cross sections of the ascending aorta analyzed for Foxp3$^+$ and representative photomicrographs (**B**) are displayed for staining of Foxp3$^+$ cells. n= 8-10 (both groups*)*.Scale bar = 200 µm. Data is presented as mean±SD. *=p<0.01

To verify our findings of an overall reduction of Treg numbers in *Apoe$^{-/-}$Cd40l$^{fl/fl}$Cd4cre$^+$* mice compared to their littermate controls, we repeated flow cytometric measurements and immunohistological stainings with lymph nodes, spleens, blood and ascending aortas of animals which consumed a WD diet for 6 weeks. Similar data were obtained by flow cytometric analysis of the systemic Treg abundance in the diet-accelerated model of atherosclerosis. The percentage of Foxp3$^+$ cells was significantly decreased in lymph nodes, spleens and blood of *Apoe$^{-/-}$Cd40l$^{fl/fll}$Cd4Cre$^+$* mice following 6 weeks of WD (Figure 14 A-C). These results suggest a cholesterol-independent connection between T cell-specific CD40L deficiency and decreased systemic Treg numbers.

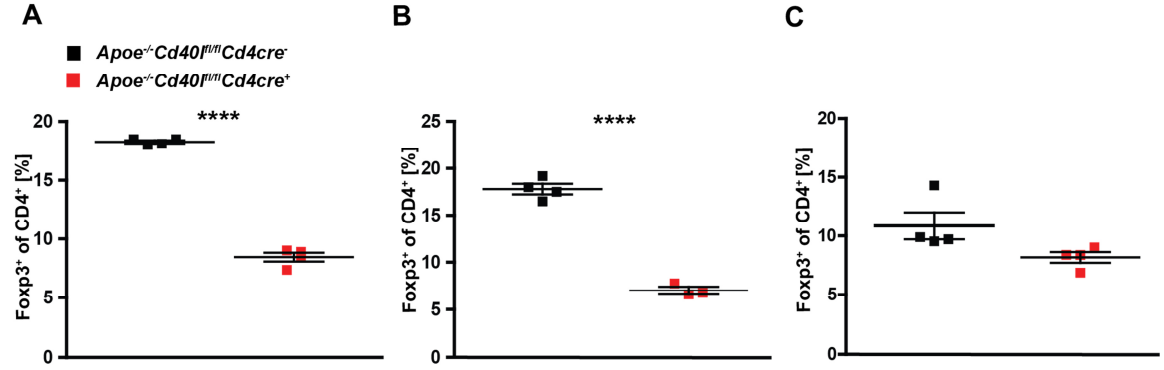

Figure 14. Loss of T cell-specific CD40L decreases systemic and aortic Treg abundance in diet-induced atherosclerosis.
Flow cytometry analysis of Foxp3+ cell distribution in cell suspensions from spleen, lymph nodes and blood from *Apoe$^{-/-}$Cd40l$^{fl/fl}$ Cd4Cre$^+$* or *Apoe$^{-/-}$Cd40l$^{fl/fl}$Cd4Cre$^-$* mice after consuming a hypercholesterolemic diet for 6 weeks. Analysis of (**A**) lymphoid, (**B**) splenic and blood cells (**C**), n= 4 (both groups). Data is presented as mean±SD. ****=p<0.00=1

To investigate whether the systemic and local reduction of Treg numbers in blood, lymphoid organs, and aortic lesions may be a consequence of decreased development or a higher apoptotic rate of these cells, thymic cell suspensions were assessed by flow cytometry. These

analyses revealed significantly decreased numbers of thymic Foxp3$^+$ cells in *Apoe*$^{-/-}$*Cd40l*$^{fl/fll}$*Cd4Cre*$^+$ mice. Both developmental stages of CD4$^+$Tregs, namely CD25$^-$Foxp3$^+$ and CD25$^+$Foxp3$^+$ cells, were significant reduced in *Apoe*$^{-/-}$*Cd40l*$^{fl/fll}$*Cd4Cre*$^+$ animals when compared to their littermate controls (Figure 15 A, B). These results suggest a role for T cell-specific CD40L in the induction and maturation of CD4$^+$Tregs.

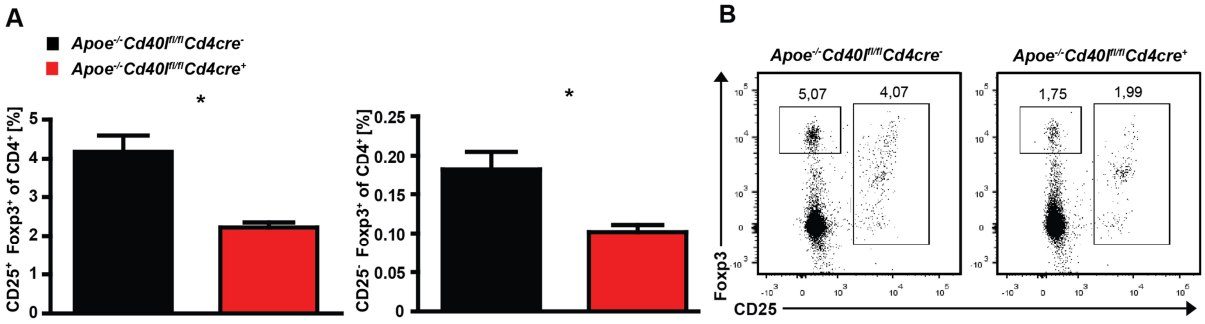

Figure 15. Lack of CD40L on T cells reduces thymic Treg abundance.
Abundance of thymic CD4$^+$Cd25$^+$Foxp3$^+$ cells and CD4$^+$CD25$^-$Foxp3$^+$ cells in *Apoe*$^{-/-}$*Cd40l*$^{fl/fll}$*Cd4Cre*$^-$ or *Apoe*$^{-/-}$*Cd40l*$^{fl/fll}$*Cd4Cre*$^+$ mice assayed by flow cytometry. (**A**) Quantification of percentage of CD4$^+$CD25$^+$Foxp3$^+$ cells (right) and CD4$^+$CD25$^-$Foxp3$^+$ cells (left). (**B**) Representative plots gated on living CD4$^+$ cells are displayed. n=5 for both genotypes. Data is presented as mean±SD.*=p<0.01

The reduced number of Treg and precursors in the thymus was not accompanied by increased Annexin-V staining of CD4$^+$CD25$^+$ cells indicating a significantly decreased rate of apoptosis of Tregs in the thymus (Figure 16 A-C).

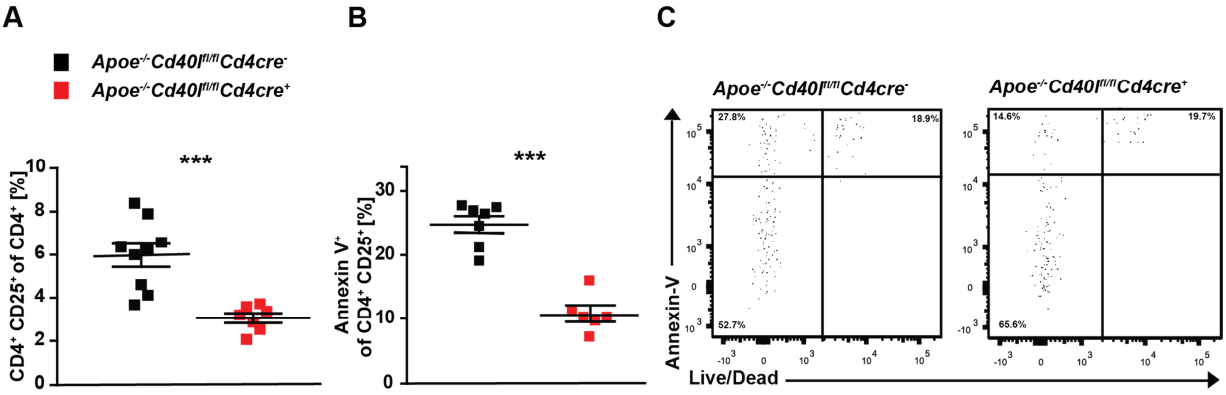

Figure 16. Lack of CD40L on T cells does not alter the apoptotic tendency of thymic Tregs.
(**A**) Quantification of thymic CD4$^+$CD25$^+$ cells in *Apoe*$^{-/-}$*Cd40l*$^{fl/fll}$*Cd4Cre*$^-$ or *Apoe*$^{-/-}$*Cd40l*$^{fl/fll}$*Cd4Cre*$^+$ mice assayed by flow cytometry. CD4$^+$CD25$^+$ cells of thymic cell suspensions were analyzed by flow cytometry for apoptosis by Annexin-V binding and Live/Dead fixable staining exclusion. Quantification (**B**) and representative plots (**C**) n=9 (*Apoe*$^{-/-}$*Cd40l*$^{fl/fll}$*Cd4Cre*$^-$); *n=6 (Apoe*$^{-/-}$*Cd40l*$^{fl/fll}$*Cd4Cre*$^+$). Data is presented as mean±SD. ***=p 0.0001-0.001

Apoe$^{-/-}$*Cd40l*$^{fl/fll}$*Cd4Cre*$^+$ mice showed a strong reduction of Tregs. However, this phenotype appeared non-linked to a higher atherosclerotic burden or a pro-inflammatory plaque phenotype as reflected in smaller lesion size and decreased numbers of immune cell infiltrates. In contrast and somewhat counterintuitive the reduced percentage of anti-inflammatory Tregs was accompanied by smaller, more stable lesions in both mild and accelerated atherosclerosis.

Accordingly, we hypothesized that the mild anti-inflammatory and anti-atherosclerotic plaque phenotype may relate to an improved suppressive capacity per single Treg in *Apoe*$^{-/-}$*Cd40l*$^{fl/fll}$*Cd4Cre*$^{+}$ mice. To validate our assumptions we performed a suppression assay by co-culturing CFSE-labeled and anti-CD3/CD28-stimulated CD4^{+} T cells with varying numbers of Tregs from *Apoe*$^{-/-}$*Cd40l*$^{fl/fll}$*Cd4Cre*$^{-}$ or *Apoe*$^{-/-}$*Cd40l*$^{fl/fll}$*Cd4Cre*$^{+}$ mice. Notably, flow cytometric analysis of CSFE dilution after 72 hours did not show any difference in the fraction of divided conventional T cells, indicating a similar suppressive capacity between wildtype- and CD40L-deficient Tregs (Figure 17 A).

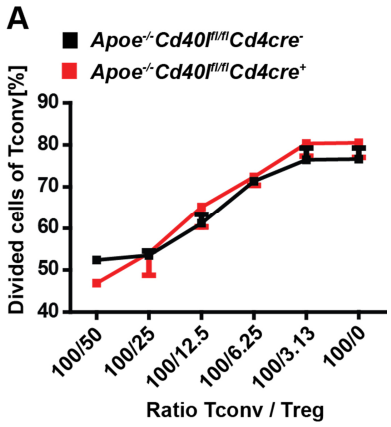

Figure 17. T cell-specific deficiency of CD40L does not influence the suppressive capacity of Treg cells.
Varying numbers of Tregs isolated from spleen of *Apoe*$^{-/-}$*Cd40l*$^{fl/fll}$*Cd4Cre*$^{-}$ or *Apoe*$^{-/-}$*Cd40l*$^{fl/fll}$*Cd4Cre*$^{+}$ mice were co-cultured with CFSE labeled CD4^{+}CD25^{-} conventional responder T cells from *Apoe*$^{-/-}$*Cd40l*$^{fl/fll}$*Cd4Cre*$^{-}$ mice and anti CD3/Cd28 stimulatory beads for 72 hours. CFSE dilution was measured and frequency of divided responder T cells is displayed. n=5 (*Apoe*$^{-/-}$*Cd40l*$^{fl/fl}$*Cd4Cre*$^{-}$*);* n= 5 *(Apoe*$^{-/-}$*Cd40l*$^{fl/fl}$*Cd4Cre*$^{+}$*).* Data is presented as mean±SD.

To recapitulate this section, we can state that the analysis of the abundance and fitness from systemic and thymic Tregs from *Apoe*$^{-/-}$*Cd40l*$^{fl/fll}$*Cd4Cre*$^{+}$ mice showed a decrease in Treg numbers, yet, their suppressive activity and apoptotic phenotype remained unchanged.

3.4 T cell-specific deletion of CD40L results in an anti-inflammatory phenotype and reduced T effector cell function due to systemically decreased concentration of IL-2

Despite of diminished abundance of Tregs, the plaque size in *Apoe*$^{-/-}$*Cd40l*$^{fl/fll}$*Cd4Cre*$^{+}$ mice was decreased. Therefore, we investigated whether the reduction of lesional CD4^{+} T cell- and Treg numbers were caused by, or resulted in changes of pro-inflammatory genes. Accordingly, we analyzed gene expression in lymph node and spleen of *Apoe*$^{-/-}$*Cd40l*$^{fl/fll}$*Cd4Cre*$^{-}$ or *Apoe*$^{-/-}$*Cd40l*$^{fl/fll}$*Cd4Cre*$^{+}$ mice at 28 weeks of age revealing a widespread modification of pro- and anti-inflammatory gene distribution in mice lacking CD40L on T cells (Figure 18 A, B).
The changes in expression pattern were accompanied by a markedly reduced expression of the *Cd4* gene. Furthermore *Cd69* as a marker for T cell activation was weakly expressed in mRNA in lymph node and spleen of *Apoe*$^{-/-}$*Cd40l*$^{fl/fll}$*Cd4Cre*$^{+}$ mice after 28 weeks of chow diet. We also

analyzed *Il2* mRNA levels finding a significant reduction of *Il2* expression in lymph node and spleen of *Apoe*$^{-/-}$*Cd40l*$^{fl/fll}$*Cd4Cre*$^{+}$ mice (Figure 21 A, B). Concurrently to the decremented expression of T cell-associated genes *Cd4*, *Cd69* and, *Il2* the pro-inflammatory Th1-associated genes *Ifng*, *Tnfa,* and *Il1b* also showed a significantly reduced expression in lymph nodes and spleen of mice lacking CD40L on CD4^{+} cells. In addition, the expression of the pro-inflammatory cytokine *Il12p35* was equally disturbed in lymphatic organs of *Apoe*$^{-/-}$*Cd40l*$^{fl/fll}$*Cd4Cre*$^{+}$ mice (Figure 18 A, B). In contrast, expression analysis of lymph node and spleen from *Apoe*$^{-/-}$ *Cd40l*$^{fl/fll}$*Cd4Cre*$^{+}$mice revealed a significant increase in the anti-inflammatory cytokines *Il10* and *Tgfb*. The diminished number of Tregs, as seen by flow cytometry (Figure 17 and 18) and the impaired expression of *Cd4*, was supported by the significantly reduced expression of the Treg-associated *Foxp3* gene (Figure 18 A, B).

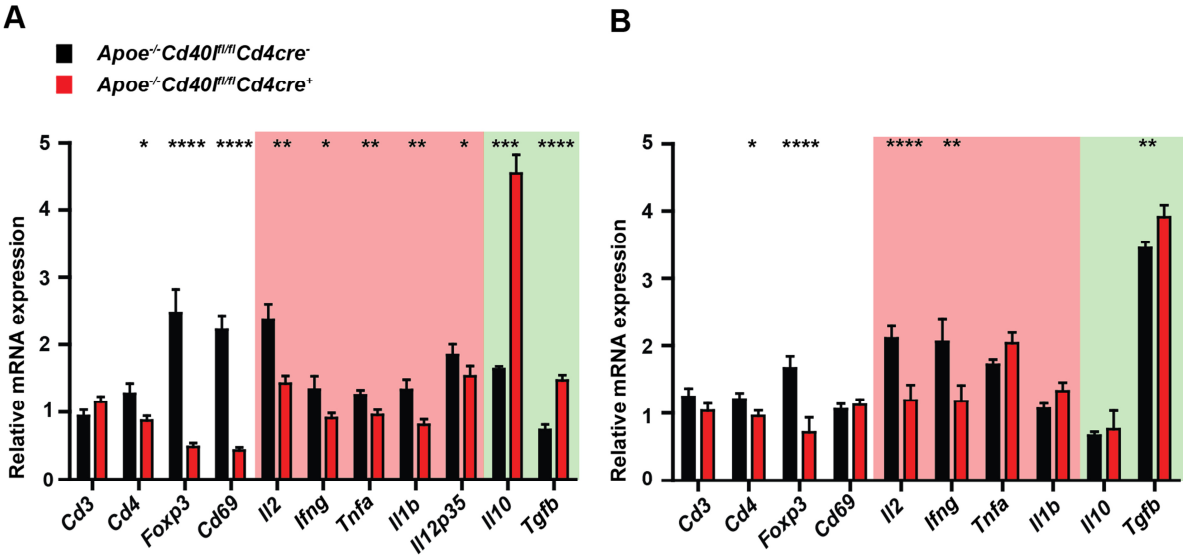

Figure 18. T cell-specific deletion of CD40L causes shift to a more anti-inflammatory milieu.
Relative mRNA expression analyzed by quantitative PCR in lymph nodes and spleen of male 28 weeks old *Apoe*$^{-/-}$ *Cd40l*$^{fl/fll}$*Cd4cre*$^{-}$ or *Apoe*$^{-/-}$*Cd40l*$^{fl/fll}$*Cd4cre*$^{+}$ mice. Red rectangles symbolize pro-inflammatory genes, green rectangle symbolizes anti-inflammatory genes. Relative mRNA expression in (**A)** lymph node and in (**B**) spleen of male 28 weeks old *Apoe*$^{-/-}$*Cd40l*$^{fl/fll}$*Cd4Cre*$^{-}$ or *Apoe*$^{-/-}$*Cd40l*$^{fl/fll}$*Cd4Cre*$^{+}$ mice. n=13-17(*Apoe*$^{-/-}$*Cd40l*$^{fl/fll}$*Cd4Cre*$^{-}$*);* n= 16-19 *(Apoe*$^{-/-}$*Cd40l*$^{fl/fll}$*Cd4Cre*$^{+}$*).* Data is presented as mean±SD. *=p<0.01;**=p<0.001;***=p 0.0001-0.001;****=p<0.0001

Taken together these data indicate an altered inflammatory phenotype in *Apoe*$^{-/-}$*Cd40l*$^{fl/fll}$*Cd4Cre*$^{+}$ mice, compared to littermate controls. This was demonstrated by the down regulation of inflammatory gene expression, the upregulation of anti-inflammatory genes and an altered activation status of the T cell and Treg population. The data of the immunohistological analyses, flow cytometry measurements and gene expression assays all suggested an altered T cell phenotype. Hence, we hypothesized that the reduced T cell abundance was due to an impaired reactivity of these cells. To test for changes in proliferation of T cells from *Apoe*$^{-/-}$*Cd40l*$^{fl/fll}$*Cd4Cre*$^{+}$ mice compared to littermate control, an *in vitro* proliferation assay was performed (Figure 19 A-D). Anti-CD3 and anti-CD28 stimulation (72h) was used to mimic the

interaction with antigen-presenting cells via TCR-Ligation and costimulation *in vivo*. Upon this stimulation, flow cytometric measurements of CFSE dilution in activated T cells and the calculation of a proliferation-index as a marker of cell-expansion demonstrated comparable values between *Apoe*$^{-/-}$*Cd40l*$^{fl/fll}$*Cd4cre*$^{-}$ and *Apoe*$^{-/-}$*Cd40l*$^{fl/fll}$*Cd4cre*$^{+}$ mice (Figure 19 A). The indistinguishable proliferation is also reflected by representative histograms of CFSE dilution in the CD4^{+} cell population from *Apoe*$^{-/-}$*Cd40l*$^{fl/fll}$*Cd4Cre*$^{-}$ and *Apoe*$^{-/-}$*Cd40l*$^{fl/fll}$*Cd4Cre*$^{+}$ mice (Figure 19 B). The percentage of cells per stage of division did also not reveal any differences in the proliferation pattern between *Apoe*$^{-/-}$*Cd40l*$^{fl/fll}$*Cd4Cre*$^{-}$ and *Apoe*$^{-/-}$*Cd40l*$^{fl/fll}$*Cd4Cre*$^{+}$ mice (Figure 19 C). Based on the fact that the majority of T cells responds to IL-2, and produce it upon activation, differences in responsiveness in a proliferative assay can be partially reflected by differences in IL-2 production by the responding T cells[311]. Indeed, ELISA of the cell culture supernatant of the cultured T cells revealed, that the concentration of IL-2 also did not differ between T cells isolated from *Apoe*$^{-/-}$*Cd40l*$^{fl/fll}$*Cd4Cre*$^{-}$ and *Apoe*$^{-/-}$*Cd40l*$^{fl/fll}$*Cd4Cre*$^{+}$ mice (Figure 19 D).

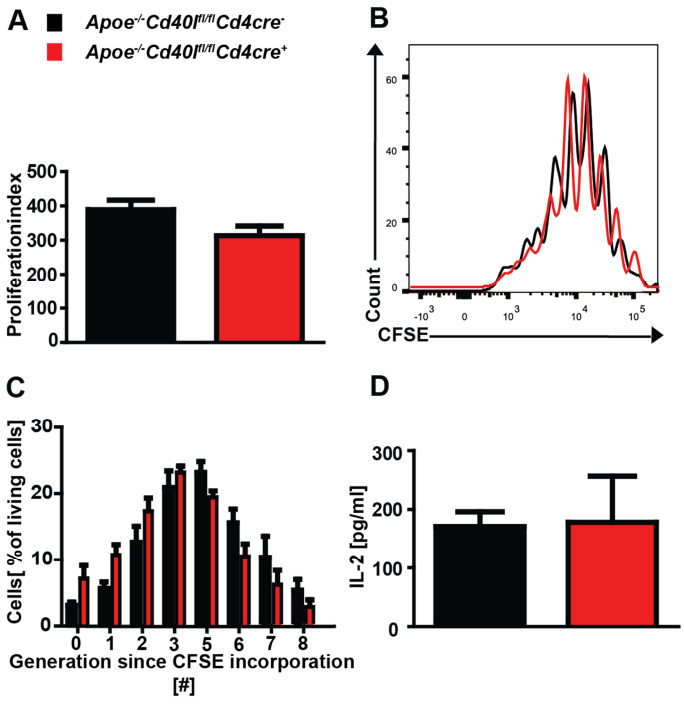

Figure 19. Lack of T cell-specific CD40L does not influence *in vitro* proliferation of CD4^{+} cells.
In vitro proliferation assay of Cd4^{+} cells of *Apoe*$^{-/-}$*Cd40l*$^{fl/fll}$*Cd4cre*$^{-}$ or *Apoe*$^{-/-}$*Cd40l*$^{fl/fll}$*Cd4Cre*$^{+}$ mice. CD4^{+} cells isolated from spleen of *Apoe*$^{-/-}$*Cd40l*$^{fl/fll}$*Cd4Cre*$^{-}$ or *Apoe*$^{-/-}$*Cd40l*$^{fl/fll}$*Cd4Cre*$^{+}$ mice were labeled with CFSE and cultured anti CD3/CD28-stimulatory beads for 72 hours. CFSE dilution was measured and frequency of divided CD4^{+} cells displayed. (**A**) Quantification of proliferation capacity displayed as proliferation index (fold expansion over the culture time). (**B**) Representative histograms for CFSE dilution of *Apoe*$^{-/-}$*Cd40l*$^{fl/fll}$*Cd4Cre*$^{-}$ and *Apoe*$^{-/-}$*Cd40l*$^{fl/fll}$*Cd4Cre*$^{+}$ CD4^{+} cells. (**C**) Alternative format to display CFSE dilution in CD4^{+} cells. (**D**) Quantification of IL-2 concentration via ELISA in cell culture supernatant after 72 hours. n=5 (*Apoe*$^{-/-}$*Cd40l*$^{fl/fl}$*Cd4Cre*$^{-}$*);* n= 5 *(Apoe*$^{-/-}$*Cd40l*$^{fl/fl}$*Cd4Cre*$^{+}$*)*. Data is presented as mean±SD.190

Taken together, in these antigen-unspecific proliferation assays we were not able to detect differences in the proliferation or in the IL-2 production of CD4^{+} cells from *Apoe*$^{-/-}$*Cd40l*$^{fl/fll}$*Cd4Cre*$^{-}$ and *Apoe*$^{-/-}$*Cd40l*$^{fl/fll}$*Cd4Cre*$^{+}$ mice.

The capability of T cells to proliferate and maintain cell-specific functions after exogenous CD28/CD3 stimulation appears unchanged in *Apoe*$^{-/-}$*Cd40l*$^{fl/fll}$*Cd4Cre*$^{+}$ mice. We questioned if the activation status of those cells differs in the two models of atherosclerosis previously employed.

By analyzing the CD62L-distribution on $CD4^+$ cells in cell suspensions of lymph nodes and spleen by flow cytometric measurements we were able to detect that $CD4^+$ cells of $Apoe^{-/-}Cd40l^{fl/fll}Cd4cre^+$ mice exposed a higher percentage of $CD62L^+$ cells after 28 weeks of age (Figure 20 A, B, C).

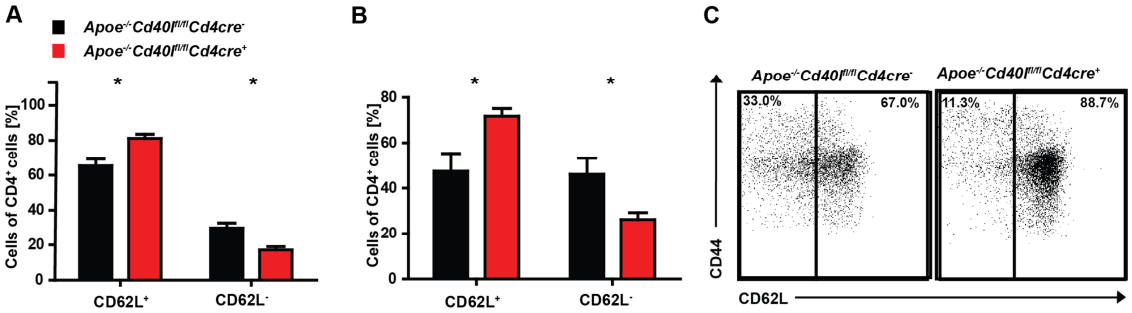

Figure 20. Lack of CD40L on T cells leads to a reduced number of activated $CD4^+$T cells.
Flow cytometric measurements of $CD4^+$ cell populations in lymph nodes and spleen of male 28 weeks old *$Apoe^{-/-}Cd40l^{fl/fll}Cd4Cre^-$* or *$Apoe^{-/-}Cd40l^{fl/fll}Cd4Cre^+$*mice. Abundance of $CD4^+$subtypes in (**A**) lymph nodes and (**B**) spleen of *$Apoe^{-/-}Cd40l^{fl/fll}Cd4Cre^-$* or *$Apoe^{-/-}Cd40l^{fl/fll}Cd4Cre^+$* mice assayed by flow cytometry. Representative plots gated on living $CD4^+$ cells (**C**) are displayed. n=13-17 (*$Apoe^{-/-}Cd40l^{fl/fll}Cd4Cre^-$); n= 17-19 ($Apoe^{-/-}Cd40l^{fl/fl}$ $Cd4Cre^+$).* Data is presented as mean±SD. *=p<0.01

CD62L is also expressed on subsets of $CD8^+$ cells, which can be further differentiated by their expression of CD44. The percentage of naïve ($CD62L^+CD44^-$) $CD8^+$ T cells, were significant higher in *$Apoe^{-/-}Cd40l^{fl/fll}Cd4Cre^+$* mice compared to *$Apoe^{-/-}Cd40l^{fl/fll}Cd4Cre^-$ mice*. At the same time the percentage of central memory ($CD62L^+CD44^+$) $CD8^+$ T cells and effector ($CD62L^-$ $CD44^+$) $CD8^+$ T cells were reduced (Figure 21 A-C).

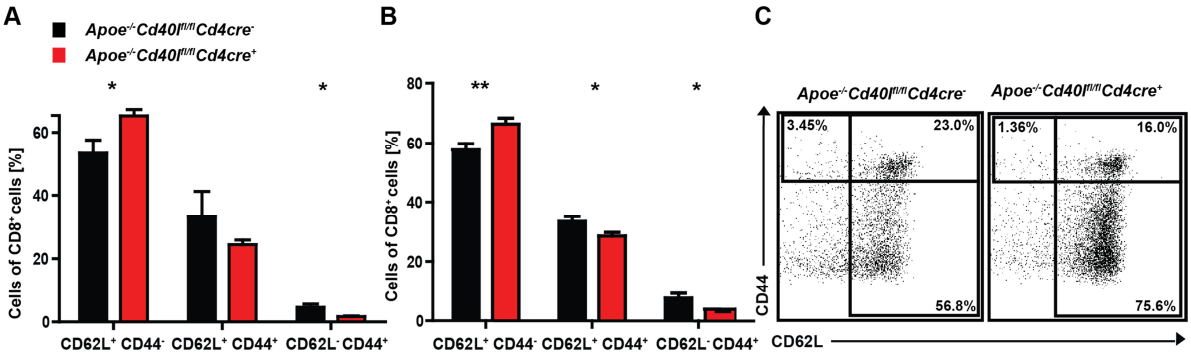

Figure 21 Lack of CD40L on $CD4^+$ cells leads to a reduced number of activated $CD8^+$T cells.
Flow cytometric measurements of $CD8^+$ T cell populations in lymph nodes and spleen of male 28 weeks old *$Apoe^{-/-}Cd40l^{fl/fll}Cd4Cre^-$* or *$Apoe^{-/-}Cd40l^{fl/fll}Cd4Cre^+$* mice. Abundance of $CD8^+$ subtypes in (**A**) lymph nodes and (**B**) spleen of *$Apoe^{-/-}Cd40l^{fl/fll}Cd4Cre^-$* or *$Apoe^{-/-}Cd40l^{fl/fll}Cd4Cre^+$* mice assayed by flow cytometry. Representative plots gated on living $CD8^+$ cells (**C**) are displayed. n=13-17 (*$Apoe^{-/-}Cd40l^{fl/fll}Cd4Cre^-$); n= 17-19 ($Apoe^{-/-}Cd40l^{fl/fl}Cd4Cre^+$).* Data is presented as mean±SD. *=p<0.01; **=p<0.001

In summary, we show that the deletion of T cell-specific CD40L results in a decrease of activated $CD4^+$ and $CD8^+$ cells and an increase of naïve cells in both T cell compartments.

3.5 T cell-specific deletion of CD40L affects B cell phenotype and decreases IgG_{2b} and IgM titers

Since our experiments showed an altered activation status in T helper and T effector cells in *Apoe*$^{-/-}$*Cd40l*$^{fl/fll}$*Cd4Cre*$^{+}$ mice we next investigated whether the specific interaction of antigen-binding and -presenting B cells and helper T cells is influenced. CD40 signaling by B cells is required for the generation of high titers of isotype-switched, high affinity antibody and for the development of humoral immune memory. The engagement of CD40 expressed on the surface of antigen-activated B cells by CD40L expressed on activated $CD4^{+}$ T cells is essential for the initiation and progression of a thymus-dependent humoral immune response[236]. *In vivo*, CD40 engagement is required for germinal center formation and progression, as well as antibody isotype switching and affinity maturation. These processes are essential for the generation of memory B cells and long-lived plasma cells[246,312]. Accordingly, we investigated the alterations of phenotypes, i.e. differentiation and activation, of B cells upon T cell-specific deletion of CD40L. In a first step we analyzed the general abundance of immunoglobulin subclasses in the plasma of atherosclerotic mice with a multiplex bead-based assay. Indeed, hyperlipidemic mice with a deficiency of CD40L on T cells displayed decreased titers of IgG_{2b}, IgE and IgM (Figure 22).

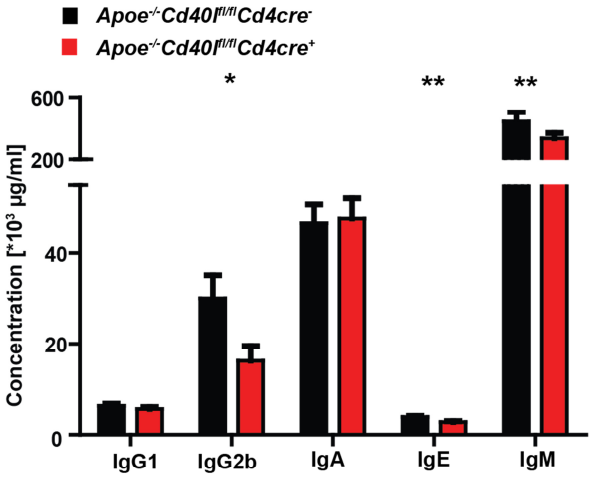

Figure 22. T cell-specific CD40L deficiency decreases IgG_{2b} and affects IgM plasma abundance.
Antibody abundance in plasma of 28 week old *Apoe*$^{-/-}$*Cd40l*$^{fl/fll}$*Cd4Cre*$^{+}$ and *Apoe*$^{-/-}$*Cd40l*$^{fl/fll}$*CdC4Cre*$^{-}$ mice as analyzed by murine multiplex bead-based technology detection antibodies. Plasma level expression for respective Ig of 28 week old *Apoe*$^{-/-}$*Cd40l*$^{fl/fll}$*Cd4Cre*$^{+}$ and *Apoe*$^{-/-}$*Cd40l*$^{fl/fll}$*Cd4Cre*$^{-}$ mice analyzed by multiplex bead-based technology n=10 (both groups). Data is presented as mean±SD. *=p<0.01; **=p<0.001

Since the general concentration of immunoglobulin subclasses does not allow predictions about reactivity and concentration of Ig specifically binding atherosclerosis-associated antigens, such as oxLDL, we performed specific ELISA detecting oxLDL-binding immunoglobulins in plasma (Figure 23 A, B). We detected significant less oxLDL-specific total IgG, total IgG_{2b} and IgM in the plasma of *Apoe*$^{-/-}$*Cd40l*$^{fl/fll}$*Cd4Cre*$^{+}$ mice (Figure 23 A). These results indicated decreased abundance of Ig subclasses which are considered as both pro-atherogenic (e.g. total IgG) and anti-atherogenic (e.g. IgM).

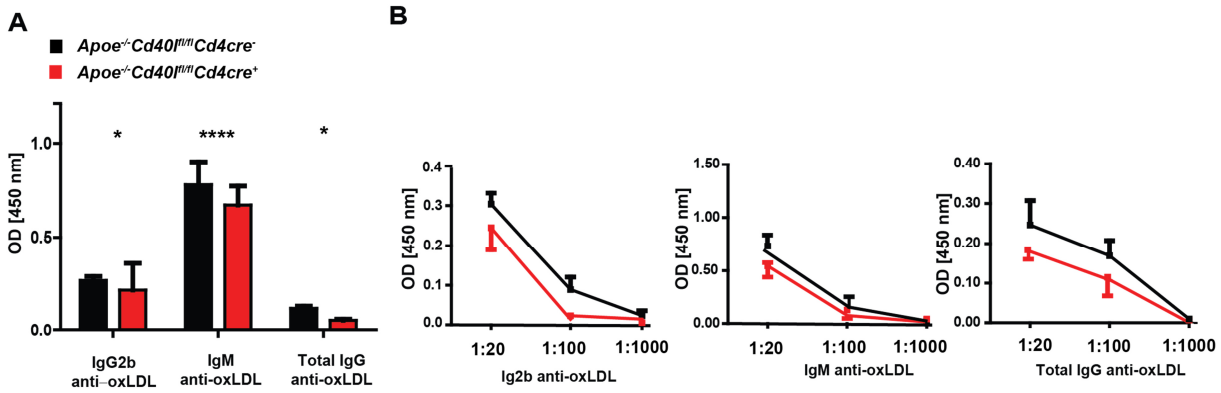

Figure 23. T cell-specific CD40L deficiency decreases oxLDL specific-IgG2b and oxLDL specific total IgG plasma abundance.
Antibody abundance in plasma of 28 week old *Apoe*$^{-/-}$*Cd40l*$^{fl/fl}$*Cd4Cre*$^{+}$ and *Apoe*$^{-/-}$*Cd40l*$^{fl/fl}$*Cd4Cre*$^{-}$ mice as analyzed by ELISA and respective murine detection antibodies. (**A**) Plasma abundance of antibodies detecting oxLDL of 28 week old *Apoe*$^{-/-}$*Cd40l*$^{fl/fl}$*Cd4Cre*$^{+}$ and *Apoe*$^{-/-}$*Cd40l*$^{fl/fl}$*Cd4Cre*$^{-}$ mice. Quantification for optic density acquired at 450nm wavelength of 1:20 diluted plasma is displayed. (**B**) Dilution series (1:20, 1:100; 1:1000) of plasma and respective ODs are displayed for each antibody. n=10 (*Apoe*$^{-/-}$*Cd40l*$^{fl/fl}$*Cd4Cre*$^{-}$);n=10 (*Apoe*$^{-/-}$*Cd40l*$^{fl/fl}$*Cd4cre*$^{+}$). Data is presented as mean±SD. *=p<0.01; ****=p<0.0001

In a seccond step we assessed the B cell phenotypes in spleens of *Apoe*$^{-/-}$*Cd40l*$^{fl/fl}$*Cd4Cre*$^{+}$ mice with particular focus on their content of marginal zone and follicular B cells. Follicles are always adjacent to T cell zones and this arrangement allows activated follicular B cells and activated T helper cells to migrate towards each other and interact at the interface of these two areas [135,136,138]. Hence, follicular B cells are particularly well-suited to participate in T cell-dependent immune responses to protein antigens. IgD^{+}CD21$^{-/low}$ or conventional follicular B cells undergo isotype switching and affinity maturation in the spleen and lymph nodes in response to T cell-dependent antigens and become either plasma cells that secrete large amounts of antibody, or memory B cells with the ability to produce specific antibodies upon re-exposure to the same antigen[135,136,138]. IgD^{-}CD21^{low} marginal zone B cells reside in the marginal sinus of the white pulp in the spleen and are positioned to immediately respond to antigens in the blood that are filtering through the spleen[139].

The analyses revealed an increased abundance of total B cells, a decreased percentage of follicular B cells and concordantly an increased percentage marginal zone B cells in spleen of *Apoe*$^{-/-}$*Cd40l*$^{fl/fl}$*Cd4Cre*$^{+}$mice (Figure 24 A,B).

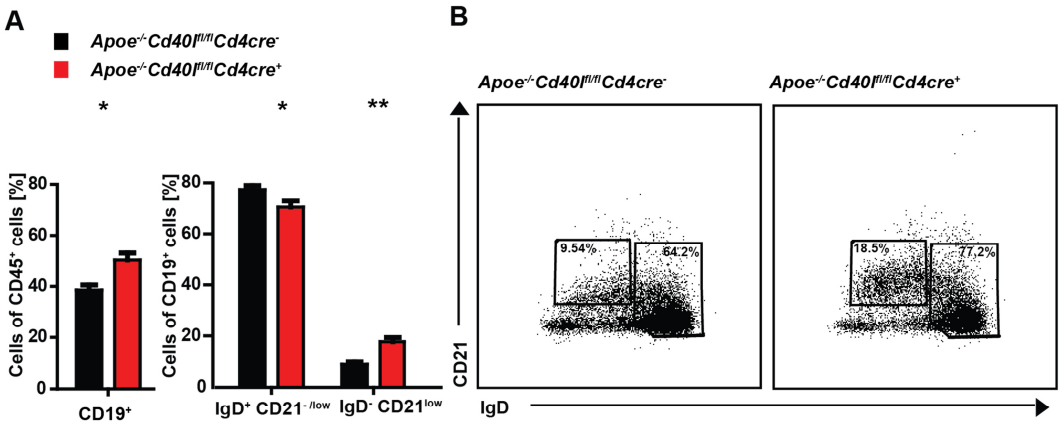

Figure 24. Lack of CD40L on T cells alters B-cell abundance and affects B cell composition.
(A) Abundance of $CD19^+$ $IgD^+CD21^{-/low}$ (follicular B cells) and IgD^-CD21^{low} (marginal zone B cells) in spleen of *Apoe*$^{-/-}$*Cd40l*$^{fl/fl}$*Cd4cre*$^-$ or *Apoe*$^{-/-}$*Cd40l*$^{fl/fl}$*Cd4Cre*$^+$ mice assayed by flow cytometry. (**B**) Representative plots gated $CD19^+$cells. n=10 (*Apoe*$^{-/-}$*Cd40l*$^{fl/fl}$*Cd4Cre*$^-$*);* n= 10 *(Apoe*$^{-/-}$*Cd40l*$^{fl/fl}$ *Cd4Cre*$^+$*)*.Data is presented as mean±SD. *=p<0.01; **=p<0.001

In sumary, we demonstrated that the lack of CD40L on Tcells led to changes in the B cell population with an increased abundance of B cells and marginal zone B cells. Changes in the B cell population co-incided with overall decreased plasma level of antigen-specific and -unspecific immunoglobulins in *Apoe*$^{-/-}$*Cd40l*$^{fl/fl}$*Cd4Cre*$^+$mice.

3.6 T cell-specific deletion of CD40L results in an impaired antigen presentation in an in vivo model of antigen-specific DC-dependent T cell activation.

Our analyses of the T and B cell population in *Apoe*$^{-/-}$*Cd40l*$^{fl/fl}$*Cd4Cre*$^-$ and *Apoe*$^{-/-}$*Cd40l*$^{fl/fl}$*Cd4Cre*$^+$ mice revealed profound discrepancies in abundance, phenotype, and activation status of those cells. Both cell types are normally tightly connected with DCs via different signals such as TCR, BCR and costimulatory molecules (e.g. CD40-CD40L). To clarify the changes in the relationship between T cells, B cells and DCs we employed an additional *in vivo* model.

Contact hypersensitivity (CHS) relies exclusively on the proper function of antigen presentation between T cells and DCs including efficient antigen capture in the skin, antigen processing, transport to lymphoid tissues such as the draining lymph nodes, and antigen presentation to naïve T cells[31,313,314]. Several studies recently suggested that CD40-CD40L interaction is required during the T cell-mediated and -dependent CHS responses[314,315].

The procedure (i.e. exposure of epidermal cells to exogenous hapten) results in a delayed-type hypersensitivity reaction that can be measured and quantified. The Langerhans cell (LC), a skin-restricted DC subpopulation, is the critical antigen-scavenging and presenting cell in this model.

LCs initiate sensitization to Th1-specific haptens (e.g.DNFB) by presenting antigens to $CD4^+$ T lymphocytes which, in turn, secrete lymphokines and recruit other cells to the site of the reaction. To investigate the involvement of T cell-specific CD40L in this process we examined DNFB-induced CHS in *Apoe*$^{-/-}$*Cd40l*$^{fl/fl}$*Cd4Cre*$^-$ and *Apoe*$^{-/-}$*Cd40l*$^{fl/fl}$*Cd4Cre*$^+$ mice. Twenty-four hours after re-challenging ears of DNFB-sensitized *Apoe*$^{-/-}$*Cd40l*$^{fl/fl}$*Cd4cre*$^-$ and *Apoe*$^{-/-}$*Cd40l*$^{fl/fl}$*Cd4Cre*$^+$ mice were excised for histological analysis. We identified that CHS was reduced in *Apoe*$^{-/-}$ *Cd40l*$^{fl/fl}$*Cd4Cre*$^+$ mice, evoked by less cellular inflammatory infiltrate and less edema in the dermal tissue of the ear of DNFB-sensitized and -challenged *Apoe*$^{-/-}$*Cd40l*$^{fl/fl}$*Cd4Cre*$^+$ mice (Figure 25 A, B).

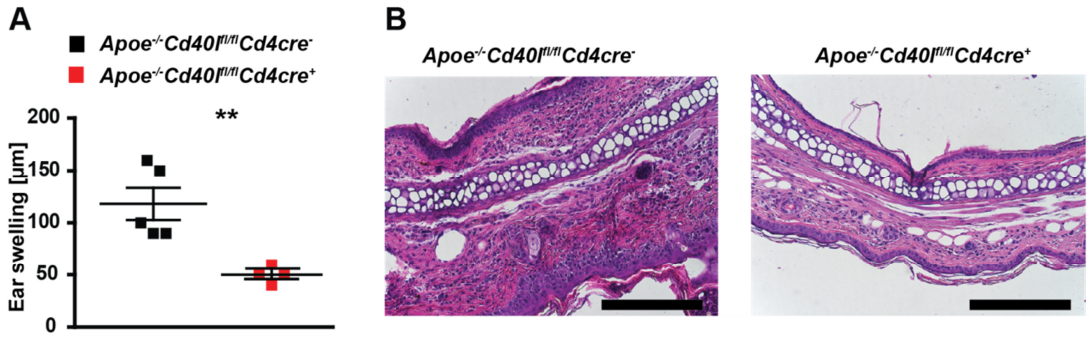

Figure 25. DNFB-induced CHS response is attenuated in mice lacking CD4 specific CD40L.
Physiologic and histologic assessment of ears during induction of CHS, in response to DNFB. (**A**) Changes in the ear measurements 24 hours after DNFB challenge of sensitized *Apoe*$^{-/-}$*Cd40l*$^{fl/fl}$*Cd4Cre*$^-$ or *Apoe*$^{-/-}$*Cd40l*$^{fl/fl}$*Cd4Cre*$^+$ mice. Data represent changes in ear thickness of the untreated ear versus the sensitized ear of each animal. (**B**) Representative histological analysis of hematoxylin-and-eosin-stained ear tissues of *Apoe*$^{-/-}$*Cd40l*$^{fl/fl}$*Cd4cre*$^-$ or *Apoe*$^{-/-}$ *Cd40l*$^{fl/fl}$*Cd4Cre*$^+$ mice. n=5 (*Apoe*$^{-/-}$*Cd40l*$^{fl/fl}$*Cd4Cre*$^-$*);* n= 5 *(Apoe*$^{-/-}$*Cd40l*$^{fl/fl}$ *Cd4Cre*$^+$*).* Scale bar = 200 µm. Data is presented as mean±SD. **=p<0.001

These results indicate that CD40L-expressing T cells are required for CHS responses to DNFB. To further investigate the underlying mechanisms, that result in an impaired mounting of an antigen-specific CHS response, we performed additional flow cytometry measurements of the ear draining lymph nodes and spleens of *Apoe*$^{-/-}$*Cd40l*$^{fl/fl}$*Cd4Cre*$^-$ and *Apoe*$^{-/-}$*Cd40l*$^{fl/fl}$*Cd4Cre*$^+$ mice to characterize the T cell population in those mice. Supporting our earlier findings in atherosclerosis, the $Foxp3^+$ Treg population was significant decreased in draining lymph nodes of *Apoe*$^{-/-}$*Cd40l*$^{fl/fl}$*Cd4Cre*$^+$ mice (Figure 26 A). Further analyses of the $CD4^+$ population in lymph nodes of *Apoe*$^{-/-}$*Cd40l*$^{fl/fl}$*Cd4Cre*$^+$ mice also revealed a significantly higher percentage of $CD62L^+$ cells as well as significant decreased percentages of activated $CD62L^-CD4^+$ cells (Figure 26 C, B). Reflecting the reduced activation status of the $CD4^+$ T cells, $CD8^+$ T cells also showed a significant higher percentage of $CD62L^+CD44^-CD8^+$ cells and a decreased ratio of $CD62L^-CD44^+CD8^+$ cells in *Apoe*$^{-/-}$*Cd40l*$^{fl/fl}$*Cd4Cre*$^+$ mice compared to *Apoe*$^{-/-}$*Cd40l*$^{fl/fl}$*Cd4Cre*$^-$ mice while central memory ($CD62L^+CD44^+$) $CD8^+$ T cells were unaffected (Figure 26. D-F).

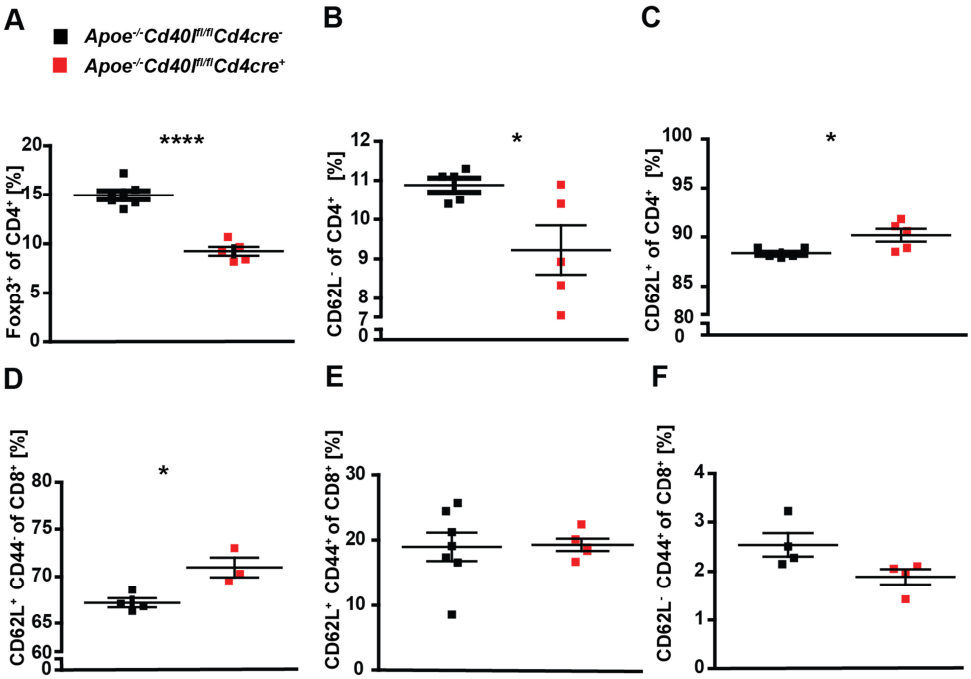

Figure 26. Deletion of CD4 specific CD40L leads to a reduced number of activated T cells and Tregs in skin induced.
Flow cytometry analysis of cell suspensions from the ear draining lymph nodes 24 hours after DNFB challenge of sensitized Apoe$^{-/-}$*Cd40l*$^{fl/fl}$*Cd4Cre*$^{+}$ or *Apoe*$^{-/-}$*Cd40l*$^{fl/fl}$*Cd4Cre*$^{-}$ mice. CD4+ cells were analyzed for their Foxp3 (**A**) and CD62L (**B, C**) distribution. CD8+ cells were analyzed for their CD44 and CD62L distribution (D, E; F). n=5 (*Apoe*$^{-/-}$*Cd40l*$^{fl/fl}$*Cd4Ccre*$^{-}$*);* n= 3-4 *(Apoe*$^{-/-}$*Cd40l*$^{fl/fl}$*Cd4Cre*$^{+}$*)*. Data is presented as mean±SD. *=p<0.01; ****=p<0.0001

We further examined the role of T cell-specific CD40L in regulating of phenotype and function of DCs. Flow cytometric analysis of draining lymph nodes from *Apoe*$^{-/-}$*Cd40l*$^{fl/fl}$*Cd4Cre*$^{-}$ and *Apoe*$^{-/-}$*Cd40l*$^{fl/fl}$*Cd4Cre*$^{+}$ mice did not reveal any differences in DC density (Figure 27 A). We therefore tested the activation status of the DCs of *Apoe*$^{-/-}$*Cd40l*$^{fl/fl}$*Cd4Cre*$^{-}$ and *Apoe*$^{-/-}$*Cd40l*$^{fl/fl}$*Cd4Cre*$^{+}$ mice and examined the effect of CD4^{+} specific deletion of CD40L on DC costimulatory expression and detected differences in the expression of the CD40-CD40L-dependent costimulatory molecules CD86 and OX40L (Figure 27 B, C). The presumably CD40/CD40L-independent expression of the costimulatory molecule CD70 appeared unchanged between *Apoe*$^{-/-}$*Cd40l*$^{fl/fl}$*Cd4cre*$^{-}$ and *Apoe*$^{-/-}$*Cd40l*$^{fl/fl}$*Cd4cre*$^{+}$ mice (Figure 27 B, C).

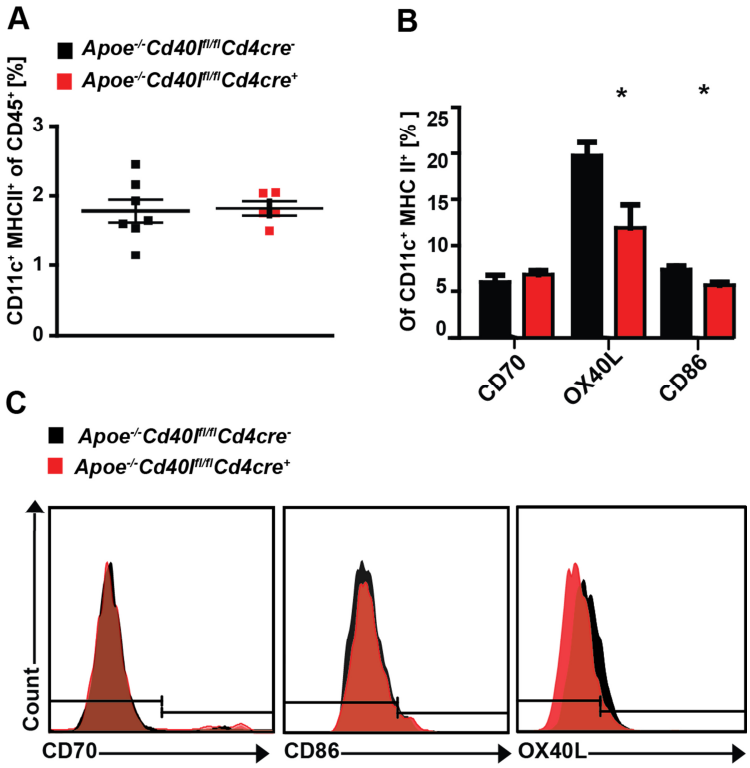

Figure 27. Lack of T cell-specific CD40L does not change DC numbers but reduces the expression of the costimulatory molecules OX40L and CD86.
Flow cytometry analysis of cell suspensions from ear draining lymph nodes 24 hours after DNFB challenge of sensitized *Apoe*$^{-/-}$*Cd40l*$^{fl/fl}$ *Cd4Cre*$^{+}$ or *Apoe*$^{-/-}$*Cd40l*$^{fl/fl}$*Cd4Cre*$^{-}$ mice. (**A**) DC percentage and (**B**) costimulatory molecule expression on DCs of *Apoe*$^{-/-}$*Cd40l*$^{fl/fl}$ *Cd4Cre*$^{+}$ *or Apoe*$^{-/-}$*Cd40l*$^{fl/fl}$*Cd4Cre*$^{-}$ *mice* were analyzed. (**C**) Representative flow cytometric histograms depicting CD70, CD86 and OX40L expression on DCs. n=7 (*Apoe*$^{-/-}$*Cd40l*$^{fl/fl}$*Cd4Cre*$^{-}$*);* n= 5 *(Apoe*$^{-/-}$ *Cd40l*$^{fl/fl}$ *Cd4Cre*$^{+}$*)*. Data is presented as mean±SD. *=p<0.01

In a second approach, we tested whether the unchanged abundance of DCs coincides with unaltered distribution of DC subtypes. Indeed, we detected an increased abundance of CD8^{-} CD11b^{+} DCs, and concordantly a decreased percentage CD8^{+}CD11b^{-} DCs in lymph nodes of *Apoe*$^{-/-}$*Cd40l*$^{fl/fl}$*Cd4Cre*$^{+}$ mice compared to controls 24 hours after DNFB-challenge (Figure 28 A, B).

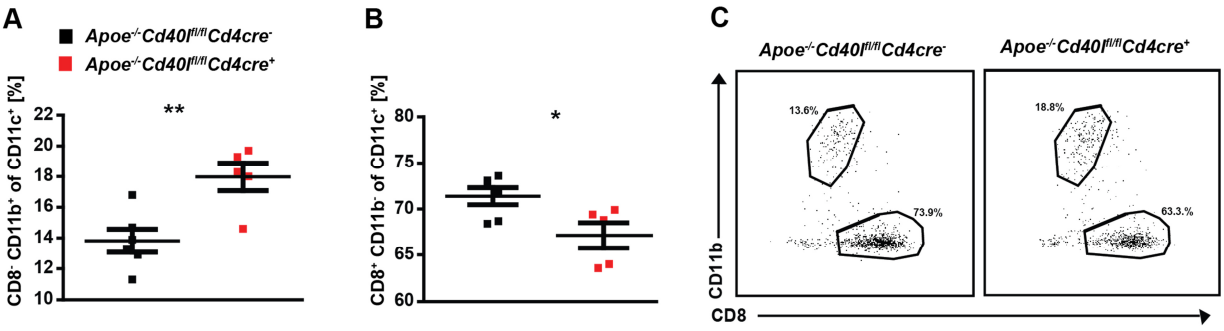

Figure 28. T cell-specific deletion of CD40L alters the ratio of CD8^{+}CD11b^{-} to CD8^{-} CD11b^{+} DCs in hapten induced hypersensitivity.
Flow cytometric measurement of the abundance of CD8^{-}CD11b^{+} and CD8^{+}CD11b^{-} in cell suspensions from ear-draining lymph nodes 24 hours after DNFB challenge of sensitized *Apoe*$^{-/-}$*Cd40l*$^{fl/fl}$*Cd4Cre*$^{+}$ or *Apoe*$^{-/-}$ *Cd40l*$^{fl/fl}$*Cd4Cre*$^{-}$ mice. Percentage of (A) CD8^{+}CD11b^{-} DCs and of (**B**) CD8^{-}CD11b^{+} DCs. (**C**) Representative flow cytometric plots pre-gated on CD11c+MHCII^{+} cells. n=5 (both groups). Data is presented as mean±SD. *=p<0.01; **=p<0.001

In summary, the activation status and morphology but not the frequency of DCs was changed in ear-draining lymph nodes between *Apoe*$^{-/-}$*Cd40l*$^{fl/fl}$*Cd4Cre*$^{-}$ and *Apoe*$^{-/-}$*Cd40l*$^{fl/fl}$*Cd4Cre*$^{+}$ mice suggesting that T cell-specific CD40L is dispensable for the generation while it is essential for the activation and maturation of T cell-stimulating CD8^{+}CD11b^{-} DCs.

3.7 DC-specific deletion of CD40 decreases atherogenesis in late stage of atherosclerosis.

The studies we conducted on the role of T cell specific CD40L in atherosclerosis demonstrated that the deficiency of CD40L primarily leads to an altered activation state of T and B cells. In general, DCs play the main role in initiating antigen-specific adaptive immune responses especially via T cell activation[32,316]. Hence, we focused on the deficiency of CD40 on DC that might lead to similar results as the lack of its counterpart CD40L on T cells. Accordingly, we generated mice lacking CD40 exclusively on DCs by crossing *Apoe*$^{-/-}$*Cd40*$^{fl/fl}$ mice to *Cd11cCre*$^{+}$ mice and evaluated atherosclerosis in *Apoe*$^{-/-}$*Cd40*$^{fl/fl}$*CD11cCre*$^{+}$ and littermate control mice at 28 week of age to maintain comparability to our previous model.

Similar to our initial experiments on mice with a deficiency of CD40L on platelets or T cell we excluded any secondary effects of DC CD40 deficiency on the cholesterol metabolism or basic blood parameters.

The analyses did not exhibit any significant differences in body weight, cholesterol level and the blood count of 28 week old male *Apoe*$^{-/-}$*Cd40*$^{fl/fl}$*Cd11cCre*$^{-}$ or *Apoe*$^{-/-}$*Cd40l*$^{fl/fl}$*Cd11cCre*$^{+}$-mice indicating that CD40 deficiency on DCs does not interfere with a proper cholesterol metabolism and blood parameters (Table 9.)

	Apoe$^{-/-}$*Cd40*$^{fl/fl}$*Cd11ccre*$^{-}$		*Apoe*$^{-/-}$*Cd40*$^{fl/fl}$*Cd11ccre*$^{+}$	
Body weight [g]	30.00	±1.28	30.13	±1.88
Lymphocytes [%]	61.08	±12.17	61.58	±14.01
Monocytes [%]	5.27	±1.07	5.05	±1.90
Granulocytes [%]	33.66	±11.32	33.37	±13.06
Platelets [10^3/µl]	1228	±248	1405	±233
Erythrocytes [10^6/µl]	8.65	±0.62	8.24	±0.69
Leukocytes [10^3/µl]	4.15	±1.56	4.13	±1.77
Lymphocytes [10^3/µl]	2.60	±0.87	2.48	±0.51
Monocytes [10^3/µl]	0.18	±0.08	0.17	±0.11
Granulocytes [10^3/µl]	1.63	±0.93	1.62	±0.83
Plasma Cholesterol [mM]	3.63	±0.20	3.53	±0.26

Table 8. Body weight, hematological parameters, and plasma cholesterol content in *Apoe*$^{-/-}$*Cd40*$^{fl/fl}$ *Cd11ccre*$^{-}$ (n= 12) or *Apoe*$^{-/-}$*Cd40*$^{fl/fl}$*Cd11ccre*$^{+}$ (n= 15) mice. Data is presented as mean±SD.

The quantitative analysis of late stage atherosclerosis and under mild hypercholesteremic conditions revealed a 24% reduction in absolute and relative lesion area between *Apoe*$^{-/-}$*Cd40l*$^{fl/fl}$*Cd11cCre*$^{+}$ mice and littermate control mice at the age of 28 weeks (Figure 29 A-C).

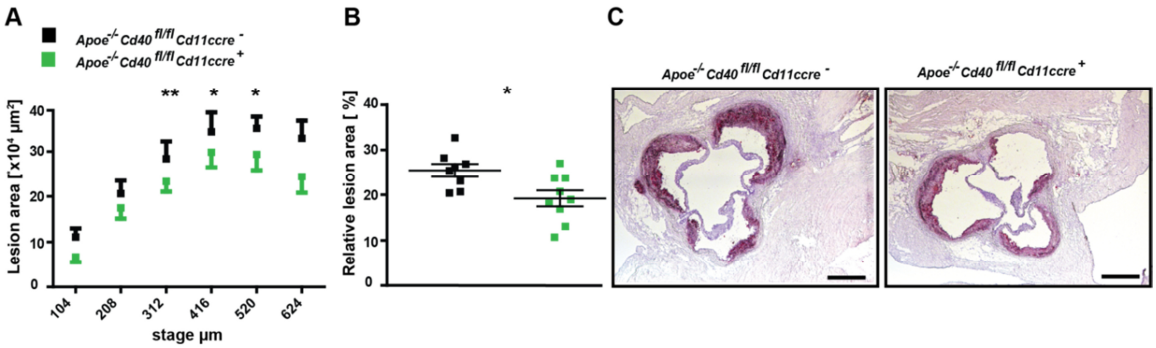

Figure 29. CD11c-specific CD40 deficiency attenuates advanced atherosclerosis.
Quantification of lesion area and atherosclerotic plaque area in cross-sections at indicated positions of the aortic root at different stages from 28-week-old, male *Apoe*$^{-/-}$*Cd40*$^{fl/fl}$*Cd11cCre*$^{-}$or *Apoe*$^{-/-}$*Cd40l*$^{fl/fl}$*Cd11Ccre*$^{+-}$mice**.** (**A**) Lesion areas in stages 104-624. (**B**) Average lesion area in stages 312-520 as percentage of total vessel area. (**C**) Representative photomicrographs of Oil Red O-stained sections; n=9 (both groups) Scale bar = 200 µm. Data is presented as mean±SD. *=p<0.01; **=p<0.001

Considering the comparability of reduction and assumed connectivity of CD40 on DCs and CD40L on T cells the next experiments addressed the question whether this alteration also involved a change in the T cell, B cell, or DC population.

3.8 DC-specific CD40 deficiency decreases systemic Treg abundance.

To examine the possible downstream impacts of the disrupted CD40-CD40L dyad between T cells and DCs in *Apoe*$^{-/-}$*Cd40l*$^{fl/fl}$*Cd11cCre*$^{+}$ mice, we determined the abundance of the Treg subpopulation. Indeed, lack of DC-specific CD40 led to significantly decreased abundance of Foxp3^{+} cells in spleen, lymph node, and blood of *Apoe*$^{-/-}$*Cd40*$^{fl/fl}$*Cd11cCre*$^{+}$ mice compared to *Apoe*$^{-/-}$*Cd40*$^{fl/fl}$*Cd11cCre*$^{-}$ controls (Figure 30 A-C).

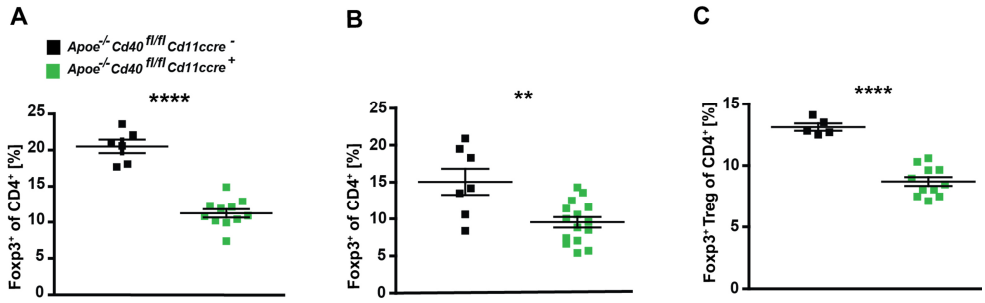

Figure 30. Loss of DC-specific CD40 decreases systemic Treg abundance.
Flow cytometric analysis of splenic, lymphoid and blood cells and immunofluorescent staining in cross-sections of the ascending aorta analyzed for Foxp3+ cells from 28 weeks old, male *Apoe*$^{-/-}$*Cd40*$^{fl/fl}$*Cd11cCre*$^{+}$ or *Apoe*$^{-/-}$*Cd40*$^{fl/fl}$*Cd11cCre*$^{-}$ mice. Flow cytometry analysis of (**A**) splenic cells, (**B**) lymphoid cells and (**C**) blood cells. n= 6-7 (*Apoe*$^{-/-}$*Cd40*$^{fl/fl}$*Cd11cCre*$^{-}$*);* n= 10-12 *(Apoe*$^{-/-}$*Cd40*$^{fl/fl}$*Cd11cCre*$^{+}$). Data is presented as mean±SD. *=p<0.01; ****=p<0.0001

Notably, the strong reduction in Tregs does not correlate to higher atherosclerotic burden, a phenomenon resembling the findings in mice with a T cell-specific CD40L deficiency.

3.9 DC-specific deletion of CD40 results in an anti-inflammatory phenotype and reduced T effector cell function due to systemically decreased concentration of IL-2

Despite diminished Tregs numbers, the lesions in *Apoe*$^{-/-}$*Cd40*$^{fl/fll}$*Cd11cCre*$^{+}$ mice were smaller in comparison to their littermate controls prompting us to examine potential mechanisms of their reduced presence by gene expression analyses of immune-relevant genes. Indeed, the examination of lymph nodes and spleen unveiled widespread modification of pro- and anti-inflammatory gene distribution in *Apoe*$^{-/-}$*Cd40*$^{fl/fll}$*Cd11cCre*$^{+}$ mice at 28 weeks of age (Figure 31 A, B). The modifications shared similarities with those already detected in spleen and lymph nodes of *Apoe*$^{-/-}$*Cd40l*$^{fl/fll}$*Cd4Cre*$^{+}$ mice (Figure 18 A, B).

The pattern of gene expression were dominated by a reduced expression of the pro-inflammatory Th1-associated genes *Ifng*, *Tnfa,* and *Il1b* in lymph node and spleen of mice lacking CD40 on CD11c^{+} cells. Furthermore, the expression of the pro-inflammatory cytokine *Il12p35* and *Il6* was also decreased in the spleen of *Apoe*$^{-/-}$*Cd40*$^{fl/fll}$*Cd11ccre*$^{+}$ mice. In contrast expression of the anti-inflammatory cytokines *Il10* and *Tgfb* was accelerated in mice lacking CD40 on DCs. The diminished number of Tregs, as seen by flow cytometry (Figure 33) and the impaired expression of *Cd4*, was corroborated by the significantly reduced mRNA expression of the Treg-associated *Foxp3* gene (Figure 31 A, B).

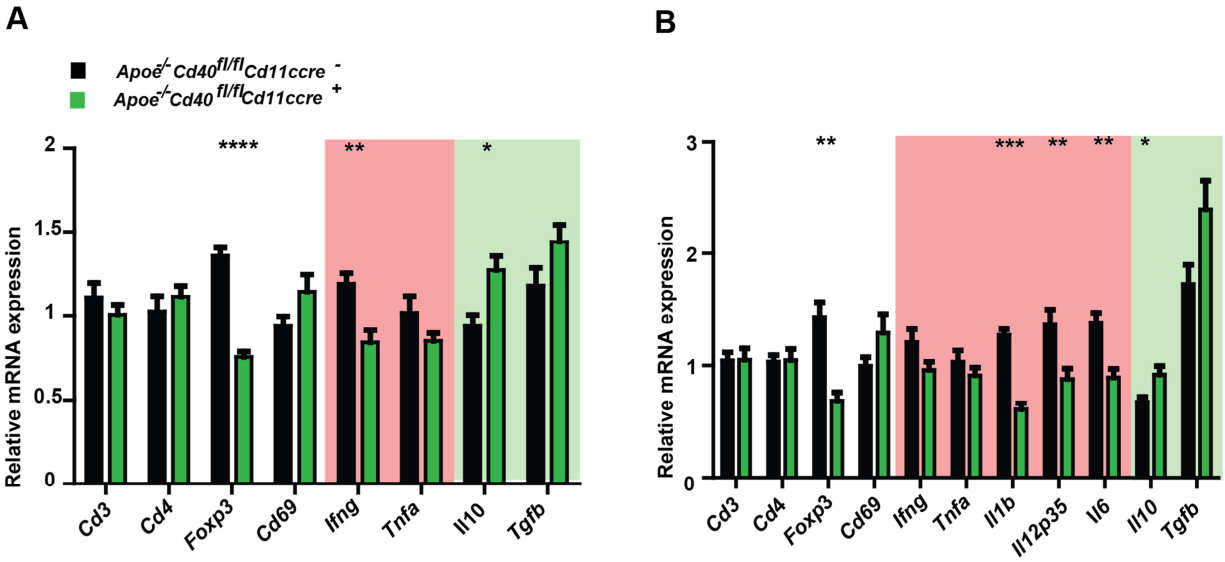

Figure 31. DC-specific deletion of CD40 causes shift to a more anti-inflammatory milieu.
Relative mRNA expression analyzed by quantitative PCR in lymph nodes and spleen of male 28 weeks old *Apoe*$^{-/-}$*Cd40*$^{fl/fll}$*Cd11cCre*$^{-}$ or *Apoe*$^{-/-}$*Cd40*$^{fl/fll}$*Cd11cCre*$^{+}$ mice. Red rectangles symbolize pro-inflammatory genes, green rectangle symbolizes anti-inflammatory genes. (**A**) Relative mRNA expression in lymph node and (**B**) in spleen of male 28 weeks *Apoe*$^{-/-}$*Cd40*$^{fl/fll}$*Cd11cCre*$^{-}$ or *Apoe*$^{-/-}$*Cd40*$^{fl/fll}$*Cd11cCre*$^{+}$ mice. n=10(*Apoe*$^{-/-}$*Cd40l*$^{fl/fl}$*Cd11cCre*$^{-}$*);* n= 12 *(Apoe*$^{-/-}$*Cd40*$^{fl/fl}$ *Cd11cCre*$^{+}$*)* Data is presented as mean±SD. *=p<0.01; **=p<0.001; ***=p 0.0001-0.001; ****=p<0.0001

To further characterize the T cell phenotype and the activation status of the $CD4^+$ and $CD8^+$ T cell subpopulation, we performed flow cytometric measurements on cell suspensions of lymph nodes and spleen from *Cd40$^{fl/fll}$Cd11cCre$^-$* and *Cd40$^{fl/fll}$Cd11cCre$^+$* mice. Indeed, $CD4^+$ cells in lymph nodes and spleen of *Apoe$^{-/-}$Cd40$^{fl/fll}$Cd11cCre$^+$* mice exhibited a higher percentage of $CD62L^+$ cells after 28 weeks of age when compared to *Apoe$^{-/-}$Cd40$^{fl/fll}$Cd11cCre$^-$* controls (Figure 32 A, B, C). The percentage of naïve ($CD62L^+CD44^-$) $CD8^+$ T cells was also significant higher in the spleen of mice with CD40-deficient DCs. This reduction was accompanied by decreased percentages of central memory ($CD62L^+CD44^+$) $CD8^+$ T cells and effector ($CD62L^-CD44^+$) $CD8^+$ T cells (Figure 32 E, F). In contrast to the splenic population the percentage of the central memory $CD8^+$ T cell population was increased in suspensions of lymph nodes from mice with a DC-specific CD40 deficiency (Figure 32 D). In summary those results demonstrated a decrease in activated $CD4^+$ and $CD8^+$ cells and a higher percentage of naïve $CD4^+$ and $CD8^+$ cells.

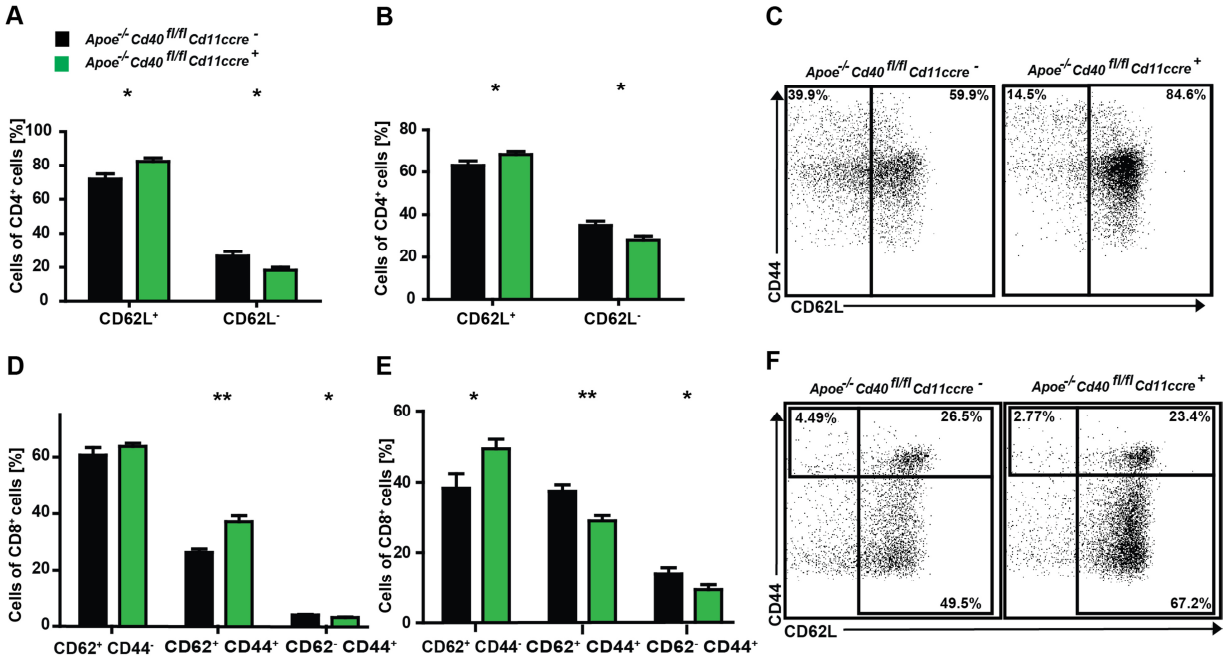

Figure 32. Lack of CD40 on DCs leads to a reduced number of activated T cells.
Flow cytometric measurements of $CD4^+$ and $CD8^+$ T cell populations in lymph nodes and spleen of male 28 weeks old *Apoe$^{-/-}$Cd40$^{fl/fll}$Cd11cCre$^-$* or *Apoe$^{-/-}$Cd40$^{fl/fll}$Cd11cCre$^+$* mice. Abundance of $CD4^+$ subtypes in (**A**) lymph nodes and (**B**) spleen *Apoe$^{-/-}$Cd40$^{fl/fll}$Cd11cCre$^-$* or *Apoe$^{-/-}$Cd40$^{fl/fll}$Cd11cCre$^+$* mice assayed by flow cytometry. Abundance $CD8^+$ subtypes in (**D**) lymph nodes and (**E**) spleen, of *Apoe$^{-/-}$Cd40$^{fl/fll}$Cd11cCre$^-$* or *Apoe$^{-/-}$Cd40$^{fl/fll}$Cd11cCre$^+$ mice* assayed by flow cytometry. Representative plots gated on living $CD4^+$ cells (**C**) and $CD8^+$ cells of lymphocytes (**F**) are displayed. n=7 (*Apoe$^{-/-}$Cd40$^{fl/fl}$Cd11cCre$^-$);* n= 9 *(Apoe$^{-/-}$Cd40$^{fl/fl}$ Cd11cCre$^+$)*. Data is presented as mean±SD. *=p<0.01

3.10 DC-specific deletion of CD40 affects B cell phenotype and decreases IgG_{2b} and IgM titers

Our experiments showed an altered activation status in T helper and T effector cells in *Apoe*$^{-/-}$*Cd40*$^{fl/fl}$*Cd11cCre*$^{+}$ mice. Maintaining our previous strategy we analyzed the B cell population regarding differences in the B cell T cell interaction and the humoral immune response in DC-specific CD40-deficient mice. We analyzed the phenotype, i.e. differentiation and activation, of B cells by measuring antigen-specific and unspecific antibodies in plasma. Using a multiplex bead-based assay to determine the concentration of antigen-unspecific Ig-subclasses we revealed a decreased abundance of IgG_{2a}, IgG_{2b}, IgE, and IgM antibodies in the plasma of *Apoe*$^{-/-}$*Cd40*$^{fl/fl}$*Cd11cCre*$^{+}$ (Figure 33).

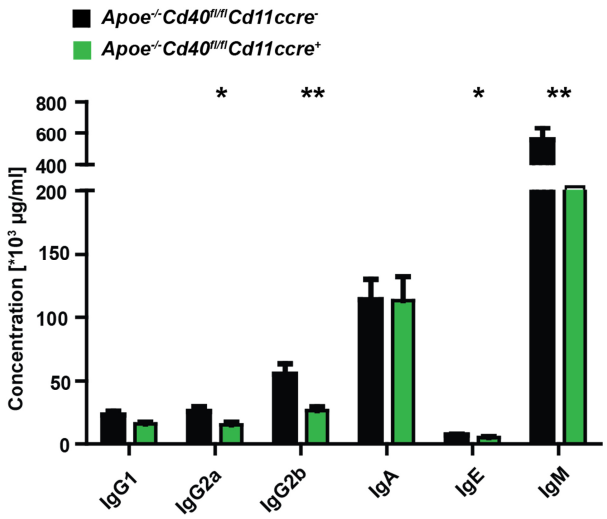

Figure 33. DC-specific CD40 deficiency decreases Ig_{G2}, IgE and IgM plasma abundance.
Antibody abundance in plasma of 28 week old *Apoe*$^{-/-}$*Cd40*$^{fl/fl}$*Cd11cCre*$^{+}$ and *Apoe*$^{-/-}$*Cd40*$^{fl/fl}$*Cd11cCre*$^{-}$ mice as analyzed by murine multiplex bead-based technology detection antibodies. Plasma level expression for respective Ig of 28 week old *Apoe*$^{-/-}$*Cd40*$^{fl/fl}$*Cd11cCre*$^{+}$ and *Apoe*$^{-/-}$*Cd40*$^{fl/fl}$*Cd11cCre*$^{-}$ mice analyzed by multiplex bead-based technology (**B**) Plasma abundance of antibodies detecting oxLDL of 28 week old *Apoe*$^{-/-}$*Cd40*$^{fl/fl}$*Cd11cCre*$^{+}$ and *Apoe*$^{-/-}$*Cd40*$^{fl/fl}$*Cd11cCre*$^{-}$ mice. Quantification for optic density acquired at 450nm wavelength of 1:20 diluted plasma is displayed. (**C**) Dilution series (1:20, 1:100; 1:1000) of plasma and respective ODs are displayed for each antibody. n=7 *Apoe*$^{-/-}$*Cd40*$^{fl/fl}$*Cd11cCre*$^{-}$*);*n=9 *(Apoe*$^{-/-}$*Cd40*$^{fl/fl}$*Cd11cCre*$^{+}$*).* Data is presented as mean±SD. *=p<0.01; **=p<0.001

In addition, when employing an ELISA for oxLDL-binding immunoglobulins, we detected significant less oxLDL-specific IgG_{2b} and IgM in the plasma of *Apoe*$^{-/-}$*Cd40*$^{fl/fl}$*Cd11cCre*$^{+}$ mice (Figure 34).

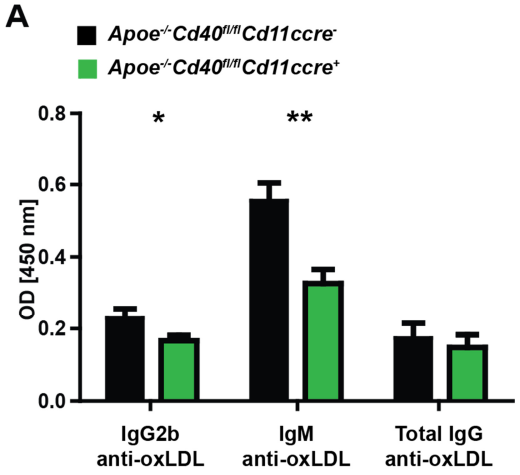

Figure 34. DC-specific CD40 deficiency decreases oxLDL specific IgG_{2b} and IgM plasma abundance.
Abundance of antibodies detecting oxLDL in plasma of 28 week-old *Apoe*$^{-/-}$*Cd40*$^{fl/fl}$*Cd11cCre*$^{+}$ and *Apoe*$^{-/-}$*Cd40*$^{fl/fl}$*Cd11cCre*$^{-}$ mice. Quantification for optic density acquired at 450nm wavelength of diluted (1:20) plasma is displayed. n=10 (both groups) Data is presented as mean±SD. *=p<0.01; **=p<0.001

In summary, the data revealed a decreased abundance of antigen-specific and unspecific immunoglobulin subclasses, which are considered both pro-atherogenic (e.g. Ig_{2b}) and anti-atherogenic (e.g. IgM) in *Apoe*$^{-/-}$*Cd40*$^{fl/fll}$*Cd11cCre*$^{+}$ mice.

3.11 DC-specific deletion of CD40 results in an impaired antigen presentation in an in vivo model of antigen specific DC-dependent T cell activation.

Our analyses of adaptive immune cells in *Apoe*$^{-/-}$*Cd40l*$^{fl/fll}$*Cd11cCre*$^{+}$ mice revealed discrepancies in abundance, phenotype, and activation status of T cells and B cells between *Apoe*$^{-/-}$*Cd40*$^{fl/fll}$*Cd11cCre*$^{+}$ and control mice.

Because of the already mentioned connection of T and B cells with DCs and to characterize this tight relationship, we once again used CHS as an additional *in vivo* model. We examined the DNFB-induced CHS in *Apoe*$^{-/-}$*Cd40*$^{fl/fll}$*Cd11cCre*$^{-}$ and *Apoe*$^{-/-}$*Cd40*$^{fl/fll}$*Cd11cCre*$^{+}$ mice. Analysis of ears from *Apoe*$^{-/-}$*Cd40*$^{fl/fll}$*Cd11cCre*$^{-}$ and *Apoe*$^{-/-}$*Cd40*$^{fl/fll}$*Cd11cCre*$^{+}$ mice collected twenty-four hours after challenging with DNFB, revealed an attenuated CHS in *Apoe*$^{-/-}$*Cd40*$^{fl/fll}$*Cd11cCre*$^{+}$ mice. The DNFB-sensitized and -challenged ears displayed less cellular inflammatory infiltrate and less edema in the dermal tissue (Figure 35 A, B).

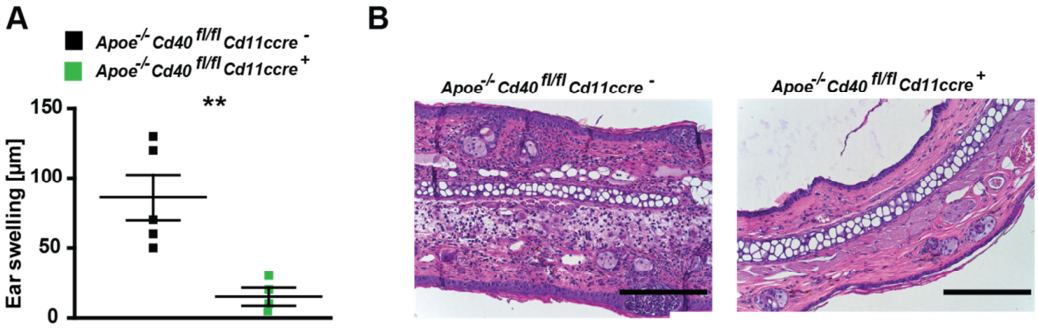

Figure 35. DNFB-induced CHS response is attenuated in mice lacking DC-specific CD40.
Physiologic and histologic assessment of ears during induction of CHS, in response to DNFB. (**A**) Changes in the ear measurements 24 hours after DNFB challenge of sensitized *Apoe*$^{-/-}$*Cd40*$^{fl/fll}$*Cd11cCre*$^{-}$ or *Apoe*$^{-/-}$*Cd40*$^{fl/fll}$*Cd11cCre*$^{+}$ mice. Data represent changes in ear thickness of the untreated ear versus the sensitized ear of each animal. (**B**) Representative histological analysis of hematoxylin-and-eosin-stained ear tissues. n=5 (for both groups). Scale bar = 200 µm. Data is presented as mean±SD. **=p<0.001

Flow cytometric analyzes of cell suspension of the ear-draining lymph nodes of DC CD40 deficient mice demonstrated a decrease in the Foxp3^{+} Treg population (Figure 36 A). Further analyses of the CD4^{+} and CD8^{+} T cell population revealed a significantly higher percentage of CD62L^{+}CD4^{+} cells as well as decreased percentage of CD62L^{-}CD44^{+}CD8^{+} cells (Figure 36 C, E), reflecting the earlier detected reduced activation status of CD4^{+} T and CD8^{+} T cells in *Apoe*$^{-/-}$*Cd40l*$^{fl/fll}$*Cd4Cre*$^{+}$ mice.

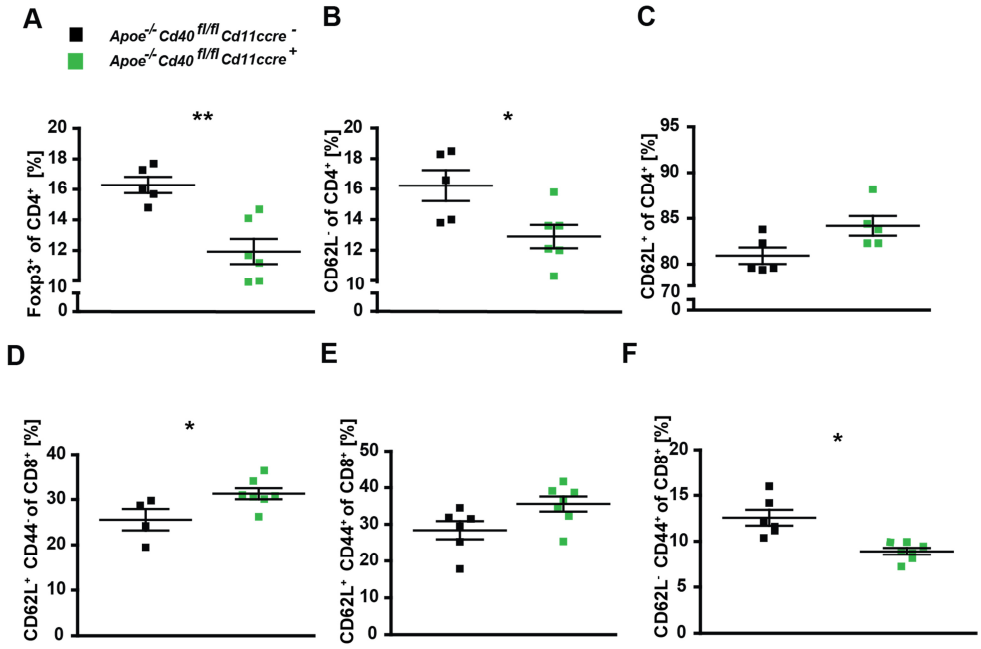

Figure 36. Deletion of DC-specific CD40 leads to a reduced number of activated T cells and Tregs in skin induced hypersensitivity.
Flow cytometry analysis of cell suspensions from the ear-draining lymph nodes 24 hours after DNFB challenge of sensitized Apoe$^{-/-}$Cd40$^{fl/fl}$Cd11cCre^{+} or Apoe$^{-/-}$Cd40$^{fl/fl}$Cd11cCre^{-} mice. CD4^{+} cells were analyzed for their Foxp3 (**A**) and CD62L (**B, C**) distribution. CD8^{+} cells were analyzed for their CD44 and CD62L distribution (**D- F**). n=4-6 (Apoe$^{-/-}$ Cd40$^{fl/fl}$Cd11cCre^{-}); n= 6-7 (Apoe$^{-/-}$Cd40$^{fl/fl}$Cd11cCre+). Data is presented as mean±SD.*=p<0.01;**=p<0.001

We further examined the role of DC-specific CD40 in the regulation of the appearance and function of DCs. Flow cytometric examination of the DC distribution in ear draining lymph nodes of *Apoe$^{-/-}$Cd40$^{fl/fl}$Cd11cCre^{-}* and *Apoe$^{-/-}$Cd40$^{fl/fl}$Cd11cCre^{+}* mice did not show any difference in percentage of CD11c^{+}MHCII^{+} DCs (Figure 37 A). In contrast to the unchanged DC density we were detected differences in the expression of the CD40-CD40L dependent costimulatory molecules CD86 and OX40L, which were significant decreased in *Apoe$^{-/-}$Cd40$^{fl/fl}$Cd11cCre^{+}* mice (Figure 37 B, C). The presumably CD40/CD40L-independent expression of the costimulatory molecule CD70 was unchanged (Figure 37 B, C).

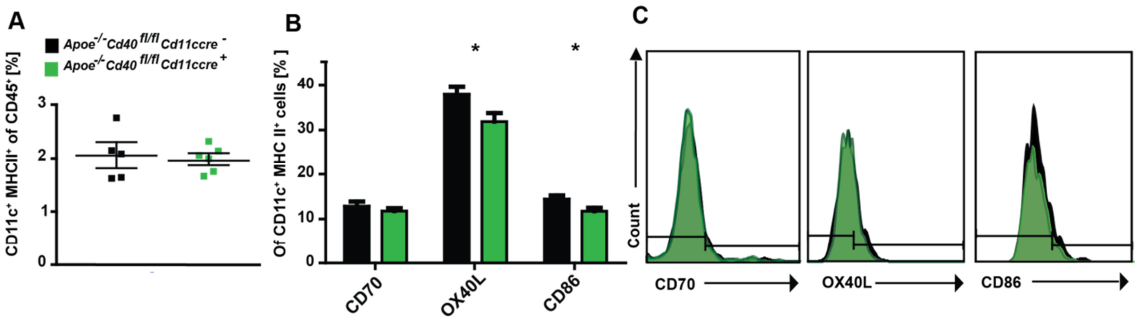

Figure 37. Lack of DC-specific CD40 does not affect DC number but their expression of the costimulatory molecules OX40L and CD86. Flow cytometry analysis of cell suspensions from ear-draining lymph nodes 24 hours after DNFB challenge of sensitized *Apoe$^{-/-}$Cd40$^{fl/fl}$ Cd11cCre^{+}* or *Apoe$^{-/-}$Cd40$^{fl/fl}$Cd11cCre^{-}* mice. (**A**) DC percentage and (**B**) costimulatory-molecule expression on DCs were analyzed. (**C**) Representative flow cytometric histograms depicting CD70, CD86 and OX40L expression on DCs. n=5 (*Apoe$^{-/-}$Cd40$^{fl/fl}$Cd11cCre^{-});* n= 6 *(Apoe$^{-/-}$Cd40$^{fl/fl}$ Cd11cCre^{+}).* Data is presented as mean±SD. *=p<0.01

In a second flow cytometry panel, we addressed unchanged abundance of DCs that may correspond to unchanged distribution of DC subtypes. We analyzed the DC population for their percentage of $CD8^+CD11b^-$ and $CD8^-CD11b^+$ DCs. Flow cytometry measurements exhibited decreased percentage $CD8^+CD11b^-$ DCs in lymph nodes of *Apoe*$^{-/-}$*Cd40*$^{fl/fl}$*Cd11cCre*$^+$mice 24 hours after DNFB-challenge (Figure 38 A, B).

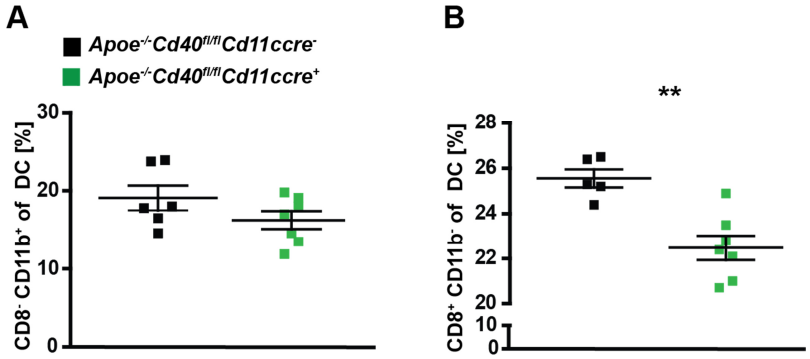

Figure 38. DC-specific deletion of CD40 alters the ratio of $CD8^+CD11b^-$ to $CD8^-CD11b^+$ DCs in hapten-induced hypersensitivity.
Flow cytometric measurement to check the abundance of $CD8^+CD11b^-$ and $CD8^-CD11b^+$ in cell suspensions from ear-draining lymph nodes 24 hours after DNFB challenge of sensitized *Apoe*$^{-/-}$*Cd40*$^{fl/fl}$*Cd11cCre*$^+$ or *Apoe*$^{-/-}$*Cd40*$^{fl/fl}$*Cd11cCre*$^-$. (**A**) Percentage of $CD8^+CD11b^-$ DCs and of (**B**) $CD8^-CD11b^+$ of sensitized *Apoe*$^{-/-}$*Cd40*$^{fl/fl}$*Cd11cCre*$^+$ or *Apoe*$^{-/-}$*Cd40*$^{fl/fl}$*Cd11cCre*$^-$ mice. n=5-6 (*Apoe*$^{-/-}$*Cd40*$^{fl/fl}$*Cd11cCre*$^-$*);* n= 7 *(Apoe*$^{-/-}$*Cd40*$^{fl/fl}$*Cd11cCre*$^+$*).* Data is presented as mean±SD. **=p<0.001

Paralleling our earlier findings in mice with a T cell-specific deletion of CD40L the summarized results provide additional support for the previously indicated requirement of CD40-CD40L interaction for CHS responses to DNFB.

3.12 Platelet specific deletion of CD40L does not affect advanced atherosclerosis.

Today platelets are seen as true immune cells and by using a platelets from *Cd40l*$^{-/-}$ mice Lievens *et al* were able to investigate the role of CD40L in atherosclerosis. They demonstrated that platelet CD40L plays a crucial role in initiation and progression of atherosclerosis by facilitating platelet–leukocyte aggregate formation and promoting adherence of platelets and leukocytes to the endothelium[125]. In addition platelets are known to be the main source for the soluble form of CD40L which serum levels in human and mice associates with cardiovascular diseases[281]. Thus, we sought to investigate the role of platelet-specific CD40L in atherosclerosis. Similar to our previous investigations we started our studies by searching for possible changes in cholesterol metabolism and blood parameters of mice lacking CD40L on platelets. These analyses did not reveal any significant differences between *Apoe*$^{-/-}$*Cd40l*$^{fl/fl}$*Pf4Cre*$^{-}$ and *Apoe*$^{-/-}$ *Cd40l*$^{fl/fl}$*Pf4Cre*$^{+}$ mice at 28 weeks of age (Table 9).

■ *Apoe*$^{-/-}$*Cd40l*$^{fl/fl}$*Pf4cre*$^{-}$ ▣ *Apoe*$^{-/-}$*Cd40l*$^{fl/fl}$*Pf4cre*$^{+}$

Body weight [g]	33.72	±2.23	33.65	±2.35
Lymphocytes [%]	63.68	±10.66	66.15	±10.25
Monocytes [%]	4.50	±0.92	4.36	±1.03
Granulocytes [%]	31.84	±10.42	29.50	±9.62
Platelets [10^3/µl]	1293	±161	1279	±179
Erythrocytes [10^6/µl]	8.33	±0.72	8.41	±2.78
Leukocytes [10^3/µl]	3.80	±1.69	3.61	±1.34
Lymphocytes [10^3/µl]	2.30	±0.65	2.27	±0.68
Monocytes [10^3/µl]	0.14	±0.08	0.11	±0.08
Granulocytes [10^3/µl]	1.39	±0.93	1.18	±0.69
Plasma Cholesterol [mM]	3.97	±0.32	3.55	±0.36

Table 9. Body weight, hematological parameters, and plasma cholesterol content in *Apoe*$^{-/-}$*Cd40l*$^{fl/fl}$*Pf4Cre*$^{-}$ mice (n=12) and *Apoe*$^{-/-}$*Cd40l*$^{fl/fl}$*Pf4Cre*$^{+}$ mice (n=14). Data is presented as mean±SD.

Once we ensured that the deletion of CD40L on platelets did not interfere with basic blood parameters or cholesterol metabolism, we analyzed the atherosclerotic lesion area in the aortic arch and the ascending aorta of the platelet CD40L-deficient and control mice in advanced stage atherosclerosis and under mild hypercholesteremic conditions. Surprisingly, the histological analyses did not reveal any differences between mice lacking CD40L on platelets and animals which expressed CD40L on platelets. The absolute atherosclerotic lesion area in the aortic arch, of *Apoe*$^{-/-}$*Cd40l*$^{fl/fl}$*Pf4Cre*$^{+}$ mice, were similar to those of littermate controls (Figure 39).

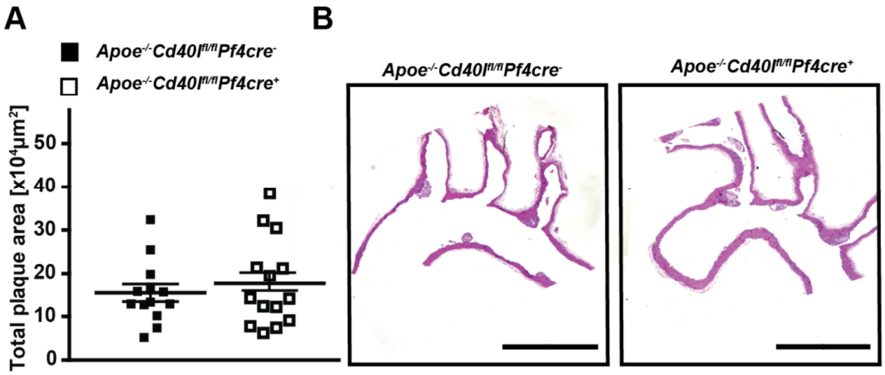

Figure 39. PF4-specific CD40L deficiency does not influence early plaque formation in the aortic arch.
Hematoxylin-and-eosin-stained longitudinal section of the aortic arch, including the brachiocephalic trunk, left carotid, and left subclavian artery from 28 week-old male *Apoe*$^{-/-}$*Cd40l*$^{fl/fl}$*Pf4Cre*$^{-}$ or *Apoe*$^{-/-}$*Cd40l*$^{fl/fl}$*Pf4Cre*$^{+}$ mice. (**A**) Quantification of total plaque size and (**B**) representative photomicrographs. n=13 (*Apoe*$^{-/-}$*Cd40l*$^{fl/fl}$*Pf4Cre*$^{-}$), n=14 (*Apoe*$^{-/-}$*Cd40l*$^{fl/fl}$*Pf4Cre*$^{+}$) Scale bar = 200 µm. Data is presented as mean±SD.

To confirm these results, atherosclerotic burden was also quantified in the aortic sinus, which, after 28 weeks of normal chow diet, contained more advanced atherosclerotic lesions than the aortic arch. Accordingly, we performed quantitative analysis of ORO- stained cryosections of the aortic sinus. Reflecting the results of the invariant lesion size in the aortic arch, the measurements did not show any differences in absolute or relative lesion area between *Apoe*$^{-/-}$*Cd40l*$^{fl/fl}$*Pf4Cre*$^{+}$ mice and *Apoe*$^{-/-}$*Cd40l*$^{fl/fl}$*Pf4Cre*$^{-}$ mice at the age of 28 weeks (Figure 40 A-C).

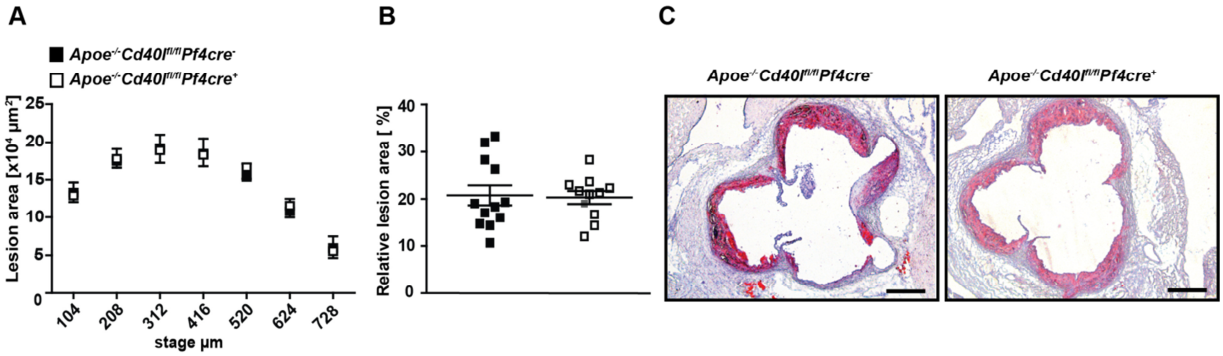

Figure 40. Platelet-specific CD40L deficiency does not affect advanced atherosclerosis.
Quantification of lesion area and atherosclerotic plaque area in cross-sections at indicated positions (µm above the appearance of the aortic valves) of the aortic sinus from 28-week-old, male *Apoe*$^{-/-}$*Cd40l*$^{fl/fl}$*Pf4Cre*$^{-}$or *Apoe*$^{-/-}$*Cd40l*$^{fl/fl}$*Pf4Cre*$^{+}$-mice. (**A**) Lesion areas in stages 104-728. (**B**) Average lesion area in stages 312-520 as percentage of total vessel area. (**C**) Representative photomicrographs of Oil Red O-stained sections. n=12-13 (*Apoe*$^{-/-}$ *Cd40l*$^{fl/fl}$*Pf4Cre*$^{-}$), n=10-13 (*Apoe*$^{-/-}$ *Cd40l*$^{fl/fl}$*Pf4Cre*$^{+}$) Scale bar = 200 µm. Data is presented as mean±SD.

Additionally, we determined the cellular composition of the lesions of the aortic sinus from *Apoe*$^{-/-}$*Cd40l*$^{fl/fl}$*Pf4Cre*$^{+}$ and *Apoe*$^{-/-}$*Cd40l*$^{fl/fl}$*Pf4Cre*$^{-}$ mice. Our detailed immunohistomorphological quantification of lesional macrophages and SMCs the most abundant cell types in atherosclerosis and the analysis of CD4^{+} cells revealed, that neither the content of lesional CD4^{+} T cells, nor macrophages or SMC content in atherosclerotic lesions of the aortic sinus differed between 28 week-old *Apoe*$^{-/-}$*Cd40l*$^{fl/fl}$*Pf4Cre*$^{+}$ and littermate controls (Figure 41 A, B, C).

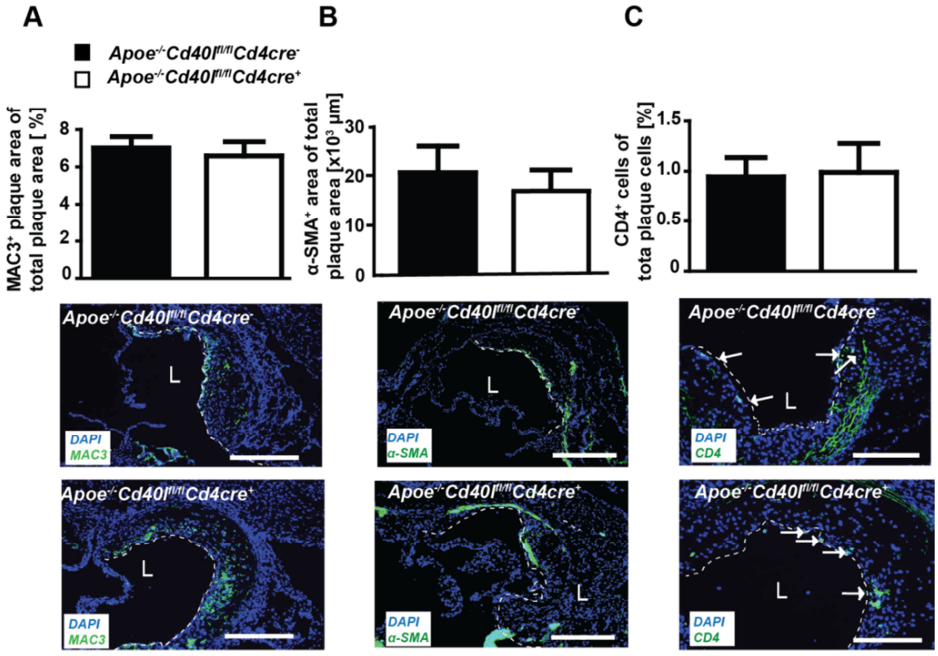

Figure 41. Platelet-specific CD40L does not affect cellular plaque composition.
Immunofluorescent stainings in cross-sections of the aortic sinus from 28 week old *Apoe*$^{-/-}$*Cd40l*$^{fl/fl}$ *Pf4Cre*$^{+}$ or *Apoe*$^{-/-}$*Cd40l*$^{fl/fl}$*Pf4Cre*$^{-}$ mice. Quantifications and representative photomicrographs are shown for each staining. The dashed lines separate the atherosclerotic lesion from the lumen (L). Analyzed for (**A**) MAC3^{+} area, (**B**) α-SMA^{+} area and (**C**) CD4^{+} cells. n=12-13 (*Apoe*$^{-/-}$*Cd40l*$^{fl/fl}$*Pf4Cre*) n=10-13 (*Apoe*$^{-/-}$*Cd40l*$^{fl/fl}$*Pf4Cre*$^{+}$). Scale bar = 200 µm. Data is presented as mean±SD.

In summary, we showed that platelet specific deficiency of the costimulatory molecule CD40L does not affect atherosclerosis progression or lesion composition. Our analyses did not show any variances in size lesions during either early or late stages of disease under conditions of mild hypercholesteremia.

3.13 Analyzing the role of platelet- and T cell-specific CD40 expression in atherosclerosis

Besides the role as the predominant CD40L-expressing cells, both T cells and platelets also express a certain amount of CD40[317]. Thus, we aimed to evaluate the consequences of a deletion of CD40 on those cell types.

In analogy to our previous studies we addressed the secondary effects of the different cell type-specific deletions of CD40 by monitoring body weight and blood parameters. Notably, body weight or blood count of male *Apoe*$^{-/-}$*Cd40*$^{fl/fl}$*Pf4Cre*$^{-}$ and *Apoe*$^{-/-}$*Cd40*$^{fl/fl}$*Pf4Cre*$^{+}$ mice at 28 week of age did not reveal significant differences (Table 10).

	Apoe$^{-/-}$*Cd40*$^{fl/fl}$*Pf4cre*$^{-}$		*Apoe*$^{-/-}$*Cd40*$^{fl/fl}$*Pf4cre*$^{+}$	
Body weight [g]	33.73	±2.23	33.65	±2.35
Lymphocytes [%]	63.69	±10.66	66.15	±10.25
Monocytes [%]	4.49	±0.92	4.36	±1.03
Granulocytes [%]	31.84	±10.24	29.50	±9.62
Platelets [10^3/µl]	1293	±161	1279	±179
Erythrocytes [10^6/µl]	8.33	±0.72	8.32	±1.04
Leukocytes [10^3/µl]	3.80	±1.69	3.98	±1.54
Lymphocytes [10^3/µl]	2.30	±0.65	2.27	±0.68
Monocytes [10^3/µl]	0.14	±0.08	0.11	±0.08
Granulocytes [10^3/µl]	1.39	±0.08	1.18	±0.69

Table 10.
Body weight and hematological parameters of *Apoe*$^{-/-}$*Cd40*$^{fl/fl}$*Pf4Cre*$^{-}$ *and* *Apoe*$^{-/-}$*Cd40*$^{fl/fl}$*Pf4Cre*$^{+}$ mice. n= 13 (*Apoe*$^{-/-}$*Cd40*$^{fl/fl}$*Pf4cre*$^{-}$) n= 19 (*Apoe*$^{-/-}$*Cd40*$^{fl/fl}$*Pf4cre*$^{+}$): Data is presented as mean±SD.

We then analyzed the lesion area of the ascending aortae in late stage atherosclerosis and under mild hypercholesteremic conditions. These measurements did not show any differences in absolute or relative lesion area between *Apoe*$^{-/-}$*Cd40*$^{fl/fl}$*Pf4Cre*$^{-}$ and *Apoe*$^{-/-}$*Cd40*$^{fl/fl}$*Pf4Cre*$^{+}$ mice (Figure 42 A-C).

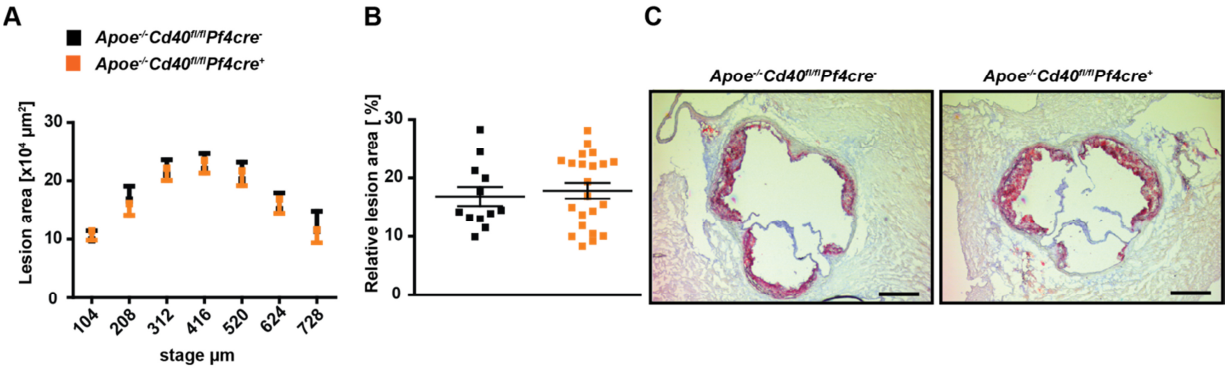

Figure 42. Platelet-specific CD40 deficiency does not influence advanced atherosclerosis.
Quantification of atherosclerotic plaque area in cross-sections of the aortic sinus from 28-week-old, male *Apoe*$^{-/-}$*Cd40*$^{fl/fl}$*Pf4Cre*$^{-}$or *Apoe*$^{-/-}$*Cd40*$^{fl/fl}$*Pf4Cre*$^{+}$mice. (**A**) Lesion areas in stages 104-728. (**B**) Average lesion area in stages 312-520 expressed as percentage of total vessel area. (**C**) Representative photomicrographs of Oil Red O-stained sections. n=13 (*Apoe*$^{-/-}$*Cd40*$^{fl/fl}$*Pf4Cre*), n=19 (*Apoe*$^{-/-}$ *Cd40*$^{fl/fl}$*Pf4Cre*$^{+}$) Scale bar = 200 µm. Data is presented as mean±SD.

Since we could not detect any alterations in lesion progression in mice lacking platelet-specific CD40 we next analyzed lesion progression in *Apoe*$^{-/-}$*Cd40*$^{fl/fl}$*Cd4Cre*$^{-}$ *and Apoe*$^{-/-}$*Cd40*$^{fl/fl}$*Cd4cre*$^{+}$ mice.

	Apoe$^{-/-}$*Cd40*$^{fl/fl}$*Cd4cre*$^{-}$		*Apoe*$^{-/-}$*Cd40*$^{fl/fl}$*CD4cre*$^{+}$	
Body weight [g]	32.40	±2.35	32.33	±1.73
Lymphocytes [%]	71.09	±8.19	75.21	±3.27
Monocytes [%]	4.87	±1.26	4.26	±0.45
Granulocytes [%]	24.04	±7.08	20.53	±3.13
Platelets [10^3/µl]	979	±315	955	±345
Erythrocytes [10^6/µl]	7.35	±3.10	8.25	±1.07
Leukocytes [10^3/µl]	3.01	±1.19	3.98	±1.54
Lymphocytes [10^3/µl]	2.13	±0.94	2.81	±1.12
Monocytes [10^3/µl]	0.10	±0.07	0.10	±0
Granulocytes [10^3/µl]	0.78	±0.29	0.73	±0.21

Table 11.
Body weight and hematological parameters of *Apoe*$^{-/-}$*Cd40*$^{fl/fl}$*Cd4cre*$^{-}$ *and Apoe*$^{-/-}$*Cd40*$^{fl/fl}$*Cd4cre*$^{+}$ mice.
n= 7 (both groups)
Data is presented as mean±SD.

Again, the data did not reveal any difference in body weight, or blood count parameters between *Apoe*$^{-/-}$*Cd40*$^{fl/fl}$*Cd4Cre*$^{-}$ and *Apoe*$^{-/-}$*Cd40*$^{fl/fl}$*Cd4Cre*$^{+}$ mice (Table 11). However, the measurement of the lesions size in ascending aortae of *Apoe*$^{-/-}$*Cd40*$^{fl/fl}$*Cd4cre*$^{-}$ and *Apoe*$^{-/-}$*Cd40*$^{fl/fl}$*Cd4cre*$^{+}$ did not display any difference in absolute or relative values in 28 week-old male mice (Figure 43. A-C).

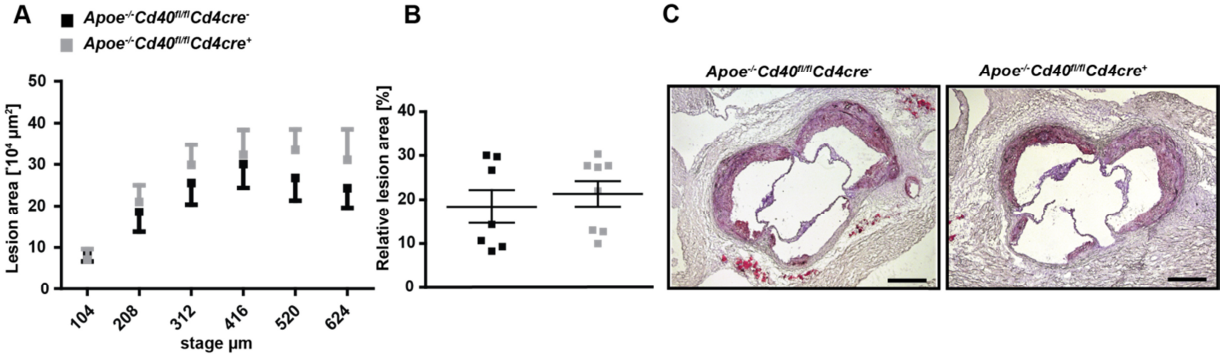

Figure 43. T cell-specific CD40 deficiency does not influence advanced atherosclerosis.
Quantification of lesion area and Atherosclerotic plaque area in cross-sections at indicated positions of the aortic root at different stages from 28-week-old, male *Apoe*$^{-/-}$*Cd40*$^{fl/fl}$*Cd4Cre*$^{-}$or *Apoe*$^{-/-}$*Cd40*$^{fl/fl}$*Cd4Cre*$^{+}$-mice. (**A**) Lesion areas in stages 104-624. (**B**) Average lesion area in stages 312-520 as percentage of total vessel area. (**C**) Representative photomicrographs of Oil Red O-stained sections. n=7 (*Apoe*$^{-/-}$*Cd40*$^{fl/fl}$*Cd4cre*), n=7 (*Apoe*$^{-/-}$ *Cd40*$^{fl/fl}$*Cd4Cre*$^{+}$) Scale bar = 200 µm. Data is presented as mean±SD.

In summary, our data do not provide any evidence for a prominent, if any, role of platelet- or T cell-specific CD40 in atherosclerosis.

4 DISCUSSION

The study of murine models of atherogenesis over the last two and a half decades has been extremely valuable in revealing the mechanisms that are operative in initiating lesion development as well as their progression and regression. The CD40-CD40L dyad is one of the most potent costimulatory pathways active in atherosclerosis[318,319]. Genetic deficiency in CD40L or pharmacological inhibition of CD40L results in the development of a stable atherosclerotic plaque phenotype[303,304]. This phenotype can even be established when antibody treatment is delayed until advanced plaques have developed in late stages of the disease[303]. However, the mechanisms of CD40-CD40L signaling are complex. In atherosclerotic lesions both CD40 and CD40L are expressed on the vast majority of immune cells present in the plaque, on vascular cells (ECs and SMCs), as well as on platelets and monocytes in the circulation[210,239,240–243]. Yet, the contribution of CD40-CD40L signaling on each of the different cell types towards plaque development has been undefined so far. Therefore, this thesis aimed to elucidate cell type-specific CD40L-CD40L interactions in atherosclerosis. To this end, we analyzed CD40-CD40L-dependent interactions of DCs, T cells, and B cells, as the central players of the adaptive immune system, in greater detail. Additionally we performed initial studies to get a surface impression of the contribution of platelet specific CD40-CD40L interactions to atherosclerosis.

4.1 Establishing the cre/loxP system to investigate the cell type-specific role of CD40-CD40L interactions in atherosclerosis

Deletion of ubiquitously expressed genes often results in severe phenotypes that interfere with the analysis of particular cell types or tissues. To overcome this limitation, we used a conditional knockout approach to examine the role of cell type-specific CD40-CD40L interactions in atherogenesis. To our knowledge, this is the first report of examining the effects of cell type-specific CD40-CD40L interactions in atherosclerosis *in vivo.* Although Lutgens and others previously tested mice with a global CD40 or CD40L deficiency in atherosclerosis, they did not report the impact of cell type-specific deficiency of CD40 or CD40L on atherosclerosis[302–305,320]. Hence, our approach resembles a further refinement of the global deficiency model in that it allows deeper understanding of the contribution of CD40-CD40L interaction on the level of a single cell population and may elucidate new potential targets and strategies to modulate cell functions in order to ameliorate the disease.

Methodologically we took advantage of the cre/loxP- system inserting by gene targeting two loxP-sites around a functionally essential part of the gene of interest, thus making a minimal change that leaves the gene completely functional[321]. The power of the cre-recombinase-based

strategies depend very much on utilization of functional and well-characterized transgenic lines expressing the recombinase with a sufficient level and specificity to achieve the desired type of gene alterations. In our studies we were able to prove that our cre-promoter constructs (CD4 and CD11c) led to specific and complete alteration of CD40L and CD40 expression on the designated cell types without any undesirable side-effects to the metabolism of mice.

4.2 Deficiency of CD40-CD40L signaling in DCs and T cells leads to insufficient DC maturation.

In peripheral tissues DCs are functionally immature, adapted to capturing and processing antigens but lack the requisite signals to stimulate T cells. Following antigen recognition in the context of a pathogenic inflammatory stimulus, immature DCs begin to mature and undergo phenotypic and functional changes that result in the complete transition from antigen-capturing cells to professional APCs[322,323].

The present study indicates that DC-specific inhibition of CD40-CD40L costimulation decreases the inflammatory T cell responses, which is associated with reduced disease symptoms. DC-specific CD40 deficiency caused a substantial decrease in atherosclerotic lesion size accompanied by less infiltration of $CD4^+$ T cell, less macrophages and more SMCs**.** The alteration in lesion size and composition was accompanied by a reduced percentage of activated T effector cells and a shift in the systemic cytokine milieu towards a Th2 cell response. In addition, CD40-deficiency in DCs alleviated inflammatory responses as demonstrated by systematically decreased expression of pro-inflammatory and increased expression of anti-inflammatory immunoglobulins. Interaction of CD40 on DCs with CD40L on T cells leads to proper DC activation and renders them potent in T cell priming and cytokine production[263,324,325].

The ability of DCs to regulate immunity is dependent on DC maturation. During their conversion from immature to mature cells, DCs undergo a number of phenotypical and functional changes. Inefficient activation leads to lacking or inadequate secondary signals, such as CD86 and OX40L, resulting in anergy of the lymphocyte[267]. Notably, our data demonstrated that DCs of *Apoe*$^{-/-}$*Cd40l*$^{fl/fl}$*Cd4Cre*$^+$ as well as *Apoe*$^{-/-}$*Cd40*$^{fl/fl}$*Cd11cCre*$^+$ mice featured a decreased expression of CD86 and OX40L compared to their respective controls despite the presence of a cognate antigen, such as oxLDL or DNFB. This may indicate that the pronounced anti-inflammatory phenotype of DC-specific CD40-deficient and T cell-specific-CD40L deficient mice is likely evoked trough insufficient DC maturation. As described earlier, a productive T cell priming depends in part on instructing cytokines provided by mature DCs[326–328]. Expression of cytokines as one of the major functions of mature DCs is regulated through ligation of CD40L to CD40 and the distinct cytokine patterns released by mature DCs ultimately determine their

Th1/Th2 polarizing capacities[252,325,329,330–333]. Mature DCs are a relevant source of IL-12, the principal cytokine that drives Th1 polarization and IL-12 production is controlled by the nature of the maturation stimulus, by environmental factors, and by feedback signals from T cells through costimulatory molecules including CD40L[66,263,264,334]. Interaction of DCs and T cells involves CD40-CD40L interaction and leads to TRAF6 recruitment to the cytoplasmatic domain of CD40. This interaction subsequently results in the activation of the p38 MAP kinase (MAPK) and Jun kinase (Jun) leading to production of cytokines such as IL-12 and IL-6[335,336]. DCs from TRAF6-deficient mice fail to upregulate maturation markers (e.g., MHCII and CD86) and cannot produce IL-6 or IL-12 in response to CD40L[336]. In agreement, our results revealed that the DC-specific deletion of CD40 as well as the T cell-specific deletion of CD40L resulted in an altered cytokine milieu characterized by upregulation of anti-inflammatory cytokines (e.g., IL-10 and TGFβ) and downregulation of pro-inflammatory cytokines (e.g. IFNγ, TNFα, IL-1β, IL-12 (IL-12p35) and IL-6) This suggests an insufficient induction of the T helper cell response since the presence of the cytokines IFNγ, IL-10, and IL-12 during the maturation process is essential for induction of the T helper cell responses[66,67]. IFNγ is produced by a variety of leukocyte populations including Th1 cells, natural killer cells, macrophages and DCs and is an important mediator for DC maturation and the DC-mediated T helper cell activation[67,79–81]. The presence of IFNγ induces DCs to release large amounts of IL-12, which can stimulate a Th1 immune response[66,264,337]. The release of autocrine IL-10, however, blocks the DC maturation process by interfering with up-regulation of costimulatory molecules and production of IL-12, subsequently limiting the ability of DCs to initiate a Th1 response[263,264,338]. Hence, the reduced number of activated T cells in *Apoe*$^{-/-}$*Cd40l*$^{fl/fl}$*Cd4Cre*$^{+}$ as well as *Apoe*$^{-/-}$*Cd40*$^{fl/fl}$*Cd11cCre*$^{+}$ may be due to the insufficient costimulatory capacity of DCs and their inability to produce inflammatory cytokines, both of which are important for the activation of T cells and generation of Th1 cells.

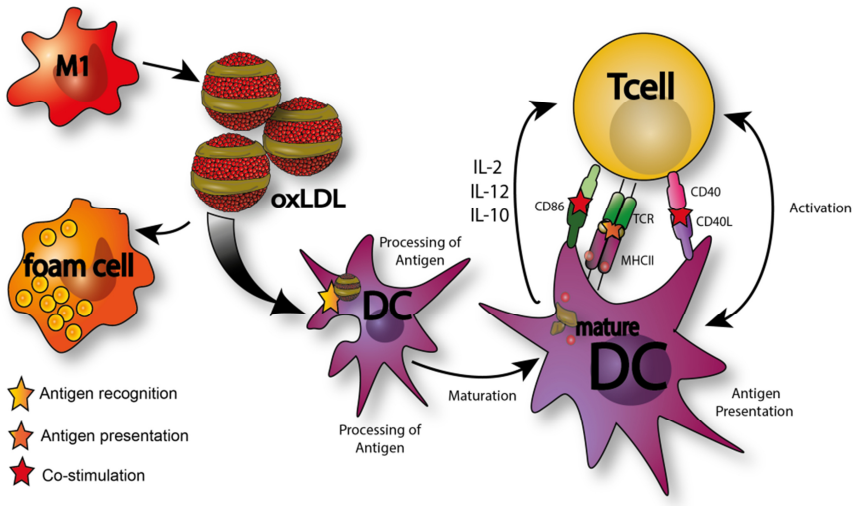

Figure 46: CD40-CD40L interactions between DCs and T cells.
CD40 is upregulated on activated mature DCs and CD40L is expressed on activated T cells. Engagement of CD40 on DCs induces positives signaling that leads to expression of CD86 and the production of IL-2, IL-12 and IL10. IL-12 skews CD4^{+} T cells towards Th1 differentiation in. In addition to IL-12, CD40L signaling in T cells induces IFNγ production (Modified from Ma and Clark[329]).

In summary, our data suggest that the requirement of Th1 cells for DC maturation in previous studies is a reflection of the fact that DCs require the CD40 maturation signals induced during cognate interaction with CD40L-bearing $CD4^+$ T cells to become efficient APCs.

To shed further light on the phenotype and maturation levels of DCs in *Apoe*$^{-/-}$*Cd40l*$^{fl/fl}$*Cd4Cre*$^+$ and *Apoe*$^{-/-}$*Cd40*$^{fl/fl}$*Cd11cCre*$^+$ mice we employed CHS as a powerful *in vivo* model. CHS exclusively relies on the proper function of antigen presentation between T cells and DCs and several studies recently suggested that CD40-CD40L interaction is required during the T cell-mediated and -dependent CHS responses[314,315]. Upon application to the skin, haptens immediately interact with keratinocytes (KC), LCs and dermal dendritic cells (dDC) [339]. Hapten binding to KCs causes them to release cytokines like IL-1β and TNFα[339]. This may activate LCs and dDCs, prompt them to take up antigen, and migrate to the draining lymph node where present the hapten-antigen to naïve T-cells[339]. DNFB application to dDCs *in vitro* upregulates MAPK and CD40[340]. Consistent with the hypothesis that CD40 plays a critical role in DC function and antigen presentation, CD40-deficient DCs seem incapable of generating a proper cell-mediated immune response to the hapten DNFB. This was associated with reduced cellular inflammatory infiltrate, less edema in the dermal tissue of the ears of *Apoe*$^{-/-}$*Cd40l*$^{fl/fl}$*Cd4Cre*$^+$ and *Apoe*$^{-/-}$*Cd40*$^{fl/fl}$*Cd11cCre*$^+$ mice. Furthermore, our data revealed decreased numbers of $CD8^+CD11b^-$ DCs in *Apoe*$^{-/-}$*Cd40l*$^{fl/fl}$*Cd4Cre*$^+$ and *Apoe*$^{-/-}$*Cd40*$^{fl/fl}$*Cd11cCre*$^+$ mice. In fact, $CD8^+CD11b^-$ lymphoid resident DCs are superior in cross-presentation, induction of Th1 cells, uptake of dead cells, production of IL-12, and capture of antigen from migratory DCs or from blood[341]. The reduction of IL12-producing $CD8^+CD11b^-$ DCs was concordantly with the aforementioned systematically reduced expression of Th1-related cytokines in mRNA from lymph nodes of *Apoe*$^{-/-}$*Cd40l*$^{fl/fl}$*Cd4Cre*$^+$ and *Apoe*$^{-/-}$*Cd40*$^{fl/fl}$*Cd11cCre*$^+$ mice. In addition, *Apoe*$^{-/-}$ *Cd40l*$^{fl/fl}$*Cd4Cre*$^+$ and *Apoe*$^{-/-}$*Cd40*$^{fl/fl}$*Cd11cCre*$^+$ mice displayed an increased ratio of $CD8^-CD11b^+$ DCs which are found in most of the lymphoid tissue (lymphoid-resident DC) but also in non-lymphoid tissues (migratory DCs)[342,343]. $CD11b^+$ DCs are less efficient in cross-presentation and production of specific cytokines, such as IL-12 but potent sources of IL-6 and IL-23[340,341341].

Taken together, these results indicate that DC-specific CD40 regulates the critical processes required for maturation, activation, and development of DCs, the primary cellular bridge between innate and adaptive immunity. In addition, they provide evidence that DC-specific CD40 and T cell-specific CD40L are important for the development of DC subsets.

4.3 Inhibition of CD40-CD40L-dependent crosstalk between DCs and T cell affects T cell proliferation and differentiation

Naïve $CD4^+$ T cells depend on the presentation of a cognate antigen and a CD40-CD40L signal by DCs to undergo activation and differentiation. *In vitro*, CD40-deficient DCs are partially defective in priming $CD8^+$ T cells, suggesting a major role for CD40-CD40L interactions in DC licensing[344].

Our studies revealed defects in mounting an effective Th1 response in *Apoe*$^{-/-}$*Cd40l*$^{fl/fl}$*Cd4Cre*$^+$ and *Apoe*$^{-/-}$*Cd40*$^{fl/fl}$*Cd11cCre*$^+$ mice. In addition, these mice with a lack of DC-specific CD40 or with a T cell-specific CD40L deficiency displayed a decrease in atherosclerotic lesion size which was accompanied by less infiltrated $CD4^+$ T cells, systematically decreased expression of cytokines related to T cell activation and polarization and a high abundance of naïve $CD4^+$ and $CD8^+$ T cells. *Apoe*$^{-/-}$*Cd40l*$^{fl/fl}$*Cd4Cre*$^+$ and *Apoe*$^{-/-}$*Cd40*$^{fl/fl}$*Cd11cCre*$^+$ mice both displayed low levels of systemic IL-2 expression which is not surprisingly since the production of IL-2 is highly CD40-CD40L dependent[72]. Without the presence of sufficient IL2- levels naïve T cell cannot enter the cell cycle[72].Upon successful activation by DCs Th1 cell polarization is then initiated in response to IFNγ and IL-12 produced by APCs[67,79–81]. The expression of both systemic IFNγ and IL-12 was significantly downregulated in *Apoe*$^{-/-}$*Cd40l*$^{fl/fl}$*Cd4Cre*$^+$ and *Apoe*$^{-/-}$*Cd40*$^{fl/fl}$*Cd11cCre*$^+$ mice. This data points to a generally hampered Th1 polarization as expression of both, a polarizing cytokine and an effector cytokine, are reduced. In summary, this led us to the assumption that *Apoe*$^{-/-}$*Cd40l*$^{fl/fl}$*Cd4Cre*$^+$ and *Apoe*$^{-/-}$*Cd40*$^{fl/fl}$*Cd11cCre*$^+$ mice harbor decreased numbers of activated and pro-atherogenic Th1 cells[58,62,76].

Furthermore, our studies provided additional information for an altered activation status of T cells in mice with a deficiency of DC-CD40 or T cell-CD40L. DCs from *Apoe*$^{-/-}$*Cd40l*$^{fl/fl}$*Cd4Cre*$^+$ and *Apoe*$^{-/-}$*Cd40*$^{fl/fl}$*Cd11cCre*$^+$ mice featured a decreased OX40L expression despite the presence of a cognate antigen. This corroborates our assumption of an insufficient T cell activation since the costimulatory signals from OX40-OX40L to T cells are essential to promote division and survival of T cells and previously studies of OX40L-deficient mice or with blocking antibodies to OX40L revealed a reduced expansion or functional priming of $CD4^+$ T cells[345–349]. Initially, an *in vitro* T cell proliferation assay did not exhibit any differences in the mitotic capacity of T cells from *Apoe*$^{-/-}$*Cd40l*$^{fl/fl}$*Cd4Cre*$^+$ or *Apoe*$^{-/-}$*Cd40*$^{fl/fl}$*Cd11cCre*$^+$ mice compared to littermate controls. However, this only holds true under an unpremeditated point of view. To interpret the results correctly one has to take into consideration that both of those mouse lines presented significant lower Treg numbers which presumably results in a lower suppressive capacity. Thus, total T cell cultures from *Apoe*$^{-/-}$*Cd40l*$^{fl/fl}$*Cd4Cre*$^+$ or *Apoe*$^{-/-}$*Cd40*$^{fl/fl}$*Cd11cCre*$^{+*}$ should be expected to proliferate at a higher rate. The comparable rates of T cell proliferation between

Apoe$^{-/-}$*Cd40l*$^{fl/fl}$*Cd4Cre*$^{+}$ or *Apoe*$^{-/-}$*Cd40*$^{fl/fl}$*Cd11cCre*$^{+}$ mice and control mice thereby indicate an altered or impaired proliferative capacity of non-regulatory T cells from *Apoe*$^{-/-}$*Cd40l*$^{fl/fl}$*Cd4Cre*$^{+}$ and *Apoe*$^{-/-}$*Cd40*$^{fl/fl}$*Cd11cCre*$^{+}$ mice. However, these results provide only room for speculation yet no evidence about the proliferation capacity of T cells. To make an accurate statement we have to conduct an additional proliferation assays with separated Tregs and T cells. As it is generally accepted that inflammatory Th1-type responses are pro-atherogenic, it is reasonable to postulate that the absence of CD40- (*Apoe*$^{-/-}$*Cd40*$^{fl/fl}$*Cd11cCre*$^{+}$) or CD40L- (*Apoe*$^{-/-}$*Cd40l*$^{fl/fl}$*Cd4Cre*$^{+}$) induced cytokine production following cognate T cell DC interaction results in a defective Th1 response which influence atherosclerotic plaque progression[58,61,62,76]. The proposed role of CD40-CD40L interactions in DC-T cell crosstalk is summarized in Figure 45.

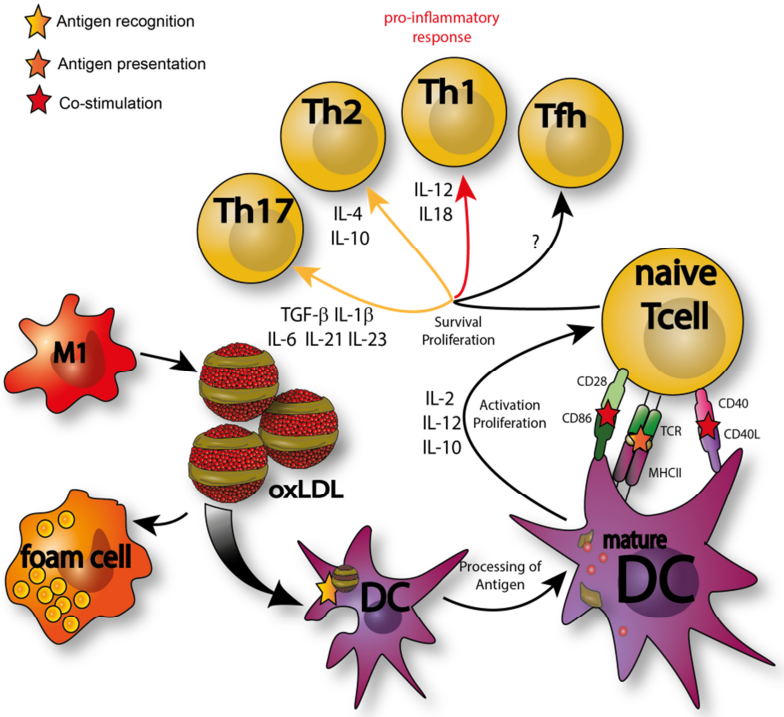

Figure 45. Role of CD40-CD40L interaction for activation and differentiation of T cells.
Mature dendritic cells (DCs) activate and polarize naïve T cells into different T helper cell (Th) subsets through antigen presentation to the T cell Receptor (TCR), secretion of cytokines and costimulatory cytokines. The presence of IL-12 and IL-18 causes Th1 skewing. Naive CD4^{+} T cells commit to a Th2 lineage under the influence of IL-4. Th17 differentiation requires a combination of several cytokines, including IL-6, TGFβ, IL-21, IL-23, and IL-1β. The mechanisms behind follicular helper T cell (Tfh) induction are not known yet. M1;classical macrophage, oxLDL; oxidized low density lipoprotein (Modified from Tse *et al*) [62].

4.4 Deficiency of CD40-CD40L signaling between DCs and T cells impedes the homeostasis of regulatory T cells by altering IL-2 levels

Several studies have shown that Treg cell development is reduced in the absence of the CD40-CD40L pathway[350–352]. However, these studies did only take global CD40- or CD40L-deficiency into account.

Here we studied the possible role of T cell- and DC-specific CD40-CD40L interactions in Treg development and homeostasis. Extensive analyses showed a significant reduction of mature Treg numbers in blood, lymph node, spleen, and aortic lesions and pre-Tregs numbers in the thymus of *Apoe*$^{-/-}$*CD40l*$^{fl/fl}$*Cd4Cre*$^{+}$ and *Apoe*$^{-/-}$*CD40*$^{fl/fl}$*Cd11cCre*$^{+}$ mice. Tregs are formed in the thymus and their development is highly dependent on the cytokine IL-2 which was also decreased systemically in both of our mouse models[311,353]. IL-2 is an autocrine T cell survival factor important for peripheral Treg maintenance since Tregs are not able to synthetize IL-2 themselves[311]. In the periphery DCs and activated T cells are the most potent producers of IL-2, however the precise mechanisms involved in the process have not been identified yet. Combined with our findings of insufficient DC maturation and T cell activation and the fact that the amount of IL-2 produced by T cells correlates with the extent of costimulation from DC *in vitro* and *in vivo*, the decreased Treg numbers strongly suggest that CD40-CD40L interactions participate in the process of Treg development[354,355]. However, CD40-CD40L interaction appears irrelevant for Treg function since neither the deficiency of T cell-specific CD40L nor the deficiency of CD40 on DCs changed the suppressive activity of Tregs. Our proposed model for the role of CD40-CD40L in Treg homeostasis is summarized in Figure 46. In summary, we have demonstrated that thymic and systemic Tregs are reduced but functional without an intact CD40–CD40L signaling on DCs or T cells. However, the exact mechanisms behind the reduction still need to be elucidated.

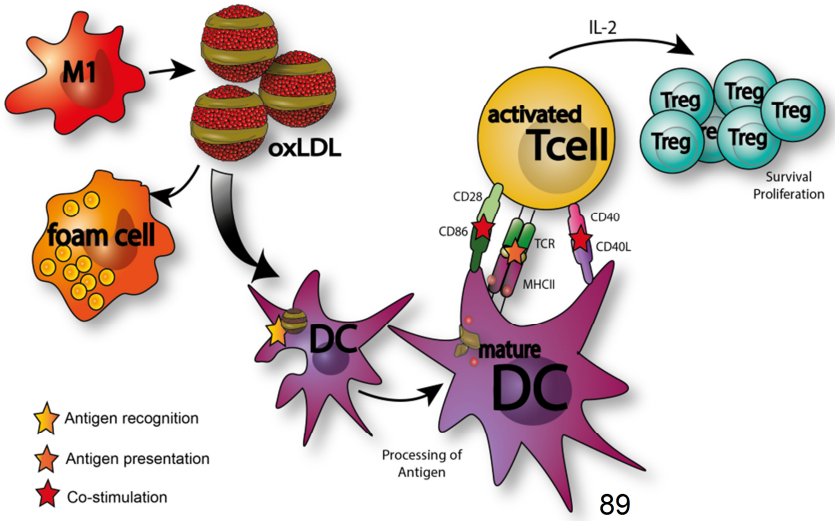

Figure 46. Proposed model for the CD40-CD40L dependent regulation of Treg homeostasis. Tregulatory cells (Tregs) are controlled by responder T cells via the level of available IL-2. Upon activation by T cell receptor (TCR) interactions and additional costimulation via CD80/CD86 and CD40/CD40L by dendritic cells (DCs), T cells produce IL-2. The secreted IL-2 then leads to proliferation and survival of Tregs. M1;classical macrophage. oxLDL; oxidized low density lipoprotein

4.5 CD40-CD40L signaling between DCs, T cells, and B cells is required for optimal B cell responses.

Both DCs and B cells express CD40 constitutively and interact with T cells via CD40L ligation. Yet, until today CD40-CD40L interactions have not been extensively studied in the context of DC-B cell interaction. The current paradigm professes that CD40L provides signals to B cells that induce proliferation, immunoglobulin switching, antibody secretion and rescue from apoptosis[244,273,274,356–365]. However, human and mouse B cells also express CD40L on their surface following activation and can release a soluble form of the ligand[366–368]. Thus it is possible that in addition to their T cell directed interaction, B cells may also interact with DCs via CD40-CD40L.

Primary B cells rapidly undergo spontaneous apoptosis in culture even in the presence of serum[369,271]. However, treatment with CD40L, B cell activating factor of the TNF family (BAFF), and LPS can all rescue B cells from apoptosis[369,271]. Furthermore, B cells undergo antibody- or Ig- class switching *in vivo* after immunization or infection or upon appropriate activation *in vitro*[246]. Engagement of the CD40 receptor on B cells by CD40L provides crucial signaling for class-switch recombination (CSR). Additionally, cytokines produced by T helper cells and DCs determine the isotype B cells will switch to[156,369,370,373]. Previous reports demonstrated a reduction in B cell responses and germinal center formation in CD40-deficient mice[265]. Plasma of *Apoe*$^{-/-}$*Cd40l*$^{fl/fl}$*Cd4Cre*$^{+}$ and *Apoe*$^{-/-}$*Cd40*$^{fl/fl}$*Cd11cCre*$^{+}$ mice showed decreased concentrations of total IgG and IgG_{2b} which are elicited through a Th1 cytokine-response and considered pro-atherogenic[148]. The concentration of plasma IgM was also decreased compared to littermate control mice. Overall decreased abundance of immunoglobulins is not necessarily affecting the presence of antigen-specific immunoglobulins. However, oxLDL-reactive immunoglobulin levels in *Apoe*$^{-/-}$*Cd40l*$^{fl/fl}$*Cd4Cre*$^{+}$ and *Apoe*$^{-/-}$*Cd40*$^{fl/fl}$*Cd11cCre*$^{+}$ mice resembled their overall abundance. The decreased immunoglobulin abundance may result from an altered activation status of B cells in both mouse models. Fully activated B cells start to produce antibodies in a secreted form rather than a membrane-bound form[157]. If they encounter specific signaling molecules via their CD40 and cytokine receptors, they then undergo antibody class switching to produce IgG, IgA or IgE antibodies (from IgM or IgD) [358,359,361]. In contrast to other immunoglobulins the IgA production is thereby partially independent of CD40-CD40L engagement since two members of the TNF-family, BAFF and APRIL, have been shown to stimulate CSR to IgG and IgA in both human and murine B cells[271,371,372]. Monocytes and DCs express BAFF, whereas APRIL is expressed by monocytes, macrophages, DCs, and activated T cells[272]. B cells express all three receptors BAFF-R, B-cell maturation antigen (BCMA) and transmembrane activator and CAML interactor (TACI) for these cytokines and previous studies showed that IgA production is not

abrogated in mice and humans deficient in CD40L or CD40[307,373]. Indeed, our studies also demonstrated comparable levels of CD40L-independent IgA in *Apoe*$^{-/-}$*Cd40l*$^{fl/fl}$*Cd4Cre*$^{+}$, *Apoe*$^{-/-}$*Cd40*$^{fl/fl}$*Cd11cCre*$^{+}$ and the respective control mice. The reduction of pro-atherogenic immunoglobulin subclasses furthermore seems linked to changes in the B2- B cell population. Total IgG, IgG1 and, IgG2b are considered pro-atherogenic and produced by B2 cells[173,174,177,178]. Depletion of B2 cells reduced the aforementioned pro-atherogenic Ig subclasses and mice were protected from atherosclerosis[148]. Notably *Apoe*$^{-/-}$*Cd40l*$^{fl/fl}$*Cd4Cre*$^{+}$ displayed a decreased percentage of follicular B2 B cells whereas the percentage of marginal zone B2 B cells was increased. Follicular B-2 B cells are known to be particularly well-suited to participate in T cell-dependent immune responses to protein antigens and undergo isotype switching and affinity maturation in the spleen and lymph nodes in response to T cell-dependent antigens to either become plasma cells that secrete large amounts of antibody, or memory B cells with the ability to produce specific antibodies upon re-exposure to the same antigen[135,136,138]. Marginal zone B cells are considered part of the innate immune system and immediately respond to antigens in the blood. Thus, they are considered T cell-independent and consequently also CD40-CD40L independent[374].

Taken together our data suggest an altered B cell activation status and therefore reduced numbers of pro-inflammatory immunoglobulins due to the missing costimulatory CD40-CD40L signal from either T cells (CD40L) or DCs (CD40). Figure 47 shows a proposed model for the role of CD40-CD40L interactions for the crosstalk between DCs, T cells and B cells in atherosclerosis.

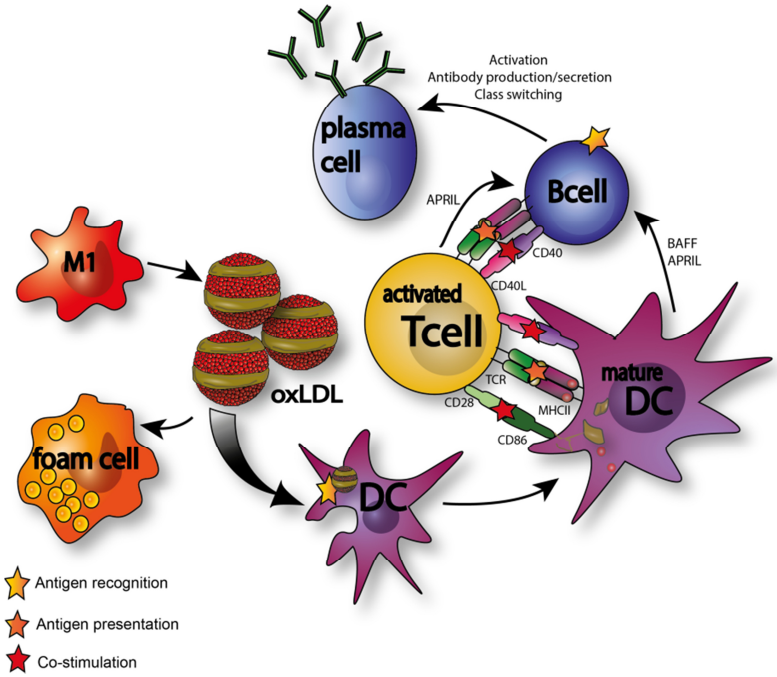

Figure 47. Proposed model of CD40-CD40L-dependent DCs, T cells and B cell crosstalk. CD40-CD40L signaling on dendritic cells (DCs) induces T cell activation which mediates class-switch recombination (CSR) and secretion of Immunoglobulin (Ig)G and IgA antibodies In general, CSR requires two signals. The first is through cytokines. Two members of the TNF- family, B cell activating factor (BAFF), and a proliferation-inducing ligand (APRIL), can stimulate CSR to IgG and IgA. Monocytes and dendritic cells express BAFF, whereas APRIL is expressed by monocytes, macrophages, dendritic cells, and activated T cells. These cytokines bind to B cells. The second signal is delivered by ligation of CD40 on B cells with its ligand CD40L on T cells. In addition DCs transfer antigen to B cells, which results in up-regulation of CD40L on B cells. M1;classical macrophage. oxLDL; oxidized low density lipoprotein. (Modified from Wykes et al.[368]).

4.6 Platelet-specific deletion of CD40L does not affect atherosclerosis

The pioneering work of Henn and coworkers established that CD40L and CD40 also exist in platelets[210]. They showed that CD40L is cryptic in unstimulated platelets but rapidly becomes exposed on the platelet surface after platelets are activated[210]. In addition elevated levels of sCD40L associate with acute coronary syndromes, percutaneous coronary interventions, and cardiopulmonary bypass[375]. Platelets are considered an important reservoir of this protein in circulation, because platelet count is correlated with levels of plasma sCD40L and essentially all of the sCD40L generated during the clotting of whole blood is derived from platelets[210].

Contrary to previous reports which ascribed platelet CD40L a key role in platelet-platelet interactions in thrombus formation and stability, our results do not point towards a crucial function of platelet CD40L in mediating inflammatory processes in atherosclerosis[317]. In this thesis we are the first to describe that neither PF4-specific CD40 nor CD40L are major contributors to atherosclerosis progression. Although we cannot completely exclude that the presence of CD40 and CD40L on the platelet surface or the interaction of other cells via CD40 and CD40L with platelets is implicated in the pathogenesis of atherosclerosis, our data seem to disqualify PF4-dependent CD40 and CD40L expression as a target for intervention.

The contradictory findings may derive from the differences to previously used models. These earlier studies were either performed with isolated platelets from mice with a systemic CD40L or CD40 deficiency or by administration of antibodies which bind systemically to CD40L or CD40[125,210,227,291,376]. Hence, it is possible that the platelet function was influenced by the systemic deficiency or inhibition of CD40L or CD40. Furthermore, the usage of isolated and *in vitro*-activated platelets bears the risk of contamination by lymphocytes which would influences lesion progression and has to be seen as a rather non-physiological model[125,295].

Although our approach allows us to eliminate certain critical points like the impact of a systemic CD40L or CD40 deficiency, the influence of other CD40L-deficient lymphocytes, and the need for an *in vitro* activation of platelets it still bears disadvantages. In contrast to our CD4- and CD11c-Cre^{+} mouse lines we were so far not able to prove that the PF4-linked cre-recombinase led to a successful deletion of CD40L or CD40 on platelets in our mice. The efficiency of the PF4-Cre-mediated excision in megakaryocytes and platelets was previously demonstrated for several proteins by Tiedt *et al*. [69.] However, Horrillo et al recently demonstrated that the floxed CD40L allele was efficiently excised in *in vitro* differentiated megakaryocytes from PF4-Cre^{+} mice but not from circulating platelets[22]. Platelets of cre^{+} mice carried similar amounts of the CD40L normal transcript which points to a deficient cre-mediated excision and that Pf4-driven cre expression fails to excise CD40L during *in vivo* differentiation of megakaryocytes[22]. Accordingly, this could also hold true for *Apoe*$^{-/-}$*Cd40l*$^{fl/fl}$*Pf4Cre*$^{+}$ mice and may explain their

unaffected atherosclerotic burden. Additionally, the origin of membrane-bound CD40L on platelets has not been clearly demonstrated yet.

The presence of CD40L or CD40 on platelets was previously demonstrated exclusively via flow cytometry or immunoblotting[210,377]. For decades, the general observation of platelet RNA and the characterization of reticulated platelets were used to estimate the rate of thrombopoiesis. However, the actual transcripts represented by this RNA were of little interest with the assumption that the RNA was merely a remnant from the precursor megakaryocyte. Over the past decade, finite but steady observations added support to the concept that platelet RNA is biologically and patho-physiologically meaningful[380–382]. Although platelets are anucleate cells, they retain mRNA, functional splicing, and translational machinery and there is a strong correlation between transcript abundance and protein expression[378–380]. In 2011 Rowley *et al* provided next-generation sequencing analysis which revealed new insights into the human and murine platelet transcriptomes. However, they also did not detect CD40L mRNA in human or murine platelets[381]. Accordingly, the lack of CD40L mRNA expression in murine platelets led to the assumption that the protein is synthesized early in platelet differentiation by megakaryocytes [377]. The Pf4-linked cre-recombinase targets all platelet progenitors, thus, CD40L-deficient megakaryocytes should pass on this deficiency to proplatelets and platelets which should presumably result in a aforementioned reduction of atherosclerosis[125]. However, our studies did not reveal any differences in the atherosclerotic burden of *Apoe*$^{-/-}$*Cd40l*$^{fl/fl}$*Pf4Cre*$^{+}$ mice.

Furthermore, the literature provides information which led us hypothesize, that platelets may not acquire CD40L from megakaryocytes but from plasma. In fact, platelets can take up fibrinogen from the plasma and release it after platelet activation and arterial thrombosis is dependent on platelet aggregation, a process mediated by the binding of soluble fibrinogen to glycoprotein IIb-IIIa (GPIIb-IIIa) on the surface of stimulated platelets[382–384]- GPIIb/IIIa antagonists are effective in these indications because they inhibit platelet aggregation[385]. It has been well documented that uptake and the delivery of fibrinogen to α-granules is mediated by GPIIb-IIIa[186,386]. Finally, during platelet activation, α-granules undergo exocytosis by which their fibrinogen content is released to the exterior and GP IIb/IIIa antagonists are capable of inhibiting platelet aggregation[385]. Two forms of CD40L are present in lymphocytes, a cell-bound form with a molecular weight of 39 kDa and various soluble forms (sCD40L) with a molecular weight of 31, 18 or14 kDa. Thus, even in a trimeric state the molecular weight of CD40L is rather small when compared to that of fibrinogen with a molecular weight of 340 kDa[185–188]. An initial study showed that sCD40L also binds directly to GP IIb/IIIa and is responsible for the formation of stable arterial thrombosis[291,387]. In addition, inhibitory effects of GPIIb/IIIa antagonists and aspirin on the release of sCD40L during platelet stimulation were demonstrated[385]. Collectively, these

observations suggest for a possible uptake and storage of CD40L in the α-granula by platelets and would explain the inefficient deletion of CD40L by PF4-dependent cre-excision. Yet, the exact mechanisms behind the presentation and origin from CD40L on the platelet surface as well as sCD40L require further investigation.
In summary, our data demonstrated the need for additional experiments to confirm the efficiency of the Pf4-linked CD40L or CD40 excision in platelets and progenitor cells and highlight the need for a proof of the validate protein depletion *in vivo* for every novel cre/loxP combination.

4.7 Conclusion and future perspectives

The continuing and increasing impact of atherosclerosis on morbidity and mortality in the western society and the rapid emergence of atherosclerosis in Asia and the rest of the world, despite the advances in diagnosis and therapy, highlights the importance to understand its pathogenesis in order to develop effective treatment or prevention[388]. The main goal of the studies in this thesis was to unravel the mechanisms of cell type-specific CD40-CD40L interactions in atherosclerosis. To this end, this thesis provides important insight into the cell type-specificity of CD40-CD40L interactions and their downstream impact on atherosclerosis progression. We demonstrate significant differences in the impact of systemic and cell type-specific CD40-CD40L interactions on atherosclerosis. We recognized that both T cell-specific CD40L and DC–specific CD40 are responsible for the pro-atherosclerotic effect of CD40-CD40L interactions. As systemic anti-CD40 or anti-CD40L intervention is not feasible, hence more specific approaches are required. In this regard, the cell type-specific modulation of CD40 on DCs and CD40L on T cells through conditional genetic approaches is more specific and results in a strong reduction of atherosclerosis. This method might circumvent problems like complete immune suppression or thromboembolemic events seen after long- term treatment with anti-CD40 antibodies[389]. It is likely that the approach of CD40 or CD40L inhibition on a specific cell population, apart from the difficulties for its technical implementation, is still too broad to use in a clinical setting as long-term treatment during atherosclerosis and could still compromise the patients´ host defense. However, cell type-specific targeting of certain cell subsets might resolve this issue, for example by targeting specific T cell- or DC subsets using the CRISPR/cas9 system, although this has to be investigated and requires many more years of development. New therapeutic approaches might induce selective suppression of pro-atherogenic immune responses or activation of anti-atherogenic responses to combat atherosclerosis. In that respect, knowledge regarding of cell type-specific CD40-CD40L interactions is of particular interest to provide new potential therapeutic targets that will be more efficient and safer than systemic CD40-CD40L inhibition.

5 SUMMARY

Cardiovascular diseases are still the leading cause of mortality worldwide. And atherosclerosis is its most underlying cause. Atherosclerosis is a lipid driven chronic inflammatory disease of the arterial wall, involving both innate and adaptive immune responses during pathogenesis. Specialized immune cells such as monocytes, B cells, T cells and dendritic cells (DCs) contribute to disease progression or by counterbalancing the inflammatory responses.

A system that has been shown to be an efficient conductor and modulator of immune cell responses is the CD40-CD40L dyad. CD40 is a member of the tumor necrosis factor receptor (TNFR) superfamily and is activated by CD40 ligand (CD40L). CD40 and CD40L both are expressed on the majority of immune and non-immune cells. However, the specific contribution of CD40-CD40L signaling on the different single cell types towards atherosclerosis progression has been undefined so far. The goal of the studies presented in this thesis was to unravel the cell type-specific mechanisms of CD40-CD40L interactions in atherosclerosis. Therefore, we used the cre/loxP system to create different, athero-prone *Apoe*$^{-/-}$ *Cd40*$^{fl/fl}$cre^{+} and *Apoe*$^{-/-}$ *Cd40l*$^{fl/fl}$cre^{+} mice with conditional CD40 or CD40L deficiencies on T cells, DCs and Platelets to investigate the cell type-specific impact of these costimulatory molecules on the generation of atherosclerosis. The main focus thereby was layed on the impact of T cell and DC specific deficiencies of CD40 and CD40L on atherosclerosis. Since platelets are also known to express CD40 or CD40L and to participate in the development and progression of atherosclerosis, a second study was established to serve as a basis for future, more detailed studies of the role of platelet- specific CD40 and CD40L interactions.

Hyperlipidemic mice with a CD40L deficiency on T cells or a CD40 deficiency on DCs developed significantly smaller atherosclerotic lesions than control animals after 28 weeks of normal diet, and after 6 weeks of a cholesterol-enriched diet. The altered lesion size was accompanied by a modified anti-inflammatory phenotype of the lesional cellular components, which was characterized by an increased proportion of stabilizing smooth muscle cells and a reduced number of anti-inflammatory immune cells, such as macrophages and T cells. Multiple mechanisms contribute to decreased athero-progression in T cell CD40- as well as DC-CD40-deficient mice. T cell CD40L-deficient and DC CD40-deficient hyperlipidemic mice displayed systematically reduced expression of pro-inflammatory cytokines such as interleukin (IL)-1 beta, IL-2, IL-12, and interferon gamma, and increased expression of anti-inflammatory cytokines IL-10 and transforming growth factor beta. This anti-inflammatory milieu ensures a reduced recruitment of immune cells into the atherosclerotic lesion and thus contributes to a decreased pathogenesis. Furthermore, we found indications in both mouse lines for a change in the development and activation status of the T cells and DCs as well as within their subpopulations.

Thus, mice with a deficiency of CD40L on T cells or a deficiency of CD40 on DCs show a systemic reduction in the expression of cytokines and gene markers associated with the activation of T cells (IL-2, CD69). This change is also reflected within the T cell populations of both mouse lines which had a reduced proportion of activated effector T cells and an increased ratio of naïve T cells. The reason for this change appears to stem from the interruption of the CD40-CD40L signals between T cells and DCs.

To unravel changes in the relationship between T cells and DCs we employed Contact hypersensitivity (CHS) as an additional *in vivo* model. The model allows to test for a proper antigen presentation between T cells and DCs including efficient antigen capture, -processing, -transport and the antigen presentation to naïve T cells. Indeed, DCs from T cell CD40L- and DC CD40-deficient mice have a higher proportion of immature inactivated DCs, which have a lower capacity for antigen presentation and T cell activation.

Furthermore, hyperlipidemic mice, with a T cell-specific CD40L deficiency and also mice with a DC-specific deficiency of CD40 show a systemic reduction of regulatory T cells (Treg), which also depend on IL-2 cytokine production. However, despite their reduced number, they have the same suppressive capacity as Tregs from control animals. The lack of costimulatory CD40-CD40L signals on T cells or DCs also lead to an insufficient activation of B cells and to a different secretion of immunoglobulins. B cells from mice with a deficiency of CD40L on T cells and from mice with a deficiency of CD40 on DCs produce fewer immunoglobulins with a smaller proportion of pro-inflammatory and an increased proportion of anti-inflammatory immunoglobulins. Therefore, the reduced atherogenesis by T cell-specific CD40L and DC-specific CD40 deficiency appears to be due to the systemic reduction of the adaptive immune response. The disturbed CD40-CD40L interactions between T cells, DCs, and B cells lead to inadequate antigen-detection and -presentation and thus to a dampened pro-inflammatory immune reaction.

In contrast to animals lacking CD40L on T cells mice with a deficiency of CD40L on platelets show no change in lesion size or phenotype. The absence of platelet-specific CD40L expression does not appear to affect their contribution to the progression of atherosclerosis.

In summary, these results underline the pro-atherosclerotic effects of CD40-CD40L interactions in a cell type-specific context, that these effects vary between different cell types and ascribe CD40-CD40L interactions between DCs and T cells a central role in atherosclerosis.

6 ZUSAMMENFASSUNG

Herz-Kreislauf-Erkrankungen sind nach wie vor die führenden Todesursache weltweit. Atherosklerose ist dabei die häufigste Ursache. Atherosklerose ist eine lipidgetriebene chronische entzündliche Erkrankung der Arterienwand, die sowohl angeborene als auch adaptive Immunantworten während der Pathogenese beinhaltet. Spezielle Immunzellen wie,T-Zellen und dendritische Zellen (DCs) tragen zum Fortschreiten der Krankheit bei.

Ein System, das sich als wirksamer Modulator von Immunzellenreaktionen erwiesen hat, ist das CD40-CD40 Ligand(L)-Paar. CD40 ist ein Mitglied der Tumor-Nekrose-Faktor-Rezeptor (TNFR)-Superfamilie und wird durch CD40L aktiviert. CD40 und CD40L sind beide auf der Mehrheit der Immun- (z.B T Zellen, B Zellen und DCs) und Nicht-Immunzellen (z.B. Plättchen) exprimiert. Der genaue Einfluss der CD40-CD40L-Signale auf einzelnen Zelltypen und die Atherosklerose entwicklung ist bisher allerdings noch unbekannt. Ziel der in dieser Arbeit vorgestellten Studien war es, diese zelltypspezifischen Mechanismen der CD40-CD40L-Wechselwirkungen innerhalb der Atherosklerose aufzuklären.

Das Hauptaugenmerk dieser Arbeit lag daher auf der Untersuchung der Auswirkungen von T Zell spezifischer Deletion von CD40L und DC-spezifischer Deletion von CD40 auf Atherosklerose. Naive T-Zellen benötigen eine Aktivierung durch DCs um in periphere Gewebe wie beispielsweise atherosklerotische Plaques einwandern zu können. Die Wechselwirkung der beiden Zellarten wird dabei unter anderem durch kostimulatorische CD40-CD40L Signale vermittelt. Die beiden Zelltypen sind daher ein viel versprechendes Ziel um mehr über die Rolle von zellspezifischen CD40-CD40L Interaktionen in der Atherosklerose entwicklung zu erfahren.

Neben der Untersuchung der T Zell- und DC-spezifischen Rolle von CD40-CD40L Interaktionen sollte mit dieser Arbeit aber auch ein Grundstein für zukünftige Untersuchungen der Plättchen spezifischen Rolle von CD40 und CD40L auf die Atherosklerose gelegt werden.

Um die Auswirkungen der jeweiligen spezifischen Deletionen auf die Atherosklerose zu analysieren etablierten wir daher mit Hilfe des Cre/loxP- Systems, Mauslinien mit zelltypspezifischen Deletionen von CD40 oder CD40L auf T Zellen, DCs und Plättchen.

Die von uns generierten hyperlipidemische Mäuse, mit einer CD40L Defizienz auf T Zellen oder eine CD40 Defizienz auf DCs entwickelten nach 28 Wochen normaler Diät sowie nach 6 Wochen einer cholesterinreichen Diät, signifikant kleinere atherosklerotische Läsionen als Kontrolltiere. Die veränderte Läsiongröße wurde dabei durch einen veränderten entzündungshemmenden Phänotyp der Läsionen ergänzt, welcher durch eine erhöhten Anteil von stabilisierenden glatten Muskelzellen und einer erniedrigten Anzahl von entzündungsfördernder Immunzellen wie Makrophagen und T Zellen begleitet wurde.

Multiple Mechanismen tragen zu der verringerten Atheroprogression in T Zell-CD40L- sowie DC-CD40-defizienten Mäusen bei. So zeigen T Zell-CD40L-defiziente und auch DC-CD40-defiziente hyperlipidemische Mäuse eine systemisch erniedrigte Expression von entzündungsfördernden Zytokinen wie z.B. Inteleukin(IL)-1b, IL-2, IL-12 und Interferon-gamma. Gleichzeitig ist eine gesteigerte Expression von entzündungshemmenden Zytokinen wie IL-10 und Transforming growth factor beta zu beobachten. Das entzündungshemmende Milieu sorgt für eine reduzierte Rekrutierung von Immunzellen in die atherosklerotische Läsion und trägt somit einen Teil zu der verminderten Pathogenese der Atherosklerose bei.

Zusätzlich finden sich in beiden Mäuselinien Hinweise auf einen veränderten Entwicklungs- und Aktivierungsstatus der T-Zellen, DCs und ihrer jeweiligen Subpopulationen. Mäuse mit einer Defizienz von CD40L auf T Zellen oder einer Defizienz von CD40 auf DCs weisen eine systemisch verminderte Expression von Genen auf, welche mit der Aktivierung von T Zellen in Verbindung stehen (IL-2, CD69). Diese Veränderung spiegelt sich auch innerhalb der T Zell-Populationen der beiden Mäuselinien wieder. So finden sich in jeweils beiden Mäuselinien ein erhöhter Anteil von naiven T Zellen, welche über geringe entzündungsfördernde Eigenschaften verfügen und ein reduzierten Anteil von aktivierten, entzündungsfördernden Effektor T Zellen.

Um die Änderungen in der Beziehung zwischen T-Zellen und DCs weiter zu entschlüsseln, benutzten wir die Kontakt-Hypersensitivität (KHS) als *in vivo* –Model zur Überprüfung der Antigenpräsentation zwischen T Zellen und DCs. Dies ermöglichte uns die genauere Analyse der Antigenpräsentation zwischen T-Zellen und DCs. Da das Model die Überprüfung der effizienten Antigen-Aufnahme, -Verarbeitung und -Präsentation durch DCs erlaubt. Dabei konnten wir zeigen, dass T Zell CD40L-defiziente und DC CD40-defiziente Mäusen über einen erhöhten Anteil an unreifer, nicht aktivierter DCs verfügen, welche eine geringere Kapazität zur Antigenpräsentation und T-Zellaktivierung aufweisen.

Des weiteren weisen hyperlipidemische Mäuse mit einer T Zell-spezifischen CD40L Defizienz und auch Mäuse mit einer DC-spezifischen Defizienz von CD40 eine systemische Reduktion regulatorischen T Zellen (Treg) auf, welche von der IL-2 Produktion durch aktivierte T Zellen und DCs abhängig sind. Trotz einer reduzierten Anzahl verfügen diese jedoch über dieselbe suppressive Kapazität wie Tregs aus Kontrolltieren.

Zusätzlich zur gestörten Aktivierung von T Zellen und DCs führt das Fehlen der kostimulatorischen CD40-CD40L Signalen, in beiden Mauslinien, zu einer nicht ausreichenden Aktivierung von B Zellen, sowie einer veränderten Sekretion von Antikörpern. B Zellen aus Mäusen mit einer Defizienz von CD40L auf T Zellen und auch aus Mäusen mit einer Defizienz von CD40 auf DCs produzieren insgesamt weniger Antikörper mit einem geringeren Anteil von entzündungsfördernden Antikörpern und einem gesteigerten Anteil von entzündungshemmenden Antikörpern.

Zusammenfassend scheint die reduzierte Atheroskleroseentwicklung durch T Zell-spezifische CD40L und DC-spezifische CD40 Defizienz daher in der systemischen Reduktion der adaptiven Immunantwort begründet zu sein. Fehlende Interaktion von CD40-CD40L zwischen T Zellen. DCs und B Zellen führen zu einer limitierten Antige-Erkennung sowie -Präsentation und somit zu einer verminderten Immunreaktion.

Im Gegensatz zu Tieren mit einer Defizienz von CD40L auf T Zellen weisen Mäuse mit einer Defizienz von CD40 oder CD40L auf Plättchen keine Veränderung der Läsionsgrößen oder des Läsionsphänotypes auf. Das Fehlen der Plättchen-spezifischen CD40 oder CD40L Expression scheint sich nicht auf deren Beitrag zur Atheroskleroseentwicklung auszuwirken.

Zusammenfassend unterstreichen diese Ergebnisse die Notwendigkeit, die unterschiedlichen pro- sowie anti-atherosklerotischen Auswirkungen von CD40-CD40L Interaktionen in einem zellspezifischen Kontext zu betrachten und das CD40-CD40L Interaktionen zwischen T Zellen und DCs als besonders wichtige Einflussfaktoren innerhalb der Atherosklerose zu sehen sind.

7 REFERENCES

1. Kumar, H., Ingle, H. & Prasad, D. Recognition of bacteriral infection by innate immune sensors. *Crit Rev Microbiol* **39,** 229–246 (2013).
2. Larsson, L. *Immunohistochemistry: Theory and practice.* (Crc Press Inc, 1988).
3. Gilmore, T. Introduction to NF-kappaB: players, pathways, perspectives. *Oncogene* **51,** 6680–6684 (2006).
4. Green, J. A., Cooperband, S. R. & Kibrick, S. Immune Specific Induction of Interferon Production in Cultures of Human Blood Lymphocytes. *Science (80-.).* **164,** 1415 LP-1417 (1969).
5. Uzman, A. Molecular biology of the cell (4th ed.): Alberts, B., Johnson, A., Lewis, J., Raff, M., Roberts, K., and Walter, P. *Biochem. Mol. Biol. Educ.* **31,** 212–214 (2003).
6. Lobstein, J. *Traité d'anatomie pathologique*. *Traité d'anatomie pathologique* (1829).
7. Weber, C. & Noels, H. Atherosclerosis: current pathogenesis and therapeutic options. *Nat Med* **17,** 1410–1422 (2011).
8. Lozano, R. *et al.* Global and regional mortality from 235 causes of death for 20 age groups in 1990 and 2010: a systematic analysis for the Global Burden of Disease Study 2010. *Lancet* **380,** 2095–2128 (2012).
9. Kochanek, K. D., Xu, J., Murphy, S. L., Minino, A. M. & Kung, H.-C. National Vital Statistics Reports Deaths : Final Data for 2009. *Natl. Cent. Heal. Stat.* **60,** 1–117 (2012).
10. Hansson, G. K. & Hermansson, A. The immune system in atherosclerosis. *Nat Immunol* **12,** 204–212 (2011).
11. Simionescu, N., Vasile, E., Lupu, F., Popescu, G. & Simionescu, M. Prelesional events in atherogenesis. Accumulation of extracellular cholesterol-rich liposomes in the arterial intima and cardiac valves of the hyperlipidemic rabbit. *Am. J. Pathol.* **123,** 109–25 (1986).
12. Davies, P. F. & Tripathi, S. C. Mechanical stress mechanisms and the cell. An endothelial paradigm. *Circ. Res.* **72,** 239 LP-245 (1993).
13. Meager, A. Cytokine regulation of cellular adhesion molecule expression in inflammation. *Cytokine Growth Factor Rev.* **10,** 27–39 (1999).
14. Weber, C., Zernecke, A. & Libby, P. The multifaceted contributions of leukocyte subsets to atherosclerosis: lessons from mouse models. *Nat Rev Immunol* **8,** 802–815 (2008).
15. Galkina, E. & Ley, K. Immune and Inflammatory Mechanisms of Atherosclerosis. *Annu. Rev. Immunol.* **27,** 165–197 (2009).
16. Steinberg, D., Parthasarathy, S., Carew, T. E., Khoo, J. C. & Witztum, J. L. Beyond Cholesterol. *N. Engl. J. Med.* **320,** 915–924 (1989).
17. Moore, K. J. & Tabas, I. The Cellular Biology of Macrophages in Atherosclerosis. *Cell*

145, 341–355 (2011).

18. Legein, B., Temmerman, L., Biessen, E. A. L. & Lutgens, E. Inflammation and immune system interactions in atherosclerosis. *Cell. Mol. Life Sci.* **70,** 3847–3869 (2013).
19. Spitz, C. *et al.* Regulatory T cells in atherosclerosis: critical immune regulatory function and therapeutic potential. *Cell. Mol. Life Sci.* **73,** 901–922 (2016).
20. Whitman, S. C. A practical approach to using mice in atherosclerosis research. *Clin. Biochem. Rev.* **25,** 81–93 (2004).
21. Ishibashi, S., Goldstein, J. L., Brown, M. S., Herz, J. & Burns, D. K. Massive xanthomatosis and atherosclerosis in cholesterol-fed low density lipoprotein receptor-negative mice. *J. Clin. Invest.* **93,** 1885–1893
22. Horrillo, A. *et al.* Generation of mice with conditional ablation of the Cd40lg gene: New insights on the role of CD40L. *Transgenic Res.* **23,** 53–66 (2014).
23. Nakashima, Y., Plump, A. S., Raines, E. W., Breslow, J. L. & Ross, R. ApoE-deficient mice develop lesions of all phases of atherosclerosis throughout the arterial tree. *Arterioscler. Thromb. Vasc. Biol.* **14,** 133 LP-140 (1994).
24. Mahley, R. W. & Ji, Z.-S. Remnant lipoprotein metabolism: key pathways involving cell-surface heparan sulfate proteoglycans and apolipoprotein E. *J. Lipid Res.* **40,** 1–16 (1999).
25. IMAIZUMI, K. Diet and Atherosclerosis in Apolipoprotein E-Deficient Mice. *Biosci. Biotechnol. Biochem.* **75,** 1023–1035 (2011).
26. Dansky, H. M., Charlton, S. A., Harper, M. M. & Smith, J. D. T and B lymphocytes play a minor role in atherosclerotic plaque formation in the apolipoprotein E-deficient mouse. *Proc. Natl. Acad. Sci. U. S. A.* **94,** 4642–6 (1997).
27. Zhou, X., Nicoletti, A., Elhage, R. & Hansson, G. K. Transfer of CD4(+) T Cells Aggravates Atherosclerosis in Immunodeficient Apolipoprotein E Knockout Mice. *Circulation* **102,** 2919 LP-2922 (2000).
28. Daugherty, A. *et al.* The effects of total lymphocyte deficiency on the extent of atherosclerosis in apolipoprotein E-/- mice. *J. Clin. Invest.* **100,** 1575–1580 (1997).
29. Song, L., Leung, C. & Schindler, C. Lymphocytes are important in early atherosclerosis. *J. Clin. Invest.* **108,** 251–259 (2001).
30. Libby, P., Lichtman, A. & Hansson, G. Immune Effector Mechanisms Implicated in Atherosclerosis: From Mice to Humans. *Immunity* **38,** 1092–1104 (2013).
31. Banchereau, J. & Steinman, R. M. Dendritic cells and the control of immunity. *Nature* **392,** 245–252 (1998).
32. Koltsova, E. K. & Ley, K. How dendritic cells shape atherosclerosis. *Trends Immunol.* **32,** 540–547 (2011).

33. Paulson, K. E. *et al.* Resident Intimal Dendritic Cells Accumulate Lipid and Contribute to the Initiation of Atherosclerosis. *Circ. Res.* **106,** 383 LP-390 (2010).
34. Satpathy, A. T. *et al.* Zbtb46 expression distinguishes classical dendritic cells and their committed progenitors from other immune lineages. *J. Exp. Med.* **209,** 1135 LP-1152 (2012).
35. Collin, M. & Milne, P. Langerhans cell origin and regulation. *Curr. Opin. Hematol.* **23,** 28–35 (2016).
36. Belz, G. T. & Nutt, S. L. Transcriptional programming of the dendritic cell network. *Nat Rev Immunol* **12,** 101–113 (2012).
37. Steinman, R. M. & Cohn, Z. A. Identification of a novel cell type in peripheral lymphoid organs of mice. *J. Exp. Med.* **137,** 1142–1162 (1973).
38. Bobryshev, Y. V & Lord, R. S. A. S-100 positive cells in human arterial intima and in atherosclerotic lesions. *Cardiovasc. Res.* **29,** 689 LP-696 (1995).
39. Dietel, B. *et al.* Decreased numbers of regulatory T cells are associated with human atherosclerotic lesion vulnerability and inversely correlate with infiltrated mature dendritic cells. *Atherosclerosis* **230,** 92–99 (2013).
40. Gautier, E. L. *et al.* Conventional Dendritic Cells at the Crossroads Between Immunity and Cholesterol Homeostasis in Atherosclerosis. *Circulation* **119,** 2367 LP-2375 (2009).
41. Busch, M., Westhofen, T. C., Koch, M., Lutz, M. B. & Zernecke, A. Dendritic Cell Subset Distributions in the Aorta in Healthy and Atherosclerotic Mice. *PLoS One* **9,** e88452 (2014).
42. Sage, A. P. *et al.* MHC Class II–Restricted Antigen Presentation by Plasmacytoid Dendritic Cells Drives Proatherogenic T Cell Immunity. *Circulation* **130,** 1363 LP-1373 (2014).
43. Koltsova, E. K. *et al.* Dynamic T cell–APC interactions sustain chronic inflammation in atherosclerosis. *J. Clin. Invest.* **122,** 3114–3126 (2012).
44. Erbel, C. *et al.* Functional profile of activated dendriticcells in unstable atherosclerotic plaque. *Basic Res. Cardiol.* **102,** 123–132 (2007).
45. Alderman, C. J. J. *et al.* Effects of oxidised low density lipoprotein on dendritic cells: a possible immunoregulatory component of the atherogenic micro-environment? *Cardiovasc. Res.* **55,** 806 LP-819 (2002).
46. Blüml, S. *et al.* Oxidized Phospholipids Negatively Regulate Dendritic Cell Maturation Induced by TLRs and CD40. *J. Immunol.* **175,** 501–508 (2005).
47. Buono, C. *et al.* B7-1/B7-2 Costimulation Regulates Plaque Antigen–Specific T-Cell Responses and Atherogenesis in Low-Density Lipoprotein Receptor–Deficient Mice. *Circulation* **109,** 2009 LP-2015 (2004).

48. Faure-André, G. *et al.* Regulation of Dendritic Cell Migration by CD74, the MHC Class II-Associated Invariant Chain. *Science (80-.).* **322,** 1705 LP-1710 (2008).
49. Sun, J. *et al.* Deficiency of Antigen-Presenting Cell Invariant Chain Reduces Atherosclerosis in Mice. *Circulation* **122,** 808 LP-820 (2010).
50. Hjerpe, C., Johansson, D., Hermansson, A., Hansson, G. K. & Zhou, X. Dendritic cells pulsed with malondialdehyde modified low density lipoprotein aggravate atherosclerosis in Apoe−/− mice. *Atherosclerosis* **209,** 436–441 (2010).
51. Hermansson, A. *et al.* Inhibition of T cell response to native low-density lipoprotein reduces atherosclerosis. *J. Exp. Med.* **207,** 1081–1093 (2010).
52. Hermansson, A. *et al.* Immunotherapy With Tolerogenic Apolipoprotein B-100–Loaded Dendritic Cells Attenuates Atherosclerosis in Hypercholesterolemic Mice. Clinical Perspective. *Circulation* **123,** 1083 LP-1091 (2011).
53. Llodrá, J. *et al.* Emigration of monocyte-derived cells from atherosclerotic lesions characterizes regressive, but not progressive, plaques. *Proc. Natl. Acad. Sci. U. S. A.* **101,** 11779–11784 (2004).
54. Schieffer, B. *et al.* Impact of Interleukin-6 on Plaque Development and Morphology in Experimental Atherosclerosis. *Circulation* **110,** 3493 LP-3500 (2004).
55. Huber, S. A., Sakkinen, P., Conze, D., Hardin, N. & Tracy, R. Interleukin-6 Exacerbates Early Atherosclerosis in Mice. *Arterioscler. Thromb. Vasc. Biol.* **19,** 2364 LP-2367 (1999).
56. Davenport, P. & Tipping, P. G. The role of interleukin-4 and interleukin-12 in the progression of atherosclerosis in apolipoprotein E-deficient mice. *Am. J. Pathol.* **163,** 1117–25 (2003).
57. Samarasinghe, R. *et al.* Induction of an Anti-Inflammatory Cytokine, IL-10, in Dendritic Cells After Toll-like Receptor Signaling. *J. Interf. Cytokine Res.* **26,** 893–900 (2006).
58. Lee, T.-S., Yen, H.-C., Pan, C.-C. & Chau, L.-Y. The Role of Interleukin 12 in the Development of Atherosclerosis in ApoE-Deficient Mice. *Arterioscler. Thromb. Vasc. Biol.* **19,** 734 LP-742 (1999).
59. Moore, K. W., de Waal Malefyt, R., Coffman, R. L. & O'Garra, A. Interleukin-10 and the Interleukin-10 receptor. *Annu. Rev. Immunol.* **19,** 683–765 (2001).
60. Daugherty, A. & Rateri, D. L. T Lymphocytes in Atherosclerosis. *Circ. Res.* **90,** 1039 LP-1040 (2002).
61. Mallat, Z. *et al.* Induction of a Regulatory T Cell Type 1 Response Reduces the Development of Atherosclerosis in Apolipoprotein E–Knockout Mice. *Circulation* **108,** 1232 LP-1237 (2003).
62. Tse, K., Tse, H., Sidney, J., Sette, A. & Ley, K. T cells in atherosclerosis. *Int. Immunol.* **25,** 615–622 (2013).

63. Elhage, R. *et al.* Deleting TCRαβ(+) or CD4(+) T Lymphocytes Leads to Opposite Effects on Site-Specific Atherosclerosis in Female Apolipoprotein E-Deficient Mice. *Am. J. Pathol.* **165,** 2013–2018 (2004).
64. Hansson, G. K., Holm, J. & Jonasson, L. Detection of activated T lymphocytes in the human atherosclerotic plaque. *Am. J. Pathol.* **135,** 169–175 (1989).
65. Khallou-Laschet, J. *et al.* The Proatherogenic Role of T Cells Requires Cell Division and Is Dependent on the Stage of the Disease. *Arterioscler. Thromb. Vasc. Biol.* **26,** 353 LP-358 (2006).
66. Trinchieri, G. in *Advances in Immunology* (ed. Immunology, F. J. D. B. T.-A. in) **Volume 70,** 83–243 (Academic Press, 1998).
67. Okamura, H., Tsutsui, H., Kashiwamura, S.-I., Yoshimoto, T. & Nakanishi, K. *Interleukin-18: A Novel Cytokine That Augments Both Innate and Acquired Immunity*. *Advances in Immunology* **70,** (Elsevier, 1998).
68. Stemme, S. *et al.* T lymphocytes from human atherosclerotic plaques recognize oxidized low density lipoprotein. *Proc. Natl. Acad. Sci. U. S. A.* **92,** 3893–3897 (1995).
69. Afek, A. *et al.* Immunization of Low-density Lipoprotein Receptor Deficient (LDL-RD) Mice with Heat Shock Protein 65 (HSP-65) Promotes Early Atherosclerosis. *J. Autoimmun.* **14,** 115–121 (2000).
70. Zhu, J. *et al.* Antibodies to Human Heat-Shock Protein 60 Are Associated With the Presence and Severity of Coronary Artery Disease. *Circulation* **103,** 1071 LP-1075 (2001).
71. Mosmann, T. R., Cherwinski, H., Bond, M. W., Giedlin, M. A. & Coffman, R. L. Two types of murine helper T cell clone. I. Definition according to profiles of lymphokine activities and secreted proteins. *J. Immunol.* **136,** 2348–2357 (1986).
72. Lin, J.-X. *et al.* The role of shared receptor motifs and common stat proteins in the generation of cytokine pleiotropy and redundancy by IL-2, IL-4, IL-7, IL-13, and IL-15. *Immunity* **2,** 331–339 (1995).
73. Szabo, S. J. *et al.* A Novel Transcription Factor, T-bet, Directs Th1 Lineage Commitment. *Cell* **100,** 655–669 (2000).
74. Szabo, S. J. *et al.* Distinct Effects of T-bet in Th1 Lineage Commitment and IFN-γ Production in CD4 and CD8 T Cells. *Science (80-.).* **295,** 338 LP-342 (2002).
75. Laurat, E. *et al.* In Vivo Downregulation of T Helper Cell 1 Immune Responses Reduces Atherogenesis in Apolipoprotein E-Knockout Mice. *Circulation* **104,** 197 LP-202 (2001).
76. Harvey, E. J. & Ramji, D. P. Interferon-γ and atherosclerosis: Pro- or anti-atherogenic? *Cardiovasc. Res.* **67,** 11 LP-20 (2005).
77. McLaren, J. E. & Ramji, D. P. Interferon gamma: A master regulator of atherosclerosis.

Cytokine Growth Factor Rev. **20,** 125–135 (2009).

78. Buono, C. *et al.* T-bet deficiency reduces atherosclerosis and alters plaque antigen-specific immune responses. *Proc. Natl. Acad. Sci. United States Am.* **102,** 1596–1601 (2005).
79. Micallef, M. J. *et al.* Interferon-γ-inducing factor enhances T helper 1 cytokine production by stimulated human T cells: synergism with interleukin-12 for interferon-γ production. *Eur. J. Immunol.* **26,** 1647–1651 (1996).
80. Gerdes, N. *et al.* Expression of interleukin (IL)-18 and functional IL-18 receptor on human vascular endothelial cells, smooth muscle cells, and macrophages: implications for atherogenesis. *J. Exp. Med.* **195,** 245–57 (2002).
81. Okamura, H. *et al.* Cloning of a new cytokine that induces IFN-gamma production by T cells. *Nature* **378,** 88–91 (1995).
82. Mallat, Z. *et al.* Expression of Interleukin-18 in Human Atherosclerotic Plaques and Relation to Plaque Instability. *Circulation* **104,** 1598–1603 (2001).
83. Wurtz, O., Bajénoff, M. & Guerder, S. IL4 mediated inhibition of IFNγ production by CD4+ T cells proceeds by several developmentally regulated mechanisms. *Int. Immunol.* **16,** 501–508 (2004).
84. King, V. L., Szilvassy, S. J. & Daugherty, A. Interleukin-4 deficiency decreases atherosclerotic lesion formation in a site-specific manner in female LDL receptor-/- mice. *Arterioscler. Thromb. Vasc. Biol.* **22,** 456–61 (2002).
85. Robertson, A.-K. L. & Hansson, G. K. T cells in atherogenesis: for better or for worse? *Arterioscler. Thromb. Vasc. Biol.* **26,** 2421–32 (2006).
86. Sica, A. & Mantovani, A. Macrophage plasticity and polarization: in vivo veritas. *J. Clin. Invest.* **122,** 787–795 (2012).
87. Leskinen, M. J., Kovanen, P. T. & Lindstedt, K. A. Regulation of smooth muscle cell growth, function and death in vitro by activated mast cells--a potential mechanism for the weakening and rupture of atherosclerotic plaques. *Biochem. Pharmacol.* **66,** 1493–8 (2003).
88. Cardilo-Reis, L. *et al.* Interleukin-13 protects from atherosclerosis and modulates plaque composition by skewing the macrophage phenotype. *EMBO Mol. Med.* **4,** 1072–86 (2012).
89. King, V. L., Cassis, L. A. & Daugherty, A. Interleukin-4 does not influence development of hypercholesterolemia or angiotensin II-induced atherosclerotic lesions in mice. *Am. J. Pathol.* **171,** 2040–7 (2007).
90. Morokata, T., Ishikawa, J., Ida, K. & Yamada, T. C57BL/6 mice are more susceptible to antigen-induced pulmonary eosinophilia than BALB/c mice, irrespective of systemic T

helper 1/T helper 2 responses. *Immunology* **98,** 345–351 (1999).

91. Stockinger, B. & Veldhoen, M. Differentiation and function of Th17 T cells. *Curr. Opin. Immunol.* **19,** 281–286 (2007).
92. Weaver, C. T., Hatton, R. D., Mangan, P. R. & Harrington, L. E. IL-17 Family Cytokines and the Expanding Diversity of Effector T Cell Lineages. *Annu. Rev. Immunol.* **25,** 821–852 (2007).
93. Taleb, S., Tedgui, A. & Mallat, Z. IL-17 and Th17 Cells in Atherosclerosis: Subtle and Contextual Roles. *Arterioscler. Thromb. Vasc. Biol.* **35,** 258–264 (2015).
94. Chung, Y. *et al.* Critical regulation of early Th17 cell differentiation by interleukin-1 signaling. *Immunity* **30,** 576–87 (2009).
95. Korn, T., Bettelli, E., Oukka, M. & Kuchroo, V. K. IL-17 and Th17 Cells. *Annu. Rev. Immunol.* **27,** 485–517 (2009).
96. Eid, R. E. *et al.* Interleukin-17 and Interferon-gamma Are Produced Concomitantly by Human Coronary Artery-Infiltrating T Cells and Act Synergistically on Vascular Smooth Muscle Cells. *Circulation* **119,** 1424–1432 (2009).
97. Butcher, M. & Galkina, E. Current views on the functions of interleukin-17A-producing cells in atherosclerosis. *Thromb. Haemost.* **106,** 787–795 (2011).
98. Erbel, C. *et al.* Inhibition of IL-17A attenuates atherosclerotic lesion development in apoE-deficient mice. *J. Immunol.* **183,** 8167–75 (2009).
99. Smith, E. *et al.* Blockade of interleukin-17A results in reduced atherosclerosis in apolipoprotein E-deficient mice. *Circulation* **121,** 1746–55 (2010).
100. Gao, Q. *et al.* A critical function of Th17 proinflammatory cells in the development of atherosclerotic plaque in mice. *J. Immunol.* **185,** 5820–7 (2010).
101. Taleb, S. *et al.* Loss of SOCS3 expression in T cells reveals a regulatory role for interleukin-17 in atherosclerosis. *J. Exp. Med.* **206,** 2067–77 (2009).
102. Gisterå, A. *et al.* Transforming growth factor-β signaling in T cells promotes stabilization of atherosclerotic plaques through an interleukin-17-dependent pathway. *Sci. Transl. Med.* **5,** 196ra100 (2013).
103. Madhur, M. S. *et al.* Role of interleukin 17 in inflammation, atherosclerosis, and vascular function in apolipoprotein e-deficient mice. *Arterioscler. Thromb. Vasc. Biol.* **31,** 1565–72 (2011).
104. Bettelli, E. *et al.* Reciprocal developmental pathways for the generation of pathogenic effector TH17 and regulatory T cells. *Nature* **441,** 235–8 (2006).
105. Berod, L. *et al.* De novo fatty acid synthesis controls the fate between regulatory T and T helper 17 cells. *Nat. Med.* **20,** 1327–33 (2014).
106. Schaerli, P. *et al.* Cxc Chemokine Receptor 5 Expression Defines Follicular Homing T

Cells with B Cell Helper Function. *J. Exp. Med.* **192,** 1553 LP-1562 (2000).

107. Nurieva, R. I. *et al.* Generation of T Follicular Helper Cells Is Mediated by Interleukin-21 but Independent of T Helper 1, 2, or 17 Cell Lineages. *Immunity* **29,** 138–149 (2008).
108. Johnston, R. J. *et al.* Bcl6 and Blimp-1 Are Reciprocal and Antagonistic Regulators of T Follicular Helper Cell Differentiation. *Science (80-.).* **325,** 1006 LP-1010 (2009).
109. Breitfeld, D. *et al.* Follicular B Helper T Cells Express Cxc Chemokine Receptor 5, Localize to B Cell Follicles, and Support Immunoglobulin Production. *J. Exp. Med.* **192,** 1545 LP-1552 (2000).
110. Crotty, S. Follicular Helper CD4 T Cells (T_{FH}). *Annu. Rev. Immunol.* **29,** 621–663 (2011).
111. Sakaguchi, S., Sakaguchi, N., Asano, M., Itoh, M. & Toda, M. Immunologic self-tolerance maintained by activated T cells expressing IL-2 receptor alpha-chains (CD25). Breakdown of a single mechanism of self-tolerance causes various autoimmune diseases. *J. Immunol.* **155,** 1151–1164 (1995).
112. Williams, L. M. & Rudensky, A. Y. Maintenance of the Foxp3-dependent developmental program in mature regulatory T cells requires continued expression of Foxp3. *Nat Immunol* **8,** 277–284 (2007).
113. Lee, Y. K., Mukasa, R., Hatton, R. D. & Weaver, C. T. Developmental plasticity of Th17 and Treg cells. *Curr. Opin. Immunol.* **21,** 274–280 (2009).
114. Chaudhry, A. *et al.* Interleukin-10 signaling in regulatory T cells is required for suppression of Th17 cell-mediated inflammation. *Immunity* **34,** 566–578 (2011).
115. Wakkach, A. *et al.* Characterization of Dendritic Cells that Induce Tolerance and T Regulatory 1 Cell Differentiation In Vivo. *Immunity* **18,** 605–617 (2003).
116. von Boehmer, H. Mechanisms of suppression by suppressor T cells. *Nat Immunol* **6,** 338–344 (2005).
117. Marson, A. *et al.* Foxp3 occupancy and regulation of key target genes during T-cell stimulation. *Nature* **445,** 931–935 (2007).
118. Qureshi, O. S. *et al.* Trans-endocytosis of CD80 and CD86: a molecular basis for the cell extrinsic function of CTLA-4 . *Science* **332,** 600–603 (2011).
119. Sakaguchi, S., Yamaguchi, T., Nomura, T. & Ono, M. Regulatory T Cells and Immune Tolerance. *Cell* **133,** 775–787 (2008).
120. Xiong, Z. *et al.* Expression of TCTP antisense in CD25(high) regulatory T cells aggravates cuff-injured vascular inflammation. *Atherosclerosis* **203,** 401–408 (2009).
121. Pastrana, J. L. *et al.* Regulatory T cells and Atherosclerosis. *J. Clin. Exp. Cardiolog.* **2012,** 2 (2012).
122. de Boer, O. J., van der Meer, J. J., Teeling, P., van der Loos, C. M. & van der Wal, A. C. Low Numbers of FOXP3 Positive Regulatory T Cells Are Present in all Developmental

Stages of Human Atherosclerotic Lesions. *PLoS One* **2,** e779 (2007).

123. Ait-Oufella, H. *et al.* Natural regulatory T cells control the development of atherosclerosis in mice. *Nat Med* **12,** 178–180 (2006).
124. Mor, A. *et al.* Role of Naturally Occurring CD4+CD25+ Regulatory T Cells in Experimental Atherosclerosis. *Arterioscler. Thromb. Vasc. Biol.* **27,** 893 LP-900 (2007).
125. Lievens, D. *et al.* Platelet CD40L mediates thrombotic and inflammatory processes in atherosclerosis. *Blood* **116,** 4317–4327 (2010).
126. Klingenberg, R. *et al.* Depletion of FOXP3+ regulatory T cells promotes hypercholesterolemia and atherosclerosis. *J. Clin. …* **123,** (2013).
127. Jonasson, L., Holm, J., Skalli, O., Bondjers, G. & Hansson, G. K. Regional accumulations of T cells, macrophages, and smooth muscle cells in the human atherosclerotic plaque. *Arterioscler. Thromb. Vasc. Biol.* **6,** 131 LP-138 (1986).
128. Cochain, C. & Zernecke, A. Macrophages and immune cells in atherosclerosis: recent advances and novel concepts. *Basic Res. Cardiol.* **110,** 34 (2015).
129. Zhou, X., Stemme, S. & Hansson, G. K. Evidence for a local immune response in atherosclerosis. CD4+ T cells infiltrate lesions of apolipoprotein-E-deficient mice. *Am. J. Pathol.* **149,** 359–366 (1996).
130. Hu, D. *et al.* Analysis of regulatory CD8 T cells in Qa-1-deficient mice. *Nat Immunol* **5,** 516–523 (2004).
131. Kyaw, T. *et al.* Cytotoxic and Proinflammatory CD8+ T Lymphocytes Promote Development of Vulnerable Atherosclerotic Plaques in ApoE-Deficient Mice Clinical Perspective. *Circulation* **127,** 1028 LP-1039 (2013).
132. Kantor, A. B. & Herzenberg, L. A. Origin of Murine B Cell Lineages. *Annu. Rev. Immunol.* **11,** 501–538 (1993).
133. Herzenberg, L. A. & Tung, J. W. B cell lineages: documented at last! *Nat Immunol* **7,** 225–226 (2006).
134. Montecino-Rodriguez, E. & Dorshkind, K. B-1 B Cell Development in the Fetus and Adult. *Immunity* **36,** 13–21 (2012).
135. Rajewsky, K. Clonal selection and learning in the antibody system. *Nature* **381,** 751–758 (1996).
136. Tarlinton, D. B-cell memory: are subsets necessary? *Nat Rev Immunol* **6,** 785–790 (2006).
137. Allen, C. D. C., Okada, T. & Cyster, J. G. Germinal Center Organization and Cellular Dynamics. *Immunity* **27,** 190–202 (2007).
138. Fairfax, K. A., Kallies, A., Nutt, S. L. & Tarlinton, D. M. Plasma cell development: From B-cell subsets to long-term survival niches. *Semin. Immunol.* **20,** 49–58 (2008).

139. Martin, F. & Kearney, J. F. Marginal-zone B cells. *Nat Rev Immunol* **2,** 323–335 (2002).
140. Cerutti, A., Cols, M. & Puga, I. Marginal zone B cells: virtues of innatelike antibody-producing lymphocytes. *Nat. Rev. Immunol.* **13,** 118–132 (2013).
141. Zhou & Hansson. Detection of B Cells and Proinflammatory Cytokines in Atherosclerotic Plaques of Hypercholesterolaemic Apolipoprotein E Knockout Mice. *Scand. J. Immunol.* **50,** 25–30 (1999).
142. Galkina, E. *et al.* Lymphocyte recruitment into the aortic wall before and during development of atherosclerosis is partially L-selectin dependent. *J. Exp. Med.* **203,** 1273 LP-1282 (2006).
143. van Leeuwen, M., Damoiseaux, J., Duijvestijn, A. & Tervaert, J. W. C. The therapeutic potential of targeting B cells and anti-oxLDL antibodies in atherosclerosis. *Autoimmun. Rev.* **9,** 53–57 (2009).
144. Perry, H., Bender, T. & McNamara, C. B Cell Subsets in Atherosclerosis. *Front. Immunol.* **3,** 373 (2012).
145. Kyaw, T., Tipping, P., Bobik, A. & Toh, B.-H. Protective Role of Natural IgM-Producing B1a Cells in Atherosclerosis. *Trends Cardiovasc. Med.* **22,** 48–53 (2012).
146. Caligiuri, G., Nicoletti, A., Poirier, B. & Hansson, G. K. Protective immunity against atherosclerosis carried by B cells of hypercholesterolemic mice. *J. Clin. Invest.* **109,** 745–753
147. Major, A. S., Fazio, S. & Linton, M. F. B-Lymphocyte Deficiency Increases Atherosclerosis in LDL Receptor–Null Mice. *Arterioscler. Thromb. Vasc. Biol.* **22,** 1892 LP-1898 (2002).
148. Ait-Oufella, H. *et al.* B cell depletion reduces the development of atherosclerosis in mice. *J. Exp. Med.* **207,** 1579–1587 (2010).
149. Kyaw, T. *et al.* Conventional B2 B Cell Depletion Ameliorates whereas Its Adoptive Transfer Aggravates Atherosclerosis. *J. Immunol.* **185,** 4410–4419 (2010).
150. Tsiantoulas, D., Diehl, C. J., Witztum, J. L. & Binder, C. J. B Cells and Humoral Immunity in Atherosclerosis. *Circ. Res.* **114,** 1743 LP-1756 (2014).
151. Wardemann, H., Boehm, T., Dear, N. & Carsetti, R. B-1a B Cells that Link the Innate and Adaptive Immune Responses Are Lacking in the Absence of the Spleen. *J. Exp. Med.* **195,** 771–780 (2002).
152. Holodick, N. E., Tumang, J. R. & Rothstein, T. L. Immunoglobulin secretion by B1 cells: Differential intensity and IRF4-dependence of spontaneous IgM secretion by peritoneal and splenic B1 cells. *Eur. J. Immunol.* **40,** 3007–3016 (2010).
153. Kyaw, T. *et al.* B1a B Lymphocytes Are Atheroprotective by Secreting Natural IgM That Increases IgM Deposits and Reduces Necrotic Cores in Atherosclerotic Lesions Novelty and Significance. *Circ. Res.* **109,** 830 LP-840 (2011).

154. Drew, P. A., Kiroff, G. K., Ferrante, A. & Cohen, R. C. Alterations in immunoglobulin synthesis by peripheral blood mononuclear cells from splenectomized patients with and without splenic regrowth. *J. Immunol.* **132,** 191–196 (1984).
155. Baumgarth, N. *et al.* Innate and acquired humoral immunities to influenza virus are mediated by distinct arms of the immune system. *Proc. Natl. Acad. Sci. U. S. A.* **96,** 2250–2255 (1999).
156. Stavnezer, J. Immunoglobulin class switching. *Curr. Opin. Immunol.* **8,** 199–205 (1996).
157. Kehry, M. *et al.* The immunoglobulin μ chains of membrane-bound and secreted IgM molecules differ in their C-terminal segments. *Cell* **21,** 393–406 (1980).
158. Ehrenstein, M. R. & Notley, C. A. The importance of natural IgM: scavenger, protector and regulator. *Nat Rev Immunol* **10,** 778–786 (2010).
159. Lewis, M. J. *et al.* Immunoglobulin M is Required for Protection Against Atherosclerosis in Low-Density Lipoprotein Receptor-Deficient Mice. *Circulation* **120,** 417–426 (2009).
160. Palinski, W. *et al.* Low density lipoprotein undergoes oxidative modification in vivo. *Proc. Natl. Acad. Sci. U. S. A.* **86,** 1372–1376 (1989).
161. Palinski, W., Tangirala, R. K., Miller, E., Young, S. G. & Witztum, J. L. Increased Autoantibody Titers Against Epitopes of Oxidized LDL in LDL Receptor–Deficient Mice With Increased Atherosclerosis. *Arterioscler. Thromb. Vasc. Biol.* **15,** 1569 LP-1576 (1995).
162. Shoenfeld, Y., Wu, R., Dearing, L. D. & Matsuura, E. Are Anti–Oxidized Low-Density Lipoprotein Antibodies Pathogenic or Protective? *Circulation* **110,** 2552 LP-2558 (2004).
163. Chou, M.-Y. *et al.* Oxidation-specific epitopes are dominant targets of innate natural antibodies in mice and humans. *J. Clin. Invest.* **119,** 1335–1349 (2009).
164. Shaw, P. X. *et al.* Natural antibodies with the T15 idiotype may act in atherosclerosis, apoptotic clearance, and protective immunity. *J. Clin. Invest.* **105,** 1731–1740 (2000).
165. Nilsson, J., Hansson, G. K. & Shah, P. K. Immunomodulation of Atherosclerosis. *Arterioscler. Thromb. Vasc. Biol.* **25,** 18 LP-28 (2004).
166. Binder, C. J. *et al.* Pneumococcal vaccination decreases atherosclerotic lesion formation: molecular mimicry between Streptococcus pneumoniae and oxidized LDL. *Nat Med* **9,** 736–743 (2003).
167. Binder, C. J. *et al.* IL-5 links adaptive and natural immunity specific for epitopes of oxidized LDL and protects from atherosclerosis. *J. Clin. Invest.* **114,** 427–437 (2004).
168. Hulthe, J. Antibodies to oxidized LDL in atherosclerosis development—clinical and animal studies. *Clin. Chim. Acta* **348,** 1–8 (2004).
169. Karvonen, J., Päivänsalo, M., Kesäniemi, Y. A. & Hörkkö, S. Immunoglobulin M Type of Autoantibodies to Oxidized Low-Density Lipoprotein Has an Inverse Relation to Carotid

Artery Atherosclerosis. *Circulation* **108,** 2107 LP-2112 (2003).

170. Nimmerjahn, F. & Ravetch, J. V. Fc gamma receptors as regulators of immune responses. *Nat Rev Immunol* **8,** 34–47 (2008).
171. Frank, M. M., Miletic, V. D. & Jiang, H. Immunoglobulin in the control of complement action. *Immunol. Res.* **22,** 137–146 (2000).
172. Lichtman, A. H., Binder, C. J., Tsimikas, S. & Witztum, J. L. Adaptive immunity in atherogenesis: new insights and therapeutic approaches. *J. Clin. Invest.* **123,** 27–36
173. Xu, Q. *et al.* Induction of arteriosclerosis in normocholesterolemic rabbits by immunization with heat shock protein 65. *Arterioscler. Thromb. Vasc. Biol.* **12,** 789 LP-799 (1992).
174. George, J., Afek, A., Gilburd, B., Shoenfeld, Y. & Harats, D. Cellular and humoral immune responses to heat shock protein 65 are both involved in promoting fatty-streak formation in LDL-receptor deficient mice. *J. Am. Coll. Cardiol.* **38,** 900–905 (2001).
175. Freigang, S., Hörkkö, S., Miller, E., Witztum, J. L. & Palinski, W. Immunization of LDL Receptor–Deficient Mice With Homologous Malondialdehyde-Modified and Native LDL Reduces Progression of Atherosclerosis by Mechanisms Other Than Induction of High Titers of Antibodies to Oxidative Neoepitopes. *Arterioscler. Thromb. Vasc. Biol.* **18,** 1972 LP-1982 (1998).
176. Zhou, X., Caligiuri, G., Hamsten, A., Lefvert, A. K. & Hansson, G. K. LDL Immunization Induces T-Cell–Dependent Antibody Formation and Protection Against Atherosclerosis. *Arterioscler. Thromb. Vasc. Biol.* **21,** 108 LP-114 (2001).
177. Schiopu, A. *et al.* Recombinant Human Antibodies Against Aldehyde-Modified Apolipoprotein B-100 Peptide Sequences Inhibit Atherosclerosis. *Circulation* **110,** 2047 LP-2052 (2004).
178. Miller, S. T. and Y. I. Oxidative Modification of Lipoproteins: Mechanisms, Role in Inflammation and Potential Clinical Applications in Cardiovascular Disease. *Current Pharmaceutical Design* **17,** 27–37 (2011).
179. Kovanen, P., Mänttäri, M., Palosuo, T., Manninen, V. & Aho, K. Prediction of myocardial infarction in dyslipidemic men by elevated levels of immunoglobulin classes A, E, and G, but not M. *Arch. Intern. Med.* **158,** 1434–1439 (1998).
180. Wang, J. *et al.* IgE stimulates human and mouse arterial cell apoptosis and cytokine expression and promotes atherogenesis in Apoe–/– mice . *J. Clin. Invest.* **121,** 3564–3577
181. Tsiantoulas, D. *et al.* Increased Plasma IgE Accelerate Atherosclerosis in Secreted IgM Deficiency. *Circ. Res.* **120,** 78 LP-84 (2017).
182. Muscari, A. *et al.* Association of serum IgA and C4 with severe atherosclerosis. *Atherosclerosis* **74,** 179–186 (1988).

183. Mizoguchi, A. & Bhan, A. K. A Case for Regulatory B Cells. *J. Immunol.* **176,** 705–710 (2006).
184. Patel, S. R., Hartwig, J. H. & Italiano, J. E. The biogenesis of platelets from megakaryocyte proplatelets. *J. Clin. Invest.* **115,** 3348–3354 (2005).
185. Handagama, P., Rappolee, D. A., Werb, Z., Levin, J. & Bainton, D. F. Platelet alpha-granule fibrinogen, albumin, and immunoglobulin G are not synthesized by rat and mouse megakaryocytes. *J. Clin. Invest.* **86,** 1364–1368 (1990).
186. Handagama, P., Scarborough, R. M., Shuman, M. A. & Bainton, D. F. Endocytosis of fibrinogen into megakaryocyte and platelet alpha- granules is mediated by alpha IIb beta 3 (glycoprotein IIb-IIIa) [published erratum appears in Blood 1993 Nov 1;82(9):2936]. *Blood* **82,** 135 LP-138 (1993).
187. Lange, W., Luig, A., Dolken, G., Mertelsmann, R. & Kanz, L. Fibrinogen gamma-chain mRNA is not detected in human megakaryocytes. *Blood* **78,** 20 LP-25 (1991).
188. Harrison, P. *et al.* Uptake of plasma fibrinogen into the alpha granules of human megakaryocytes and platelets. *J. Clin. Invest.* **84,** 1320–1324 (1989).
189. Heijnen, H. F. G. *et al.* Multivesicular Bodies Are an Intermediate Stage in the Formation of Platelet α-Granules. *Blood* **91,** 2313 LP-2325 (1998).
190. Munnix, I. C. A., Cosemans, J. M. E. M., Auger, J. M. & Heemskerk, J. W. M. Platelet response heterogeneity in thrombus formation. *Thromb. Haemost.* **102,** 1149–1156 (2009).
191. Denis, C. V & Wagner, D. D. Platelet Adhesion Receptors and Their Ligands in Mouse Models of Thrombosis. *Arterioscler. Thromb. Vasc. Biol.* **27,** 728 LP-739 (2007).
192. Smyth, S. S. *et al.* Platelet functions beyond hemostasis. *J. Thromb. Haemost.* **7,** 1759–1766 (2009).
193. Clark, S. R. *et al.* Platelet TLR4 activates neutrophil extracellular traps to ensnare bacteria in septic blood. *Nat Med* **13,** 463–469 (2007).
194. Langer, H. F. *et al.* Platelets contribute to the pathogenesis of experimental autoimmune encephalomyelitis. *Circ. Res.* **110,** 1202–1210 (2012).
195. Boilard, E. *et al.* Platelets Amplify Inflammation in Arthritis via Collagen-Dependent Microparticle Production. *Science* **327,** 580–583 (2010).
196. Wong, C. H. Y., Jenne, C. N., Petri, B., Chrobok, N. L. & Kubes, P. Nucleation of platelets with blood-borne pathogens on Kupffer cells precedes other innate immunity and contributes to bacterial clearance. *Nat Immunol* **14,** 785–792 (2013).
197. Coupland, L. A. & Parish, C. R. Platelets, Selectins, and the Control of Tumor Metastasis. *Semin. Oncol.* **41,** 422–434 (2014).
198. Huo, Y. & Ley, K. F. Role of Platelets in the Development of Atherosclerosis. *Trends*

Cardiovasc. Med. **14,** 18–22 (2004).

199. Lusis, A. J. Atherosclerosis. *Nature* **407,** 233–241 (2000).
200. Chandraratne, S. *et al.* Critical Role of Platelet Glycoprotein Ibα in Arterial Remodeling. *Arterioscler. Thromb. Vasc. Biol.* **35,** 589 LP-597 (2015).
201. Koenen, R. R. *et al.* Disrupting functional interactions between platelet chemokines inhibits atherosclerosis in hyperlipidemic mice. *Nat Med* **15,** 97–103 (2009).
202. von Hundelshausen, P. *et al.* RANTES Deposition by Platelets Triggers Monocyte Arrest on Inflamed and Atherosclerotic Endothelium. *Circulation* **103,** 1772 LP-1777 (2001).
203. Sarma, J. *et al.* Increased Platelet Binding to Circulating Monocytes in Acute Coronary Syndromes. *Circulation* **105,** 2166 LP-2171 (2002).
204. Drechsler, M., Megens, R. T. A., van Zandvoort, M., Weber, C. & Soehnlein, O. Hyperlipidemia-Triggered Neutrophilia Promotes Early Atherosclerosis. *Circulation* **122,** 1837 LP-1845 (2010).
205. Kornerup, K. N., Salmon, G. P., Pitchford, S. C., Liu, W. L. & Page, C. P. Circulating platelet-neutrophil complexes are important for subsequent neutrophil activation and migration. *J. Appl. Physiol.* **109,** 758 LP-767 (2010).
206. Duffau, P. *et al.* Platelet CD154 Potentiates Interferon-α Secretion by Plasmacytoid Dendritic Cells in Systemic Lupus Erythematosus. *Sci. Transl. Med.* **2,** 47ra63 LP-47ra63 (2010).
207. Gerdes, N. *et al.* Platelets regulate CD4+ T-cell differentiation via multiple chemokines in humans. *Thromb. Haemost.* **106,** 353–362 (2011).
208. Psaltis, P. J. & Simari, R. D. Vascular Wall Progenitor Cells in Health and Disease. *Circ. Res.* **116,** 1392 LP-1412 (2015).
209. Bültmann, A. *et al.* Impact of glycoprotein VI and platelet adhesion on atherosclerosis—A possible role of fibronectin. *J. Mol. Cell. Cardiol.* **49,** 532–542 (2010).
210. Henn, V. *et al.* CD40 ligand on activated platelets triggers an inflammatory reaction of endothelial cells. *Nature* **391,** 591–594 (1998).
211. Santoso, S. *et al.* The Junctional Adhesion Molecule 3 (JAM-3) on Human Platelets is a Counterreceptor for the Leukocyte Integrin Mac-1. *J. Exp. Med.* **196,** 679–691 (2002).
212. Aslam, R. *et al.* Platelet Toll-like receptor expression modulates lipopolysaccharide-induced thrombocytopenia and tumor necrosis factor-α production in vivo. *Blood* **107,** 637 LP-641 (2006).
213. Karshovska, E., Weber, C. & von Hundelshausen, P. Platelet chemokines in health and disease. *Thromb. Haemost.* **110,** 894–902 (2013).
214. Nergiz-Unal, R., Rademakers, T., Heemskerk, J. & Cosemans, J. CD36 as a Multiple-Ligand Signaling Receptor in Atherothrombosis. *Cardiovascular & Hematological Agents*

in Medicinal Chemistry **9,** 42–55 (2011).

215. Fitzgerald, D. J., Roy, L., Catella, F. & FitzGerald, G. A. Platelet Activation in Unstable Coronary Disease. *N. Engl. J. Med.* **315,** 983–989 (1986).
216. Tsao, P. S., Theilmeier, G., Singer, A. H., Leung, L. L. & Cooke, J. P. L-arginine attenuates platelet reactivity in hypercholesterolemic rabbits. *Arterioscler. Thromb. Vasc. Biol.* **14,** 1529 LP-1533 (1994).
217. Furman, M. I. *et al.* Increased Platelet Reactivity and Circulating Monocyte-Platelet Aggregates in Patients With Stable Coronary Artery Disease. *J. Am. Coll. Cardiol.* **31,** 352–358 (1998).
218. Tailor, A. & Granger, D. N. Hypercholesterolemia Promotes P-Selectin–Dependent Platelet–Endothelial Cell Adhesion in Postcapillary Venules. *Arterioscler. Thromb. Vasc. Biol.* **23,** 675 LP-680 (2003).
219. Frenette, P. S., Johnson, R. C., Hynes, R. O. & Wagner, D. D. Platelets roll on stimulated endothelium in vivo: an interaction mediated by endothelial P-selectin. *Proc. Natl. Acad. Sci. U. S. A.* **92,** 7450–7454 (1995).
220. Huo, Y. *et al.* Circulating activated platelets exacerbate atherosclerosis in mice deficient in apolipoprotein E. *Nat Med* **9,** 61–67 (2003).
221. Massberg, S. *et al.* A Critical Role of Platelet Adhesion in the Initiation of Atherosclerotic Lesion Formation. *J. Exp. Med.* **196,** 887–896 (2002).
222. Theilmeier, G. *et al.* Endothelial von Willebrand factor recruits platelets to atherosclerosis-prone sites in response to hypercholesterolemia. *Blood* **99,** 4486 LP-4493 (2002).
223. May, A. E. *et al.* Engagement of Glycoprotein IIb/IIIa on Platelets Upregulates CD40L and Triggers CD40L-Dependent Matrix Degradation by Endothelial Cells. *Circulation* **106,** 2111 LP-2117 (2002).
224. Springer, T. A. Traffic signals for lymphocyte recirculation and leukocyte emigration: The multistep paradigm. *Cell* **76,** 301–314 (1994).
225. Nassar, T. *et al.* Platelet Factor 4 Enhances the Binding of Oxidized Low-density Lipoprotein to Vascular Wall Cells. *J. Biol. Chem.* **278,** 6187–6193 (2003).
226. von Hundelshausen, P. *et al.* Heterophilic interactions of platelet factor 4 and RANTES promote monocyte arrest on endothelium. *Blood* **105,** 924 LP-930 (2005).
227. Henn, V., Steinbach, S., Büchner, K., Presek, P. & Kroczek, R. A. The inflammatory action of CD40 ligand (CD154) expressed on activated human platelets is temporally limited by coexpressed CD40. *Blood* **98,** 1047 LP-1054 (2001).
228. Andre, P. *et al.* CD40L stabilizes arterial thrombi by a beta3 integrin-dependent mechanism. *Nat Med* **8,** 247–252 (2002).
229. Bromley, S. K. *et al.* The immunological synapse and CD28-CD80 interactions. *Nat*

Immunol **2,** 1159–1166 (2001).

230. Au, P.-Y. B. & Yeh, W.-C. in *TNF Receptor Associated Factors (TRAFs)* (ed. Wu, H.) 32–47 (Springer New York, 2007). doi:10.1007/978-0-387-70630-6_3
231. Walsh, M. C. & Choi, Y. Biology of the RANKL–RANK–OPG System in Immunity, Bone, and Beyond. *Front. Immunol.* **5,** 511 (2014).
232. Rickert, R. C., Jellusova, J. & Miletic, A. V. Signaling by the TNFR superfamily in B-cell biology and disease. *Immunol. Rev.* **244,** 115–133 (2011).
233. Linsley, P. S. *et al.* Immunosuppression in vivo by a soluble form of the CTLA-4 T cell activation molecule. *Science (80-.).* **257,** 792 LP-795 (1992).
234. Koho, H. *et al.* Monoclonal antibodies to antigens associated with transitional cell carcinoma of the human urinary bladder. *Cancer Immunol. Immunother.* **17,** 165–172 (1984).
235. Koho, H. *et al.* Cancer mmunology mmunotherapy Monoclonal antibodies to antigens associated with transitional cell carcinoma of the human urinary bladder I . Determination of the selectivity of six antibodies by cell ELISA and immunofluorescence. 165–172 (1984).
236. Clark, E. a & Ledbetter, J. a. Activation of human B cells mediated through two distinct cell surface differentiation antigens, Bp35 and Bp50. *Proc. Natl. Acad. Sci. U. S. A.* **83,** 4494–8 (1986).
237. Graf, D., Korthauer, U., Mages, H. W., Senger, G. & Kroczek, R. a. Cloning of TRAP, a ligand for CD40 on human T cells. *Eur. J. Immunol.* **22,** 3191–3194 (1992).
238. Lederman, B. S. *et al.* Identification of a novel surface protein on activated CD4+ T cells that induces contact-dependent B cell differentiation. *J. Exp. Med.* **175,** 1091–1101 (1992).
239. Elgueta, R. *et al.* Molecular mechanism and function of CD40/CD40L engagement in the immune system. *Immunol. Rev.* **229,** 10.1111/j.1600-065X.2009.00782.x (2009).
240. Krzesz, R., Wagner, A. H., Cattaruzza, M. & Hecker, M. Cytokine-inducible CD40 gene expression in vascular smooth muscle cells is mediated by nuclear factor κB and signal transducer and activato of transcription-1. *FEBS Lett.* **453,** 191–196 (1999).
241. Alderson, M. *et al.* CD40 expression by human monocytes: regulation by cytokines and activation of monocytes by the ligand for CD40. *J. Exp. Med.* **178,** 669–674 (1993).
242. Yellin, M. *et al.* Functional interactions of T cells with endothelial cells: the role of CD40L-CD40-mediated signals. *J. Exp. Med.* **182,** 1857–1864 (1995).
243. Karmann, K., Hughes, C. C., Schechner, J., Fanslow, W. C. & Pober, J. S. CD40 on human endothelial cells: inducibility by cytokines and functional regulation of adhesion molecule expression. *Proc. Natl. Acad. Sci. U. S. A.* **92,** 4342–4346 (1995).

244. Noelle, R. J. *et al.* A 39-kDa protein on activated helper T cells binds CD40 and transduces the signal for cognate activation of B cells. *Proc. Natl. Acad. Sci. U. S. A.* **89,** 6550–6554 (1992).
245. Van den Eertwegh, A. *et al.* In vivo CD40-gp39 interactions are essential for thymus-dependent humoral immunity. I. In vivo expression of CD40 ligand, cytokines, and antibody production delineates sites of cognate T-B cell interactions. *J. Exp. Med.* **178,** 1555–1565 (1993).
246. Foy, T. M. *et al.* gp39-CD40 interactions are essential for germinal center formation and the development of B cell memory. *J. Exp. Med.* **180,** 157 LP-163 (1994).
247. Winkelstein, J. & al, et. The X-Linked Hyper-IgM Syndrome: Clinical and Immunologic Features of 79 Patients. *Pediatr. Infect. Dis. J.* **23,** (2004).
248. Hardy, R. R., Hayakawa, K., Parks, D. R. & Herzenberg, L. A. Demonstration of B-cell maturation in X-linked immunodeficient mice by simultaneous three-colour immunofluorescence. *Nature* **306,** 270–272 (1983).
249. Davies, E. G. & Thrasher, A. J. Update on the hyper immunoglobulin M syndromes. *Br. J. Haematol.* **149,** 167–180 (2010).
250. Durandy, A. *et al.* Induction by anti-CD40 antibody or soluble CD40 ligand and cytokines of IgG, IgA and IgE production by B cells from patients with X-linked hyper IgM syndrome. *Eur. J. Immunol.* **23,** 2294–2299 (1993).
251. Grewal, I. S. & Flavell, R. A. CD40 and CD154 in cell-mediated immunity. *Annu. Rev. Immunol.* **16,** 111–135 (1998).
252. Schönbeck, U. & Libby, P. The CD40 / CD154 receptor / ligand dyad. *Cell. Mol. life Sci.* **58,** 4–43 (2001).
253. Bishop, G. A., Moore, C. R., Xie, P., Stunz, L. L. & Kraus, Z. J. in *TNF Receptor Associated Factors (TRAFs)* (ed. Wu, H.) 131–151 (Springer New York, 2007). doi:10.1007/978-0-387-70630-6_11
254. Pullen, S. S. *et al.* High-Affinity Interactions of Tumor Necrosis Factor Receptor-Associated Factors (TRAFs) and CD40 Require TRAF Trimerization and CD40 Multimerization. *Biochemistry* **38,** 10168–10177 (1999).
255. Pullen, S. S. *et al.* CD40−Tumor Necrosis Factor Receptor-Associated Factor (TRAF) Interactions: Regulation of CD40 Signaling through Multiple TRAF Binding Sites and TRAF Hetero-Oligomerization. *Biochemistry* **37,** 11836–11845 (1998).
256. Lu, L.-F. *et al.* The in vivo function of a noncanonical TRAF2-binding domain in the C-terminus of CD40 in driving B-cell growth and differentiation. *Blood* **110,** 193–200 (2007).
257. Zapata, J. M. TNF-receptor-associated factors as targets for drug development. *Expert Opin. Ther. Targets* **7,** 411–425 (2003).

258. Ishida, T. K. *et al.* TRAF5, a novel tumor necrosis factor receptor-associated factor family protein, mediates CD40 signaling. *Proc. Natl. Acad. Sci. U. S. A.* **93,** 9437–9442 (1996).
259. Xie, P. TRAF molecules in cell signaling and in human diseases. *J. Mol. Signal.* **8,** 7 (2013).
260. Mildner, A. & Jung, S. Development and Function of Dendritic Cell Subsets. *Immunity* **40,** 642–656 (2014).
261. Ma, D. Y. & Clark, E. a. The role of CD40 and CD40L in Dendritic Cells. *Semin Immunol. 2009* **21,** 265–272 (2010).
262. Kiener, P. A. *et al.* Stimulation of CD40 with purified soluble gp39 induces proinflammatory responses in human monocytes. *J. Immunol.* **155,** 4917–4925 (1995).
263. Koch, F. *et al.* High level IL-12 production by murine dendritic cells: upregulation via MHC class II and CD40 molecules and downregulation by IL-4 and IL-10. *J. Exp. Med.* **184,** 741 LP-746 (1996).
264. Macatonia, S. E. *et al.* Dendritic cells produce IL-12 and direct the development of Th1 cells from naive CD4+ T cells. *J. Immunol.* **154,** 5071–5079 (1995).
265. Kawabe, T. *et al.* The immune responses in CD40-deficient mice: Impaired immunoglobulin class switching and germinal center formation. *Immunity* **1,** 167–178 (1994).
266. Castigli, E. *et al.* CD40-deficient mice generated by recombination-activating gene-2-deficient blastocyst complementation. *Proc. Natl. Acad. Sci. U. S. A.* **91,** 12135–12139 (1994).
267. Frleta, D. *et al.* Distinctive Maturation of In Vitro Versus In Vivo Anti-CD40 mAb-Matured Dendritic Cells in Mice. *J. Immunother.* **26,** (2003).
268. Ouaaz, F., Arron, J., Zheng, Y., Choi, Y. & Beg, A. A. Dendritic Cell Development and Survival Require Distinct NF-κB Subunits. *Immunity* **16,** 257–270 (2002).
269. Wong, B. R. *et al.* TRANCE (Tumor Necrosis Factor [TNF]-related Activation-induced Cytokine), a New TNF Family Member Predominantly Expressed in T cells, Is a Dendritic Cell–specific Survival Factor . *J. Exp. Med.* **186,** 2075–2080 (1997).
270. Wykes, M. & Macpherson, G. Dendritic cell–B-cell interaction: dendritic cells provide B cells with CD40-independent proliferation signals and CD40-dependent survival signals. *Immunology* **100,** 1–3 (2000).
271. Litinskiy, M. B. *et al.* DCs induce CD40-independent immunoglobulin class switching through BLyS and APRIL. *Nat. Immunol.* **3,** 822–829 (2002).
272. Mackay, F., Schneider, P., Rennert, P. & Browning, J. BAFF AND APRIL: A Tutorial on B Cell Survival. *Annu. Rev. Immunol.* **21,** 231–264 (2003).
273. Lane, P. *et al.* Activated human T cells express a ligand for the human B cell-associated

antigen CD40 which participates in T cell-dependent activation of B lymphocytes. *Eur. J. Immunol.* **22,** 2573–2578 (1992).

274. Nonoyama, S., Hollenbaugh, D., Aruffo, A., Ledbetter, J. A. & Ochs, H. D. B cell activation via CD40 is required for specific antibody production by antigen-stimulated human B cells. *J. Exp. Med.* **178,** 1097 LP-1102 (1993).
275. Al-Daccak, R., Mooney, N. & Charron, D. MHC class II signaling in antigen-presenting cells. *Curr. Opin. Immunol.* **16,** 108–113 (2004).
276. Kumanogoh, a *et al.* Increased T cell autoreactivity in the absence of CD40-CD40 ligand interactions: a role of CD40 in regulatory T cell development. *J. Immunol.* **166,** 353–360 (2001).
277. Smook, M. L. F. *et al.* Leukocyte CD40L deficiency affects the CD25+ CD4 T cell population but does not affect atherosclerosis. *Atherosclerosis* **183,** 275–282 (2005).
278. Wells, A. D. *et al.* Requirement for T-cell apoptosis in the induction of peripheral transplantation tolerance. *Nat Med* **5,** 1303–1307 (1999).
279. Li, Y. *et al.* Blocking both signal 1 and signal 2 of T-cell activation prevents apoptosis of alloreactive T cells and induction of peripheral allograft tolerance. *Nat Med* **5,** 1298–1302 (1999).
280. Wekerle, T. *et al.* Peripheral Deletion After Bone Marrow Transplantation with Costimulatory Blockade Has Features of Both Activation-Induced Cell Death and Passive Cell Death. *J. Immunol.* **166,** 2311–2316 (2001).
281. Danese, S. *et al.* Activated platelets are the source of elevated levels of soluble CD40 ligand in the circulation of inflammatory bowel disease patients. *Gut* **52,** 1435–1441 (2003).
282. Matthies, K. M. G., Newman, J. L., Hodzic, A. & Wingett, D. G. Differential regulation of soluble and membrane CD40L proteins in T cells. *Cell. Immunol.* **241,** 47–58 (2006).
283. Garlichs, C. *et al.* Patients with acute coronary syndromes express enhanced CD40 ligand/CD154 on platelets. *Heart* **86,** 649–655 (2001).
284. Bourgeois, C., Rocha, B. & Tanchot, C. A Role for CD40 Expression on CD8+ T Cells in the Generation of CD8+ T Cell Memory. *Science (80-.).* **297,** 2060 LP-2063 (2002).
285. Linker, R., Gold, R. & Luhder, F. Function of Neurotrophic Factors Beyond the Nervous System. *CritRevImmunl* **29,** 43–68 (2009).
286. Zhu, L. M., Fang, Y. S., Sun, Z. G., Yu, L. Z. & Xu, H. Monocyte-Derived CD40 Expression Is Regulated by Interferon-γ/Interferon-γ Receptor-1 Pathway when Acting as a Bridge During Their Interaction with T Cells and Allogeneic Endothelial Cells. *Transplant. Proc.* **44,** 996–998 (2012).
287. Peng, X., Remacle, J. E., Kasran, A., Huylebroeck, D. & Ceuppens, J. L. IL-12 Up-

Regulates CD40 Ligand (CD154) Expression on Human T Cells. *J. Immunol.* **160,** 1166–1172 (1998).

288. Tian, L., Noelle, R. J. & Lawrence, D. A. Activated T cells enhance nitric oxide production by murine splenic macrophages through gp39 and LFA-1. *Eur. J. Immunol.* **25,** 306–309 (1995).
289. Malik, N., Greenfield, B. W., Wahl, A. F. & Kiener, P. A. Activation of human monocytes through CD40 induces matrix metalloproteinases. *J. Immunol.* **156,** 3952–3960 (1996).
290. Stout, R. D., Suttles, J., Xu, J., Grewal, I. S. & Flavell, R. A. Impaired T cell-mediated macrophage activation in CD40 ligand-deficient mice. *J. Immunol.* **156,** 8–11 (1996).
291. André, P., Nannizzi-Alaimo, L., Prasad, S. K. & Phillips, D. R. Platelet-derived CD40L: The switch-hitting player of cardiovascular disease. *Circulation* **106,** 896–899 (2002).
292. Danese, S. *et al.* Cutting Edge: T Cells Trigger CD40-Dependent Platelet Activation and Granular RANTES Release: A Novel Pathway for Immune Response Amplification. *J. Immunol.* **172,** 2011–2015 (2004).
293. Vanichakarn, P., Blair, P., Wu, C., Freedman, J. E. & Chakrabarti, S. Neutrophil CD40 enhances platelet-mediated inflammation. *Thromb. Res.* **122,** 346–358 (2008).
294. Li, G. *et al.* CD40 Ligand Promotes Mac-1 Expression, Leukocyte Recruitment, and Neointima Formation after Vascular Injury. *Am. J. Pathol.* **172,** 1141–1152 (2008).
295. Gerdes, N. *et al.* Platelet CD40 Exacerbates Atherosclerosis by Transcellular Activation of Endothelial Cells and Leukocytes. *Arterioscler. Thromb. Vasc. Biol.* **36,** 482 LP-490 (2016).
296. Kotowicz, K., Dixon, G. L. J., Klein, N. J., Peters, M. J. & Callard, R. E. Biological function of CD40 on human endothelial cells: costimulation with CD40 ligand and interleukin-4 selectively induces expression of vascular cell adhesion molecule-1 and P-selectin resulting in preferential adhesion of lymphocytes. *Immunology* **100,** 441–448 (2000).
297. Schönbeck, U. & Libby, P. CD40 signaling and plaque instability. *Circ. Res.* **89,** 1092–1103 (2001).
298. Lutgens, E. *et al.* Deficient CD40-TRAF6 signaling in leukocytes prevents atherosclerosis by skewing the immune response toward an antiinflammatory profile. *J. Exp. Med.* **207,** 391–404 (2010).
299. Lutgens, E. & Daemen, M. J. a P. CD40-CD40L interactions in atherosclerosis. *Trends Cardiovasc. Med.* **12,** 27–32 (2002).
300. Mach, F., Schönbeck, U. & Libby, P. CD40 signaling in vascular cells: A key role in atherosclerosis? *Atherosclerosis* **137, Suppl,** S89–S95 (1998).
301. Mach, F. *et al.* Functional CD40 ligand is expressed on human vascular endothelial cells, smooth muscle cells, and macrophages: implications for CD40-CD40 ligand signaling in

atherosclerosis. *Proc. Natl. Acad. Sci. U. S. A.* **94,** 1931–1936 (1997).

302. Mach, F., Schönbeck, U., Sukhova, G. K., Atkinson, E. & Libby, P. Reduction of atherosclerosis in mice by inhibition of CD40 signalling. *Nature* **394,** 200–203 (1998).
303. Lutgens, E. *et al.* Requirement for CD154 in the progression of atherosclerosis. *Nat. Med.* **5,** 1313–1316 (1999).
304. Lutgens, E. *et al.* Both early and delayed anti-CD40L antibody treatment induces a stable plaque phenotype. *Proc. Natl. Acad. Sci. U. S. A.* **97,** 7464–7469 (2000).
305. Schönbeck, U., Sukhova, G. K., Shimizu, K., Mach, F. & Libby, P. Inhibition of CD40 signaling limits evolution of established atherosclerosis in mice. *Proc. Natl. Acad. Sci. U. S. A.* **97,** 7458–7463 (2000).
306. Zirlik, A. *et al.* CD40 ligand mediates inflammation independently of CD40 by interaction with Mac-1. *Circulation* **115,** 1571–1580 (2007).
307. Renshaw, B. R. *et al.* Humoral immune responses in CD40 ligand-deficient mice. *J. Exp. Med.* **180,** 1889 LP-1900 (1994).
308. Sawada, S., Scarborough, J. D., Killeen, N. & Littman, D. R. A lineage-specific transcriptional silencer regulates CD4 gene expression during T lymphocyte development. *Cell* **77,** 917–929 (1994).
309. Caton, M. L., Smith-Raska, M. R. & Reizis, B. Notch–RBP-J signaling controls the homeostasis of CD8(−) dendritic cells in the spleen. *J. Exp. Med.* **204,** 1653–1664 (2007).
310. Tiedt, R., Schomber, T., Hao-Shen, H. & Skoda, R. C. Pf4-Cre transgenic mice allow the generation of lineage-restricted gene knockouts for studying megakaryocyte and platelet function in vivo. *Blood* **109,** 1503–1506 (2007).
311. Maloy, K. J. & Powrie, F. Fueling regulation: IL-2 keeps CD4+ Treg cells fit. *Nat Immunol* **6,** 1071–1072 (2005).
312. Foy, T. M. *et al.* In vivo CD40-gp39 interactions are essential for thymus-dependent humoral immunity. II. Prolonged suppression of the humoral immune response by an antibody to the ligand for CD40, gp39. *J. Exp. Med.* **178,** 1567–75 (1993).
313. Kripke, M. L., Munn, C. G., Jeevan, A., Tang, J. M. & Bucana, C. Evidence that cutaneous antigen-presenting cells migrate to regional lymph nodes during contact sensitization. *J. Immunol.* **145,** 2833–2838 (1990).
314. Moodycliffe, a M. *et al.* CD40-CD40 ligand interactions in vivo regulate migration of antigen-bearing dendritic cells from the skin to draining lymph nodes. *J. Exp. Med.* **191,** 2011–2020 (2000).
315. Tang, A., Judge, T. A. & Turka, L. A. Blockade of CD40-CD40 ligand pathway induces tolerance in murine contact hypersensitivity. *Eur. J. Immunol.* **27,** 3143–3150 (1997).
316. Schraml, B. U. & Reis e Sousa, C. Defining dendritic cells. *Curr. Opin. Immunol.* **32,** 13–

20 (2015).
317. Lievens, D. *et al.* Platelet CD40L mediates thrombotic and inflammatory processes in atherosclerosis. *Blood* **116,** 4317 LP-4327 (2010).
318. Engel, D. *et al.* The immunobiology of CD154–CD40–TRAF interactions in atherosclerosis. *Semin. Immunol.* **21,** 308–312 (2009).
319. Lievens, D., Eijgelaar, W. J., Biessen, E. a L., Daemen, M. J. a P. & Lutgens, E. The multi-functionality of CD40L and its receptor CD40 in atherosclerosis. *Thromb. Haemost.* **102,** 206–214 (2009).
320. Bavendiek, U. *et al.* Atherogenesis in mice does not require CD40 ligand from bone marrow-derived cells. *Arterioscler. Thromb. Vasc. Biol.* **25,** 1244–1249 (2005).
321. Nagy, A. Cre recombinase: The universal reagent for genome tailoring. *genesis* **26,** 99–109 (2000).
322. Celia, B. M. *et al.* Brief Definitive Report. *J. Exp. Med.* **184,** 0–5 (1996).
323. Chistiakov, D. A., Sobenin, I. A., Orekhov, A. N. & Bobryshev, Y. V. Dendritic cells in atherosclerotic inflammation: the complexity of functions and the peculiarities of pathophysiological effects. *Front. Physiol.* **5,** 196 (2014).
324. Mackey, M. F. *et al.* Cutting Edge: Dendritic Cells Require Maturation via CD40 to Generate Protective Antitumor Immunity. *J. Immunol.* **161,** 2094–2098 (1998).
325. McLellan, A. D., Heiser, A. & Hart, D. N. J. Induction of dendritic cell costimulator molecule expression is suppressed by T cells in the absence of antigen-specific signalling: Role of cluster formation, CD40 and HLA-class II for dendritic cell activation. *Immunology* **98,** 171–180 (1999).
326. Weiss, A. & Imboden, J. B. in (ed. Frank J. Dixon Leroy E. Hood and Jonathan W. Uhr BT - Advances in Immunology, K. F. A.) **Volume 41,** 1–38 (Academic Press, 1987).
327. Essen, D. van, Kikutani, H. & Gray, D. CD40 ligand-transduced co-stimulation of T cells in the development of helper function. *Nature* **378,** 620–623 (1995).
328. Smith-Garvin, J. E., Koretzky, G. A. & Jordan, M. S. T Cell Activation. *Annu. Rev. Immunol.* **27,** 591–619 (2009).
329. Ma, D. Y. & Clark, E. A. The role of CD40 and CD40L in Dendritic Cells. *Semin. Immunol.* **21,** 265–272 (2009).
330. Lanzavecchia, A. & Sallusto, F. Dynamics of T Lymphocyte Responses: Intermediates, Effectors, and Memory Cells. *Science (80-.).* **290,** 92 LP-97 (2000).
331. Moser, M. & Murphy, K. M. Dendritic cell regulation of TH1-TH2 development. *Nat Immunol* **1,** 199–205 (2000).
332. Liu, Y.-J., Kanzler, H., Soumelis, V. & Gilliet, M. Dendritic cell lineage, plasticity and cross-regulation. *Nat Immunol* **2,** 585–589 (2001).

333. Morelli, A. E. *et al.* Cytokine production by mouse myeloid dendritic cells in relation to differentiation and terminal maturation induced by lipopolysaccharide or CD40 ligation. *Blood* **98,** 1512 LP-1523 (2001).
334. Kaliński, P., Hilkens, C. M. U., Wierenga, E. A. & Kapsenberg, M. L. T-cell priming by type-1and type-2 polarized dendritic cells: the concept of a third signal. *Immunol. Today* **20,** 561–567 (1999).
335. Cella, M. *et al.* Ligation of CD40 on dendritic cells triggers production of high levels of interleukin-12 and enhances T cell stimulatory capacity: T-T help via APC activation. *J. Exp. Med.* **184,** 747–752 (1996).
336. Kobayashi, T. *et al.* TRAF6 Is a Critical Factor for Dendritic Cell Maturation and Development. *Immunity* **19,** 353–363 (2003).
337. Trinchieri, G. Interleukin-12 and the regulation of innate resistance and adaptive immunity. *Nat Rev Immunol* **3,** 133–146 (2003).
338. de Smedt, T. *et al.* Effect of interleukin-10 on dendritic cell maturation and function. *Eur. J. Immunol.* **27,** 1229–1235 (1997).
339. Erkes, D. A. & Selvan, S. R. Hapten-induced contact hypersensitivity, autoimmune reactions, and tumor regression: Plausibility of mediating antitumor immunity. *J. Immunol. Res.* **2014,** (2014).
340. Matos, T. J., Duarte, C. B., Gonçalo, M. & Lopes, M. C. DNFB activates MAPKs and upregulates CD40 in skin-derived dendritic cells. *J. Dermatol. Sci.* **39,** 113–123 (2005).
341. Heath, W. R. & Carbone, F. R. The skin-resident and migratory immune system in steady state and memory: innate lymphocytes, dendritic cells and T cells. *Nat. Immunol.* **14,** 978–85 (2013).
342. Schlitzer, A. *et al.* IRF4 Transcription Factor-Dependent CD11b+ Dendritic Cells in Human and Mouse Control Mucosal IL-17 Cytokine Responses. *Immunity* **38,** 970–983 (2013).
343. Persson, E. K. *et al.* IRF4 Transcription-Factor-Dependent CD103+CD11b+ Dendritic Cells Drive Mucosal T Helper 17 Cell Differentiation. *Immunity* **38,** 958–969 (2013).
344. Lu, Z. *et al.* Cd40-Independent Pathways of T Cell Help for Priming of Cd8(+) Cytotoxic T Lymphocytes. *J. Exp. Med.* **191,** 541–550 (2000).
345. Ohshima, Y. *et al.* Expression and function of OX40 ligand on human dendritic cells. *J. Immunol.* **159,** 3838–3848 (1997).
346. Weinberg, A. D., Wegmann3, K. W., Funatake, C. & Whitham, R. H. Blocking OX-40/OX-40 Ligand Interaction In Vitro and In Vivo Leads to Decreased T Cell Function and Amelioration of Experimental Allergic Encephalomyelitis. *J. Immunol.* **162,** 1818–1826 (1999).

347. Walker, L. S. K. *et al.* Compromised Ox40 Function in Cd28-Deficient Mice Is Linked with Failure to Develop Cxc Chemokine Receptor 5–Positive Cd4 Cells and Germinal Centers. *J. Exp. Med.* **190,** 1115–1122 (1999).
348. Murata, K. *et al.* Impairment of Antigen-Presenting Cell Function in Mice Lacking Expression of Ox40 Ligand. *J. Exp. Med.* **191,** 365–374 (2000).
349. Song, J. *et al.* The costimulation-regulated duration of PKB activation controls T cell longevity. *Nat Immunol* **5,** 150–158 (2004).
350. Spence, P. J. & Green, E. A. Foxp3+ regulatory T cells promiscuously accept thymic signals critical for their development. *Proc. Natl. Acad. Sci.* **105,** 973–978 (2008).
351. Zhan, Y., Bourges, D., Dromey, J. A., Harrison, L. C. & Lew, A. M. The origin of thymic CD4+CD25+ regulatory T cells and their co-stimulatory requirements are determined after elimination of recirculating peripheral CD4+ cells. *Int. Immunol.* **19,** 455–463 (2007).
352. Guiducci, C., Valzasina, B., Dislich, H. & Colombo, M. P. CD40/CD40L interaction regulates CD4+CD25+ T reg homeostasis through dendritic cell-produced IL-2. *Eur. J. Immunol.* **35,** 557–567 (2005).
353. de la Rosa, M., Rutz, S., Dorninger, H. & Scheffold, A. Interleukin-2 is essential for CD4+CD25+ regulatory T cell function. *Eur. J. Immunol.* **34,** 2480–2488 (2004).
354. Shahinian, A. *et al.* Differential T cell costimulatory requirements in CD28-deficient mice. *Science (80-.).* **261,** 609 LP-612 (1993).
355. Kastenmuller, W. *et al.* Regulatory T Cells Selectively Control CD8+ T Cell Effector Pool Size via IL-2 Restriction. *J. Immunol.* **187,** 3186–3197 (2011).
356. Armitage, R. J. *et al.* Molecular and biological characterization of a murine ligand for CD40. *Nature* **357,** 80–82 (1992).
357. Aruffo, a *et al.* The CD40 ligand, gp39, is defective in activated T cells from patients with X-linked hyper-IgM syndrome. *Cell* **72,** 291–300 (1993).
358. Korthauer, U. *et al.* Defective expression of T-cell CD40 ligand causes X-linked immunodeficiency with hyper-IgM. *Nature* **361,** 539–541 (1993).
359. Gordon, J., Millsum, M. J., Guy, G. R. & Ledbetter, J. A. Resting B lymphocytes can be triggered directly through the CDw40 (Bp50) antigen. A comparison with IL-4-mediated signaling. *J. Immunol.* **140,** 1425–1430 (1988).
360. Vallé, A. *et al.* Activation of human B lymphocytes through CD40 and interleukin 4. *Eur. J. Immunol.* **19,** 1463–1467 (1989).
361. Fuleihan, R., Ramesh, N. & Geha, R. S. Role of CD40-CD40-ligand interaction in Ig-isotype switching. *Curr. Opin. Immunol.* **5,** 963–967 (1993).
362. Rousset, F., Garcia, E. & Banchereau, J. Cytokine-induced proliferation and immunoglobulin production of human B lymphocytes triggered through their CD40

antigen. *J. Exp. Med.* **173,** 705 LP-710 (1991).

363. Grabstein, K. H. *et al.* The regulation of T cell-dependent antibody formation in vitro by CD40 ligand and IL-2. *J. Immunol.* **150,** 3141–3147 (1993).
364. Liu, Y.-J. *et al.* Mechanism of antigen-driven selection in germinal centres. *Nature* **342,** 929–931 (1989).
365. Liu, Y.-J. *et al.* Germinal center cells express bcl-2 protein after activation by signals which prevent their entry into apoptosis. *Eur. J. Immunol.* **21,** 1905–1910 (1991).
366. Nüsslein, H. G. *et al.* Increase of intracellular calcium is the essential signal for the expression of CD40 ligand. *Eur. J. Immunol.* **26,** 846–850 (1996).
367. Wykes, M., Poudrier, J., Lindstedt, R. & Gray, D. Regulation of cytoplasmic, surface and soluble forms of CD40 ligand in mouse B cells. *Eur. J. Immunol.* **28,** 548–559 (1998).
368. Wykes, M. Why do B cells produce CD40 ligand ? 328–331 (2003).
369. Zarnegar, B. *et al.* Unique CD40-mediated biological program in B cell activation requires both type 1 and type 2 NF-κB activation pathways. *Proc. Natl. Acad. Sci. United States Am.* **101,** 8108–8113 (2004).
370. Stavnezer, J., Guikema, J. E. J. & Schrader, C. E. Mechanism and Regulation of Class Switch Recombination. *Annu. Rev. Immunol.* **26,** 261–292 (2008).
371. Macpherson, A. J. *et al.* A Primitive T Cell-Independent Mechanism of Intestinal Mucosal IgA Responses to Commensal Bacteria. *Science (80-.).* **288,** 2222 LP-2226 (2000).
372. Castigli, E. *et al.* TACI and BAFF-R mediate isotype switching in B cells. *J. Exp. Med.* **201,** 35 LP-39 (2005).
373. Bergqvist, P., Gärdby, E., Stensson, A., Bemark, M. & Lycke, N. Y. Gut IgA Class Switch Recombination in the Absence of CD40 Does Not Occur in the Lamina Propria and Is Independent of Germinal Centers. *J. Immunol.* **177,** 7772–7783 (2006).
374. Martin, F., Oliver, A. M. & Kearney, J. F. Marginal Zone and B1 B Cells Unite in the Early Response against T-Independent Blood-Borne Particulate Antigens. *Immunity* **14,** 617–629 (2001).
375. Verma, S. *et al.* The relationship between soluble CD40 ligand levels and Framingham coronary heart disease risk score in healthy volunteers. *Atherosclerosis* **182,** 361–365 (2005).
376. Dewitte, A. *et al.* New frontiers for platelet CD154. *Exp. Hematol. Oncol.* **4,** 6 (2015).
377. Inwald, D. P., McDowall, A., Peters, M. J., Callard, R. E. & Klein, N. J. CD40 Is Constitutively Expressed on Platelets and Provides a Novel Mechanism for Platelet Activation. *Circ. Res.* **92,** 1041 LP-1048 (2003).
378. Weyrich, A. S. *et al.* mTOR-dependent synthesis of Bcl-3 controls the retraction of fibrin clots by activated human platelets. *Blood* **109,** 1975 LP-1983 (2007).

379. Gnatenko, D. V *et al.* Transcript profiling of human platelets using microarray and serial analysis of gene expression. *Blood* **101,** 2285 LP-2293 (2003).
380. Bugert, P., Dugrillon, A., Günaydin, A., Eichler, H. & Klüter, H. Messenger RNA profiling of human platelets by microarray hybridization. *Thromb. Haemost.* **90,** 738–748 (2003).
381. Rowley, J. W. *et al.* Genome-wide RNA-seq analysis of human and mouse platelet transcriptomes. *Blood* **118,** e101–e111 (2011).
382. Bennett, J. S. & Vilaire, G. Exposure of platelet fibrinogen receptors by ADP and epinephrine. *J. Clin. Invest.* **64,** 1393–1401 (1979).
383. Phillips, D. R., Charo, I. F. & Scarborough, R. M. GPIIb-IIIa: The responsive integrin. *Cell* **65,** 359–362 (1991).
384. Bennett, J. S. Structural biology of glycoprotein IIb-IIIa. *Trends Cardiovasc. Med.* **6,** 31–36 (1996).
385. Nannizzi-Alaimo, L., Alves, V. L. & Phillips, D. R. Inhibitory Effects of Glycoprotein IIb/IIIa Antagonists and Aspirin on the Release of Soluble CD40 Ligand During Platelet Stimulation. *Circulation* **107,** 1123 LP-1128 (2003).
386. Coller, B. S., Seligsohn, U., West, S. M., Scudder, L. E. & Norton, K. J. Platelet fibrinogen and vitronectin in Glanzmann thrombasthenia: evidence consistent with specific roles for glycoprotein IIb/IIIA and alpha v beta 3 integrins in platelet protein trafficking [see comments]. *Blood* **78,** 2603 LP-2610 (1991).
387. Aoui, C. *et al.* The Signaling Role of CD40 Ligand in Platelet Biology and in Platelet Component Transfusion. *Int. J. Mol. Sci.* **15,** 22342–22364 (2014).
388. Wong, M. C. S., Zhang, D. X. & Wang, H. H. X. Rapid emergence of atherosclerosis in Asia: a systematic review of coronary atherosclerotic heart disease epidemiology and implications for prevention and control strategies. *Curr. Opin. Lipidol.* **26,** (2015).
389. Boumpas, D. T. *et al.* A short course of BG9588 (anti–CD40 ligand antibody) improves serologic activity and decreases hematuria in patients with proliferative lupus glomerulonephritis. *Arthritis Rheum.* **48,** 719–727 (2003).

8 ACKNOWLEGMENTS

An dieser Stelle möchte ich mich bei allen Personen bedanken, die mich auf meinem Weg zur Promotion unterstützt und begleitet haben. Der Weg zur Promotion ist eine intensive Phase, die häufig, aber nicht immer, glücklich und erfolgreich endet. Daher bin ich umso glücklicher darüber nun an diesem Punkt zu stehen.

Ein großes Dankeschön geht an meine Doktormutter Prof. Dr. Sabine Steffens, für die Betreuung und wissenschaftliche Zusammenarbeit während meiner Promotion. Liebe Sabine, vielen Dank für die fachliche Unterstützung, die guten Gespräche und dafür, dass Du für mich immer weibliches Vorbild innerhalb der maskulinen Welt der universitären Forschung warst.

Lieber Norbert, liebe Esther, nicht nur in wissenschaftlicher Hinsicht habe ich viel von Euch gelernt. Ihr beiden wart für mich immer ein Beispiel für die erfolgreiche Vereinbarkeit von Familie und Forschung, selbst über Ländergrenzen hinaus. Esther war dabei stets der ruhige und fröhliche Pol innerhalb unserer Arbeitsgruppe und dank Deinem unermüdliches Engagement mussten wir uns nie Gedanken um unsere Ressourcen machen. Norbert möchte ich dabei besonders dafür danken, dass Du meine Selbstständigkeit gefördert hast und als Diskussionspartner einen großen Teil zu meiner persönlichen Weiterentwicklung beitragen konnte.

Liebe/r Charlotte, Sigrid, Tobi, Sandra, Geli, Holger und Svenja. Vielen Dank für all die gemeinsamen Jahre innerhalb und außerhalb des Labors. Ohne Euch hätte das Arbeiten definitiv nur halb so viel Spaß gemacht. Ihr seid oft genug der Grund für ein dickes Grinsen in meinem Gesicht, auch nach den längsten Labortagen oder Katastrophen. Ihr wisst genau, dass ich eigentlich Steine vorziehe und den direkten persönlichen Dank sowieso, daher werde ich mich hier kurzfassen und sage nur nochmals: DANKE!!!!

Liebe Siess Mädels , oder auch 3 (+1) Engel für Siess. Danke für die Zeit als meine Büropartnerinnen, für all die guten Gespräche auf höchst wissenschaftlichem Niveau und eure Unterstützung gerade in den letzten Monaten meiner Doktorarbeit. Janina, Du hast mich von Anfang an als Büropartnerin begleitet und mich an manch dunklem Tag, an dem ich an mir und meinen Fähigkeiten gezweifelt habe, gerettet. Auch wenn das „Frag´Chrissy, die weiß alles!“ meistens nur auf den richtigen Umgang mit irgendeiner Software bezogen war, reichte dies um mein Ego wieder aufzubauen. Und im Zweifelsfall hatten wir ja auch immer noch „Alors dance!“.

Ich möchte hier auch Herrn Haupt nicht unerwähnt lassen. Obwohl es Ihnen wahrscheinlich niemals wirklich bewusst war, so haben Sie doch dafür gesorgt, mein Interesse an der Biologie zu wecken. Ich danke Ihnen für die Amselprotokolle, dem extrahieren von Kiwi-DNA und Ihrer unermütlichen Begeisterung für die Biologie!

Es gibt es auch noch eine nicht zu vernachlässigende Anzahl an Menschen, welche mich außerhalb des Elfenbeinturmes namens Wissenschaft immer tatkräftig unterstützt haben.

Stellvertretend für diese Menschen möchte ich mich hier bei Alex, Fetty und Jule bedanken. Ich bin stolz und froh euch als „Meine Menschen“ bezeichnen zu können! Ohne euch wäre ich nicht ansatzweise die Person, die ich heute bin und ich weiß nicht, ob ich ohne euch bis zum Schreiben dieser Danksagung gekommen wäre.

Der finale Dank gilt meiner Familie. Worte können nur schlecht beschreiben, wie dankbar ich bin Euch zu haben. Ihr seid der beste Rückhalt, den man sich vorstellen kann. Ihr habt mir in meinem Leben all die Schritte ermöglicht, die mich zu diesem Punkt geführt haben. Euer unerschütterlicher Glaube an mich und meine Entscheidungen waren oft genug Grund genug über meinen Schatten zu springen und die nächsten Schritte in Angriff zu nehmen. Ich kann mich glücklich schätzen, ein Teil von dieser Familie zu sein!